UiT The Arctic University of Norway

Faculty of Health Sciences
Department of Pharmacy

Synthesis and structure-activity relationship studies of marine-derived antimicrobial peptides and small cyclic peptidomimetics

Danijela Simonovic

A dissertation for the degree of Philosophiae Doctor

April 2023

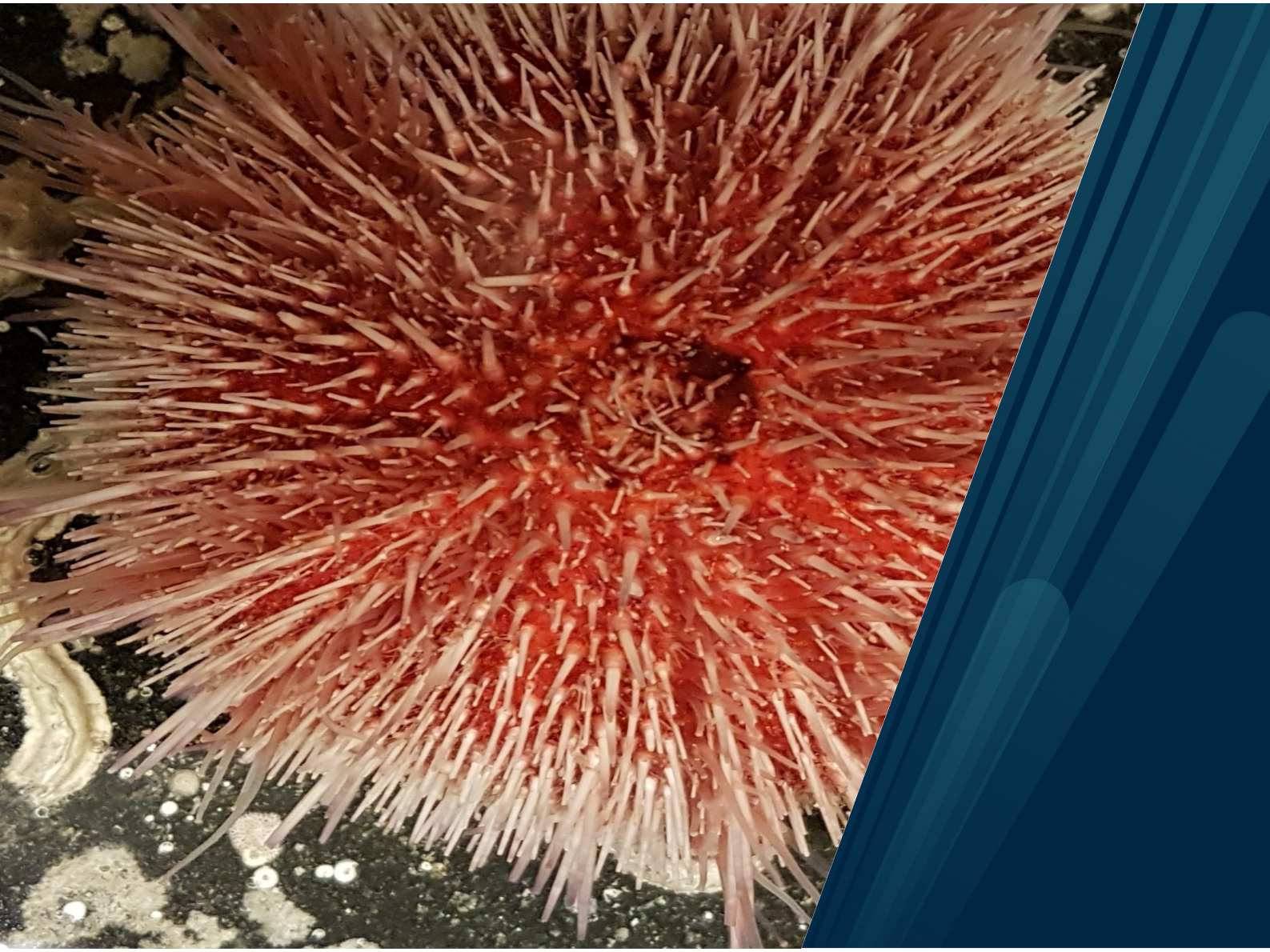

A dissertation for the degree of Philosophiae Doctor

Synthesis and structure-activity relationship studies of marine-derived antimicrobial peptides and small cyclic peptidomimetics

Danijela Simonovic

Tromsø, 2023

Natural products and medicinal chemistry research group

Department of Pharmacy

Faculty of Health Sciences

UiT The Arctic University of Norway

Norway

Acknowledgements

The time I spent at the Department of Pharmacy, at the UiT was in many respects unique. It was a privilege to be part of such a stimulating and creative environment for the past four years. Living and working in the Arctic was something far more than I could have ever expected. The magic of this journey was fascinating and the people I have met along the way have made me realise how fulfilling and inspiring scientific work can be. However, it seems that now the time has come for this PhD-chapter to close. But I can by no means close it, not before expressing my gratitude to many people who have shaped this incredible Arctic journey.

First and foremost, I am deeply grateful to my supervisor, Prof. Morten B. Strøm, for his support and guidance over the past four years and for the sharp scientific discussions. My appreciation also goes to my co-supervisor, Prof. Tor Haug, whose assistance and advice were invaluable. I am grateful to all my co-authors, without whom this work would not be possible. I would further like to thank Manuel, Marianne, and Aaron for their greatly appreciated assistance during my PhD, and Hymonti, with whom I had a pleasure of working on this project.

However, this experience would not have been so fulfilling, had there not been for my group members, as well as former master students, Ingrid, Natascha and Nima. Thank you all for making the work environment so enjoyable. For all the great discussions in and outside the lab, I am deeply grateful to Ingrid. Thank you Olga for the memorable Turku experience! Thank you Ana, Marina and Aleksandra for always being there for me! And to my amazing friends, Nina, Slavica, Irena and Kim – I am so grateful that our paths crossed.

I would also like to thank all my friends and former colleagues for helping me steer my way through calm, blue waters, but also rough and stormy seas. How would I have otherwise found my way to the Arctic?

Last, but not least, I would like to thank my family for their encouragement, love and support.

There are indeed bonds that never break.

Tromsø, April 2023

Danijela Simonović

Table of Contents

Abstract

Antibiotic-resistant bacterial pathogens pose a serious threat to human health. It is foreseeable that current, antibiotic-based regimes to treat bacterial infections will become ineffective in the coming decades, mainly due to the overuse and misuse of currently available antibiotics in both clinical and non-clinical settings. Therefore, there is an urgent need for new treatment options to conventional antibiotics.

Antimicrobial peptides, also known as host defense peptides, are one such option. These compounds are an important part of the innate immune system of different organisms and they are generally characterised by being short, structurally diverse, positively charged and amphipathic in nature. However, their toxicity to host (mammalian) cells, along with their often moderate antimicrobial activity, pose a major obstacle for their development as antibiotics. To effectively address this challenge, we need to better understand the relationship between structure and activity of these compounds.

In the present work we investigated how different structural modifications affect antimicrobial and haemolytic properties of various marine-derived short antimicrobial peptides and cyclic peptidomimetics. We used three different peptide scaffolds: firstly, a 12-residue loop region of the marine antimicrobial peptide Turgencin A, secondly, a previously reported lead peptide (P6) derived from the heavy chain of the marine peptide EeCentrocin 1, and finally, a tetrapeptide scaffold containing non-canonical amino acid. We have shown that antimicrobial and haemolytic properties of Turgencin A and EeCentrocin 1 analogues can be fine-tuned by incorporating bulky, hydrophobic amino acids in the native sequence, by lysine to arginine substitution, and *N*-terminal acylation. However, cyclisation of the linear peptides, either via formation of disulphide bridges or backbone cyclisation, did not significantly affect peptide selectivity. For much smaller, tetrapeptide scaffold our structure-activity relationship study revealed that changes in amphipathicity (from amphipathic to non-amphipathic) and stereochemistry (*L*- to *D*-amino acid substitution of a single cationic residue) could be used to decrease the mammalian cell toxicity, while not significantly affecting potency of such analogues.

In summary, our findings show that structural modifications performed in the present work could serve as viable strategies for the development of potent, non-haemolytic antimicrobial agents.

Abbreviations

AMPs	Antimicrobial peptides
AR	Antimicrobial resistance
ATP	Adenosin triphosphate
DAP	Daptomycin
DNA	Deoxyribonucleic acid
FDA	Food and Drug Administration
GAS	Group A *Streptococcus*
GBS	Group B *Streptococcus*
HCTU	*O*-(1*H*-6-Chlorobenzotriazole-1-yl)-1,1,3,3-tetramethyluronium hexafluorophosphate
LPS	Lipopolysaccharides
MDR	Multidrug-resistant
MIC	Minimal inhibitory concentration
GlcNAc	*N*-Acetyl-*D*-glucosamine
MurNAc	*N*-Acetylmuramic acid
RBC	Red blood cells
RNA	Ribonucleic acid
SAK	Staphylokinase
SAR	Structure-activity relationship
SPPS	Solid phase peptide synthesis
TA	Teichoic acid
UPLC	Ultra-Performance Liquid Chromatography
UPP	Undecaprenyl pyrophosphate

List of papers

This thesis is based on the following papers, which are referred to in the text of the thesis by their Roman numerals.

Paper I

Dey, H., **Simonovic, D**., Norberg-Schulz Hagen, I., Vasskog, T., Fredheim, E. G. A., Blencke, H.-M., Anderssen, T., Strøm, M. B., & Haug, T. (2022). Synthesis and Antimicrobial Activity of Short Analogues of the Marine Antimicrobial Peptide Turgencin A: Effects of SAR Optimizations, Cys-Cys Cyclization and Lipopeptide Modifications. International Journal of Molecular Sciences, 23(22). DOI: 10.3390/ijms232213844

Paper II

Danijela Simonovic, Hymonti Dey, Natascha Johansen, Trude Anderssen, Hege Devold, Terje Vasskog, Hans-Matti Blencke, Elizabeth G. Aarag Fredheim, Tor Haug, and Morten B. Strøm. Antimicrobial activity of short analogues of the marine peptide *EeCentrocin 1*: Synthesis of lipopeptides and head-to-tail cyclic peptides. (**Manuscript**)

Paper III

Danijela Simonovic, Fredrik G. Rylandsholm, Martin Jakubec, Johan Mattias Isaksson, Hege Devold, Trude Anderssen, Annette Bayer, Tor Haug, Morten B. Strøm. The role of amphipathicity and *L*- to *D*-amino acid substitution in a small antimicrobial cyclic tetrapeptide scaffold containing a halogenated α,α-disubstituted $\beta^{2,2}$-amino acid residue. (**Manuscript**)

1 Introduction

1.1 Antibiotics

Since their discovery, more than a century ago, antibacterial drugs have become indispensable for the treatment of bacterial infections. The preludium of the "antibiotic era" started in 1909, with the synthesis of arsphenamine (Salvarsan®), followed by the discovery of its analogue and active metabolite, neoarsphenamine (Neosalvarsan®) and oxophenarsine (Mapharsen®), respectively. (1-3) These synthetic compounds were used to treat syphilis, and they served as a replacement for highly toxic mercury-based formulations (*e.g.*, inunction, tablets, injections). (4) A few decades later, in the 1930s, yet another milestone was reached – the discovery of sulfonamidochrysoidine (KI-730, Prontosil), an antimicrobial prodrug which paved the way for the synthesis of a large and diverse group of sulphonamides, out of which sulfamethoxazole, sulfisoxazole and sulfadiazine, are still in use today. (1, 5)

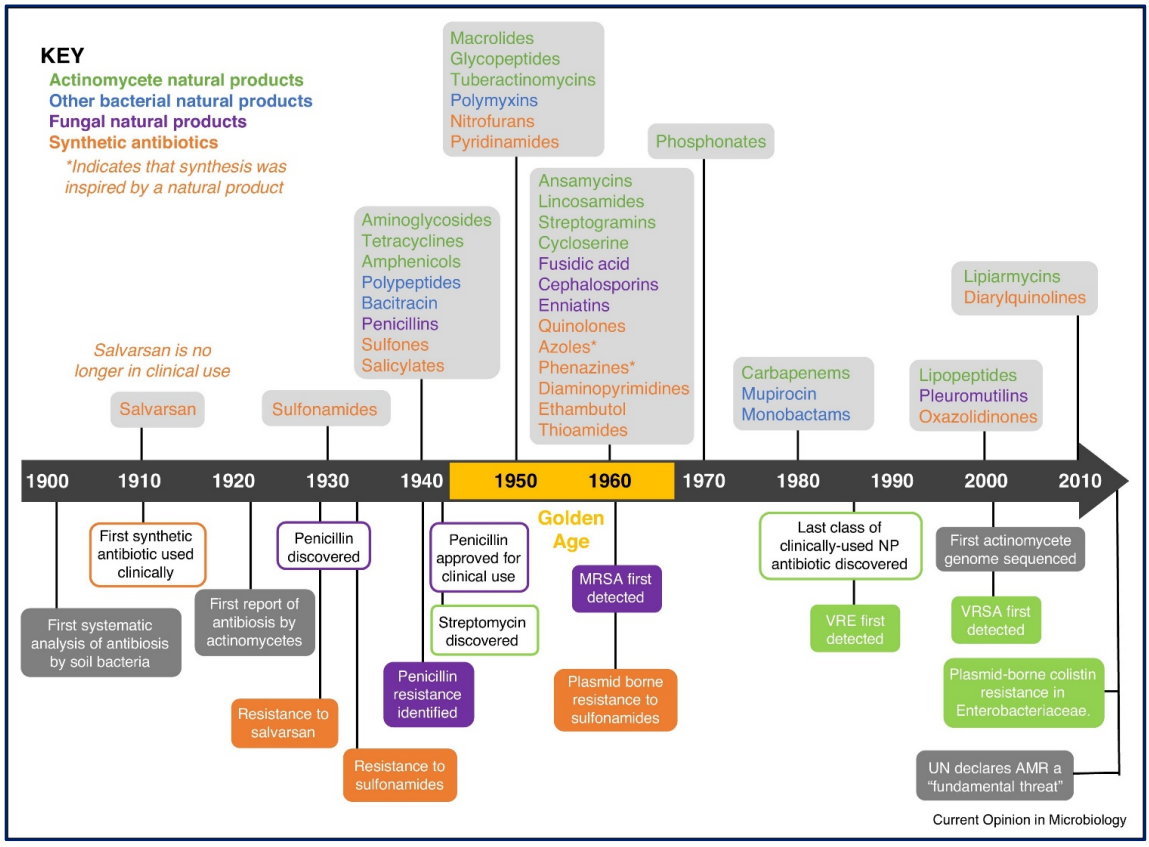

Figure 1. Timeline showing the decade when new antibiotic classes reached the clinic. (MRSA – methicillin-resistant *Staphylococcus aureus*; VRE – vancomycin-resistant enterococci; VRSA – vancomycin-resistant *S. aureus*. (Reprinted with permission from ref. 3.)

Often referred to as one of the greatest medical breakthroughs in the 20th century, the discovery of penicillin by Alexander Fleming in 1928 profoundly changed the antimicrobial therapy landscape, marking the beginning of the golden age of natural product antibiotic discovery (1943–1960). (6) (Figure 1) During this period, many new antibiotic classes were introduced, such as aminoglycosides, macrolides, tetracyclines, and glycopeptides. Since then, despite the increasing rates of antibiotic resistance, there has been a gradual decline in the discovery of new antibiotics. This trend has become more pronounced in recent years as major pharmaceutical companies have decided to leave the market in favour of more profitable research areas, such as cancer treatment. Nonetheless, during the last two decades many new antimicrobials, mostly derivatives of existing classes, reached the market. Some of the examples include oxazolidinones – linezolid and tedizolid, cyclic lipopepetide daptomycin, the first pleuromutilin – retapamulin, semisynthetic macrolide antibiotic fidaxomicin, and siderophore-cefalosporine cefiderocol. (7, 8)

1.2 Antimicrobial resistance

It is commonly held that antimicrobial resistance (AR) is a modern phenomenon tightly linked to the use of antibiotics. (9-11) However, findings from a number of studies have shown that AR is a widespread naturally occurring phenomenon predating human antibiotic use. (12-14) In other words, many bacterial species have evolved the ability to tolerate antibiotics even before their introduction into the clinic. However, the population-wide use of antibiotics to treat infections provided unprecedented selection pressure on human, animal and environmental macrobiota. Such selection pressure has facilitated mobilisation and horizontal transfer of AR genes among bacterial populations, rendering current antibiotic arsenal increasingly ineffective. (15) The severity of the problem has been recently highlighted in the study done by Murray *et al*., which found that in 2019, 1.27 million deaths were attributable to bacterial AR, killing more people than HIV/AIDS or malaria. (16) This burden of resistance is further compounded by the drug-related toxicity of the available treatment options, such as nephrotoxicity of colistin or oto- and nephrotoxicity of aminoglycosides, both of which are currently used to treat multidrug-resistant Gram-negative bacteria. (17, 18)

1.3 Global efforts to curb antimicrobial resistance

The problem of resistance, as well as emergence of multidrug-resistant pathogens, was recognised in the World Health Assembly Resolution of 1998. (19) A few years later, in 2001, the World Health Organisation global strategy to contain antimicrobial resistance was published. (20) In May 2015, the World Health Assembly adopted a global action plan on AR to insure adequate prevention and treatment of infectious diseases. (21) The need for urgent action was also recognised by the UN General Assembly in 2016 with the adoption of political declaration on AR. (22) A few years later, the Ad hoc Interagency Coordination Group (IACG) on Antimicrobial Resistance issued a report advocating for more holistic, One Health response to AR, underlying the importance of innovation, engagement and global governance. (23) On the IACG recommendation, in November 2020, the Global Leaders Group on Antimicrobial Resistance was established with joint effort by the Food and Agriculture Organisation of the United Nations, the World Health Organisation, the World Organisation for Animal Health and The United Nations Environment Programme. (24) The group acts, among others, as a global advisory body on issues, such as development of national and global strategies to fight AR. Most recently, in November 2022, the Antimicrobial Resistance Multi-Stakeholder Partnership Platform was launched to further improve the global collaboration towards resource efficient and sustainable solutions and help curb AR on a global scale. (25)

1.4 Public-private partnerships

As collaboration between public and private stakeholders has become increasingly important, if not indispensable, many partnerships have been established in order to provide greater impetus for the research and development within the field of AR. The Global Antibiotic Research and Development Partnership (GARDP) – a not-for-profit organisation, was created by the World Health Organisation and Drugs for Neglected Diseases *initiative (*DND*i)*. It includes a network of partners, *e.g.*, private sector, academia, civil society and public actors, and its main goal is to accelerate development of new treatments for drug-resistant infections. (26) Another example of successful partnership is the Combating Antibiotic-Resistant Bacteria Biopharmaceutical Accelerator (CARB-X), set up as a global consortium with uniquely diverse portfolio, which includes projects on the development of new classes of antibiotics, non-traditional therapeutics, vaccines and preventatives. With CARB-X support, a number of lead compounds have recently entered phase I clinical trial: a novel topoisomerase inhibitor, BWC0977 (Bugworks); small-molecule drug targeting *Escherichia coli* adhesion protein,

FimH GSK3882347 (GlaxoSmithKline), a polymyxin analogue for the treatment of infections caused by multidrug-resistant (MDR) Gram-negative bacteria, MRX-8 (MicuRx Pharmaceuticals), and a human monoclonal antibody as an antibiofilm agent for the treatment of prosthetic joint infections, TRL1068 (Trellis Bioscience). (27, 28)

1.5 Cyclic (lipo)peptides as antibiotics-inspiration from nature

Cyclic (lipo)peptides are a diverse group of compounds that have several unique features and distinct modes of action. They are used in the treatment of systemic infections, often caused by MDR strains of both Gram-positive and Gram-negative bacteria. Due to their poor oral bioavailability, they are generally administered intravenously, and their targets are predominantly localised on the outer membrane of the bacterial cell. Having a cyclic structure along with non-proteinogenic amino acids, makes them more tolerant to proteases degradation. Unlike proteins, cyclic lipopeptide antibiotics are biosynthesised via non-ribosomal peptide synthetases. (29) The lipid moiety, generally found at the *N*-terminus of the peptide is important for their amphipathic character. (30) A few examples of the cyclic lipopeptide-based antibiotics currently in clinical use will be presented in the following concise overview: daptomycin, teicoplanin and more recently approved telavancin, oritavancin and dalbavancin. In addition, two cyclic polypeptide antibiotics isolated from bacterial species will be described, namely bacitracin and polymyxin E.

1.5.1 Daptomycin – a calcium-dependent antibiotic

The family of calcium-dependent antibiotics consists of two main classes: the lipodepsipeptides and the lipopeptides. The compounds of both classes share some common chemical features: 10 amino acid macrolactone ring and an exocyclic region with an acylated *N*-terminus. (31) They have an overall negative charge, in contrast to cationic antimicrobial peptides, and a conserved Asp-X-Asp-Gly motif that is thought to facilitate calcium binding. (32, 33) It should be noted that the malacidins, a recently discovered class of antibiotics, do not contain this motif, and yet they exert their effect in a calcium-dependent manner. (34)

Daptomycin (DAP) is an acidic cyclic lipopeptide antibiotic with *in vitro* bactericidal activity against Gram-positive bacteria. It is an *N*-decanoyl analogue of the lipopeptide antibiotic complex A21889C, produced by a soil actinomycete *Streptomyces roseosporus*. (30, 35) Chemically, it consists of a cyclic depsipeptide core attached to the short linear segment (tripeptide) with an *N*-terminal fatty acid tail. DAP contains 13 amino acids, three of which are

with *D*-configuration: *D*-asparagine, *D*-alanine and *D*-serine, whereas three, the non-canonical ones, are present in its peptide core: *L*-kynurenine, *L*-ornithine, and (2S, 3R)-3-methylglutamic acid. (30, 36) (Figure 2) It was initially approved by the Food and Drug Administration (FDA) in 2003, for the treatment of complicated skin and skin structure infections and subsequently, in 2006, for two additional therapeutic indications, *Staphylococcus aureus* bacteraemia and right-sided endocarditis. (37)

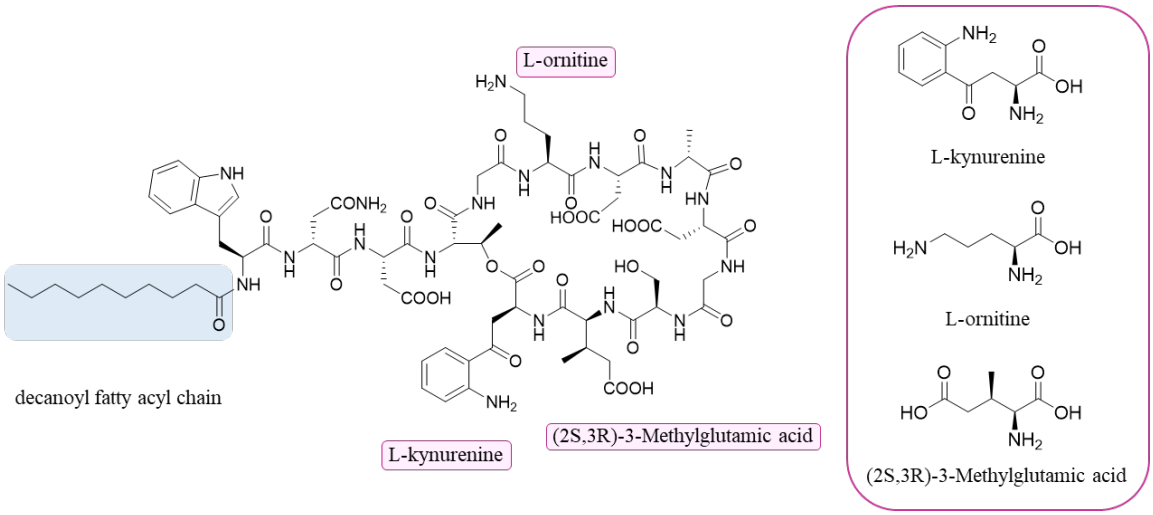

Figure 2. Structure of daptomycin.

Although its mechanism of action is not yet fully understood, existing evidence suggests that effect of DAP is mediated via calcium-dependent aggregation resulting in permeabilisation and depolarisation of the bacterial cell membrane. (38-41) Observation that membrane depolarisation occurs after cell death, led Jung *et al.* to suggest the possibility of DAP having multiple targets. (33) This lipopeptide interacts with membrane lipids (preferentially phosphatidylglycerol) in a calcium-dependent manner. Moreover, susceptibility to DAP is shown to correlate with the amount of phosphatidylglycerol in the target membrane. (42) While examining the interactions between DAP and *B. subtilis*, Pogliano *et al.* observed that it induces membrane distortion, which leads to aberrant recruitment of essential membrane proteins and hence disruption of cell wall biosynthesis – an event that ultimately leads to cell death. (43) A later study done by Muller *et al.* found no evidence for altered membrane curvature, but rather for the rearrangement of the fluid lipid domains with the consequent displacement of enzymes crucial for peptidoglycan synthesis, namely the membrane-associated lipid II synthase MurG and the phospholipid synthase PlsX. (44) Most recently undecaprenyl-coupled cell wall precursors have been identified as a specific target of DAP, indicating that membrane

reorganisation is most likely the primary mode of action of this antibiotic, whereas membrane leakage and depolarisation appear not to be essential for its activity. In addition, the authors demonstrated that DAP forms tripartite complex with lipid II and phosphatidylglycerol *in vitro*, what could explain its specificity for bacterial cell wall. (45) In their recent isothermal titration calorimetry study, Kotsogianni *et al.* were not able to detect signal of direct binding of DAP to lipid II, as was observed for lanthipeptide nisin. Nevertheless, they showed that binding of DAP to Ca^{2+} entirely depends on the presence of phospholipids, most notably phosphatidylglycerol. (46)

1.5.2 Teicoplanin

Teicoplanin, initially known as teichomycin A2, is a lipoglycopeptide isolated from actinomycete *Actinoplanes teichomyceticus*, found in a soil sample collected near Nimodi village, Indore (India). (47) It is composed of six closely related glycopeptide components, five of which, known as Teicoplanin-A2, represent 90% of the mixture, whereas the remaining 10% is known as Teicoplanin-A3. (48) Apart from a linear heptapeptide aglycone core, teicoplanin components contain different *N*-acylglucosamine moieties, with a C_{10}- or C_{11}-fatty acid acyl chains. (49) (Figure 3) Similarly to vancomycin, teicoplanin inhibits the synthesis of peptidoglycan. Specifically, it binds to the *D*-Ala-*D*-Ala unit of lipid II through a network of five hydrogen bonds and multiple van der Waals interactions, thereby interfering with both the transglycosylation and the transpeptidation step in the cell wall biosynthesis pathway. (50, 51) The presence of hydrophobic tail is believed to anchor the antibiotic into the bacterial membrane, facilitating interaction between teicoplanin glycopeptide core and its lipid II target. (49, 52) Teicoplanin is currently approved in Europe and other countries as intravenous and intramuscular formulation for the treatment of susceptible Gram-positive infections, including skin infections, endocarditis, complicated urinary tract infections, bone and joint infections, pneumonia, and bacteraemia. (53) Furthermore, oral formulations are available for the treatment of *Clostridium difficile* infection-associated diarrhoea and colitis. (48) Teicoplanin has a long half-life of 100-170 h as it binds extensively to plasma proteins. (54) In contrast to vancomycin, it possesses more favourable toxicity profile. (55)

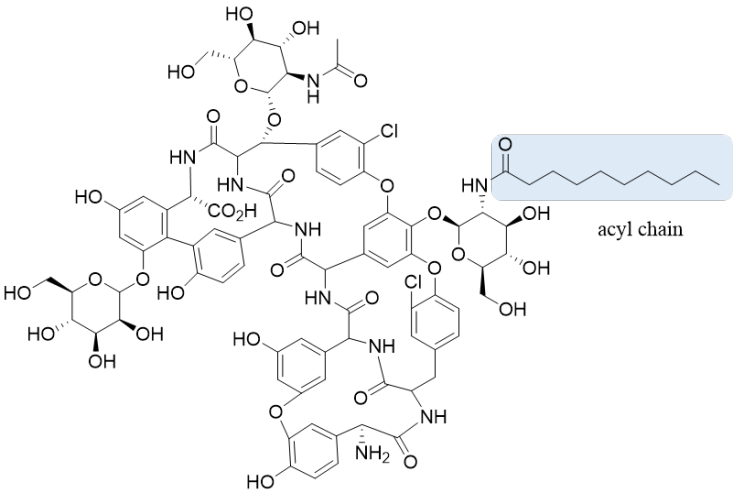

Figure 3. Structure of teicoplanin.

1.5.3 Telavancin, oritavancin and dalbavancin

The increased resistance among Gram-positive bacteria, especially vancomycin resistant strains, has accentuated the need for new antibiotics. The great efforts in this direction led to the clinical approval of three semisynthetic lipoglycopeptides: telavancin, oritavancin and dalbavancin. Similar to vancomycin, they all inhibit cell wall synthesis in Gram-positive bacteria, including MDR strains of staphylococci and enterococci by binding to the carboxyl terminal *D*-alanyl-*D*-alanine residue of the growing peptide chains. (31) However, unlike vancomycin, which is primarily bacteriostatic, these compounds have a rapid bactericidal effect. Their increased binding affinity and thus potency is mostly attributed to the presence of the hydrophobic side chains (as in teicoplanin) and/or the ability of lipoglycopeptide molecules to form dimers, which can stabilise their binding to the cell wall. (52, 56, 57)

Telavancin

The first to be introduced to the clinic in 2009 was Telavancin developed by Theravance, Inc., (South San Francisco, CA) and Astellas Pharma US, Inc., (Deerfield, IL). (58) Its structure is similar to that of vancomycin with two main modifications, a (decylaminoethyl) lipophilic tail on the vancosamine unit, and the presence of a (phosphonomethyl)aminomethyl on the 4′-position of aromatic amino acid 7. (Figure 4) The former modification is thought to be responsible for improved potency against a range of Gram-positive pathogens, whereas the latter provides favourable absorption, distribution, metabolism, and excretion (ADME)

properties. (59, 60) Telavancin was reported to have a dual mode of action. Apart from inhibiting cell wall biosynthesis by binding to the lipid II, it causes concentration-dependent dissipation of cell membrane potential, leading to increased membrane permeability and subsequent leakage of potassium ions and adenosine triphosphate (ATP). (61, 62) Telavancin is indicated for the treatment of complicated skin and skin structure infections, as well as hospital-acquired and ventilator-associated bacterial pneumonia caused by susceptible isolates of *S. aureus* when no alternative treatments are suitable. (63) Due to its poor oral bioavailability, telavancin is administered intravenously. It binds extensively to human plasma proteins (~93%) and has a half-life of approximately 7−9 h. (64, 65)

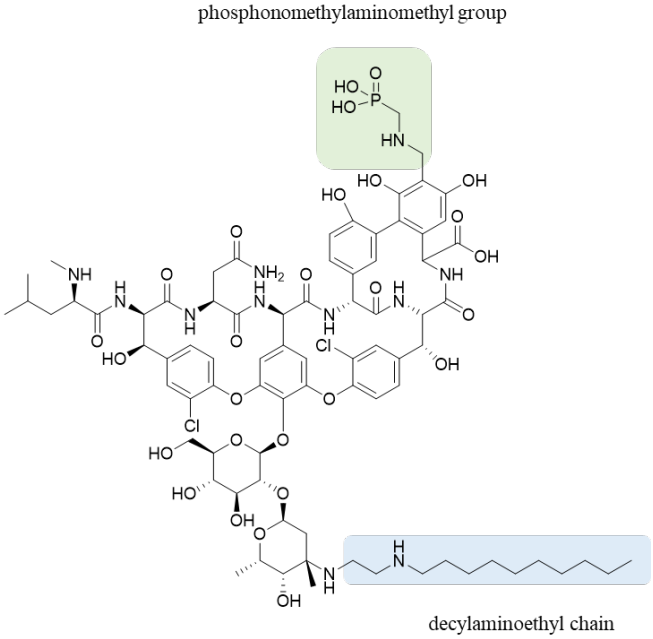

Figure 4. Structure of telavancin.

Oritavancin

Oritavancin (Orbactiv), originally developed by Eli Lilly was approved by the FDA in 2014. (66, 67) It was obtained by modifications of a naturally occurring glycopeptide chloroeremomycin, a fermentation product of a Gram-positive filamentous actinomycete, *Amycolatopsis orientalis*. (31) Although structurally similar to vancomycin, it possesses two 4-epi-vancosamine units and a highly hydrophobic *N*-alkyl-*p*-chlorophenylbenzyl moiety. (Figure 5) These pharmacophores, along with associated alterations in stereochemistry, are believed to largely contribute to the enhanced activity of oritavancin against vancomycin-resistant Gram-positive bacteria. (68) In addition, oritavancin is reported to target different

secondary binding sites on lipid II, such as the pentaglycine in *S. aureus*, and the *D*-aspartate/*D*-asparagine (*D*-Asx) cross-bridge in *Enterococcus faecium*. (69-71) These multiple modes of action enable oritavancin to retain activity (in contrast to telavancin and dalbavancin) against vancomycin-resistant organisms, such as vancomycin-resistant enterococci (VRE) and vancomycin-resistant *S. aureus* (VRSA) with *D*-Ala-*D*-Lac peptidoglycan termini. (69, 71) Oritavancin is indicated for the treatment of acute bacterial skin and skin structure infections. (67, 72) It is administered as a 3h-intravenous infusion and has a high degree of protein binding (approx. 85%) and extensive tissue distribution. (73, 74)

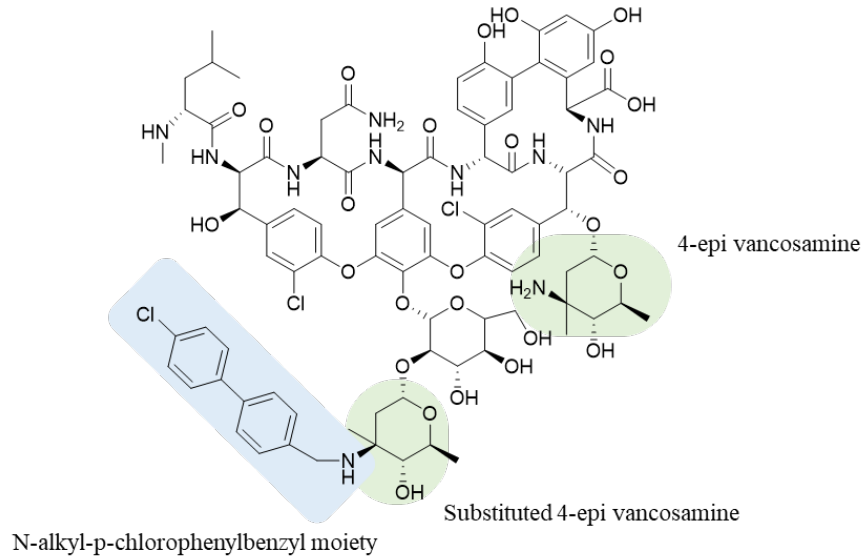

Figure 5. Structure of oritavancin.

Dalbavancin

Dalbavancin is a lipoglycopeptide whose structure and antimicrobial spectrum resembles that of teicoplanin. It is a *N*,*N*-dimethyl-1,3-diaminopropane derivative of the natural compound A40926 factor Bo, initially isolated in 1987 from a *Nonomuraea* species. (75, 76) It is believed that its hydrophobic acyl chain serves as an anchorage point, while the positively charged *C*-terminal dimethylaminopropyl side chain interacts with anionic phospholipid headgroups on bacterial surface. (77) (Figure 6) Unlike oritavancin, dalbavancin is far less active against vancomycin-resistant enterococci (VRE) that possess *vanA* gene (*VanA* type VRE). (74, 78) Apart from its initial indication, namely treatment of acute bacterial skin and skin structure infections in adults, dalbavancin has been successfully used off-label, for the treatment of osteomyelitis, endocarditis and bacteraemia. (79) Similar to other lipoglycopeptides,

dalbavancin is administered intravenously due to its poor oral bioavailability. It has high plasma protein binding (93−98%) and a long half-life allowing for once-weekly administration. (80)

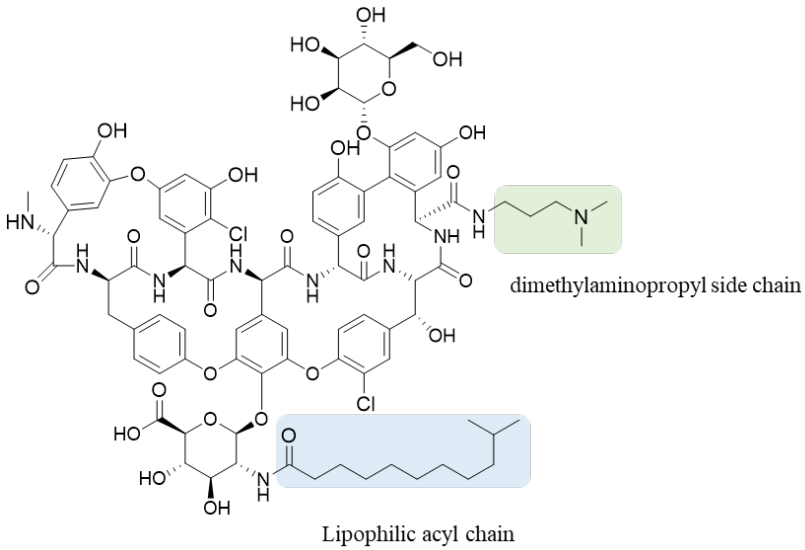

Figure 6. Structure of dalbavancin homolog B0. (Dalbavancin is a mixture of five active homologs).

1.5.4 Bacitracin

Bacitracin is a cyclic, non-ribosomally synthesised polypeptide antibiotic. It was discovered in 1943 in the debrided tissue removed from a compound fracture of the tibia in a 7-year-old girl. (81-83) It is produced by *Bacillus subtilis* and *B. licheniformis*, as a mixture of several closely related dodecapeptides which contain both *L*- and *D*-amino acids, as well as a cyclic ring formed between the ε-amino group of a lysine side chain and the peptide *C*-terminus (*L*-Lys^{6} and *C*-terminal *D*-Asn^{12}). (84, 85) (Figure 7) A major component (60-80%) of the bacitracin congeners, and the most potent one, bacitracin A, contains a thiazoline ring at its *N*-terminus formed by the condensation of Ile^{1} and Cys^{2}. (86-88) Its mechanism of action involves inhibition of dephosphorylation of the undecaprenyl pyrophosphate (UPP), a lipid carrier involved in the transport of oligosaccharide components in the peptidoglycan biosynthesis. (89) By forming a complex with lipid pyrophosphate molecule and divalent metal ions (most readily Zn^{2+}), bacitracin inhibits membrane bound pyrophosphatase, and hence recycling of UPP to undecaprenyl monophosphate. (90, 91) Bacitracin is predominantly active against Gram-positive bacteria and due to its nephrotoxicity, it is commonly used as a topical agent, either alone or in combination with neomycin and polymyxin B. However, it can be administered

intramuscularly for the treatment of infants with pneumonia and empyema caused by susceptible staphylococci strains. (84)

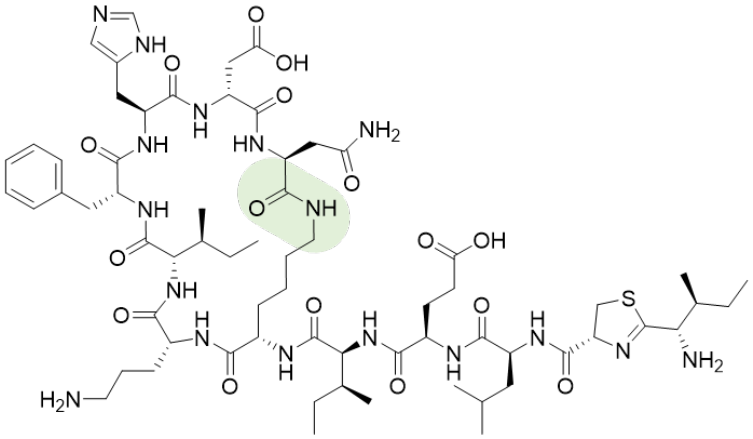

Figure 7. Structure of Bacitracin A.

1.5.5 Polymyxins

The polymyxins are a family of chemically distinct antibiotics independently discovered in 1947 by three different research groups. (92-94) They are produced by the Gram-positive spore-forming soil bacterium *Paenibacillus polymyxa*, previously known as *Bacillus polymyxa*. Synthesised non-ribosomally, these secondary metabolites contain non-proteogenic amino acids, such as *L*-2,4-diaminobutyric acid (*L*-Dab) and various *D*-amino acids. (Figure 8) Apart from the heptapeptide macrocyclic core, additional structural feature includes the presence of the exocyclic tripeptide, which is modified at the *N*-terminus by different, branched or linear, saturated fatty acids of varying length (7-9 carbons). (95)

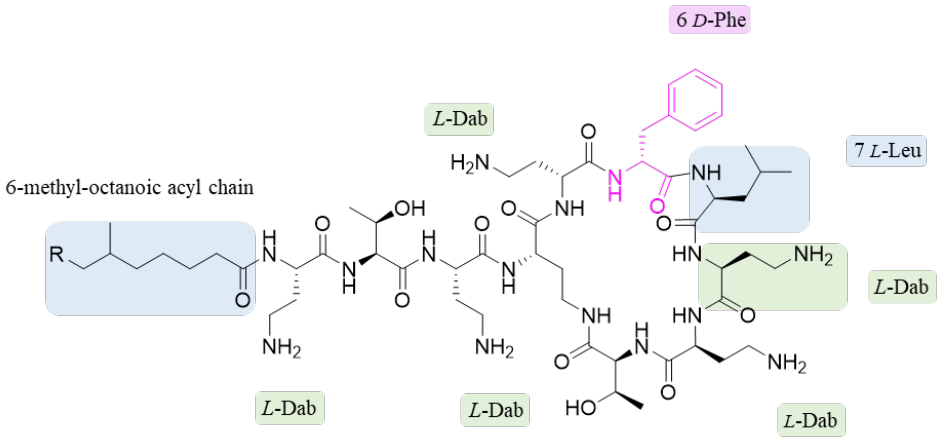

Polymyxin B1: R=CH_3

Polymyxin B2: R=H

Figure 8. Structure of polymyxin B which is a mixture of polymyxins B1 and B2; *L*-Dab: *L*-2,4-diaminobutyric acid.

Polymyxins exert their bactericidal effect by interacting with lipid A of the polyanionic lipopolysaccharides (LPS) present in the outer membrane of Gram-negative bacteria. The subsequent displacement of divalent cations, in particular LPS-bound Mg^{2+} and Ca^{2+} ions, leads to increased bilayer permeability, membrane disruption and cell death. (31, 96) The polymyxins, colistin and polymyxin B, are indicated for the treatment of serious infections caused by aerobic Gram-negative bacteria. (97) However, their use is limited due to their nephro- and neurotoxicity. Colistin is available commercially as colistin sulphate for oral and topical application, and as sulphomethylated derivative, (also known as colistimethate sodium) for parenteral application. Polymyxin B, on the other hand, is only available as polymyxin B sulphate, which is administered parenterally. (98, 99)

1.6 Antimicrobial peptides

1.6.1 Sources and discovery

The discovery of antimicrobial peptides (AMPs) dates back to 1939 when René J. Dubos isolated tyrothricin in the extracts of an unidentified soil-dwelling bacterium of the *Bacillus* genus. (100, 101) The identified compound was reported to consist of two antibiotic substances, tyrocidine and gramicidin. (102, 103) The latter was found to be active against a wide range of Gram-positive bacteria both *in vivo* and *in vitro*. Being highly haemolytic, it was successfully used as a topical agent for the treatment of wounds and ulcers during the Second World War. (104, 105) Similar antibacterial compounds were also identified in eukaryotes. The observation that wheat flower contains substance which is lethal to bread yeast was reported as early as 1895. (106) The active substance, later designated purothionin, was isolated from wheat (*Triticum aestivum*) endosperm in 1942. (107) Many studies conducted in the following decades (mainly in the 1950s and 1960s) were crucial as they marked the beginning of antimicrobial peptide research. The first such study reported on discovery of "basic bactericidal proteins" in lysosomes of the polymorphonuclear leukocytes. These substances, later named defensins, were first identified in rabbit and guinea-pig neutrophils, and much later in rabbit alveolar macrophages and human neutrophils. (108-114) The presence of AMPs in invertebrates was confirmed by the research work carried out in the 1980s by the Boman group. The landmark study involved the discovery of two AMPs, termed cecropins A and B, isolated from the hemolymph of immunised pupae of the giant silk moth *Hyalophora cecropia.* (115) Cecropins were found to have a potent antimicrobial activity against *Escherichia coli,* and moderate against *Enterobacter cloacae* and *Pseudomonas aeruginosa*. Further analysis demonstrated their basic, amphiphilic character. (116)

In the decades that followed, a large number of AMPs have been discovered in the skin secretions of amphibians, with the first study dating back to 1970, when Csordas *at al.* reported on bombinin, a haemolytic 24-residue peptide from skin secretion of the European Bombina species. (117-119) Shortly after, two peptides, bombesin and alytesin, derived from the skin of the European amphibians of the family *Discoglossidae* were isolated and characterised by Anastasi *et al*. (120) However, it was not until the discovery of magainins, extracted from the skin of the African clawed frog *Xenopus laevis*, that this new research avenue started attracting much wider scientific interest. (121) Since then AMPs have been discovered in diverse species

of fungi (peptaibols), plants (thionins, defensins, cyclotides), and animals (cathelicidin, brevinin). (122-124) (Figure 9)

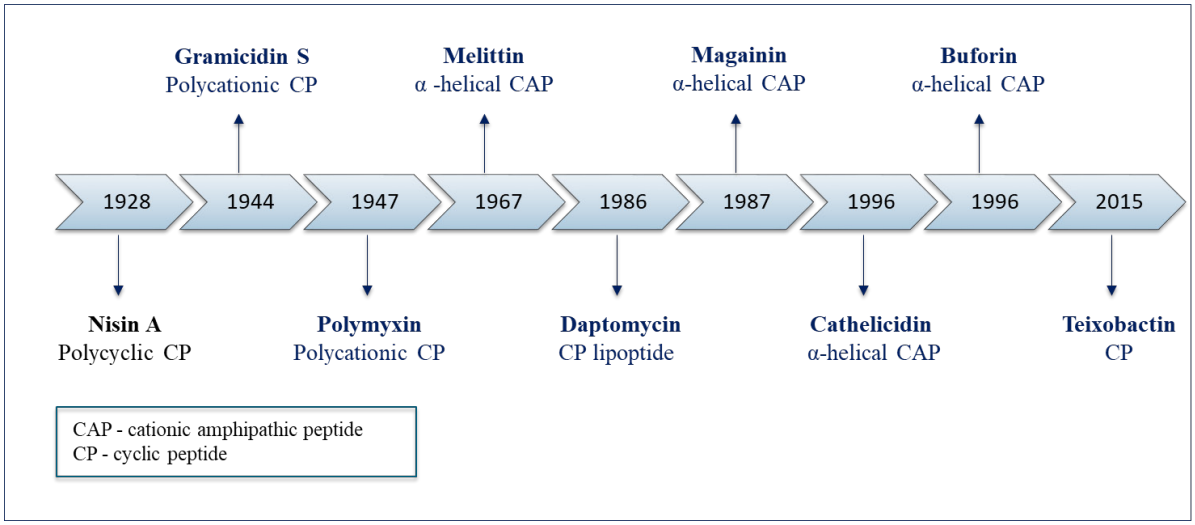

Figure 9. Representative examples of antimicrobial peptides and their discovery. (125)

1.6.2 AMPs biosynthesis

According to their biosynthetic pathway, AMPs can be grouped into two classes, non-ribosomally and ribosomally synthesised peptides. The biosynthesis of the former class, which includes many of the antibiotics in clinical use today (*e.g.*, gramicidins, polymyxins, bacitracins and glycopeptides), are performed by multimodular peptide synthetases, resulting in products with great chemical diversity. This diversity is reflected in the presence of unique structural features, such as hydroxy-, *D*-, or non-proteinogenic amino acids, which can be further modified by acylation, glycosylation, *N*-methylation, or heterocyclic ring formation. (126) Non-ribosomally synthesised peptides are mostly produced by members of the Gram-positive Actinomycetes and Bacilli genera, filamentous fungi and marine microorganisms. (127, 128)

In contrast, ribosomally synthesised AMPs are found in all kingdoms of life. Nearly all of them are initially synthesised as a longer precursor peptides, typically 20 – 110 residues in length. (129) They can be extensively post-translationally modified: their side chains may be altered through dehydration and heterocyclisation of Ser and Thr, lanthionine- and disulphide-bond formation and prenylation. In addition, structural changes of the peptide backbone often seen in this class of AMPs are mediated by macrocyclisation, formylation and formation of lactone rings. (130) Some of the examples of gene-encoded AMPs include lasso peptides,

cyanobactins from cyanobacteria, microcins from enterobacteria, conopeptides from molluscs, cyclotides from plants, and the fungal amanitins and phallacidins. (129, 131-135)

1.6.3 AMPs secondary structure

AMPs are an important component of the innate immune system found in all species of life, with broad-spectrum activity against bacteria fungi, protozoa and viruses. They are typically composed of fewer than 100 amino acids, and although highly diverse, they share some common features: they are mostly cationic, hydrophobic and amphiphilic. (136)

AMPs are commonly divided into four major classes based on their secondary structure:

1. linear α-helical peptides
2. β-sheet peptides, often stabilised with one or more disulphide bonds
3. non-αβ peptides (known as extended structures, typically rich in one particular amino acid, such as Gly, Pro, Arg, Trp, or His)
4. αβ-peptides having both α-helix and β-sheet structures, and
5. cyclic, unusual or complex peptide topologies. (137-139) (Table 1) (Figure 10)

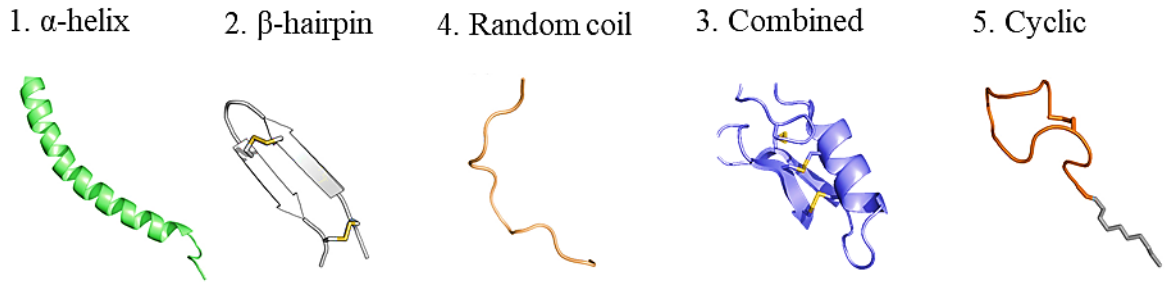

Figure 10. Examples of peptide structural classes. 1. α-helix, represented by LL-37 (PDB ID: 2K6O), 2. β-hairpin, represented by tachyplesin I (PDB ID: 2RTV) with disulphide bonds shown in yellow, 3. random coil, represented by indolicidin (PDB ID: 1G89), 3. combined α-helix and β-sheet elements, represented by plectasin (PDB ID: 3E7U) with disulphide bonds in yellow, and 5. a cyclic lipopeptide with lipid tail (in grey), represented by daptomycin (PDB ID: 1T5M). (Adapted with permission from ref. 140)

Linear α-helical AMPs

Helical peptides are most abundant and widely studied group of AMPs. (141) They are predominantly found in frogs, insects, and mammals. Some of the examples include frog magainins, the honeybee-venom component melittin and insect cecropins, and the mammalian cathelicidins. (121, 142-145) Most of these peptides are cysteine-free, linear and unstructured in solution. However, upon interaction with target membranes they assume amphipathic structure, which seems to be necessary for their interaction with bacterial membrane. (146, 147)

The cationic β-sheet AMPs

Peptides belonging to this group are typically 16-40 residues in length. (148) They contain one or more disulphide bonds, which play an important role in further structure stabilisation. Based on cysteine content and structural characteristics, they can be grouped into:

1. β-hairpin peptides, and
2. vertebrate defensins. (139, 149)

Some of the examples of β-hairpin peptides include bactenecin from bovine neutrophils (stabilised by one disulphide bridge), tachyplesin I from horseshoe crab hemocytes (containing two Cys-Cys bridges) and hepcidin from human hepatocytes (stabilised by four disulphide bridges). (150-154) (Figure 10, Figure 11) This group of peptides is often rich in Ala, Leu, Gly, and Lys residues. (149, 155)

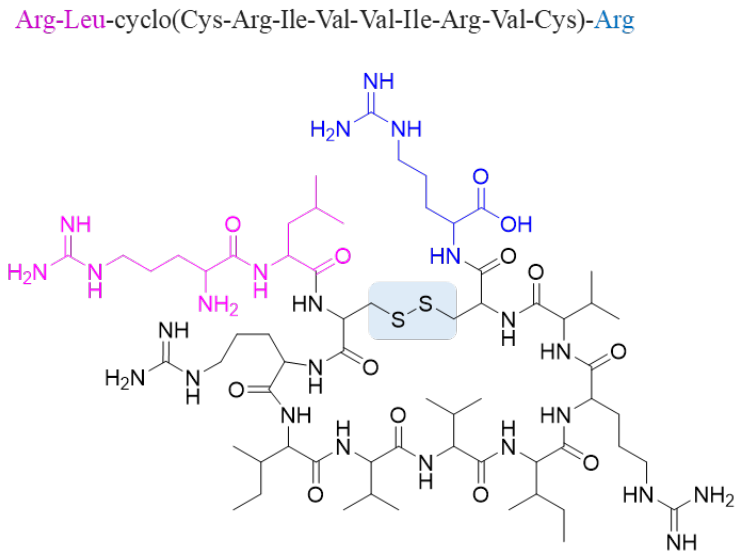

Figure 11. Structure of a β-hairpin peptide Bactenecin.

Vertebrate defensins are diverse members of a large family of AMPs expressed predominantly in leukocytes and epithelial cells. (156) They are classified into three subfamilies, the α-, β- and θ-defensins based primarily on the spacing between the cysteine residues and the topology of the disulphide bridges. (157) They are cationic, with a triple-stranded β-sheet conformation stabilised by three intramolecular disulphide bonds. (158, 159) θ-defensins, which were isolated from the rhesus monkey leukocytes, are the only known fully cyclic peptides of animal origin. (160, 161)

Non-α/β-containing AMPs

Non-αβ AMPs are also called extended or loop peptides. (155) Although they do not adopt any particular secondary structure while in solution or upon contact with membranes, they can be classified based on the most abundant amino acid in their sequence, typically glycine, proline, tryptophan or histidine. (137, 139) Examples include tryptophan-rich peptide indolicidin from cattle, histatins (small histidine-rich salivary polypeptides), drosocin from *Drosophila* and the mammalian PR-39 which adopts a polyproline II helix conformation. (162-166)

Peptides with α- and β-structural elements

Two prominent examples of this class of peptides are defensins, isolated from plants and some invertebrates, such as insect defensin A (phormicin) from the larvae of the flesh fly *Phormia terranovae*, and the plant defensin NaD1, antifungal and insecticidal peptide isolated from the flowers of *Nicotiana alata*. (167-169) (Figure 12, Figure 13) They both contain a conserved structural αβ-motif, consisting of an α-helix which is connected via disulphide bonds to a triple-stranded antiparallel β-sheet. (167) This group of AMPs belongs to the so-called *cis*-defensins, where disulphide (S-S) bonds are pointing in the same direction and are bound to the same α-helix. In contrast, human β-defensins have *N*-terminal α-helix and disulphides from the final β-strand that point in opposite directions. (167, 170)

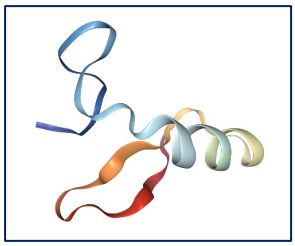

Figure 12. Insect defensin A is a basic 4 kDa protein secreted by *Phormia terranovae* larvae in response to bacterial challenges or injuries. (https://www.rcsb.org/3d-view/ngl/1ICA)

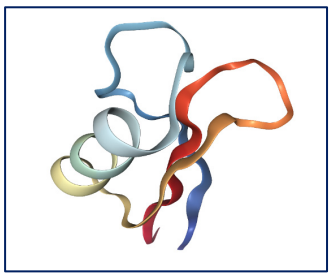

Figure 13. Solution structure of NaD1 from *Nicotiana alata*. (https://www.rcsb.org/3d-view/ngl/1mr4)

Cyclic, Unusual or Complex Peptide Topologies

AMPs belonging to this highly diverse class may be further classified based on their cyclisation pattern (*e.g.*, 'head-to-tail' or 'head-to-side chain') and/or the presence of distinct cross-links such as, disulphide or thioether bridges. (139) Examples of backbone-cyclised peptides include cyclic bacteriocins (Enterocin AS-48, Amylocyclin A) and plant cyclotides (Kalata b1). (171-173) They are both ribosomally synthesised and remarkably stable compared to their linear counterparts. (174, 175) Cyclotides, in contrast to bacteriocins, have an additional feature, a structural motif known as cyclic cystine knot (CCK), which comprises a cyclic backbone cross-braced with three disulphide bridges. (176) (Figure 14) Many AMPs in this class undergo extensive post-translational modifications, which add further to their structural diversity. Lanthipeptides, for example, are characterised by the presence of the thioether cross-linked amino acids (2S, 6R)-lanthionine (Lan) or (2S, 3S, 6R)-3-methyllanthionine (MeLan). (177) A prototypical lanthipeptide is Nisin A which, apart from five lanthionine rings, contains two unnatural (non-canonical) amino acid residues, dehydrobutyrine and dehydroalanine. (178) Some interesting structural features of this class of AMPs also include threaded-loop topologies (lasso peptides), cysteine sulphur to α-carbon bonds (the sactibiotic subclass of bacteriocins, subtilosin A) and glycosylation of cysteine residues (glycocins). (179-182)

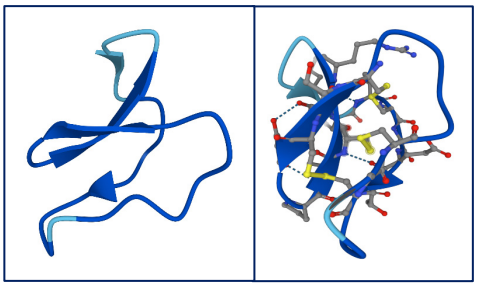

Figure 14. Structure of Kalata S from *Oldenlandia affinis.* Disulphide bridges are presented as yellow bonds. (https://alphafold.ebi.ac.uk/entry/P58458)

Table 1. Classes of antimicrobial peptides based on their secondary structure. (Adapted from ref. 342 and ref. 124.)

Secondary structure	Peptide	Predominant amino acid	Source
α-helical peptides	Melittin		Bees
	Buforin		Toad
	Cathelicidins		
	LL-37 [a]		Humans
	Magainins		Frogs
	Cecropin		Insects
β-sheet peptides	Cathelicidins		
	Protegrin	Cysteine	Pigs
	Bactenecin	Cysteine and Arginine	Bovine
	Defensins		
	α-defensins	Cysteine	Mammals
	β-defensins	Cysteine	Mammals
	θ-defensins	Cysteine	Rhesus macaque, Baboons
	Tachyplesins		Horseshoe crab
Non-α/β-containing AMPs	Indolicidin	Tryptophane	Cattle
	Histatins	Histidine	Mammals
	Apidaecins	Proline	Honeybee
	Drosocin	Proline	*Drosophila melanogaster*
	PR-39	Proline and arginine	
Peptides with α- and β-structural elements	Insect defensin A-phormicin		*Phormia terranovae*
	Plant defensin NaD1		*Nicotiana alata*
Cyclic, unusual or complex peptide topologies	Cyclic bacteriocins		Bacteria
	Lanthipeptides-Nisin A		*Lactococcus lactis*
	Glycocins		Diverse, genome mining
	Subtilosin A		*Bacillus subtilis* 168
	Lasso peptides-Microcin J25		
	Cyclotides	Cysteine	Plants

[a]The only cathelicidin-derived antimicrobial peptide found in humans. (183)

1.6.4 Molecular targets and mechanisms of action

Membrane Targeting AMPs

AMPs exert their effect by either permeabilising the cell membrane or translocating across the membrane to reach their intracellular targets. (184) The basis for selectivity of AMPs is thought to arise from the different charges of bacterial and mammalian membranes. Namely, human cell membranes have a neutral net charge as they are rich in zwitterionic phospholipids, such as phosphatidylethanolamine, phosphatidylcholine and sphingomyelin. In contrast to human cell membrane, bacterial membranes are rich in negatively charged phospholipids, such as phosphatidylserine, phosphatidylglycerol, and cardiolipin, which are stabilised by divalent cations (*e.g.*, Mg^{2+} and Ca^{2+}). (185) (Figure 15)

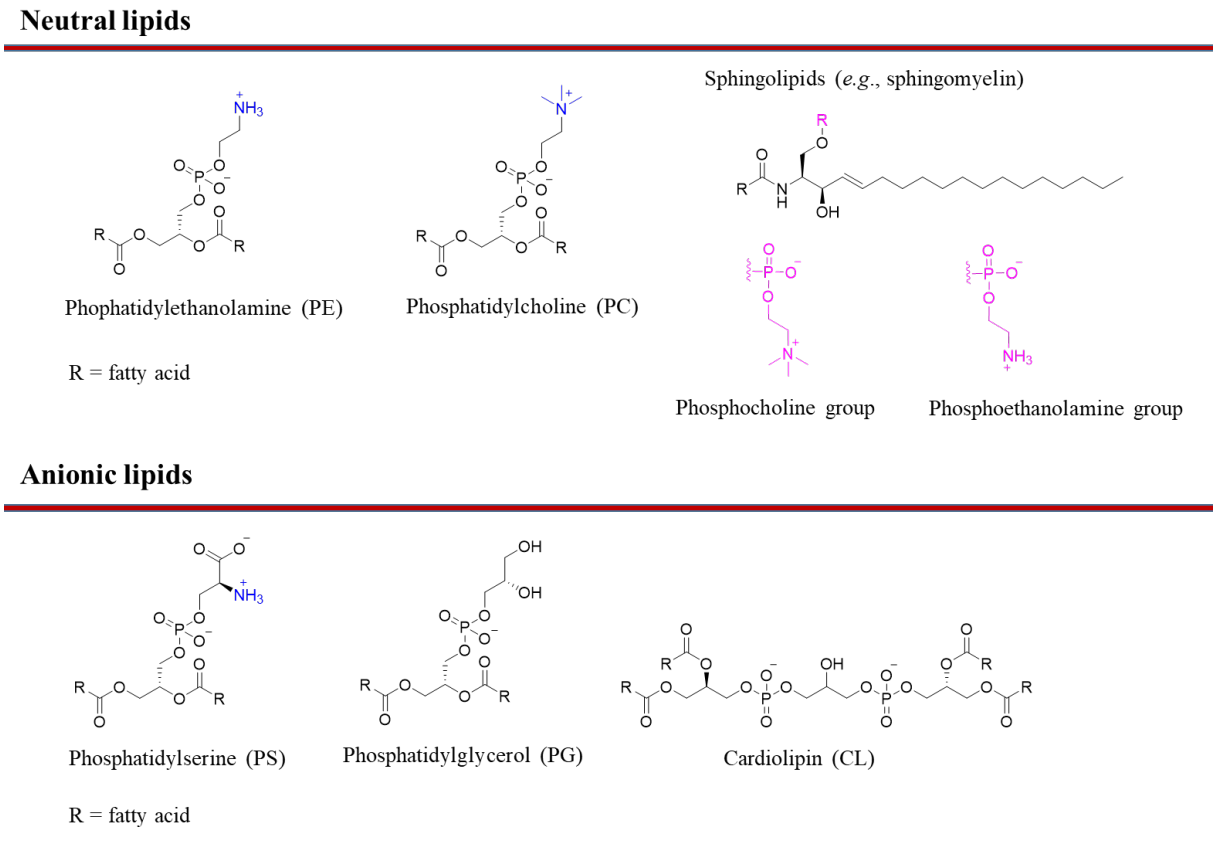

Figure 15. Neutral and anionic phospholipids present in membranes of eukaryotic and bacterial cells, respectively.

Apart from the above-mentioned difference between bacterial and human cell membrane, there is also an important intrinsic difference between Gram-positive and Gram-negative bacteria. The cell wall of Gram-positive bacteria consists of a single lipid membrane and a

thick, outer layer of peptidoglycan and lipoteichoic acids (LTAs). The peptidoglycan layer is usually densely functionalised with anionic glycopolymers called wall teichoic acids (WTAs). (186, 187) (Figure 16)

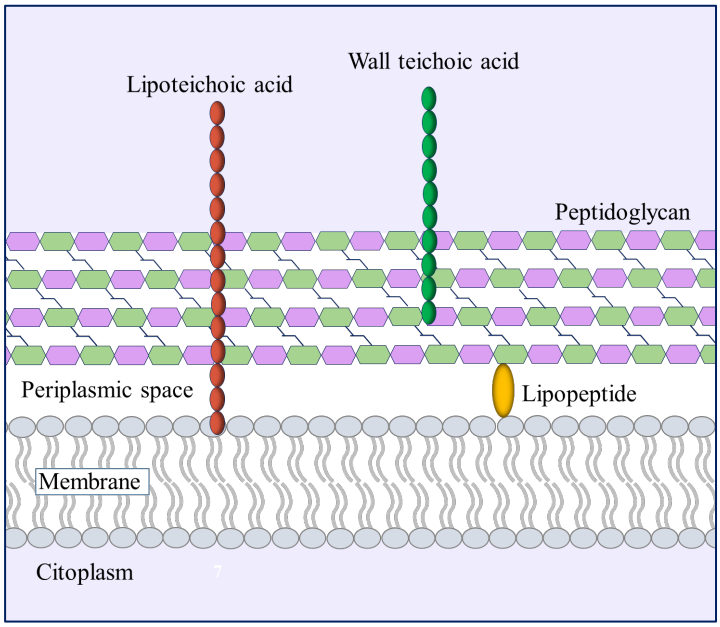

Figure 16. Composition of the cell wall of Gram-positive bacteria. (Adapted with permission from ref. 187-189)

Peptidoglycan-attached WTAs are usually formed by glycerol or ribitol groups that are connected by phosphodiester bonds, whereas the membrane-anchored LTAs are usually formed by glycerol-phosphate repeating units, which are connected to glycolipids. (190) (Figure 17)

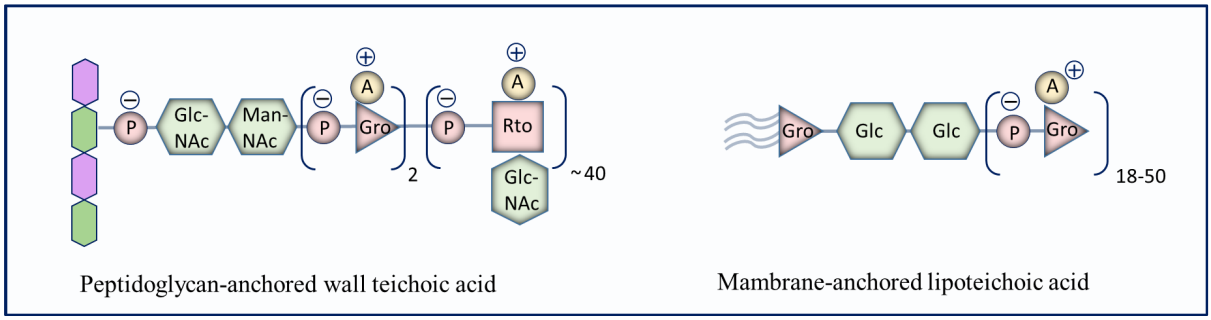

Figure 17. Schematic structures of cell-wall glycopolymers in *S. aureus*. Non-glycosyl residues: A, *D*-alanine; P, phosphate. Glycosyl residues: GlcNAc, *N*-acetylglucosamine; Glc, glucose; Gro, glycerol; ManNAc, *N*-acetylmannosamine; Rto, ribitol. (Adapted with permission from ref. 190)

In contrast to Gram-positive bacteria, the cell wall of Gram-negative bacteria contains a thin peptidoglycan layer within a periplasmic space and additional outer membrane. The outer leaflet of the outer membrane is composed of lipopolysaccharides, which are organised into

three distinct regions: the membrane-anchored lipid A, the phosphorylated, non-repetitive core oligosaccharide (inner and outer core) and the O-antigen (O polysaccharide). (187-189) (Figure 18)

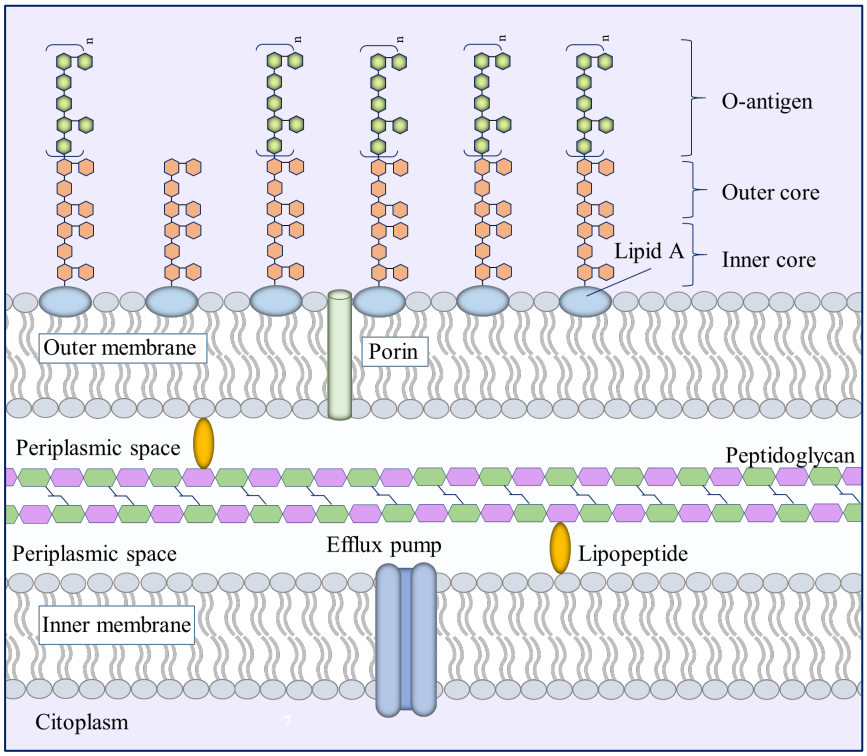

Figure 18. Composition of the cell wall of Gram-negative bacteria. (Adapted with permission from ref. 187-189.)

Mechanisms of action

Most AMPs interact with negatively charged bacterial membrane causing disruption to the lipid bilayer. (191) Three main mechanisms have been proposed to describe the action of antimicrobial peptides once they bind the membrane: the barrel-stave, the toroidal pore, and the carpet-like model. (192) (Figure 19)

In **the barrel-stave model**, first postulated by Baumann and Mueller, peptides aggregate to form a barrel-like ring around an aqueous pore. (193) The amphipathic character of AMPs plays an important role in this mechanism, since the hydrophilic residues form the inner lining of the pore while the hydrophobic face of the ring interacts with the lipid acyl chains of the membrane. (184) To date, only a few AMPs, alamethicin and possibly pardaxin, are thought to act via the barrel-stave model. (194-196)

In the **toroidal-pore model**, the peptides only interact with the headgroups of the membrane lipids, thereby inducing a positive curvature strain, resulting in the formation of the pores. (197-

199) The lining of these pores contains both, the inserted peptide molecules and polar lipid headgroups. The peptides, unlike those which mechanism of action could be described by the barrel-stave model, are always in contact with the polar headgroups even after their insertion into the lipid bilayer. (200) This model explains the activity of a number of AMPs, such as magainin 2, aurein 2.2, protegrins, melittin and pleurocidin. (199, 201-204)

In the **carpet-like model** (detergent-like model), first proposed for the action of dermaseptin S, disruption of the membrane occurs in a dispersive-like manner rather than by formation of the stable pores, as observed with previous two mechanisms. (205) In this model, AMPs interact with anionic phospholipid headgroups at various points, covering the bilayer surface in a carpet-like manner. At certain peptide-to-lipid ratio, the membranes lose their integrity and eventually disintegrate via micelle formation. (206) Interactions with the membrane of a short peptide aurein 1.2, which is expressed in the skin secretions of various species of the *Litoria* genus of Australian frogs, are consistent with this model. (207)

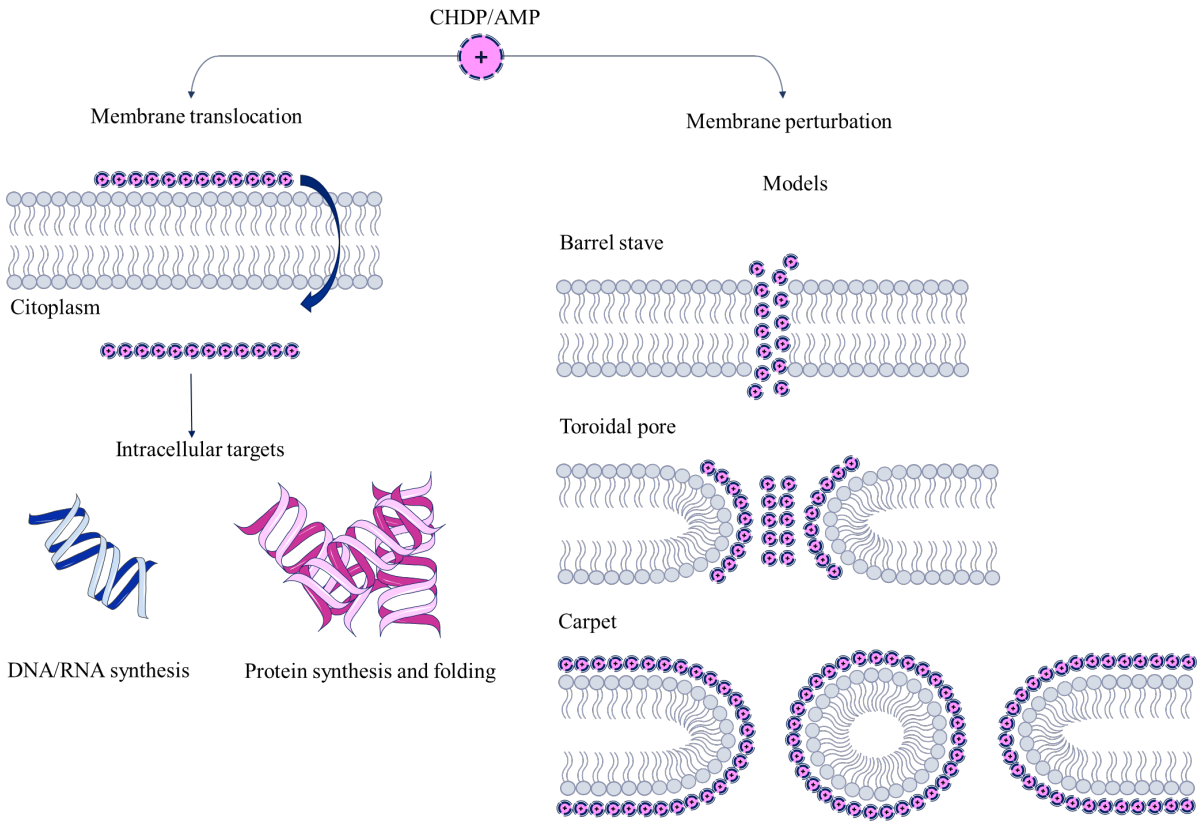

Figure 19. Models of antibacterial mechanisms of cationic host defense peptides (CHDP)/AMPs. Short cationic and/or amphipathic peptides, known as cell-penetrating peptides cross biological membranes and localise to specific intracellular compartments, whereas the majority of AMPs cause membrane perturbation and subsequent lysis of the bacterial cell. (Adapted with permission from ref. 192.)

While the three aforementioned mechanisms are still the most frequently proposed, a number of models, some of which share common features with those described, have been also used to explain the modes of action of various AMPs. Examples include aggregate model, the leaky slit model (Plantaricin A and Bacteriocin AS-48), electroporation (NK-lysin), and sinking raft model. (126, 208-212).

Non-Membrane Targeting/Intracellular AMPs

While many antimicrobial peptides kill bacteria through some type of membrane disruption, an increasing number appear to penetrate the cell membrane without causing substantial membrane permeabilisation. (213) These AMPs can bind directly to cellular components (RNA, DNA) and thus interfere with essential biological processes, such as replication, transcription and translation. (184)

Buforin II, a linear amphipathic α-helical peptide, has been shown to cause a rapid cell death of *E.coli* by inhibiting cellular functions via DNA- and RNA-binding. (214) Similarly, cathelicidin PR-39 and indolicidin were found to inhibit DNA synthesis in *E.coli*. (215-217) The cyclic lasso peptide, microcin J25, in addition to being membranolytic, as shown in *Salmonella newport*, inhibits transcription by binding to the β' subunit of the bacterial RNA polymerase. (218, 219)

Many AMPs interfere with protein synthesis by interacting with ribosomal machinery or subsequent chaperone-assisted folding of proteins. Proline-rich antimicrobial peptide, Onc112 has been found to inhibit protein synthesis by simultaneously blocking the peptidyl transferase centre and the peptide-exit tunnel of the ribosome. (220) In contrast to Onc112, which arrests translation at the start codon, a derivative of the insect-produced antimicrobial peptide apidaecin, Api137 arrests translation at a stop codon before polypeptide release. (221-223) Furthermore, the insect-derived proline-rich peptides, drosocin and pyrrhocoricin induce permanent closure of the DnaK peptide-binding cavity resulting in aberrant protein folding. (224) AMPs can also act on various biocellular pathways. Recently, using an *E. coli* proteome microarray, Ho *et al.* have shown that bovine lactoferricin (LfcinB) and a proline and arginine rich cathelicidin, PR-39, target lipopolysaccharide biosynthesis while purine metabolism emerged as a target for both Bac7 and LfcinB. (225)

Other examples of AMPs and their respective intracellular mechanism of action include cysteine-rich peptide, eNAP-2, which selectively inhibits microbial serine proteases, and nisin,

a polycyclic peptide, which binds to the peptidoglycan precursor Lipid II, and thereby interferes with cell wall biosynthesis. (226-228) The latter mechanism was also observed in human β-defensin (hBD3) and copsin (from basidiomycete *Coprinopsis cinerea*). (229, 230) The lanthipeptide mersacidin, however, inhibits the cell wall synthesis at the transglycosylation step. (231)

Oncolytic AMPs

Many AMPs exhibit selective cytotoxicity against tumour cells. This selectivity is believed to predominantly stem from the differences in surface-charge between tumour and normal cells. Tumour cell surface tends to be more anionic due to the presence of the negatively charged phosphatidylserines, which are exposed on the outer leaflet of the cancer cell membrane during malignant transformation. (232, 233) In contrast, membrane of non-cancerous cell is neutral, composed mainly of zwitterionic phosphatidylcholine and sphingomyelin. (234)

Oncolytic AMPs are shown to exert their activity by three following mechanisms: lysis of the cell membrane, mitochondrial membrane disruption, or via various non-membranolytic modes of action. (235) Examples of peptides with anti-tumour activity are found both among α-helical peptides (LL-37 and magainin II) and those having β-sheet secondary structure (defensins, lactoferricin and tachyplesins). (236-240)

1.6.5 AMPs determinants of action

Structure-activity relationship (SAR) approaches have become a useful tool for elucidating determinants of action of AMPs. To date, a great number of studies have demonstrated the correlation between biological activity of AMPs and their specific physicochemical and structural properties, such as length, net charge, primary and secondary structure, hydrophobicity and amphipathicity. (141) (Figure 20)

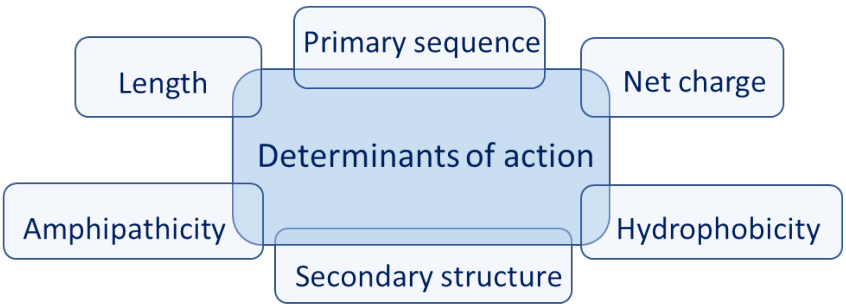

Figure 20. Determinants of action of AMPs.

The majority of AMPs have an overall positive charge at physiological pH (+2 to +9), most often conferred by cationic amino acids, Arg and Lys. (241) This charge is an important selectivity determinant, as cationic AMPs specifically target negatively charged bacterial membrane, as opposed to mainly neutral zwitterionic membrane of the eukaryotic cell. (242, 243) Similarly, antifungal properties of AMPs, at least in terms of initial interaction, may be attributed to the overall negative charge of the fungal cell surface, most likely due to the presence of phosphorylated mannosyl side chains. (244)

Many studies have reported on the positive correlation between charge and antimicrobial activity. (245) However, the potential of peptide charge to modulate membrane activity is limited, indicating that other factors need to be considered when optimising properties of AMPs. (246) One such factor is hydrophobicity, defined as a percentage of hydrophobic amino acids in a given sequence. (247) Apart from positively charged amino acids, AMPs sequence include typically ~50 % of hydrophobic residues, such as Phe, Trp, Tyr, Leu. These residues are essential as they facilitate hydrophobic interactions and subsequent partitioning of the peptide into the membrane layer. (248) Apart from hydrophobicity, distribution of residues is yet another important parameter, which has been shown to affect peptide properties. (249, 250) For instance, for the interfacial binding, the helical amphipathicity was found to have a much greater role than simple hydrophobicity. (251) Furthermore, changing the degree of amphipathicity in a peptide sequence could also be used to fine-tune properties of AMPs. (249)

1.6.6 Anionic AMPs

While majority of known antimicrobial peptides are cationic, a small number, consisting of short Asp-rich sequences, have a net negative charge ranging from –1 to –8. (252) These, so called anionic AMPs, are an important part of the innate immune system of prokaryotes and eukaryotes (vertebrates, invertebrates and plants). They are found to be active against various microorganisms and cancer cells. (253) In some instances, the formation of salt bridges between anionic AMPs and metal ions is necessary for their biological activity. However, for some peptides interaction with membranes occurs independently of cationic metal ions, probably via their association with positively charged components of the microbial membrane, such as cationic lipids and the ammonium moiety of phospatidylethanolamine. (254) Prominent examples of anionic AMPs include human dermcidin and amphibian maximin H5. (255, 256)

1.6.7 Resistance to AMPs

Bacteria resist the action of human AMPs by five main molecular mechanisms:

a) secretion of proteases
b) protein mediated sequestration
c) alterations in the target structures (cell surface/membrane)
d) extrusion via efflux systems, and
e) antimicrobial peptide sensing systems. (257-259)

a) Extracellular proteins

Secretion of extracellular proteins (*e.g.*, proteases) has been implicated in the virulence of many pathogenic bacterial species. (260) Some of the examples of AMP degrading proteases in staphylococci include metalloprotease aureolysin and glutamyl endopeptidase V8, both of which are found to degrade linear cationic AMPs (*e.g.*, human cathelicidin LL-37) to a varying extent. (261) SepA (or SepP1) is a metalloprotease secreted by *S. epidermidis* that can cleave and inactivate dermcidin, an anionic AMP constitutively expressed in human sweat glands. (262) Another example include SpeB, a Gram-positive cysteine protease, which is secreted by the pathogenic bacterium *Streptococcus pyogenes*. (263) Due to its broad substrate specificity, it cleaves not only host proteins, but also AMPs, such as LL-37. (264, 265) During infection, surface bound complexes between a major proteinase inhibitor of human plasma α2-macroglobulin (α2M) and SpeB are formed. This complex formation is mediated by the surface protein called G-related α2M-binding protein (GRAB). (266) SpeB, being entrapped on the bacterial surface is unable to cleave bacterial membrane proteins, although its proteolytic activity is conserved against smaller substrates, such as AMPs. (267) Apart from cleaving LL-37, SpeB degrades proteoglycans, thereby releasing dermatan sulphate, which can bind and inactivate human α-defensin HNP-1. (268) Although proteoglycan shedding is one of the responses normally seen during tissue injury, enhanced proteoglycan degradation, in particular Syndecan-1 shedding, can be induced via virulence factor LasA secreted by *P. aeruginosa* during infection. Shed Syndecan-1 ectodomains can bind to Arg and Pro reach AMPs preventing them from interacting with bacterial cells. (269)

b) Protein-mediated sequestration

Protein-mediated sequestration is another extracellular mechanism of resistance to AMPs. (257) Some Gram-positive bacteria produce surface-linked or extracellular proteins that bind to AMPs, and thus prevent them from reaching their targets. Although mechanisms of protein-mediated AMP sequestration vary considerably, in this section only a few examples will be discussed. Streptococcal inhibitor of complement (SIC) secreted by *S. pyogenes* is a hydrophilic protein which binds to and consequently inactivates several AMPs: complement C5b67, lysozyme, secretory leukocyte proteinase inhibitor, human catelicidin LL-37 and α-defensins. (270-272) Another example is Staphylokinase (SAK), a 136 amino acid long bacteriophage-encoded plasminogen activator, which is expressed by lysogenic strains of *S. aureus.* (273) It binds to mouse cathelicidin *in vitro* thereby promoting SAK-dependent fibrinolysis during the early stage of *S. aureus* airway infection. (274) In addition, SAK directly binds to human neutrophil peptides (HNP-1 and 2), causing almost complete inhibition of their bactericidal effect. (275)

Cell-surface proteins, such as the M1 protein of *S. pyogenes* and the pilus subunit, PilB of *Streptococcus agalactiae,* bind AMPs, thereby preventing their contact to cell-specific targets. M1 protein is recognised as a critical virulence factor in Group A *Streptococcus* (GAS) pathogenesis. Despite its ability to induce the formation of neutrophil extracellular traps (NETs), where pathogens are eliminated upon entrapment, M-protein was also found to promote GAS survival by inhibiting cathelicidin present in the NETs. (276) This effect is mediated by the extracellular, hypervariable *N*-terminal segment of the M-protein. (277, 278) Like the M proteins in *S. pyogenes*, pili identified in Group B *Streptococcus* (GBS) also contribute to systemic virulence. (279, 280) Pili (fimbriae) are non-flagellar polymeric organelles, which have long been recognised as mediators of initial host-pathogen interactions. (281, 282) They are expressed on the cell surface of many Gram-positive bacteria, including *S. agalactiae.* (283) The major pilus subunit protein, PilB was found to promote resistance to murine cathelicidin *in vitro*, most likely via binding/sequestering the defence molecule before it can reach its cell membrane target. In addition, the PilB deficient GBS strain was shown to be more susceptible to phagocytic killing by macrophages and neutrophils, resulting in attenuation of virulence. (280)

Another group of membrane-associated AMP resistance proteins are LanI immunity proteins, identified in some lantibiotic-producing strains. LanI-type immunity proteins are lipoproteins that anchor to the bacterial cell surface and confer resistance by either binding

directly to AMPs or outcompeting AMPs by interacting with cellular target. (284) In this way they prevent toxicity of bacterial own lantibiotics, often working in concert with the specific transporters (lanFEG) involved in transport of toxic peptides to the extracellular space. (285) The most studied examples of the transporter-associated LanI proteins are the SpaI and NisI lipoproteins, produced by *Lactococcus lactis* and *B. subtilis*, respectively. (286-288) Mechanisms of resistance of Gram-positive bacteria is presented in Figure 21.

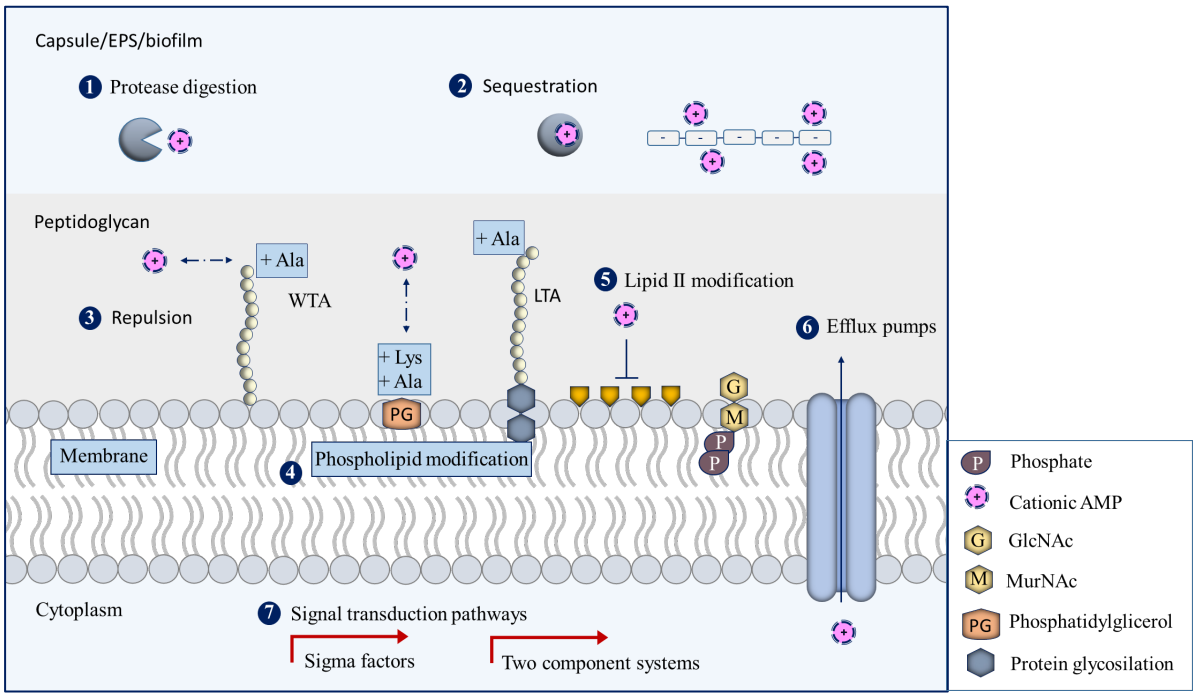

Figure 21. Mechanisms of resistance to cationic AMPs in Gram-positive bacteria. EPS–exopolysaccharides; WTA–wall teichoic acid; LTA–lipoteichoic acid; GlcNAc–N-acetylglucosamine; MurNAc–N-acetylmuramic acid. (Adapted with permission from ref. 192.)

Bacterial extracellular polysaccharides are structurally diverse polymeric compounds classified into two distinct groups: capsular polysaccharides (CPS) and exopolysaccharides (EPS). While CPS are covalently bound to the cell surface, EPS are weakly attached to the cell wall and often sloughed off to form slime. (289) These compounds are thought to form a physical barrier, which favours evasion from the host immune defences by shielding the bacterial cell surface. Moreover, when anionic, they can bind positively charged species (*e.g.*, cationic AMPs), thereby reducing the amount of peptides reaching its target. (290, 291) The production of exopolysaccharide intercellular adhesin (PIA) in *S. epidermidis* has been shown to mediate protection against polymorphonuclear leukocyte phagocytosis, partly due to enhanced electrostatic repulsion to cationic AMPs, such as LL-37 and human β-defensin-3

(HBD-3). (292, 293) In most instances, exopolysaccharide capsules protect bacteria from the effects of AMPs, although with some exceptions. For example, it has been shown that encapsulated pneumococci are efficiently killed by α-defensins, such as human neutrophil proteins 1 to 3 (HNP1-3) at physiological concentrations, whereas non-encapsulated pneumococci were less sensitive to α-defensins. (294-296) This, rather unexpected finding is thought to be due to specific surface charge modification in non-virulent strain, such as introduction of positively charged *D*-alanylation of surface-exposed lipoteichoic acids, which is masked by the presence of the capsule. (294)

c) Membrane and Cell Wall Modifications

Changing the composition of the cell membrane is used by bacteria as an effective strategy to evade the bactericidal effects of AMPs. This is mainly achieved by three mechanisms:

- reduction of the surface net charge
- modification of AMPs target, and
- alterations in membrane fluidity.

Reduction of the net negative membrane charge

Many AMPs exert their effect by interacting with the negatively charged bacterial membrane. One of the strategies that can limit such interactions is the reduction of the membrane net surface charge, either through the incorporation of *L*-lysine into phosphatidylglycerol, and/or increase in *D*-alanylation of teichoic acids. (297, 298)

Phosphatidylglycerol is the major membrane lipid shown to be modified by lysination. Addition of positively charged amino acid lysine via aminoacylation by multipeptide resistance factor protein (MprF) decreases the net negative charge on the bacterial surface, thereby diminishing the bacterial affinity for cationic AMPs. (298, 299) The *D*-alanylation of teichoic acid has also been shown to impart resistance to cationic AMPs as well as to infection-induced antibacterial proteins. (300, 301) Teichoic acids are anionic carbohydrate-containing polymers, which are referred to as either lipoteichoic acids, when associated with the cytoplasmic membrane, or wall teichoic acids, when covalently linked by phosphodiester bridges to peptidoglycan muramic acid residues. (190) These polymers are modified with *D*-alanine residues through a process mediated by *D*-alanyl lipoteichoic acid pathway (DLT). (302) Apart from modulating the net anionic charge on the bacterial membrane, the esterification of teichoic acids with *D*-alanyl

esters can increase surface rigidity and consequently reduce AMPs penetration through the cell wall. (303)

Mechanisms of resistance of Gram-negative bacteria are presented in Figure 22.

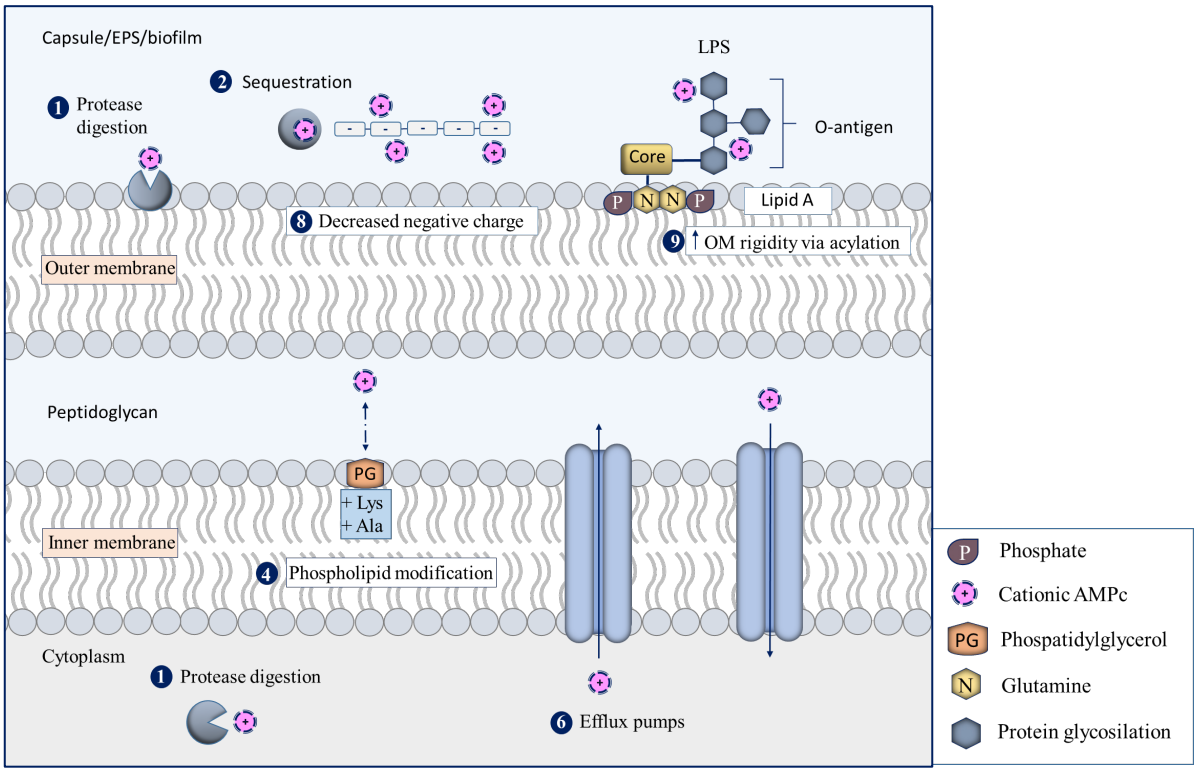

Figure 22. Common resistance mechanisms to cationic AMPs in Gram-negative bacteria. LPS–lipopolysaccharide; OM–Outer membrane. (Adapted with permission from ref. 192)

Target Modification

The peptidoglycan is an essential component of the bacterial cell wall. This complex biopolymer is targeted by the lysozyme, a cationic antimicrobial enzyme found in neutrophils, monocytes, macrophages, and epithelial cells. Lysozyme catalyses the hydrolysis of the β-(1,4)-glycosidic bond between *N*-acetylmuramic acid (MurNAc) and *N*-acetylglucosamine (GlcNAc) of the peptidoglycan, thus causing breakdown of its structure and eventual lysis of the cell. (304) Two main mechanisms of lysozyme resistance have been characterised in different bacterial species. The first mechanism confers resistance via either *O*-acetylation of the C-6 hydroxyl moiety of the MurNAc residues or the deacetylation of the GlcNAc residues. (305-309) These modifications act as a steric hindrance, preventing binding of the lysozyme to its polymeric substrate. The second mechanism involves production of lysozyme inhibitors, such as the periplasmic lysozyme inhibitor Ivy (inhibitor of vertebrate lysozyme) and the factor Sic

(streptococcal inhibitor of complement), identified in *E. coli* and *S. pyogenes,* respectively. (310, 311)

Alterations to Membrane Order

Other mechanisms that confer resistance to AMPs include alterations in the membrane composition and changes in the transmembrane pH and potential. (312-314)

d) AMP efflux mechanisms

Bacteria express a plethora of integral membrane transport proteins, called efflux pumps, which transport molecules across the inner membrane or the entire cell envelope. (315) These protein assemblies can be either selective for a given compound or extrude structurally varied molecules, such as antibiotics, thereby conferring a MDR phenotype. (316) Currently, six families of bacterial drug efflux pumps have been identified, out of which the ATP-binding cassette (ABC) family is most frequently encountered. Its members utilise adenosin triphosphate (ATP) as a source of energy to drive transport across cell membrane, as opposed to members of other five families that use electrochemical gradients as an energy source. (315) A new family of bacterial multidrug efflux pumps in *Acinetobacter baumannii* was only recently described by Hassan *et al.* (317) It is found to be widespread among Gram-negative bacteria, but its role in the resistance to AMPs is still not clear. (318)

In Gram-positive bacteria, three transporters have been shown to contribute to the development of resistance to AMPs: three-component ABC-transporters, two-component ABC-transporters, and single protein multidrug-resistance transporters, or MDR pumps. (319) The LanFEG system, a three component ABC transporter, is the best characterised in AMP-producing Gram-positive bacteria. Along with a specific immunity peptide (LanI), it confers self-immunity to lantibiotic-producing strains. (320) Unlike most LanFEG systems, two-component ABC transporters, called BceAB type, often provide resistance to multiple AMPs, including lantibiotics, cyclic AMPs, glycopeptides, defensins and cathelicidin. (321) The dual efflux pump of both the major facilitator superfamily (MFS) and ABC families in *Streptococcus pneumoniae*, MefE/Mel has been found to be inducible by human cathelicidin, and confers resistance to LL-37, as well as macrolides. (322) Efflux pumps found in many Gram-negative bacteria, described as the resistance/nodulation/cell division (RND) family transporters have been extensively studied. They have been shown to confer resistance to a number of AMPs. Examples include MtrCDE of *Neisseria gonorrhoeae* and *N. meningitides,* which confers

resistance to LL-37 and protegrin-1, AcrAB-TolC in *Klebsiella pneumoniae* to human defensins, and *Vibrio cholerae* VexAB-TolC to polymyxin B. (257, 323-326) However, some RND family efflux pumps do not exhibit such function. (327)

e) Antimicrobial peptide sensing systems

Many bacterial AMP resistance mechanisms are regulated by so-called sensor/regulators. These two-component regulatory systems contribute to bacterial adaptation to environmental stress by modulating target gene expression. (283) The antimicrobial peptide sensor (Aps), first observed in *S. epidermidis,* regulates the expression of genes such as the *dlt* operon for teichoic acid alanylation and the *mprF* gene for phosphatidylglycerol lysinylation. Sensing systems have also been found in other Gram-positive bacteria, such as *BceSR* in *B. subtilis*, *BraSR* in *S. aureus* and *LiaFSR* in streptococci, and they often act in concert with their designated ABC transporters. (328-330) The central two-component system (TCS) in Gram-negative bacteria is the PhoPQ two-component system, whose two main components are the histidine kinase sensor PhoQ, located in the cytoplasmic membrane and the DNA binding regulator PhoP. (331, 332) Together with another two-component system, designated PmrAB, PhoPQ regulates lipid A modifications and thus the mechanisms of resistance to cationic AMPs. (331, 333-335)

Apart from TCS, sigma (σ) factors are another common mechanism for the regulation of gene expression in response to extracellular signals. These factors are found to regulate resistance to antimicrobial compounds in many bacteria. Some examples include sigma factors σB and σL in *Listeria monocytogenes*, and the sigma factor V (sigV) in *B. subtilis,* which is activated in the presence of lysozyme. (336)

1.7 Converting AMPs into drug leads

Natural AMPs have several properties, which make their translation into drugs particularly challenging. They are prone to proteolytic degradation, often possess modest antimicrobial activity, chemical/physical instability, and they are usually toxic to mammalian cells. Thus far, many chemical modifications have been developed with the goal of improving proteolytic stability and activity of AMPs while minimising their toxicity to mammalian cell. These modifications broadly include amino acid substitution, *N*-terminal acetylation and *C*-terminal amidation, introduction of unnatural amino acids, PEGylation and other hybrid approaches. (337, 338)

1.7.1 Amino acid substitution

The most straightforward approach includes substitution of one or more amino acids in the peptide chain for other *L*-proteinogenic residues. This approach was shown to be successful in the synthesis of pexiganan, whose antibacterial activity was significantly improved by selective substitution of neutral and anionic amino acids in the sequence of magainin-2, for cationic and hydrophobic residues. (339) Similarly, *L*-amino acid substitution in protegrin and indolicidin resulted in two clinical trial candidates, iseganan and omiganan, respectively. (340) Although none of the peptides have been licensed for clinical use, the encouraging results indicate that modifying peptide sequence may be a viable strategy for improving peptide properties. Furthermore, AMPs can be modified by replacing *L*-amino acids with their *D* analogues. (341, 342) Partial *L*- to *D*-amino acid substitution can result in analogues with improved proteolytic stability, without largely affecting antimicrobial activity of peptides. (343) It should be noted, however, that partial substitution may result in reduction, if not complete loss of activity due to the disruption of an α-helical structure, as demonstrated in the study done by Zhao *et al*. (344) The authors also found that all-*D*-amino acid sequence had greatly improved stability towards proteases while still maintaining antimicrobial activity, indicating that peptide target may be non-stereospecific. In addition, many studies have shown that the presence of *D*-amino acids in the sequence of different AMP-analogues could improve their proteolytic, as well as serum stability. (341, 345, 346)

1.7.2 *N*-Terminal acetylation and *C*-terminal amidation

Modifications, such as *N*-terminal acetylation and *C*-terminal amidation, are common approaches used mainly to increase proteolytic stability of peptides. (347) Apart from its ability to prevent enzymatic degradation by aminopeptidases, *N*-terminal acetylation reduces the overall net charge of the peptide by one, and thus may cause reduction in antimicrobial activity. Saikia *et al.* developed four analogues of the 9-residue long lipid-binding stretch of cytoskeleton protein of *E. coli* (MreB). (348) Capping of *N*-terminus with acetyl group rendered the peptide less effective, particularly against *S. aureus* and *P. aeruginosa,* while activity against *Candida albicans* and gentamicin- and methicillin-resistant *S. aureus* remained unchanged. Unlike the acetyl-capping of the *N*-terminus, *C*-amidation is a very common posttranslational modification that is widely observed among AMPs and it is thought to influence both peptide antimicrobial activity and proteolytic stability. (347, 349) For some AMPs, such as anoplin, an antimicrobial, helical decapeptide from wasp venom, this structural feature appears to be essential for antibacterial activity. (350) It has been suggested that the main driver of increased efficacy by amidation is related to the stability of the α-helix at a peptide-membrane interface. (351, 352) Using circular dichroism measurements and molecular dynamics analysis, Mura *et al.* showed that peptides with amidated *C*-terminus do have greater propensity to form an α-helical structure compared to non-amidated analogues. (353) However, effect of *C*-terminal amidation on the peptides efficacy is rather inconclusive, considering that such modification can result in peptide analogues with unchanged or even decreased efficacy. (354) As for proteolytic stability, Kuzman *et al.* demonstrated that it was greatly enhanced for tachyplasin I analogue which was modified by both *N*-acetylation and *C*-amidation. (355) The same modifications to the peptide termini of the host defense peptides derived from apolipoprotein E(B) led to the 4-fold increase in proteolytic stability. (356) This increase, however, cannot be exclusively attributed to modifications of the peptide termini, as the presence of hydrophobic amino acids (2-Nal and S-*tert*-butylthio *L*-cysteine residues) in the peptide sequences may also have contributed to the resistance to serum proteases. More recently, *N*-terminal cholesterol modifications of various AMPs have been successfully introduced, resulting in analogues with reduced haemolytic activity and improved potency. (357, 358)

1.7.3 PEGylation

PEGylation refers to the modification of bioactive compounds with polyethylene glycol (PEG) moieties. This type of peptide modification has been widely used as a post-production methodology for improving undesirable pharmacokinetic properties of peptides/proteins, such as short half-life and fast serum degradation. (359) Moreover, PEGylation modifies peptide physicochemical properties, and hence affects its biodistribution and solubility. (360) Many studies with AMPs demonstrated the utility of such modification in developing peptide analogues with high tolerance to proteolytic degradation. (361)

Although PEGylation is considered to confer favourable properties to peptides and proteins, it is not without its own limitations. (360) PEGylation can result in the reduced biological activity of conjugates compared to unmodified peptides. (362) This is most likely owing to the steric hindrance imposed by PEG-molecules, which can limit peptide-membrane interactions. (363)

To overcome this limitation, temporary PEGylation strategies can be used that rely on the presence of cleavable, protease-susceptible linker between PEG molecules and *N*-terminus of a therapeutic peptide. Upon exposure to blood proteases, the tracer-free peptide is released. Prodrugs designed in such a way have been shown to have prolonged half-life and greater efficacy compared to their permanently PEGylated analogues. (364, 365) Furthermore, Gong *et al.* demonstrated that traceless releasable pegylation of Arg residues in Arg-rich peptides can serve as a promising tool in developing highly protease-resistant conjugates, with full *in vitro* bioactivity. (366)

1.7.4 Incorporation of unnatural amino acids

Susceptibility of AMPs to host and bacterial proteases (*e.g.*, human proteases in serum, *Staphylococcus* aureolysin and *Pseudomonas* elastase) is one of the major impediments to the translation of AMPs into effective therapeutics. Incorporation of unnatural (non-canonical) amino acids (either through addition or substitution) has shown to increase the proteolytic stability of peptides, and in some instances, their antimicrobial activity. (347) This backbone modification can be achieved using shorter amino acid analogues, such as ornithine, 2,4-diamino-butyric acid (Dab) and 2,3-diaminopropionic acid (Dap), *N*-methylated amino acids, β-amino acids and peptoids (*N*-alkyl-glycine oligomers). (347, 367) Arias *et al.* have recently shown that substitution of Arg and Lys residues in the Trp-rich peptides for their corresponding analogues with shorter side chain length, resulted in peptides highly resistant to hydrolysis by

trypsin, with mostly unaltered activity against *E. coli.* (368) Of note, although referred to as unnatural, β-amino acids are found in many naturally occurring peptides. These amino acids are important constituents of biologically active natural products, such as the anticancer agents taxol (paclitaxel) and bleomycin (with β-aminoalanine) produced by the Western yew (*Taxus brevifolia)* and *Streptomyces verticillus*, respectively. (369-371) Furthermore, Rhodopeptins, a family of antifungal cyclic lipopeptides, isolated from *Rhodococcus* species, are characterised by the presence of lapidated β-amino acids. (372)

The utility of amino acid replacement strategy, together with incorporation of unnatural amino acids was demonstrated in the recent work done by Roberts *et al.* (373) By systematically optimising multiple non-conserved positions in the polymyxin scaffold, the authors successfully synthesised a clinical candidate F365 (QPX9003) with favourable safety profile and higher potency against MDR pathogens *P. aeruginosa*, *A. baumannii* and *K. pneumoniae*. These optimisations resulted in an analogue with following structural features: the presence of 2,4-dichlorobenzoyl group at the *N*-terminus, as well as *L*-2,3-diaminopropionic acid (Dap), *D*-Leu and *L*-2-aminobutyric acid (Abu) at positions 3, 6 and 7, respectively. According to the data from recently ended Phase I clinical trial, F365 was well tolerated with no significant adverse effects during the treatment with doses sufficient to achieve clinical efficacy. (374)

Up to date, hundreds of non-canonical amino acids have been incorporated into recombinant proteins using Flexizyme technology. (375) Some examples of AMPs modified by genetically encoded non-canonical building blocks were also reported. (376-379)

A most prominent example of a peptide containing non-canonical amino acid is Lytixar (LTX-109), a synthetic tripeptide with broad antimicrobial activity and high stability towards proteolytic degradation. (380, 381) Similar to other AMPs, its main mode of action is bacterial disruption and cell lysis. (382, 383) LTX-109 completed Phase II clinical trial, which evaluated the efficacy and safety of the drug in the treatment of impetigo. In addition, two new clinical trials have been recently registered for the following indications: hidradenitis suppurativa (an Open label Phase II//proof of concept-study) and nasal decolonisation of *S. aureus* (Phase I/IIa). (384)

1.8 Peptidomimetics/AMP optimisation

Peptidomimetics are molecules that mimic the natural structure and/or biological activity of natural peptides. In general, the antimicrobial peptidomimetics can have high structural similarity to their native analogues, such as when native peptide backbone is modified via, among others, amino acid substitution, incorporation of non-canonical amino acids, or acylation. However, some peptidomimetics bear no resemblance to their native analogues, having only general structural features known to promote antimicrobial activity, such as net positive charge and amphipathicity. Compared to their native analogues, peptidomimetics are usually easier to synthesise as they tend to be less structurally complex. In addition, apart from being less prone to resistance development, they can possess favourable physicochemical properties mirrored in greater metabolic and proteolytic stability, enhanced activity and reduced toxicity. Chemical modifications often employed in designing peptidomimetics include cyclisation, PEGylation, lipidation, glycosilation, grafting and formation of dendrimers. Here we highlight two of these strategies, cyclisation and lipidation. For more detailed overview, the reader is referred to several recent reviews. (337, 361)

1.8.1 Cyclisation

Naturally occurring cyclic peptides are found in all kingdoms of life. They exhibit a wide variety of biological activities, such as antibacterial (bacteriocins), cytotoxic (*e.g.*, cyclopeptide RA-V and plant cyclotides) haemolytic (*e.g.*, cycloviolacin H4) and antiviral (*e.g.*, cyclic depsipeptide plitidepsin). (385-389)

Peptide cyclisation can be achieved either between *N*- and *C*-terminus (head-to-tail cyclisation), one of the termini and one of the side chain groups (head-to-side chain or tail-to-side chain), or between two side chain groups (side chain-to-side chain). (Figure 23)

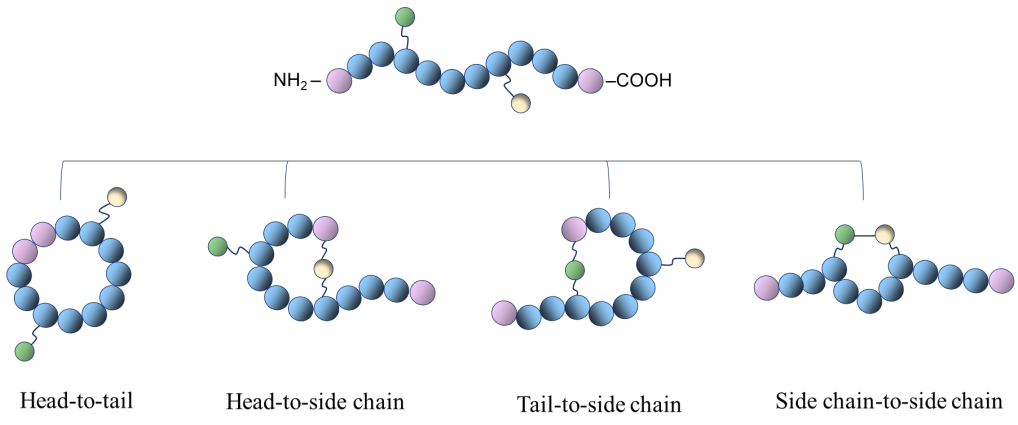

Figure 23. Different cyclisation strategies. The blue and purple spheres denote amino acid residues.

The fourth group, according to terminology proposed by Zhang *et al*., includes plant-derived cyclotides, where apart from a head-to-tail macrocycle the peptide structure is further stabilised with three disulphide bonds. This unique structural motif endows cyclotides with a number of advantages over conventional (i.e. acyclic) peptides, such as exceptional stability against thermal, chemical or enzymatic degradation, as well as amenability to grafting. (390, 391) The presence of a cyclic motif is found to impart a number of favourable properties to peptides, as discussed previously, making them an attractive modality for drug development. (387)

Head-to-tail cyclisation can result in analogues with improved stability and activity, as demonstrated for the cyclic analogue of gomesin, an 18-residue peptide originally isolated from the hemocytes of the Brazilian spider *Acanthoscurria gomesiana*. (392) Furthermore, cyclic antimicrobial peptoids, as well as cyclic Arg/Trp-rich hexapeptides have been found to have increased antimicrobial activity compared to their linear analogues. (393, 394). For disulphide-rich host defence peptides (protegrins, defensins), backbone cyclisation has been reported to increase not only their stability and selectivity, but also their tolerance to high-salt concentrations. (395, 396) In a recent study, Mwangi *et al.* synthesised a cyclic peptide ZY4 by introducing two cysteines next to the valines at both ends of the cathelicidin-BF-15-a3. The obtained peptide had an excellent activity against *P. aeruginosa* and *A. baumannii*. Moreover, it inhibited planktonic growth and biofilm formation, displayed high stability *in vivo* and law propensity to induce resistance. (397) Inspired by the properties of constrained cyclic peptides, Hancock and co-workers synthesised cyclomimetics by following three different strategies: head-to-tail cyclisation, glutamate side chain-to-tail cyclisation and Cys-Cys cyclisation. The analogues resulting from glutamate side chain-to-tail cyclisation were non-haemolytic, displayed high proteolytic stability and improved activity against *S. aureus* skin infections. (398)

1.8.2 Lipopeptides and lipidation

Lipopeptides constitute a structurally diverse group of secondary metabolites produced by various fungal and bacterial genera. They are amphipathic molecules consisting of an aliphatic hydrocarbon tail linked to the linear or cyclic peptide chain. (399) Lipopeptides produced by *Bacillus* strains are widely studied. All of them are synthesised by non-ribosomal peptide synthetases (NRPS) (*e.g.*, surfactin, fengycin) or by hybrid polyketide synthases and non-ribosomal peptide synthetases (PKSs/NRPSs) (*e.g.*, iturin or locillomycin). (400) This mode of

biosynthesis endows them with highly versatile structural features, such as β-hydroxy or β-amino fatty acid chains, *D*-amino acids, or saturation. In addition, the amphipathic nature of these compounds imparts specific physicochemical properties, such as reduction of surface tension and their ability to self-assembly in aqueous environment at the critical aggregation (micellar) concentration. Lipopeptides produced by *Bacillus* species, are shown to have, among others, antimicrobial, antifungal, anticancer, and immunomodulatory activity. (401) Of note, in their recent study Hubrich *et al*. reported on a genome-guided discovery of ribosomally derived, fatty-acylated cyclic peptides, termed selidamides. They were found to have a cyclic peptide structure and acylated (hydroxy)ornithine or lysine side chains with C_{10}, C_{12} or C_{16} fatty acids. (402)

In general, lipidation has been shown to modulate the AMPs antimicrobial activity, which is greatly influenced by the length of the acyl chain and overall hydrophobicity of the peptide. (403) Chu-Kung *et al*. developed a series of acylated nanopeptides derived from an α-helical region of coprisin, a 43-mer insect defensin-like peptide produced by the dung beetle *Copris tripartitus*. (404) The study showed that elongation of the acyl chain affected both antimicrobial and haemolytic activity of the lipopeptides, whereas conjugation with fatty acid with 16 carbons in length resulted in an analogue having no antimicrobial activity. Albada *et al.* demonstrated that acylation of Lys, positioned either on *C*- or *N*-terminus, could increase the activity of short AMPs. (405) Acyl conjugation was also shown to be an effective tool for improving antimicrobial activity against Gram-positive bacteria (up to 30-fold increase), as demonstrated by Mayo and co-workers. (406)

By varying acyl chain length in the pseudodesmin, a cyclic lipodepsipeptide produced by *Pseudomonas* analogues, Steigenberger *et al.* showed that the optimal chain length for antimicrobial activity is governed by a balance between membrane partitioning, favoured by longer chains, and local membrane perturbation which is weakened following acyl chain elongation. (407)

Increased proteolytic stability

Lipidation may result in increased stability towards serum proteases, probably due to the reversible binding of the lipidated peptides to serum albumin, as observed for the *N*-terminal fatty acyl chain of daptomycin. (408) Lee *et al*. designed a series of acylated *D*-analogues with high serum stability. (409) Apart from acylation, the higher stability could be, at least in part, attributed to the presence of *D*-amino acids in the peptide chain.

Making non-active peptides active

Lipidation of the *D*-lysine by acyl chains of varying lengths ($C_6 – C_{16}$) was successfully used to convert otherwise non-active *D*,*L* tetrapeptides into AMPs with antifungal and antibacterial properties. (410) The authors suggested that acylation could be therefore used as a method to endow peptides with antimicrobial activity by compensating for their short length and low hydrophobicity. (411) Similarly, it was shown that conjugation of inactive diastereomers of magainin with undecanoic acid and palmitic acid greatly improved their activity towards *Cryptococcus neoformans*. (412)

Improvement of antibacterial activity and/or serum stability

Liu *et al.* designed an *N*-terminal myristoylated antimicrobial peptide Myr-36PW, which exerted high activity against four tested bacterial strains (minimum inhibitory concentration (MIC): 0.0020 – 8 μg/mL). The greatest improvement in activity was seen for *S. aureus* with nearly 4-fold increase in MIC compared to its non-acylated analogue. In addition, Myr-36PW had relatively good stability in serum, although with considerable toxicity. (413) Peptides with improved antimicrobial activity and serum stability were designed by acylation of anoplin (GLLKRIKTLL-NH_2), a natural AMP isolated from the venom sac of solitary spider wasps. Acyl chains were linked to the side chain of one of the *D*-lysines at the positions 4 and 7 in the peptide sequence. The optimal acyl chain length was found to be in the range of C_8 to C_{10}. (414) Zhong *et al.* made a series of acylated lipopeptides with fatty acids ranging from 8 –18 carbon atoms in length. Among these, C_{14}-R1 (C_{14}-RWW-NH_2) and C_{12}-R2 (C_{12}-RRW-NH_2) had the best antimicrobial profile and higher selectivity than other analogues. In addition, when used in combination with antibiotics they showed synergistic effect. (415) Siano *et al.* investigated the effect of amino acid substitution and *N*-terminal acylation on antimicrobial activity of peptide analogues of Plantaricin, a bacteriocin produced by *Lactobacillus plantarum* NRIC 149 isolated from pineapple. (416) Acylated peptides exhibited improved antimicrobial activity against *S. aureus*, whereas substitution of Phe^{17} for Trp without acylation, rendered the peptide analogue less effective. Interestingly, its further conjugation with n-octanoic acid increased 8-fold the antimicrobial activity against the two tested strains, *S. aureus* and *Listeria monocytogenes.* An unusual but simple approach in designing lipopeptides was adopted by Ghosh *et al.* The synthesised membrane active peptides consisted of only one amino acid, namely Lys, with two lipid tails with the length ranging from hexyl to decyl. (417) Similarly, Greber *et al*. synthesised *N*-α-acyl-*N*-ε-acyl lysine analogues, however, with only modest

antimicrobial activity. (418) Chionis *et al.* designed a series of analogues of a short natural cationic antimicrobial peptide derived from the venom sac of the solitary wasp, *Anoplius samariensis*. The *N*-terminal acylation of one of the analogues, GLLKF^{5}IKK^{8}LL-NH_2 with octanoic-, decanoic- and dodecanoic acid, resulted in peptides with increased potency against tested Gram-positive and Gram-negative bacteria. (419) In an interesting recent study, Zhang and co-workers designed a truncated and lipidated analogue of the short AMP (KR12) derived from LL-37. Additional optimisation led to the all-*D* analogue (KRIWQRIK) conjugated with decanoic acid. This lipopeptide displayed good selectivity, stability, and robust antimicrobial activity *in vitro* against both Gram-positive and Gram-negative bacteria. In addition, it had antibiofilm and immunomodulatory properties. (346) Improvement in potency due to *N*-acylation was also demonstrated for the peptide dimers against Gram-negative bacteria, including carbapenem-resistant *Enterobacteriaceae*. (420)

1.9 Cyclisation chemistry

The most used ring-closing strategies include lactamisation, lactonisation and disulphide bridge formation, as well as more recently developed diverse set of ligation methods. (421, 422)

1.9.1 Lactamisation in solid phase peptide synthesis

Solid phase peptide synthesis (SPPS) has been widely used to generate precursors of cyclic peptides, namely their linear analogues. In the SPPS, typically a linear sequence of the desired cyclic peptide is first assembled on the solid support. A subsequent cyclisation step is performed either in solution after the cleavage of the assembled sequence from the resin, or on the support, following selective side chain deprotection. In the former method, the ring closing reactions tend to be slow and side reactions, such as oligomerisation and dimerisation, may even predominate. These reactions can be minimised when the cyclisation is done under high dilution conditions ((10^{-4} to 10^{-3} M). Amount of solvent can be also reduced by performing reaction under pseudo-high dilution conditions, namely when both the linear precursor and the coupling reagent are added simultaneously to the small amount of solvent and a base. (423)

Another efficient approach includes formation of a macrocyclic ring while the linear peptide is still bound to the solid support. In this strategy, pseudo-dilution conditions can be approximated by the low loading of the resin, which favours intramolecular reactions over unwanted intermolecular. Linear peptide can be anchored to the solid support via backbone amide or, more commonly via *C*-terminal amino acids such as Asp, Glu, Lys, Ser, or Tyr, choice of which should be carefully considered to minimise the formation of diketopiperazine side product. (424)

For small and medium-sized cyclic peptides, such as those with three, four, and five amino acid residues, cyclisation might be difficult, if not impossible. This is mainly attributable to the planar transoid conformation of the peptide bond, which hinders linear precursor from folding in a way that would enable reactive ends to come in close proximity. In addition, transannular interactions may further interfere with the conformational preorganisation of the linear peptide. (425, 426)

1.9.2 Lactonisation

Macrolactonisation, although similar to macrolactamisation, offers some unique opportunities for ring formation, as both an alcohol and a carboxylate can act as a nucleophile. Some successful examples of macrolactonisation through acid activation include the Corey–Nicolaou reaction, Mukaiyama esterification, Yamaguchi esterification, and Shiina

macrolactonisation, among others. (427-430) A more detailed description of macrolactonisation methods used in the synthesis of natural products can be found in a review by Campagne and co-workers. (431)

1.9.3 Disulphide bond formation

Disulphide bonds formed between thiol groups of the cysteine residues are indispensable for proper folding and thus structural stability of many biologically active peptides, such as oxytocin, vasopressin and calcitonin. (432-434) These bonds can be formed intramolecularly, in rare cases even between two adjacent cysteines, and intermolecularly, leading sometimes to increased protein aggregation. (435, 436) *In vivo*, formation, as well reduction, of disulphide bonds is tightly regulated by the cellular enzymes known as thiol-disulphide oxidoreductases that catalyse thiol-disulphide exchange reactions. (437) On the other hand, formation of monocyclic disulphide bridges *in vitro* is usually straightforward, including removal of all or just thiol protecting groups and subsequent macrocyclisation under high dilution conditions. A great variety of oxidants have been used to facilitate cyclisation, some of which are air oxidation, dimethyl sulfoxide (DMSO) and oxidation using potassium ferricyanide ($K_3Fe(CN)_6$). (438)

1.9.4 Peptide ligation methods

Peptide ligation methods have greatly expanded the toolbox of peptide chemists by enabling the formation of a peptide bond in aqueous solution without the need of having protected peptide fragments. The mechanism, in general, includes a chemoselective capture step, followed by an intramolecular rearrangement. According to Agouridas *et al.* these methods could be classified into three distinct types based on the position of the functional group(s) within the amine component involved in the capture step. Methods where the side chain is involved in the capture step are designated Type I, whereas those involving the reactivity of α-nitrogen are referred to as Type II. The last type, Type III, is considered to be a combination of the previous two types. (439)

The Type I ligation method, the native chemical ligation (NCL), was first introduced by Kent and co-workers in 1994. (440) (Figure 24) The reaction involves coupling of a *C*-terminal peptide thioester with an *N*-terminal cysteinyl peptide and subsequent rearrangement of a thioester intermediate via an *S,N*-acyl transfer. This regioselective reaction allows for the synthesis of larger peptides with native peptide bond at the ligation site, thereby overcoming the inherent limitation of the SPPS with respect to the length of the peptide chain.

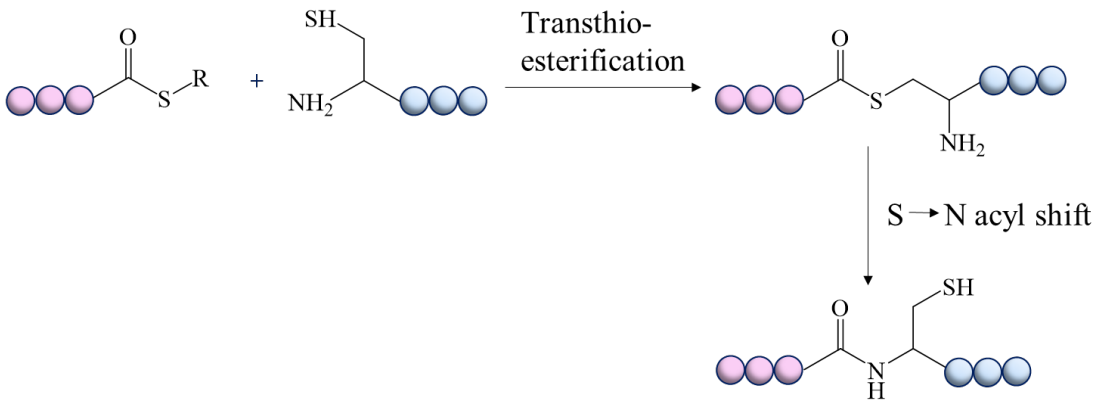

Figure 24. Peptide bond formation by native chemical ligation. (Adapted with permission from ref. 441 with permission from the Royal Society of Chemistry.)

In addition to NCL, other peptide ligation methods were developed, such as the traceless Staudinger ligation, simultaneously reported in 2000 by the groups of Bertozzi and Raines; (Figure 25A), the ketoacid-hydroxylamine ligation (KAHA), which was introduced in 2006 (Figure 25B) and serine/threonine ligation (STL) reported in 2013. (Figure 25C) (442-445). In addition, copper(I)-catalyzed azide–alkyne cycloaddition (CuAAC) ("click chemistry") has been reported for cyclisation of peptidic molecules. (Figure 25D) (446-448)

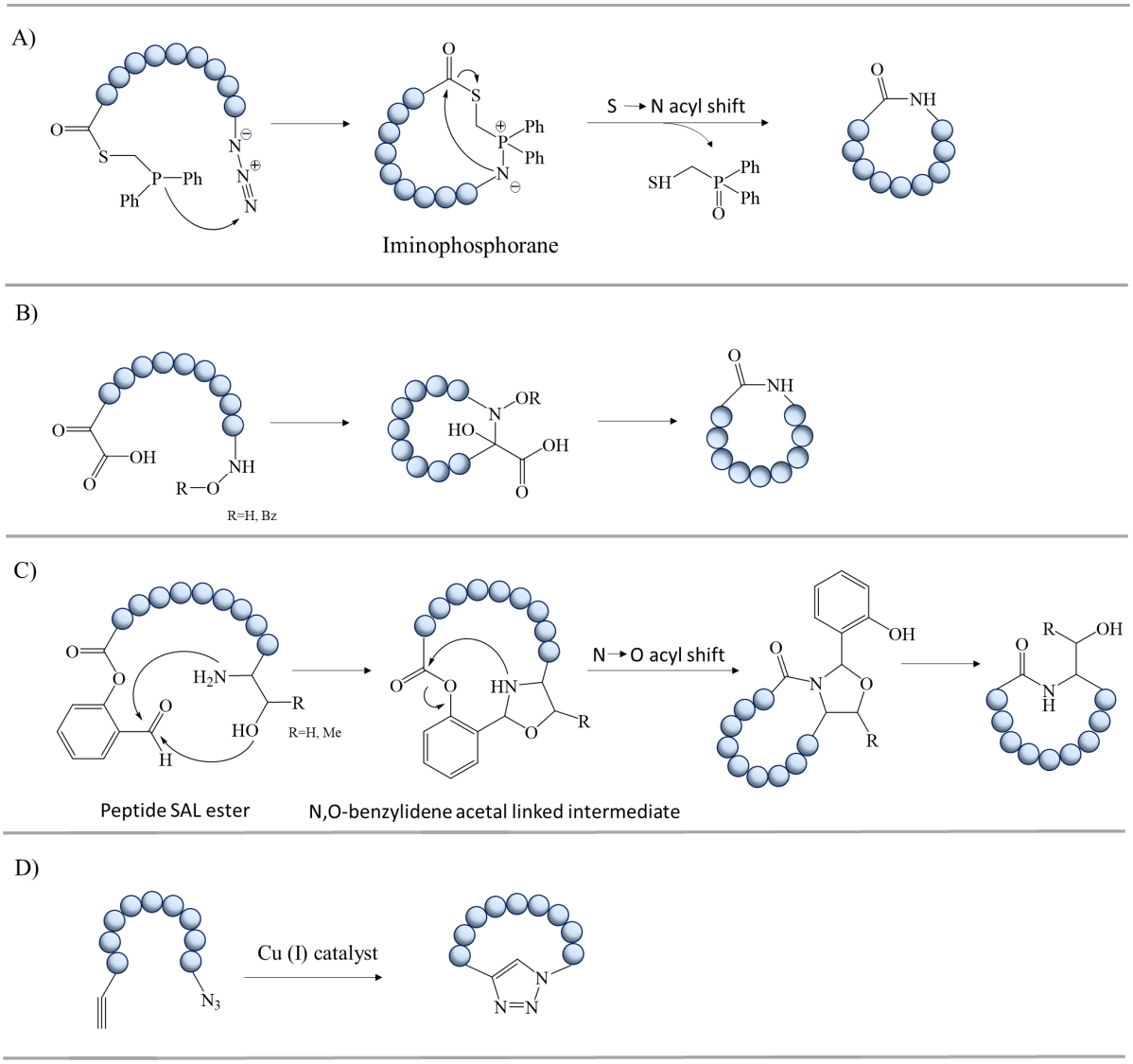

Figure 25. Selected ligation methods for peptide/protein cyclisation: A) traceless Staudinger ligation, B) type II KAHA ligation, C) Serine/Threonine ligation (C-terminal peptide salicylaldehyde (SAL) ester is required) and D) CuAAC. (Adapted from ref. 441 with permission from the Royal Society of Chemistry and from ref. 449.)

1.9.5 Enzyme-mediated cyclisation methods

In recent years, enzyme-catalysed peptide ligation strategies have generated great interest due to their excellent regio- and chemoselectivity. (450) These reactions are mediated by enzymes, such as sortase A, a transpeptidase isolated from *S. aureus* (451, 452), asparaginyl endoproteases like butelase 1, an asparagine/aspartate (Asx)-specific cysteine transpeptidase from a tropical cyclotide-producing plant (*Clitoria ternatea*) (453) and the subtilisin variants like peptiligase or omniligase (454, 455). Although not without their own limitations, these enzymatic approaches offer a valuable addition to the currently used chemical strategies for peptide macrocyclisation.

2 Aims of the thesis

The main objectives of this thesis were:

1. Synthesis of novel linear and cyclic antimicrobial peptides using either marine antimicrobial peptides (**Paper I** and **II**) or a synthetic cyclic tetrapeptide scaffold (**Paper III**) as a template.

2. SAR optimisation studies – Investigation of the effects of various structural modifications on antimicrobial and haemolytic activities of the synthesised peptides.

The following modifications were explored:

Investigated structural modifications	**Paper(s)**
L-Amino acid substitution	I, II, III
N-Terminal acylation	I, II
Cys-Cys side chain cyclisation	I
Head-to-tail cyclisation	II, III
Single *L*- to *D*-amino acid substitution	III

Biological and biophysical investigations that were performed by our collaborators in the LEADScAMR project are listed below:

Investigated biological properties	**Paper(s)**
Antibacterial minimum inhibitory concentration (MIC)	I, II, III
Antifungal MIC	I, II
Haemolytic activity against human red blood cells (RBC)	I, II, III
Effects on bacterial membrane integrity	I, II
Effects on bacterial viability	I, II
Effects on outer membrane permeability	I
Biophysical studies	
Interactions with the membrane by surface plasmon resonance	III
NMR studies	III

3 Summary of papers

Paper I – Synthesis and antimicrobial activity of short analogues of the marine antimicrobial peptide Turgencin A: Effects of SAR Optimisations, Cys-Cys Cyclisation and Lipopeptide Modifications. *International Journal of Molecular Sciences* 23, no. 22. (2022).
Hymonti Dey*, **Danijela Simonovic***, Ingrid Norberg-Schulz Hagen, Terje Vasskog, Elizabeth G. Aarag Fredheim, Hans-Matti Blencke, Trude Anderssen, Morten B. Strøm, and Tor Haug (*shared first authorship)

In this SAR optimisation study, we designed a series of truncated analogues of the marine antimicrobial peptide Turgencin A. These analogues included the core sequence of Turgencin A, composed of 12 amino acid residues with amidated *C*-terminus. To investigate the effects of cyclisation, this sequence was modified by intramolecular Cys-Cys side chain cyclisation. Next, the effects of hydrophobicity and the presence of different cationic residues in the peptide sequence were explored via *L*-amino acid substitutions, namely Pro/Leu to Trp and Lys to Arg substitution. Selected linear and cyclic analogues were further modified by *N*-terminal acylation with octanoic- (C_8), decanoic- (C_{10}) or dodecanoic acid (C_{12}). The highest antimicrobial activity was obtained for the two cyclic Turgencin A analogues, **C_{12}-cTurg-1** and **C_8-cTurg-2**, that were acylated with dodecanoic- and octanoic acid, respectively. These peptides had similar antimicrobial profiles against the Gram-positive bacteria (MIC: 2 – 4 µg/mL) and against *E. coli* (MIC: 4 µg/mL), with relatively low toxicity against human red blood cells. Mode of action studies confirmed their membranolytic activity.

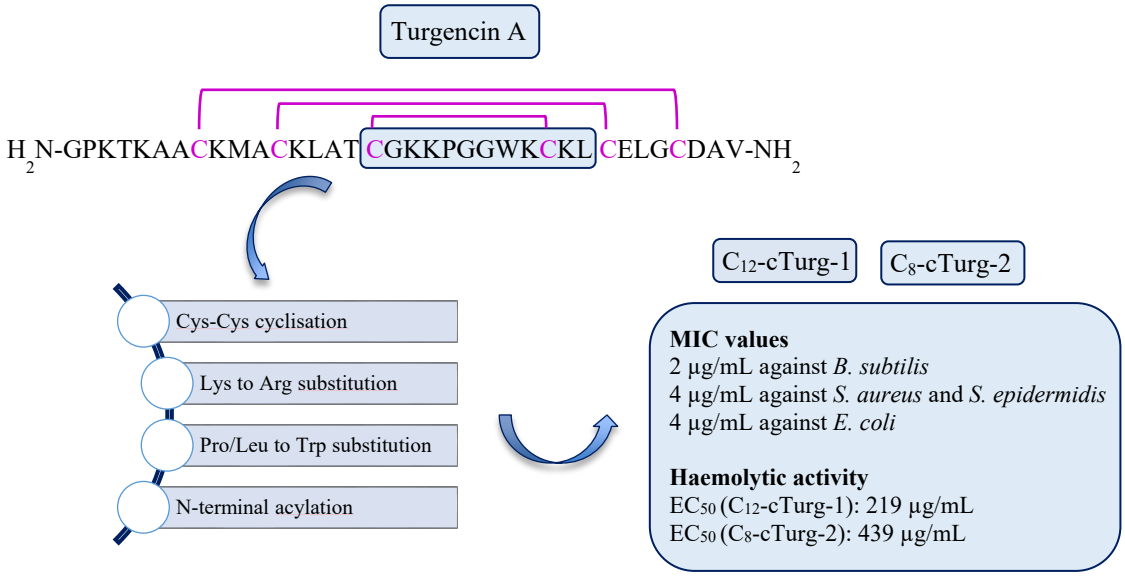

Paper II – Antimicrobial activity of short analogues of the marine peptide EeCentrocin 1: Synthesis of lipopeptides and head-to-tail cyclic peptides. (**Manuscript**)

In this work a series of 12-residue analogues of the previously reported lead peptide **P6** was synthesised. The sequence of **P6** was derived from a segment of the heavy chain (HC) of the marine antimicrobial heterodimeric peptide EeCentrocin 1, isolated from the red sea urchin *Echinus esculentus*. To further optimise properties of the lead peptide, the following modifications were employed: amino-acid substitution (Ala^8 to Lys/Arg, Thr^6 to Trp, and simultaneous Arg^4 to Trp and Trp^6 to Arg substitution), *N*-terminal acylation and head-to-tail cyclisation using pseudo-high dilution conditions. The synthesised analogues were tested for antibacterial and antifungal activity. In addition, their haemolytic activity was evaluated against human red blood cells. The two most potent analogues, the linear peptide, **P6-W6R8** and its head-to-tail cyclic counterpart **cP6-W6R8**, had MIC values ranging from 0.4 to 1.6 µM against tested Gram-positive and Gram-negative bacteria, and MIC values from 1.6 to 6.6 µM against fungi. They were both non-haemolytic (EC_{50} > 500 µM). Mode of action studies indicated that both linear and cyclic peptides disrupt bacterial membrane, although targeting intracellular components could not be excluded.

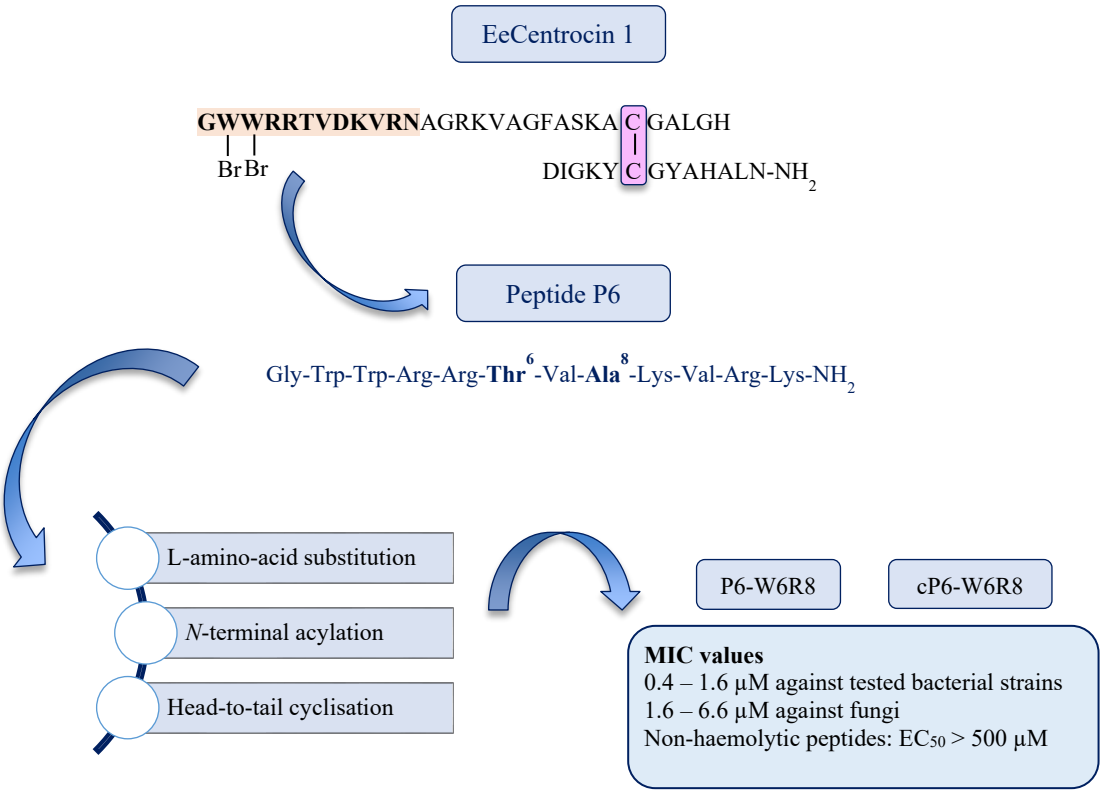

Paper III – The role of amphipathicity and *L*- to *D*-amino acid substitution in a small antimicrobial cyclic tetrapeptide scaffold containing a halogenated α,α-disubstituted $\beta^{2,2}$-amino acid residue. (**Manuscript**)

In this paper a series of cyclic tetrapeptides was synthesised. This series was based on a synthetic scaffold previously developed in our group containing a lipophilic $\beta^{2,2}$-amino acid residue, termed $\beta^{2,2}$. Structural characteristics of the synthesised peptides were altered in a way that allowed for the investigation of the effects of *L*-amino acid substitution, changes in stereochemistry and amhipathicity on antimicrobial and haemolytic properties of resultant peptides.

The most potent cyclic tetrapeptide in this series **cArg-$\beta^{2,2}$-Arg-Arg** had MIC values in the low micromolar range (1 – 4 μg/mL). It had low haemolytic activity (EC_{50}: 279 μg/mL), and the highest selectivity for bacterial cells. Lys to Arg substitution resulted in an equally potent antibacterial analogue, but with increased haemolytic toxicity. The non-amphipathic peptides exhibited reduced potency against Gram-negative bacteria, whereas activity against Gram-positive bacteria was largely unaffected. In addition, their haemolytic activity was considerably reduced. Similar reduction in haemolytic activity was observed following *L*- to *D*-amino acid substitution. This modification only slightly influenced antimicrobial activities of the resultant *D*-analogues. Lastly, Leu to Phe substitution resulted in peptides with slightly increased activity against both Gram-positive and Gram-negative bacteria, while their haemolytic activity was either unchanged (both analogues were non-haemolytic) or increased, in the case of Arg-containing analogue.

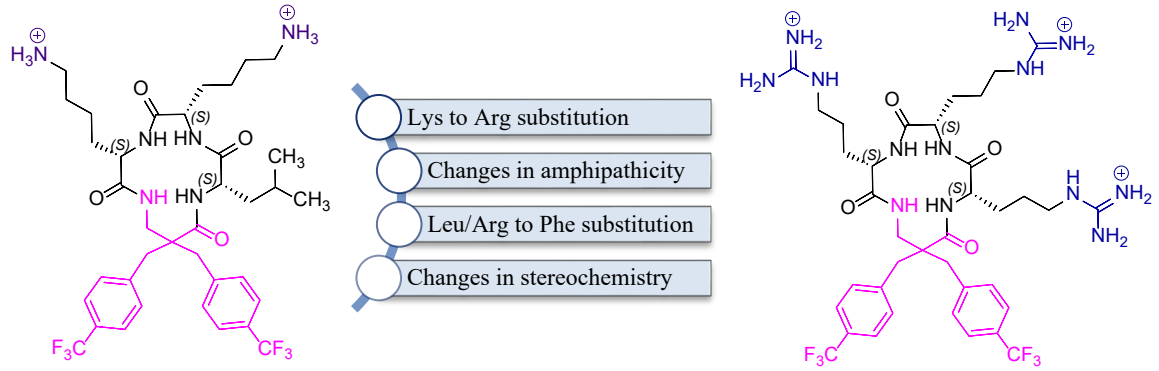

MIC values for c(Lys-$\beta^{2,2}$-Lys-Lys)
1 – 2 μg/mL against Gram-positive bacteria
8 μg/mL against Gram-negative bacteria

Haemolytic activity
EC_{50} >500 μg/mL

MIC values for c(Arg-$\beta^{2,2}$-Arg-Arg)
1 μg/mL – 2 μg/mL against Gram-positive bacteria
2 μg/mL – 4 μg/mL against Gram-negative bacteria

Haemolytic activity
EC_{50} 279 μg/mL

4 Results and discussion

Antimicrobial peptides are generally characterised by being short, structurally diverse, positively charged and amphipathic in nature. (456) Their wide spectrum of antimicrobial activity along with their non-specific mode of action (although some have specific targets and/or act intracellularly), make them promising compounds in the treatment of infections. (136) Despite these advantages, their further development into drug leads has been hindered by their relatively high production cost, insufficient antimicrobial potency, poor proteolytic stability, and low selectivity. (457, 458) One of the strategies to overcome these limitations includes the synthesis of much shorter peptides, which are regarded as a viable therapeutic alternative to classical antibiotics. (459) In order to improve their potency, protease stability and selectivity, these peptides are usually modified by amino acid substitution, modification of their *C*- and/or *N*-terminus, and by various cyclisation strategies. In the present thesis, the effects of such modifications on the antimicrobial and haemolytic properties of peptides with three unique scaffolds were investigated.

Our first model peptide (**Paper I**) was a 12-residue sequence, termed **cTurg-1**, derived from the much longer antimicrobial peptide, Turgencin A, isolated from the Arctic marine colonial ascidian *Synoicum turgens*. Turgencin A consists of 36 amino acid residues with three intramolecular disulphide bridges and an amidated *C*-terminus. (460) In a previous study a series of shortened linear 10-residue peptides was designed using an amino acid replacement strategy. (461) In the present work, we focused on a 12-residue long sequence in the native peptide Turgencin A (C^{17}GKKPGGWKC^{26}KL), as we further wanted to explore the effects of intramolecular Cys-Cys cyclisation on peptide antimicrobial and haemolytic properties.

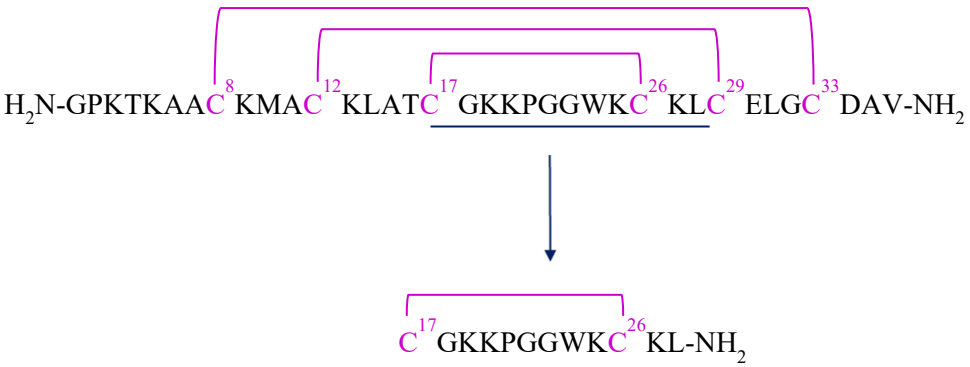

Figure 26. Sequence of Turgencin A with three Cys-Cys connectivities presented as pink lines. Underlined is the sequence of **cTurg-1**.

Main features of **cTurg-1** included four Lys residues, a central Pro-Gly-Gly (PGG) sequence, an amidated *C*-terminus and a Cys-Cys disulphide bridge. (Figure 26) Previous research has shown that the presence of both bulky, lipophilic residues and cationic charge are important for antimicrobial activity of short peptides. (462-464) Therefore, to increase hydrophobicity of the peptides we used two strategies: 1) stepwise substitution of two out of three amino acids in the PGG core sequence for tryptophan, and 2) *N*-terminal acylation with fatty acids of different length. Furthermore, we wanted to investigate if Lys to Arg substitution would affect the antimicrobial and haemolytic activities of the newly synthesised peptides. As Arg has been shown to interact much stronger with negatively charged phospholipids than Lys, we reasoned that by introducing Arg into the model sequence along with incorporating bulky, aromatic residues we would be able to generate peptides with improved selectivity. (465)

For the second paper (**Paper II**) we continued exploring similar modifications (amino acid substitution and *N*-terminal acylation), as well as a method for head-to-tail peptide cyclisation, which was used for the synthesis of cyclic analogues. Our model peptide **P6** was derived from EeCentrocin 1, an AMP previously isolated from the edible sea urchin *Echinus esculentus* and further characterised by researchers at UiT, The Arctic University of Norway. (466)
EeCentrocin 1 was shown to have a heterodimeric structure, where a 30-amino acid long heavy chain (HC) was connected via a disulphide bond to a light chain (LC) of 13 amino acids. It was further demonstrated that the HC is responsible for antimicrobial activity. (466) As the presence of brominated Trp residues in the peptide sequence of HC was not crucial for its antimicrobial activity, Solstad *et al.* successfully developed a truncated and optimised lead peptide **P6** with a sequence GWWRRTVA^{8}KVRK^{12}. (467) (Figure 27) This truncated and modified peptide

contained the first 12, *N*-terminally localised amino acids of the original HC sequence, with the following amino acid substitutions: Asp[8] to Ala, Asn[12] to Lys and brominated Trp[2,3] to non-brominated Trp. In addition, the *C*-terminal Lys residue was amidated.

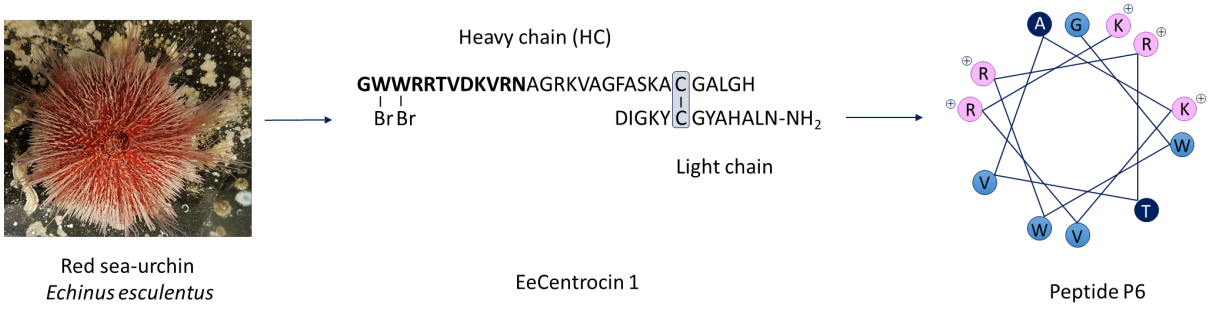

Figure 27. Peptide **P6** was derived from the antimicrobial peptide EeCentrocin 1 which was isolated from the red sea urchin *Echinus esculentus*. («W-Br» in the heavy chain stands for 6-Br-Trp.) Image credit: Prof. Tor Haug.

The third paper (**Paper III)** was based on a previous study showing that cyclic tetrapeptides containing non-canonical β[2,2]-amino acid possess antimicrobial properties. (468) Starting with a similar tetrapeptide scaffold with slightly modified sequence c(Lys-β[2,2]-Leu-Lys), we designed a series of tetrapeptides with the aim of investigating the role of single *L*-amino acid substitution (*L*-Lys to *L*-Arg, *L*-Leu to *L*-Phe), as well as changes in both amphipathicity and stereochemistry, on the peptide antimicrobial and haemolytic properties. (Figure 28)

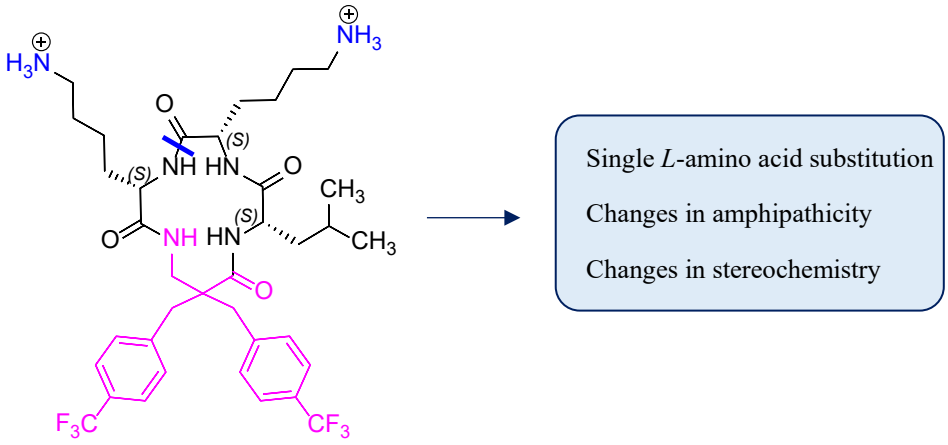

Figure 28. The model peptide **c(Lys-β[2,2]-Leu-Lys)** and the performed modifications.

4.1 Effects of *L*-amino acid substitution

4.1.1 Substitution of *L*-Lys with *L*-Arg in Turgencin A analogues

In the first series of cyclic peptides, **cTurg-1 – cTurg-7**, the change of cationic residues by Lys to Arg substitution, resulted in mostly non-haemolytic analogues, which were slightly more potent against Gram-positive bacteria. (Table 2) Interestingly, against Gram-negative bacteria the increase in activity was much more pronounced, with up to an 8-fold reduction in MIC values.

Table 2. Antimicrobial activity of cyclic Turgencin A analogues (MIC in µg/mL) and their haemolytic activity against human RBC (EC_{50} in µg/mL). Sequence modifications are shown in pink. Sequences in parenthesis denote Cys-Cys cyclic peptides.

		Peptide	Sequence	Charge[2]	Antimicrobial activity (MIC)[1]						RBC Tox. (EC_{50})
					Gram +			Gram -			
					Bs	*Cg*	*Sa*	*Se*	*Ec*	*Pa*	
Cyclic peptides		**cTurg-1**	(CGKKPGGWKC)KL-NH_2	+5	256	16	>256	>256	>256	>256	nt[3]
	W	**cTurg-2**	(CGKKWWGWKC)KL-NH_2	+5	8	4	32	16	64	64	>1045
	W	**cTurg-3**	(CGKKWGWWKC)KL-NH_2	+5	4	4	32	16	32	128	849
	W	**cTurg-4**	(CGKKPWWWKC)KL-NH_2	+5	8	4	64	32	64	256	>1065
	R / W	**cTurg-5**	(CGRRWWGWRC)RL-NH_2	+5	8	4	16	8	8	16	>1101
	R / W	**cTurg-6**	(CGRRWGWWRC)RL-NH_2	+5	4	4	16	8	8	16	1101
	R / W	**cTurg-7**	(CGRRPWWWRC)RL-NH_2	+5	4	4	16	8	16	32	197

[1]Microbial strains; Bs – Bacillus subtilis, Cg – Corynebacterium glutamicum, Sa – Staphylococcus aureus, Se – Staphylococcus epidermidis, Ec – Escherichia coli, Pa – Pseudomonas aeruginosa. [2] Charge at physiological pH (7.4). [3] nt: not tested.

Lys and Arg are similar in several respects. They are both basic amino acids with high aqueous pKa's, (~10.5 and ~13.8) respectively. (469, 470) By being protonated at physiological pH they both engage in electrostatic interactions with anionic membrane components. (Figure 29) However, the nature of these interactions is greatly influenced by the chemical characteristics of their side chain functional groups, guanidine and amine. The guanidinium group (protonated form of guanidine at physiological pH) has a delocalised positive charge and it can form multiple hydrogen bonds with anionic and polar molecules, such as glycerol and phosphate groups. (465, 471, 472) However, Lys having a charge more centred around its side chain amino group, forms only monodentate hydrogen bonds with phosphate groups. As a result, the electrostatic Arg–membrane interaction is believed to be much stronger than that of Lys, what could partly explain the greater efficacy of Arg-containing peptides seen in this work. (473, 474)

Despite its positive effect on peptide potency, we observed that the Lys to Arg substitution in **cTurg-4** gave a more haemolytic peptide, **cTurg-7**. However, the same substitution in cTurg-

2 and cTurg-3 did not increase the degree of haemolysis, indicating that the effect of Arg to Lys substitution on haemolytic properties of peptides is sequence dependant.

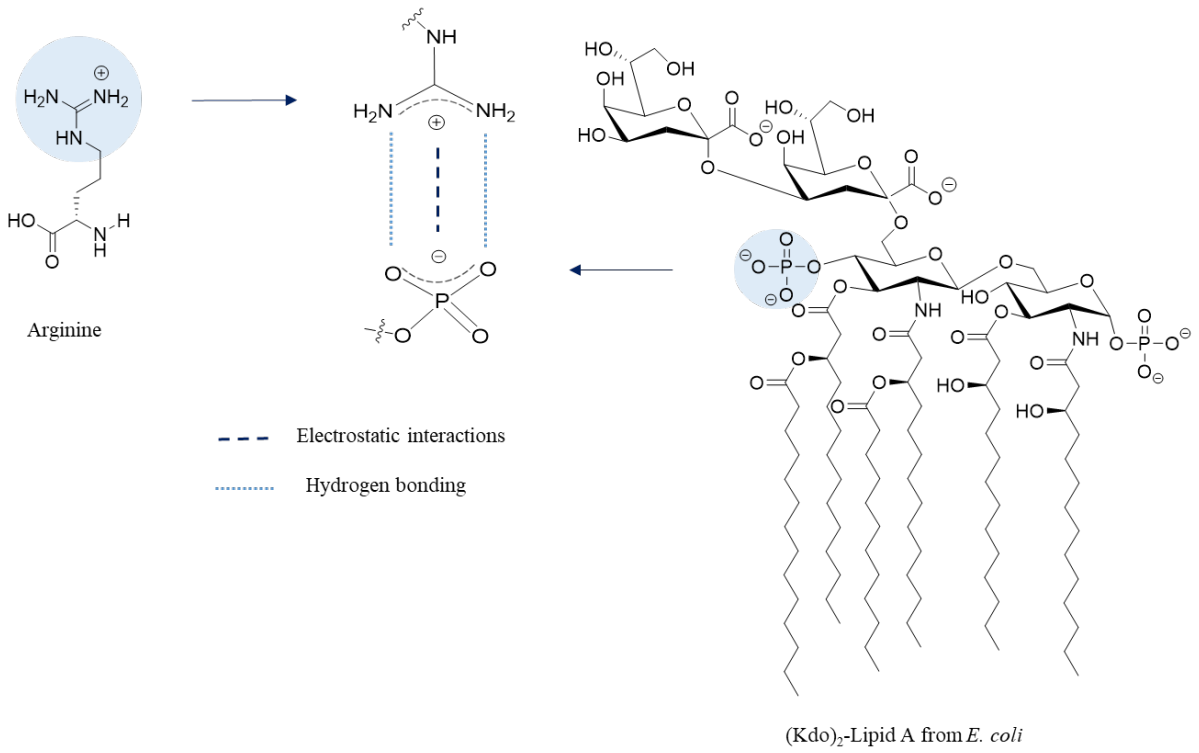

Figure 29. Interactions between the guanidinium group of arginine and oxygen atoms on a phosphate group of $(Kdo)_2$-Lipid A. (Adapted with permission from ref. 472, and ref 189.)

4.1.2 Increasing hydrophobicity by *L*-tryptophan substitution in Turgencin A analogues

Due to its unique structure, a Pro residue limits the conformational space available to the peptide backbone. Turgencin A had only one such residue positioned within its most inner core (between Cys^{17} and Cys^{26}), most likely facilitating the formation of the three disulphide bridges. As opposed to Pro, Gly is an amino acid with the highest conformational freedom allowing neighbouring residues to assume an optimal conformation for binding. (475) By substituting both Pro^5 and $Gly^{6,7}$ for Trp, we wanted to increase hydrophobicity of **Turg-1** while retaining net positive charge of the resultant analogue. Furthermore, such substitution gave us the opportunity to investigate whether Cys-Cys cyclisation would occur in a peptide analogue lacking turn-inducing segment (PG-segment). To our surprise, cyclic peptides were successfully synthesised although reactions were somewhat slow. Substitution of Pro^5 and Gly^6 in **cTurg-1** for Trp, resulted in **cTurg-2**, which had dramatically improved potency, especially against Gram-positive bacteria**.** However, further changes in the positioning of the two Trp residues, either in Lys or Arg analogues, resulted in minor changes in potency.

4.1.3 Increasing charge and amphipathicity of EeCentrocin 1 analogues

In **Paper II,** the first modification of the model peptide **P6** included substitution of Ala^8 for either Lys or Arg to give **P6-K8** and **P6-R8**, respectively. This modification was employed to increase the amhipathicity of the putative α-helical peptide and its net positive charge. Although the overall antimicrobial profile did not change considerably following these changes in the sequence, both analogues had a slightly higher antimicrobial activity against *S. aureus* compared to their parent peptide **P6**, with the Arg analogue being twice as potent as its Lys counterpart. (Table 3) Although both Lys and Arg carry one positive charge, they differ in their interactions with the bacterial membrane as mentioned previously. It is, however, unclear why such increase in activity was not observed for other tested Gram-positive bacteria.

Next, we substituted Thr in position 6 for Trp to further increase hydrophobicity in the non-polar face of the putative α-helix of both **P6-K8** and **P6-R8.** (Figure 30) For the resulting peptides, **P6-W6K8** and **P6-W6R8** this modification had only minor effect on potency. (Table 3) Contrary to our expectations, it seemed that neither amhipathicity nor Ala^8 to Lys/Arg substitution played a significant role in shaping antimicrobial and haemolytic properties of this series of cyclic peptides. Considering the initial high potency of **P6,** it may be that no further improvements in activity could be achieved. In addition, all the above-mentioned modifications resulted in non-haemolytic peptides.

Table 3. Antimicrobial activity of synthesised peptides (MIC in μM) and their toxicity against human RBC (EC_{50} in μM). Sequence modifications compared to the lead peptide **P6** are shown in pink.

Peptide	Sequence	Charge[2]	Rt[3]	Antimicrobial activity (MIC)[1]						RBC Tox (EC_{50})
				Gram +				Gram –		
				Bs	*Cg*	*Sa*	*Se*	*Ec*	*Pa*	
P6	GWWRRTVAKVRK-NH_2	+6	3.32	0.9	0.9	28	1.8	3.5	3.5	>500
P6-K8	GWWRRTVKKVRK-NH_2	+7	3.18	0.8	0.8	13	1.6	3.3	3.3	>500
P6-R8	GWWRRTVRKVRK-NH_2	+7	3.20	0.8	0.8	6.4	1.6	3.2	3.2	>500
P6-W6K8	GWWRRWVKKVRK-NH_2	+7	3.67	1.6	0.8	1.6	1.6	3.1	1.6	>500
P6-W6R8	GWWRRWVRKVRK-NH_2	+7	3.61	1.6	0.8	1.6	0.8	1.6	1.6	>500

[1] Microbial strain; Bs – *Bacillus subtilis* (ATCC 23857), Cg – *Corynebacterium glutamicum* (ATCC 13032), Sa – *Staphylococcus aureus* (ATCC 9144), Se – *Staphylococcus epidermidis* RP62A (ATCC 35984), Ec – *Escherichia coli* (ATCC 25922), Pa – *Pseudomonas aeruginosa* (ATCC 27853). [2] Charge at physiological pH (7.4). [3] Retention time (min) on RP-UPLC.

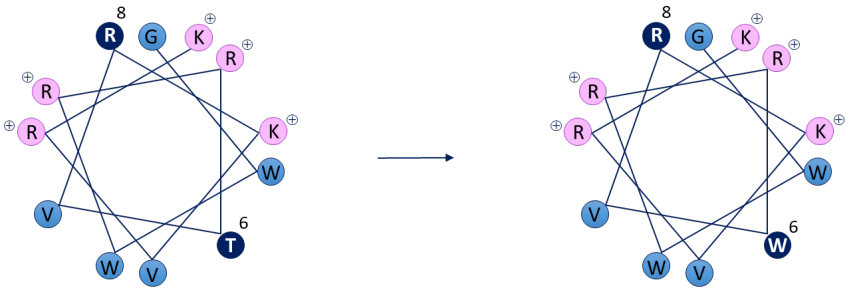

P6-R8
GWWRR**T**^{6}VRKVRK-NH_2
μH=5.01

P6-W6R8
GWWRR**W**^{6}VRKVRK-NH_2
μH=6.84

Figure 30. The helical wheel diagram of the peptide **P6-R8** and its optimised analogue **P6-W6R8**: Thr^{6} in the sequence of **P6-R8** was replaced with Trp to give **P6-W6R8**. The hydrophobic moment (μH), as a measure of amphipathicity of an α-helix for each peptide, was calculated using the MPEx software. (*https://blanco.biomol.uci.edu/mpex/*).

4.2 Effects of acylation of Turgencin A and EeCentrocin 1 analogues

N-Terminal acylation is yet another modification used to improve stability and potency of AMPs. Some lipopeptides (*e.g.*, colistin and daptomycin) are already in clinical use as essential antibiotics. (476, 477) Acylated peptides are more hydrophobic and in some instances more potent than their non-acylated analogues. However, it is generally recognised that hydrophobicity of amphipathic α-helical peptides positively correlates with their haemolytic activity. (478, 479) Therefore, tuning the length of the acyl chain may serve as a promising strategy for improving peptide selectivity. Therefore, we further wanted to investigate the effects of *N*-terminal acylation on the antimicrobial activity and mammalian cell toxicity of both Turgencin A and EeCentrocin-1 derived analogues. (**Papers I** and **Paper II**)

In **Paper I** we introduced fatty acids of different length at the *N*-terminus of selected cyclic peptides: **cTurg-1** (inactive peptide), **cTurg-2** (the most potent peptide among the Lys analogues) and **cTurg-6** (the most potent peptide among the Arg analogues). (Table 4) *N*-terminally acylated linear peptides were also synthesised for comparison. All lipopeptides had the same charge of +4. The conjugation was done with aliphatic fatty acids reported to be of optimal length for achieving improved activity: octanoic acid (C_8), decanoic acid (C_{10}) and dodecanoic acid (C_{12}). (403) For both linear and cyclic **Turg-1** lipopeptides, we observed a positive correlation between elongation of the fatty acid chain and the lipopeptide antimicrobial activity. This correlation was, however, reverse for the **cTurg-2** and **cTurg-6** lipopeptide

analogues, probably due to their slightly higher intrinsic hydrophobicity, as evidenced by their longer retention times (3.87 min and 4.02 min) measured by reversed-phase ultra-performance liquid chromatography (RP-UPLC). Moreover, conjugates with longer acyl chains may have reduced antibacterial activity because of aggregation and self-assembly, as demonstrated by Sikorska *et al.* in their study on short acylated Arg-rich AMPs. (480) The increase in the acyl chain length was also positively correlated with haemolytic activity, except for the linear **Turg-1** lipopeptides, which were all non-haemolytic. Our results support previous research indicating that there is a hydrophobicity window within which good peptide selectivity could be obtained. (481) The lower and the upper limit, in terms of fatty acid chain length, may vary depending on the initial hydrophobicity of the peptide.

Table 4. Antimicrobial activity of selected lipopeptides (MIC in µg/mL) and their haemolytic activity against human RBC (EC_{50} in µg/mL). Sequence modifications are shown in pink. Sequences in parenthesis denote Cys-Cys cyclic peptides.

		Peptide	Sequence	Rt[2]	Antimicrobial activity (MIC)[1]						RBC tox. (EC_{50})
					Gram +			Gram –			
					Bs	*Cg*	*Sa*	*Se*	*Ec*	*Pa*	
Linear lipopeptides		**C_8-Turg-1**	C_8-CGKKPGGWKC KL-NH_2	4.38	8	4	128	32	32	128	>943
		C_{10}-Turg-1	C_{10}-CGKKPGGWKC KL-NH_2	4.89	4	4	16	8	16	32	>957
		C_{12}-Turg-1	C_{12}-CGKKPGGWKC KL-NH_2	5.44	4	4	8	4	8	16	>971
		C_8-Turg-2	C_8-CGKKWWGWKC KL-NH_2	4.97	8	4	8	8	16	16	198
	W	**C_{10}-Turg-2**	C_{10}-CGKKWWGWKC KL-NH_2	5.41	8	4	8	8	8	16	64
		C_{12}-Turg-2	C_{12}-CGKKWWGWKC KL-NH_2	5.89	8	16	16	8	16	32	55
Cyclic lipopeptides		**C_8-cTurg-1**	C_8-(CGKKPGGWKC)KL-NH_2	4.27	4	4	128	32	32	128	>942
		C_{10}-cTurg-1	C_{10}-(CGKKPGGWKC)KL-NH_2	4.74	2	2	16	4	8	32	>956
		C_{12}-cTurg-1	C_{12}-(CGKKPGGWKC)KL-NH_2	5.22	2	2	4	4	4	16	219
		C_8-cTurg-2	C_8-(CGKKWWGWKC)KL-NH_2	4.70	2	2	4	4	4	8	439
	W	**C_{10}-cTurg-2**	C_{10}-(CGKKWWGWKC)KL-NH_2	5.11	2	4	4	4	8	8	106
		C_{12}-cTurg-2	C_{12}-(CGKKWWGWKC)KL-NH_2	5.55	4	8	8	8	16	16	32

[1] Microbial strain; Bs – Bacillus subtilis (ATCC 23857), Cg – Corynebacterium glutamicum (ATCC 13032), Sa – Staphylococcus aureus (ATCC 9144), Se – Staphylococcus epidermidis RP62A (ATCC 35984), Ec – Escherichia coli (ATCC 25922), Pa – Pseudomonas aeruginosa (ATCC 27853). [2] Retention time (min) on RP-UPLC.

An interesting observation was made in a recent review by Rounds *et al.* (403) While investigating the determinants of action for the most potent linear amphipathic lipopeptides reported in the literature, the authors noticed that the sum of the number of amino acids in the peptide sequence and the number of acyl carbons was fairly constant at 20, with the corresponding length of ~31-33 Å. This length is found to be relatively close to the thickness of the 1-palmitoyl-2-oleoyl-phosphatidylcholine/1-palmitoyl-2-oleoyl-phosphatidylglycerol bilayer (~39 Å), leading the authors to suggest that lipopeptides insertion into the bilayer might

be easier compared to their non-acylated analogues. Although this assumption may be valid for our linear and cyclic **Turg-2** and **Turg-6** lipopeptides, they were contrary to our observation for corresponding **Turg-1** analogues. As all three peptides had 12 amino acid residues, according to the "number 20" criteria the acyl chain with 8 carbons, namely acylation with octanoic acid, would be the most optimal for activity. However, for the **Turg-1** analogues, conjugation with octanoic acid did not result in the lipopeptide with the highest potency but rather acylation with dodecanoic acid, violating the "number 20" criteria. This indicates, as previously mentioned, that the peptide initial hydrophobicity may be an important factor influencing the properties of corresponding acylated analogues.

It is worth noting that the concept proposed by Rounds *et al.* may be in part applicable even when peptide sequence of the molecule is composed of only one cationic amino acid, namely Lys. (403) By coupling aliphatic amines to the *C*-terminus of Lys, Ghosh *et al.* were able to design a short series of compounds, focusing only on two physicochemical properties, positive charge and hydrophobicity. (417) Among the mono-substituted analogues, the palmitylamine (C_{16}) conjugate had the highest antimicrobial and haemolytic activity (what is a bit higher than what would be expected according to the mentioned "number 20" criteria, (approx. 12 – 14 carbons), whereas further increase in the amine chain length to either stearylamine (C_{18}) or arachidylamine (C_{20}) analogues led to a complete loss of activity. Next, they designed di-substituted (dialkylamidated) analogues containing aliphatic chains half the size of the corresponding mono-substituted counterparts. This modification resulted in three relatively potent conjugates: C_8-Lys-C_8, C_8-Lys-C_{10}, C_{10}-Lys-C_{10}. These findings indicate that not only the overall length of the lipophilic segment (shown to be pertinent to α-helical lipopeptides), but also its structure could be an important determinant of action. Single-chain analogues (which mimicked linear lipopeptides) in the above-mentioned study required longer aliphatic chain (in this case 16 carbons) to gain optimal antimicrobial activity, than what would be expected if they were to fulfil the criteria of optimal proposed length of 31-33 Å (12–13 carbon unites). This might be because the initial peptide sequence composed of only Lys was not hydrophobic. Therefore, acylation with a longer hydrocarbon chain was required to achieve optimal hydrophobicity. Interestingly, the trend was quite different for the di-substituted analogues. Presence of yet another lipid chain adds to the overall hydrophobicity of the Lys conjugate, rendering even those analogues with much shorter lipophilic segment antimicrobial. However, it cannot be excluded that structural resemblance to phospholipid molecules may in

part explain increased affinity of di-substituted analogues towards membrane bilayer. (It should be noted that fatty acids have been also reported to have antimicrobial properties, although research efforts were mostly focused on those having polyunsaturated character.) (482)

For the design of lipopeptides in **Paper II**, we chose the linear Arg[8] modified peptide **P6-R8** as a template for lipidation, as it was more potent than its Lys analogue. (Figure 31)

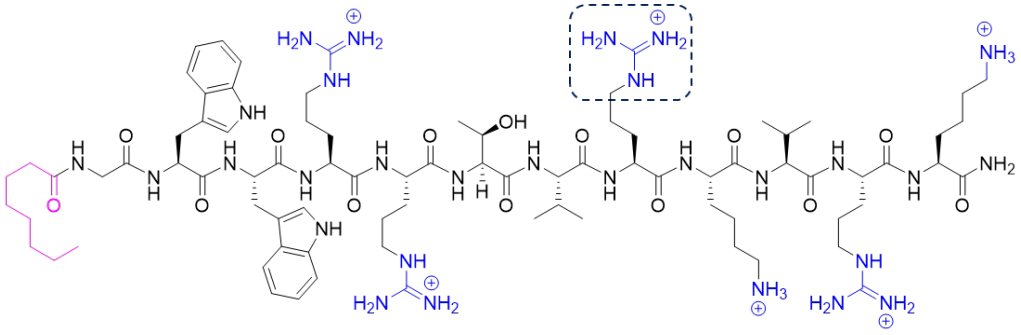

Figure 31. Lipopeptide **C_8-P6-R8**. Lipid chain is coloured in pink, whereas Arg at position 8 is marked with a dashed dark-blue square. Cationic side groups are coloured in light blue.

According to our results, all three synthesised lipopeptides, **C_8-P6-R8**, **C_{10}-P6-R8** and **C_{12}-P6-R8** had in general either unchanged or slightly reduced activity compared to their parent peptide, **P6-R8**. (Table 5) However, their activity against *S. aureus* was slightly improved.

Table 5. Antimicrobial activity (MIC in μM) and haemolytic activity against human RBC (EC_{50} in μM) of synthesised lipopeptides and their parent sequence **P6-R8**.

Peptide	Sequence	Charge[2]	Rt[3]	Antimicrobial activity (MIC)[1]						RBC tox. (EC_{50})
				Gram +				Gram –		
				Bs	*Cg*	*Sa*	*Se*	*Ec*	*Pa*	
P6-R8	GWWRRTVRKVRK-NH_2	+7	3.20	0.8	0.8	6.4	1.6	3.2	3.2	>500
C_8-P6-R8	C_8-GWWRRTVRKVRK-NH_2	+6	4.70	1.6	1.6	1.6	1.6	6.4	6.4	>500
C_{10}-P6-R8	C_{10}-GWWRRTVRKVRK-NH_2	+6	5.16	3.2	3.2	3.2	1.6	3.2	6.3	173
C_{12}-P6-R8	C_{12}-GWWRRTVRKVRK-NH_2	+6	5.67	3.1	3.1	3.1	3.1	3.1	6.3	26

[1] Microbial strain; Bs – *Bacillus subtilis* (ATCC 23857), Cg – *Corynebacterium glutamicum* (ATCC 13032), Sa – *Staphylococcus aureus* (ATCC 9144), Se – *Staphylococcus epidermidis* RP62A (ATCC 35984), Ec – *Escherichia coli* (ATCC 25922), Pa – *Pseudomonas aeruginosa* (ATCC 27853). [2] Charge at physiological pH (7.4). [3] Retention time (min) on RP-UPLC.

Surprisingly, the potency against *P. aeruginosa* was reduced 2-fold, and against both *B. subtilis* and *C. glutamicum* 2- to 4-fold, regardless of the lipid-chain length. Given that further acyl chain elongation did not improve potency of the Arg analogue, **C_8-P6-R8,** it seems that the hydrophobicity threshold might have been achieved already with the C_8-acyl chain. An interesting observation was made pertaining to haemolytic activity of the three synthesised

lipopeptides. Namely, stepwise elongation with only two carbons resulted in a dramatic increase in haemolytic activity, from the non-haemolytic C_8 analogue, **C_8-P6-R8** to the highly haemolytic C_{12} analogue, **C_{12}-P6-R8**. These results were in line with the previous research showing a positive correlation between acyl chain length and degree of haemolysis. (479, 483) Moreover, these results were also in accordance with the "number 20" criteria. (403)
In general, our results demonstrated that antimicrobial activity could be successfully fine-tuned by incorporating hydrophobic residues in a peptide sequence and/or via *N*-terminal acylation.

4.3 Effects of Cys-Cys side chain cyclisation of Turgencin A analogues

Turgencin A is a Cys-rich AMP with following Cys-Cys connectivities: Cys^8-Cys^{33}, Cys^{12}-Cys^{29}, and Cys^{17}-Cys^{26}. (Figure 32) As we focused on the cationic inner loop region flanked by two Cys residues (Cys^{17} and Cys^{26}) in the native sequence, we decided to mimic this structure by performing Cys-Cys cyclisation of our short linear analogues. This reaction was performed either under open air conditions or with an additional, continuous supply of oxygen ($O_{2\ (g)}$). The purified lipopeptides (5 mg) were dissolved in Milli-Q water to a concentration of 250 µg/mL. The reaction proceeded at room temperature (r.t.) under continuous magnetic stirring. The progress of the reaction was monitored by Ultra-Performance Liquid Chromatography–High-Resolution Mass Spectrometry (UPLC-HRMS). For the more hydrophobic cyclic Turg-peptides (Turg-2 and Turg-6) we observed significant reduction in the reaction rate. This was especially prominent for the peptides acylated with dodecanoic acid, most likely due to their reduced water solubility and the lack of turn-inducing Pro residue.

Figure 32. Amino acid sequence of Turgencin A with the 12-residue loop region underlined (residues 17–28). Disulphide connectivities in the native Turgencin A peptide, Cys^8-Cys^{33}, Cys^{12}-Cys^{29} and Cys^{17}-Cys^{26} are presented in dark blue lines. (460)

Cys-Cys cyclisation of the linear Turg-lipopeptides designed in **Paper I** gave analogues with either unchanged or slightly increased antimicrobial activity. (Table 4) The observed increase in potency may have resulted from the additional structural stabilisation of the Turg-lipopeptides. As for haemolytic activity, it has been shown that intramolecular cyclisation may cause a reduction in haemolysis, as observed for melittin and magainin 2 analogues. (484) Moreover, Cys-Cys cyclisation can reduce haemolytic activity of cyclic peptides and

consequently improve their selectivity towards bacterial cells. (485) By contrast, our results showed no consistent pattern, as we observed both increase (*e.g.*, **C_{12}-cTurg-1**) and reduction in haemolytic activity (*e.g.*, **C_8-cTurg-2, C_{10}-cTurg-2**) following Cys-Cys cyclisation of linear analogues.

4.4 Effects of head-to-tail cyclisation of EeCentrocin 1 analogues

Backbone cyclisation results in conformationally more constrained peptides with an overall charge reduced by one unit for *C*-terminally amidated peptides. Many studies have shown that this type of cyclisation is effective in increasing proteolytic stability of cyclic analogues against exopeptidases and their cell-membrane permeability. (486, 487) Additionally, cyclisation may also enhance cell selectivity by reducing host cytotoxicity. (347) Thus, in **Paper II** our aim was to study the effects of head-to-tail cyclisation of selected EeCentrocin 1 analogues on their antimicrobial and haemolytic activity.

For the head-to-tail cyclisation of linear peptides a pseudo-high dilution cyclisation method was used. (Figure 33, step 2)

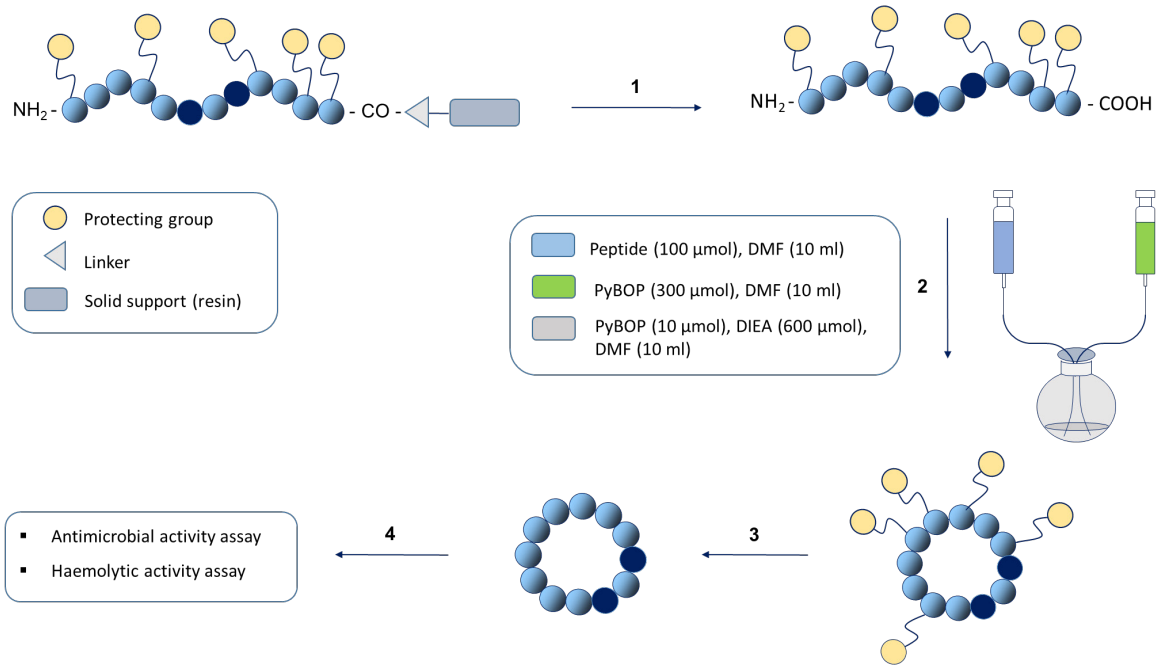

Figure 33. Strategy for preparing head-to-tail cyclic peptides using two syringes attached to a mechanical pump for creating pseudo-high dilution conditions. 1) Fmoc-SPPS synthesis using a preloaded 2-Cl-Trt resin and subsequent cleavage from the resin with HFIP/DCM. 2) Head-to-tail cyclisation. 3) Deprotection of side chain protecting groups. 4) Bioactivity screening following RP-HPLC peptide purification. (PyBOP-Benzotriazole-1-yl-oxy-tris-pyrrolidino-phosphonium hexafluorophosphate; DMF-*N,N*-dimethylformamide)

The setup allowed for very slow addition (0.01 mL/min) of a linear peptide (contained in syringe 1) and a coupling reagent (contained in syringe 2), thereby creating pseudo-high dilution conditions. (423) The method required a low amount of solvent in total (50 mL *N,N*-dimethylformamide (DMF), for cyclisation of 100 µmol of linear protected peptide). No dimers or polymers of the peptides were isolated after the head-to-tail cyclisation procedures. Total isolated yield after RP-HPLC purification for the cyclised peptides, ranged from 9.8% to 14.5%. The overview of the synthesis flow is shown in Figure 33.

According to our findings, cyclisation did not adversely affect haemolytic properties of the peptides since all cyclic, as well as linear analogues, were non-haemolytic. (Table 6). Cyclisation did, however, result in peptides with overall lower antimicrobial potency possibly due to disruption of a putative α-helical structure and decrease in the overall net positive charge. The only improvements in activity were observed for **cP6-R8** and **cP6-W6R8** against *C. glutamicum*. Interestingly, whereas linear peptides exerted similar or identical activity against both *E. coli* and *P. aeruginosa*, the cyclic peptides **cP6** and **cP6-R8** showed 17-fold reduction in potency against *P. aeruginosa* compared to their linear analogues. This may be due to lower permeability of the outer membrane of *P. aeruginosa* compared to that of *E. coli,* protease production, and/or the presence of efflux pumps capable of extruding antimicrobials from the bacterial cell. (488, 489) The latter mechanism would, however, be an option only if peptides were able to reach intracellular compartment.

Table 6. Antimicrobial activity of synthesised peptides against bacteria (MIC in µM), and their toxicity against human RBCs (EC_{50} in µM). Sequence modifications are shown in pink, and sequences in parentheses denote head-to-tail cyclic peptides.

	Peptide	Sequence	Charge[2]	Rt[3]	Antimicrobial activity (MIC)[1]						RBC tox. (EC_{50})
					Gram +			Gram –			
					Bs	*Cg*	*Sa*	*Se*	*Ec*	*Pa*	
Linear peptides	**P6**	GWWRRTVAKVRK-NH_2	+6	3.32	0.9	0.9	28	1.8	3.5	3.5	>500
	P6-R8	GWWRRTVRKVRK-NH_2	+7	3.20	0.8	0.8	6.4	1.6	3.2	3.2	>500
	P6-W6R8	GWWRRWVRKVRK-NH_2	+7	3.61	1.6	0.8	1.6	0.8	1.6	1.6	>500
Cyclic peptides	**cP6**	c(GWWRRTVAKVRK)	+5	3.36	1.9	0.9	60	15	7.5	60	>500
	cP6-R8	c(GWWRRTVRKVRK)	+6	3.20	1.7	0.1	6.8	1.7	3.4	55	>500
	cP6-W6R8	c(GWWRRWVRKVRK)	+6	3.76	0.8	0.4	1.6	0.8	6.6	3.3	>500
	cP6-W4R6,8	c(GWWWRRVRKVRK)	+6	3.62	0.8	0.8	3.3	1.6	3.3	6.6	>500

[1] Microbial strain; Bs – Bacillus subtilis (ATCC 23857), Cg – Corynebacterium glutamicum (ATCC 13032), Sa – Staphylococcus aureus (ATCC 9144), Se – Staphylococcus epidermidis RP62A (ATCC 35984), Ec – Escherichia coli (ATCC 25922), Pa – Pseudomonas aeruginosa (ATCC 27853). [2] Charge at physiological pH (7.4). [3] Retention time (min) on RP-UPLC.

Our last modification included grouping three Trp residues by exchanging positions between Arg[4] and Trp[6] in the sequence of **cP6-W6R8**. Contrary to our expectation, the resultant peptide cP6-W4R6,8 had similar properties to those of **cP6-W6R8**, suggesting that having three adjacent Trp residues does not confer additional favourable properties. **(**Figure 34)

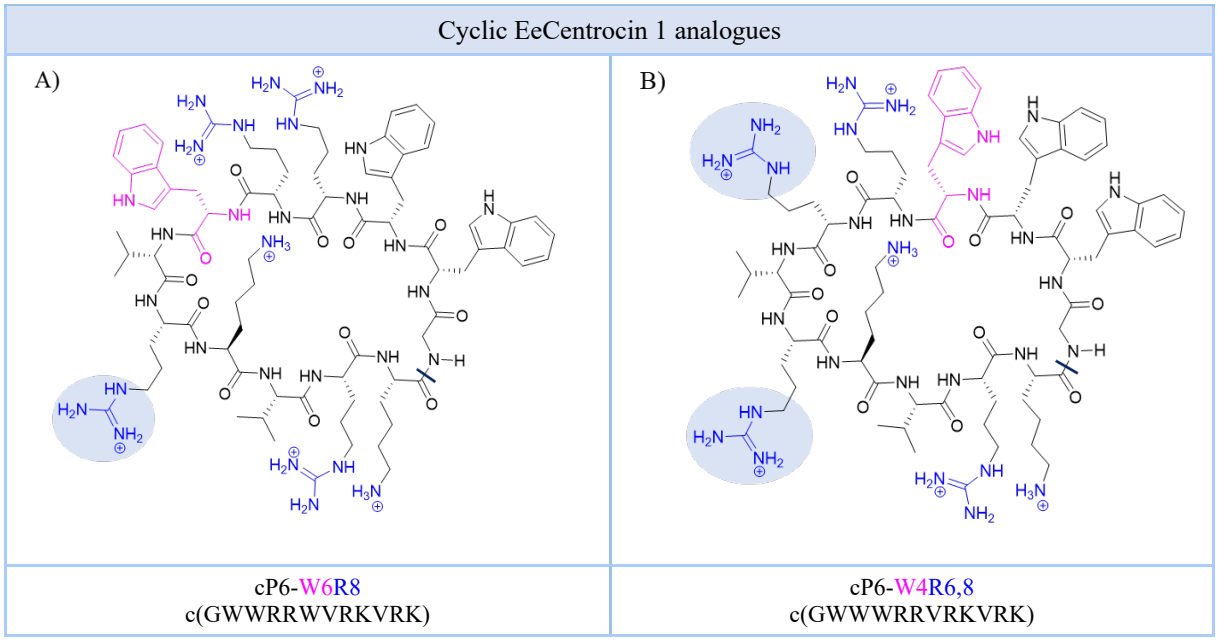

Figure 34. A) Head-to-tail cyclised **P6** analogue, **cP6-W6R8**. **B)** Structure of **cP6-W4R6,8** with a compact hydrophobic region containing three adjacent Trp residues. The dark blue line shows the site of head-to-tail cyclisation.

4.5 Cyclic tetrapeptide analogues-synthesis

4.5.1 Synthesis of Fmoc-β^{2,2}-amino acid

The α,α-disubstituted β^{2,2}-amino acid containing two 4-(trifluoromethyl)benzyl side chains, termed β^{2,2}, was synthesised following the protocol described by Paulsen *et al.* (490) (Figure 35). In brief the initial dialkylation of methyl cyanoacetate by 1,8-diazabicyclo-[5.4.0]undec-7-ene (DBU) was followed by nitrile reduction with H_2 (g)/Raney Nickel. The resulting β^{2,2}-amino ester was hydrolysed with lithium hydroxide (LiOH) pre-dissolved in water. After pH adjustment to pH=8, the final step included the protection of the free amine by subsequent addition of N-(9-fluorenylmethoxy-carbonyloxy) succinimide (Fmoc-OSu). The reaction was followed by thin layer chromatography (TLC) and visualised with either UV light (A_{254nm}) or by immersion in potassium permanganate after light heating of the plates with a heating gun.

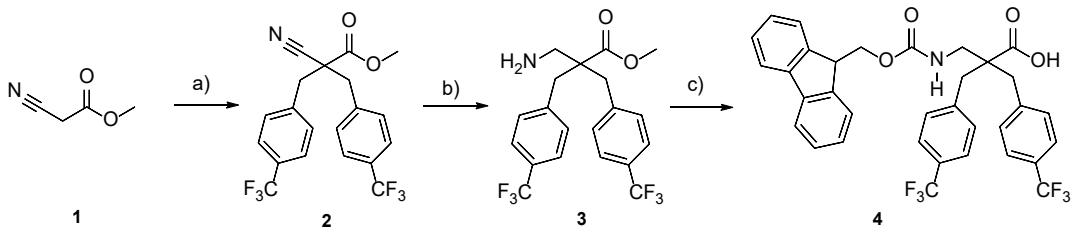

Figure 35. Synthesis of the $\beta^{2,2}$-amino acid building block, termed $\beta^{2,2}$ a) $CF_3C_6H_4CH_2Br$ (4-(trifluoromethyl)benzyl bromide), DBU, CH_2Cl_2, r.t.; b) Raney-Nickel, H_2 (g), ethylacetate (EtOAc), 45 °C, 18 h; c) i. LiOH, dioxane:water (4:1) reflux, 2 h, ii. aq. HCl to pH 8 then Fmoc-OSu, r.t. 18 h. (490)

4.5.2 Synthesis of linear tetrapeptides

In the next step, the linear tetrapeptides were synthesised by microwave solid-phase peptide synthesis on preloaded 2-chlorotrityl chloride resin. Removal of the Fmoc group was performed under standard conditions using 20% piperidine/DMF. Coupling reaction was performed in the presence of HCTU (3 equiv.) and a base, *N,N*-diisopropylethylamine (DIEA) (6 equiv.). Microwave heating (75°C, 15 min) was applied during coupling of all amino acids, except for arginine, where coupling was done at room temperature (r.t.) for 60 min to avoid side reactions.

4.5.3 Head-to-tail cyclisation of linear tetrapeptides

As the head-to-tail cyclisation of the EeCentrocin analogues was shown to be successful, we aimed at evaluated the applicability of the same method for the synthesis of much smaller, constrained rings. The overview of the synthesis flow is presented in Figure 33. However, for more detailed explanation, the reader is referred to the **Paper II**, Method section.

4.6 The role of amphipathicity and *L*- to *L*/*D*-amino acid substitution in the cyclic tetrapeptide scaffold

Development of effective drug candidates based on α-peptides is often limited by their low proteolytic stability *in vivo* and high conformational freedom. One of the strategies to overcome these limitations is to introduce β-amino acid(s) in the sequence of α-peptides. (491) By incorporating aromatic, fluorinated $\beta^{2,2}$-amino acid in a tetrapeptide sequence c(Lys-$\beta^{2,2}$-Lys-Lys), Paulsen *et al.* successfully designed relatively potent analogues with low haemolytic activity. (468) In particular, analogues containing $\beta^{2,2}$-amino acid with two 4-(trifluoromethyl)benzyl side chain groups were most promising candidates for further optimisation, as they were relatively potent and mostly non-haemolytic. This work served as a starting point in the design of our series of tetrapeptides **(Paper III**), enabling us to further investigate the role of *L*-amino acid substitution (Lys to Arg and Leu to Phe), as well as changes

in both amphipathicity and stereochemistry, on peptide antimicrobial and haemolytic properties.

4.6.1 Effects of *L*-amino acid substitution

The first peptide in the tetrapeptide series, **001** c(Lys-$\beta^{2,2}$-Leu-Lys) was shown to have good antimicrobial activity against all tested bacterial strains (MIC: 2 – 8 µg/mL), although with considerable cell toxicity (EC_{50} 105 µg/mL). (Table 7) Replacement of each *L*-Lys residue in the initial tetrapeptide sequence **001** with *L*-Arg, resulted in an equally potent, but more haemolytic analogue, **002** c(Arg-$\beta^{2,2}$-Leu-Arg) (EC_{50} 33 µg/mL). This difference in selectivity towards RBCs may be attributed to different interactions with membrane components of these cells and those of bacterial cells, as previously discussed. Lys residues have been shown to interact weakly with zwitterionic phospholipids, but much stronger with anionic phospholipids, whereas Arg residues interact strongly with both membrane components. (492) Further incorporation of a third Arg residue, via Leu to Arg substitution, gave an overall most potent tetrapeptide, **006** c(Arg-$\beta^{2,2}$-Arg-Arg), with MIC values ranging from 1–2 µg/mL against Gram-positive bacteria, and MIC values from 2–4 µg/mL against Gram-negative bacteria.

Table 7. Antimicrobial activity (MIC in µg/mL) and haemolytic activity against human RBC (EC_{50} in µg/mL) of selected tetrapeptides.

Peptide	Sequence	Charge[2]	Rt[3]	Antimicrobial activity (MIC)[1]						RBC tox. EC_{50}
				Gram +				Gram –		
				Bs	*Cg*	*Sa*	*Se*	*Ec*	*Pa*	
001	c(Lys-$\beta^{2,2}$-Leu-Lys)	+2	6.23	2	2	4	4	4	8	105
002	c(Arg-$\beta^{2,2}$-Leu-Arg)	+2	6.38	2	2	4	4	4	8	33
006	c(Arg-$\beta^{2,2}$-Arg-Arg)	+3	5.08	1	2	1	1	2	4	279

[1] Microbial strain; Bs – *Bacillus subtilis* (ATCC 23857), Cg – *Corynebacterium glutamicum* (ATCC 13032), Sa – *Staphylococcus aureus* (ATCC 9144), Se – *Staphylococcus epidermidis* RP62A (ATCC 35984), Ec – *Escherichia coli* (ATCC 25922), Pa – *Pseudomonas aeruginosa* (ATCC 27853). [2] Charge at physiological pH (7.4). [3] Retention time (min) on RP-UPLC.

4.6.2 Changes in amphipathicity

Previous studies have shown that amphipathicity is an important determinant of antimicrobial action of AMPs. (337) Although these studies mainly focused on relatively longer amphipathic peptides, which assume α-helical secondary structure upon interaction with bacterial membranes, amphipathicity may as well be an important factor influencing antimicrobial properties of much smaller, cyclic tetrapeptides. An indication of this could be found in a more recent work done by Paulsen *et al*., where the authors synthesised a short series of relatively potent amphipathic tetrapeptides with the following sequence: c(Lys-$\beta^{2,2}$-Xaa-Lys) (Xaa stands for Gly, Ala or Phe). (468)

In this work, we wanted to explore the effects of amphipathicity (denoting presence of separated hydrophilic and hydrophobic regions in a molecule) on the antimicrobial activity and RBC toxicity of such cyclic tetrapeptides. To do so, we designed analogues with alternating cationic and hydrophobic residues, **003** c(Leu-Lys-$\beta^{2,2}$-Lys) and **004** c(Leu-Arg-$\beta^{2,2}$-Arg). (Figure 36)

Amphipathic cyclic tetrapeptides	Non-amphipathic cyclic tetrapeptides
A) 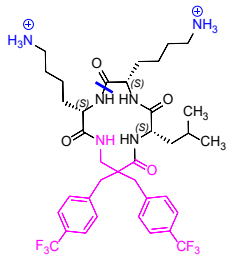	B) 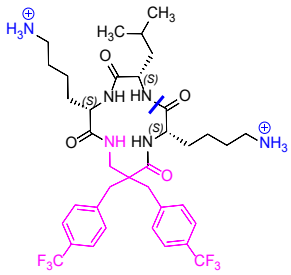
c(Lys-$\beta^{2,2}$-Leu-Lys) **001**	c(Leu-Lys-$\beta^{2,2}$-Lys) **003**
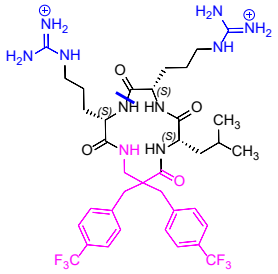	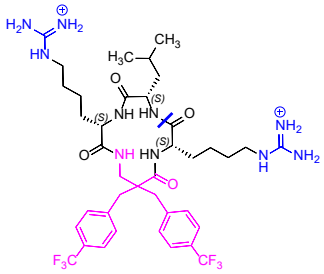
c(Arg-$\beta^{2,2}$-Leu-Arg) **002**	c(Leu-Arg-$\beta^{2,2}$-Arg) **004**

Figure 36. Structure of amphipathic **(A)** and corresponding non-amphipathic **(B)** Lys and Arg analogues.

For the resulting non-amphipathic cyclic tetrapeptides, **003 and 004,** we observed minor changes in MIC against Gram-positive bacteria and a significant reduction in potency against Gram-negative bacteria, compared to their amphipathic analogues. (Table 8) This reduction was especially prominent for the Lys-containing analogue, **003** with 8-fold reduction in potency against both *E. coli* and *P. aeruginosa*. Importantly, the non-amphipathic analogues had greatly reduced toxicity towards RBCs.

Table 8. Antimicrobial activity (MIC in µg/mL) and haemolytic activity against human RBC (EC_{50} in µg/mL) of selected tetrapeptides.

Peptide	Sequence	Charge[2]	Rt[3]	Antimicrobial activity (MIC)[1]						RBC tox. EC_{50}
				Gram +			Gram –			
				Bs	*Cg*	*Sa*	*Se*	*Ec*	*Pa*	
001	c(Lys-$\beta^{2,2}$-Leu-Lys)	+2	6.23	2	2	4	4	4	8	105
003	c(Leu-Lys-$\beta^{2,2}$-Lys)	+2	5.30	4	2	8	8	32	64	>492
002	c(Arg-$\beta^{2,2}$-Leu-Arg)	+2	6.38	2	2	4	4	4	8	33
004	c(Leu-Arg-$\beta^{2,2}$-Arg)	+2	5.46	2	2	4	2	8	32	215

[1] Microbial strain; Bs – *Bacillus subtilis* (ATCC 23857), Cg – *Corynebacterium glutamicum* (ATCC 13032), Sa – *Staphylococcus aureus* (ATCC 9144), Se – *Staphylococcus epidermidis* RP62A (ATCC 35984), Ec – *Escherichia coli* (ATCC 25922), Pa – *Pseudomonas aeruginosa* (ATCC 27853). [2] Charge at physiological pH (7.4). [3] Retention time (min) on RP-UPLC.

As shown in Figure 36 the amphipathic cyclic tetrapeptide **001** had two adjacent Lys residues and a clear delineation between cationic and hydrophobic segments in the molecule, in contrast to its non-amphipathic analogue **003,** whose cationic residues, although with the same orientation, were further apart. Our results suggest that amphipathicity is important for the initial electrostatic interactions with the bacterial membrane, especially that of Gram-negative bacteria. These interactions may be considerably reduced due to the conformational constraints induced by the ring, as well as the distance between the two cationic side chains. Our findings suggest that "breaking" amphipathicity could be used to improve selectivity of short cyclic peptides, by reducing undesirable haemolytic toxicity.

4.6.3 *L*-Leu to *L*-Phe substitution

The previous work in our group showed that an amphipathic cyclic tetrapeptide c(Lys- $\beta^{2,2}$-Phe-Lys) exerted high antimicrobial and haemolytic activity (compound **5d**). (468) To investigate whether changes in amphipathicity could reduce undesirable haemolytic properties of this peptide and its Arg analogue, we replaced *L*-Leu with *L*-Phe in the sequences of the two non-amphipathic analogues, **003** c(Leu-Lys-$\beta^{2,2}$-Lys) and **004** c(Leu-Arg-$\beta^{2,2}$-Arg). For the modified peptides, **031** c(Phe-Lys-$\beta^{2,2}$-Lys) and **041** c(Phe-Arg-$\beta^{2,2}$-Arg), antimicrobial activity

was mostly improved, with 2-fold reduction in MIC compared to their corresponding Leu counterparts. (Table 9) However, activity against Gram-negative bacteria was still relatively low compared to that of Gram-positive bacteria. The *L*-Leu to *L*-Phe substitution had unfavourable effect only on Arg-Phe analogue, **041,** which was more haemolytic (EC_{50} 116 µg/mL) than its Arg-Leu counterpart, **004** (EC_{50} 215 µg/mL). The corresponding Lys-Phe-containing analogue remained non-haemolytic (EC_{50} >509 µg/mL). However, we could not ascertain with the data at hand whether cell toxicity of the Lys analogues changed, since haemolytic activity was not tested above EC_{50} 500 µg/mL. Compared with the previously synthesised amphipathic Lys-Phe-containing tetrapeptide (compound **5d**), its non-amphipathic analogue **031**, was non-haemolytic, although with reduced antimicrobial activity.

Of note, Phe-containing analogues did not differ from their Leu-containing parent peptides with respect to either hydrophobicity (comparison of retention times obtained from RP-UPLC), or their net charge (+2). However, compared to Leu, Phe has a larger hydrophobic surface and a strong preference for the interfacial water-lipid region. (493, 494) These properties of Phe residue seemed to be important in shaping both antimicrobial and haemolytic properties of our cyclic tetrapeptides.

Table 9. Antimicrobial activity (MIC in µg/mL) and haemolytic activity against human RBC (EC_{50} in µg/mL) of selected cyclic tetrapeptides.

Peptide	Sequence	Charge[2]	Rt[3]	Antimicrobial activity (MIC)[1]						RBC tox. EC_{50}
				Gram +			Gram –			
				Bs	*Cg*	*Sa*	*Se*	*Ec*	*Pa*	
003	c(Leu-Lys-$\beta^{2,2}$-Lys)	+2	5.30	4	2	8	8	32	64	>492
031	c(Phe-Lys-$\beta^{2,2}$-Lys)	+2	5.33	2	1	8	4	16	32	>509
5d	c(Lys-$\beta^{2,2}$-Phe-Lys) (Paulsen *et al.*)	+2	-	-	0.1	2	-	4	2	88
004	c(Leu-Arg-$\beta^{2,2}$-Arg)	+2	5.46	2	2	4	2	8	32	215
041	c(Phe-Arg-$\beta^{2,2}$-Arg)	+2	5.47	1	0.3	2	2	4	16	116

[1] Microbial strain; Bs – *Bacillus subtilis* (ATCC 23857), Cg – *Corynebacterium glutamicum* (ATCC 13032), Sa – *Staphylococcus aureus* (ATCC 9144), Se – *Staphylococcus epidermidis* RP62A (ATCC 35984), Ec – *Escherichia coli* (ATCC 25922), Pa – *Pseudomonas aeruginosa* (ATCC 27853). [2] Charge at physiological pH (7.4). [3] Retention time (min) on RP-UPLC.

4.6.4 Changes in amino acid stereochemistry

To investigate further the role of stereochemistry (chirality) on the bioactivity of cyclic tetrapeptides, we decided to replace *N*-terminal amino acids in both **001** and **002**, with their corresponding *D*-enantiomers. (Figure 37)

L- to *D*-substitution in the cyclic tetrapeptide scaffold	
A) 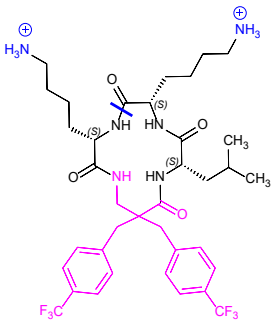	B) 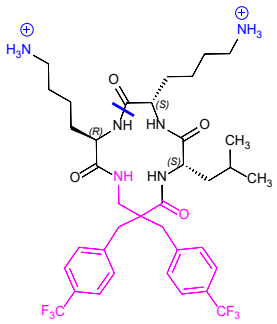
c(Lys-$\beta^{2,2}$-Leu-Lys) **001**	c(*D*-Lys-$\beta^{2,2}$-Leu-Lys) **011**

Figure 37. Stereochemical modification of Lys analogue: A) Structure of the all-*L*-tetrapeptide, c(Lys-$\beta^{2,2}$-Leu-Lys); and B) the diastereomer obtained by replacing *L*-Lys to *D*-Lys at the *N*-terminus, c(*D*-Lys-$\beta^{2,2}$-Leu-Lys).

Changing chirality of these residues in the sequences of all-*L*-peptides led to seemingly inconsistent results. For the *D*-Lys analogue **011** antimicrobial activity was slightly reduced, although activity against *C. glutamicum* (MIC: 2 µg/mL) and *P. aeruginosa* (MIC: 8 µg/mL) remained unchanged. (Table 10) On the other hand, having *D*-Arg in the sequence of **002** (021 c(*D*-Arg-$\beta^{2,2}$-Leu-Arg)) did not influence the activity against Gram-negative bacteria, whereas the activity against Gram-positive bacteria was mostly improved (2-fold decrease in MIC). Importantly, both *D* analogues had greatly reduced haemolytic toxicity. Although further research is needed to demonstrate improved enzymatic stability of these peptides, *L*- to *D*-amino acid substitution may be a useful modification for improving selectivity of this series of cyclic tetrapeptides.

Table 10. Antimicrobial activity (MIC in μg/mL) and haemolytic activity against human RBC (EC_{50} in μg/mL) of selected cyclic tetrapeptides.

Peptide	Sequence	Charge[2]	Rt[3]	Antimicrobial activity (MIC)[1]						RBC tox. EC_{50}
				Gram +			Gram –			
				Bs	*Cg*	*Sa*	*Se*	*Ec*	*Pa*	
001	c(Lys-β^{2,2}-Leu-Lys)	+2	6.23	2	2	4	4	4	8	105
011	c(*D*-Lys-β^{2,2}-Leu-Lys)	+2	6.07	4	2	8	8	8	8	426
002	c(Arg-β^{2,2}-Leu-Arg)	+2	6.38	2	2	4	4	4	8	33
021	c(*D*-Arg-β^{2,2}-Leu-Arg)	+2	5.25	1	4	2	2	4	8	181

[1] Microbial strain; Bs – *Bacillus subtilis* (ATCC 23857), Cg – *Corynebacterium glutamicum* (ATCC 13032), Sa – *Staphylococcus aureus* (ATCC 9144), Se – *Staphylococcus epidermidis* RP62A (ATCC 35984), Ec – *Escherichia coli* (ATCC 25922), Pa – *Pseudomonas aeruginosa* (ATCC 27853). [2] Charge at physiological pH (7.4). [3] Retention time (min) on RP-UPLC.

4.6.5 Recent studies on short diastereomeric antimicrobial peptides and peptidomimetics

Previous studies of cationic linear AMPs indicate that antimicrobial activity of diastereomers may be influenced by their ability to form well defined amphipathic structures in solution. (495, 496)

In one such study, the authors investigated the antimicrobial and haemolytic activities of diastereomers of an antimicrobial linear peptide, LTX 109. (495) This short peptidomimetic was composed of a tri-tert-butyl substituted Trp residue (Tbt) flanked by two Arg residues. In order to impart additional hydrophobicity and enzymatic stability to the peptide, the *C*-terminus was capped by an ethylphenyl ester group. Varying stereochemistry of its three residues, the authors synthesised a series of eight diastereomers. They found that isomers whose second (Tbt) and third residue had the same chirality, either *L,L* or *D,D*, were the most potent against tested bacterial strains. Furthermore, molecular dynamics simulation and nuclear magnetic resonance (NMR) studies revealed that these diastereomers, in contrast to their non-amphipathic analogues, easily adopted amphipathic conformation, which allowed for the effective permeation of the membrane. Of note, diastereomers with greatly decreased retention times compared to those of their *L,L* and *D,D* stereoisomers were found to be much less haemolytic, although with reduced potency.

A similar study recently done by Grant *et al.,* investigated, among others, the activity of cyclic Arg-derived 2,5-diketopiperazines with different stereochemistry: *L,L*, *D,D* and *L,D*. (496) The two enantiomers had very similar potency against a panel of tested bacteria, including MDR clinical isolates. Potency of *L,D* stereoisomer was only slightly reduced, whereas far greater reduction was observed against *P. aeruginosa*. In addition, substitution of Arg for Lys

in the *L,L* stereoisomer, resulted in an analogue with similar potency, except against pandrug resistant *K. pneumonia*. Although the authors did report retention times of all diastereomers, presented as retention factors, their haemolytic activity was unfortunately not evaluated.

In our work with cyclic tetrapeptide diastereomers, there was not much variation in the MIC values for both Gram-positive and Gram-negative bacteria. That may be expected considering that their retention times were quite similar, as opposed to the observations made in both above-mentioned studies. Therefore, it seemed that in our cyclic tetrapeptide scaffold, orientation of the side chain groups was not the crucial determinant of antimicrobial activity, but rather their proximity, maintained by the rigid cyclic structure. Nonetheless, single *L*- to *D*- amino acid substitution did have a favorable effect on peptides haemolytic activity. Namely, the non-amphipathic analogues (those containing *D*-amino acid where two cationic side chains were oriented in opposite directions relative to the plane of the cyclic ring) were considerably less prone to cause haemolysis, whereas all-*L*-diastereomer were more haemolytic. Although amhipathicity of our cyclic diastereomers seem to be important for reducing mammalian cell toxicity, further studies are needed to ascertain whether such modification is case dependent or might have more broad applicability.

A short summary of the modifications of the cyclic tetrapeptide scaffold and the corresponding outcomes is given bellow.

Lys to Arg substitution

- Activity against both Gram-positive and Gram-negative bacteria remained the same.
- Haemolytic activity was greatly reduced.

Changes in amphipathicity

- Activity against Gram-positive bacteria was mostly reduced 2-fold or remained unchanged.
- Activity against Gram-negative bacteria was greatly reduced for both Lys- and Arg- analogue.
- Haemolytic activity was greatly reduced.

Leu to Phe substitution

- Activity against Gram-positive bacteria was mostly improved (2-fold decrease in MIC).
- Activity against Gram-negative bacteria was improved 2-fold. The overall potency of Arg-analogues was slightly higher than that of the corresponding Lys-analogues.
- There was no significant change in haemolytic activity for Lys-containing analogue. However, for the Arg-containing analogue, Leu to Phe substitution resulted in more haemolytic peptide.

***L*- to *D*-amino acid substitution**

- Activity against both Gram-positive and Gram-negative bacteria remained relatively high, although with some variations (e.g., 2-fold reduction/increase in MIC).
- Activity against Gram-negative bacteria was mostly unchanged.
- Haemolytic activity was greatly reduced.

4.7 Mode of action studies

Luciferase-based assays were used to investigate whether synthesised Turgencin analogues (**Paper I**) had an immediate effect (within 3 min) on bacterial viability and membrane integrity. In general, against *B. subtilis*, (lipo)peptides caused decrease in bacterial cell viability due to immediate damage of the bacterial cell membrane, although the degree of this damage varied considerably. However, against *E. coli*, the immediate effect on cell viability was hardly observable for most of the peptides within the short timeframe of the experiments. Moreover, in some instances, the effect was present only for the highest concentration of the tested peptide (50 μg/mL), most likely due to the high concentration of bacterial inoculum (1000-fold greater than that used for the MIC assay) that was used in these experiments. An interesting finding for some of the lipopeptides was the delayed effect on *E. coli* membrane, indicating that the outer membrane might be a considerable obstacle for these analogues to exert their activity against Gram-negative bacteria. This was confirmed for most peptides that were tested against an *E. coli* mutant strain with an impaired outer membrane. The most potent lipopeptides (**C_{12}-cTurg-1** and **C_8-cTurg-2**) were also shown to enable the hydrophobic 1-*N*-phenylnapthylamine (NPN) to immediately cross the outer membrane of *E. coli*, further supporting their action on bacterial membranes. These two peptides were also shown to have a bactericidal effect against both *S. aureus* and *E. coli* at MIC-values.

Similar to the Turgencin analogues, the selected linear and cyclic analogues of EeCentrocin 1 (**Paper II**) were shown to affect the viability of *B. subtilis* in a concentration-dependent manner. In addition, their membrane related mode of action against *B. subtilis* was more pronounced at higher concentrations (5xMIC). Against *E. coli* their effect on viability and membrane integrity was greatly reduced compared to their effect on *B. subtilis*. Both **P6-W6R8** and **cP6-W6R8** showed a concentration-dependent increase in NPN entry, indicating a membrane-permeabilising effect. However, their mode of action might be dual: apart from causing membrane disruption, they might also target intracellular components.

5 Conclusions

In the present work we explored how different structural modifications affect the antimicrobial and haemolytic activities of short antimicrobial peptides (AMPs). We used three different peptide scaffolds: firstly, a 12-residue loop region of the marine AMP Turgencin A, secondly, a previously reported lead peptide (P6) derived from the heavy chain of the marine peptide EeCentrocin 1, and finally, a tetrapeptide scaffold containing non-canonical amino acid. To investigate structure-activity (SAR) relationships of short AMPs with putative membrane-disruptive properties, we performed following structural modifications: *L*- to *L/D*-amino acid substitutions, N-terminal acylation, and Cys-Cys and head-to-tail cyclisation.

For both Turgencin A and EeCentrocin 1 analogues we observed that AMPs properties could be easily tuned by increasing peptide hydrophobicity, either by incorporating bulky, hydrophobic amino acids in the native sequence, as for example Trp, or by N-terminal acylation. These modifications do not necessarily result in peptides with greater potency, considering that there is a threshold in hydrophobicity above which potency starts to decline. Another observation was that the Arg-containing peptides were in general more potent than their Lys analogues, indicating that Arg to Lys substitution may lead to more active peptides, which are, however, likely to be more haemolytic. Cys-Cys cyclisation of the Turgencin 1 analogues did slightly improve antimicrobial activity of the lipopeptides, and apart from few exceptions, it did not greatly influence haemolytic activity. By contrast, backbone cyclisation of EeCentrocin 1 analogues resulted in peptides with mostly reduced potency, while haemolytic activity remained unchanged compared to their linear analogues (all peptides were non-haemolytic).

For the much smaller tetrapeptide scaffold, changes in amphipathicity (from amphipathic to non-amphipathic) resulted in peptides with similar antimicrobial profile (2-fold variations) and considerable reduction in haemolytic toxicity. This same trend was present with the change in stereochemistry, namely *L*- to *D*-amino acid substitution of a single cationic residue. Finally, Leu to Phe substitution of non-amphipathic peptides resulted in moderate increase in potency, while results with respect to haemolytic activity were somewhat inconsistent.

In summary, our findings demonstrate that simple modifications in the peptide sequence and structure could be used to fine-tune the properties of marine-derived peptides and short peptidomimetics, making them potential drug leads for the treatment of bacterial infections.

6 Perspectives

For the peptides synthesised in this work one avenue of future research could be to investigate peptide-membrane interactions with model membranes (*e.g.*, large unilamellar vesicles - LUVs). For example, for Trp-containing peptides, fluorescent spectroscopy could be used, as well as quenching of the Trp fluorescence by small molecules, such as a neutral quencher acrylamide. In addition, fluorescence correlation spectroscopy would enable us to study the effect of peptides on LUVs, namely, to quantify peptide-induced leakage of fluorescent molecules from LUVs, and furthermore ascertain whether leakage is associated with aggregation, fusion or micellisation of the LUVs.

Activity of many natural AMPs is greatly reduced, and in some instances even completely lost, under physiological conditions. Thus, another potential avenue could be the investigation of peptides stability in serum and physiological concentrations of salts.

Exploring the possibility of peptides having intracellular target would give us a more complete picture of their mechanism of action. For example, changes in cell morphology induced by AMPs can be visualized using atomic force microscopy and electron microscopy (*e.g.*, SEM). Electrophoretic mobility shift assay may help reveal putative interactions between peptides with DNA/RNA molecules. In addition, both mass spectrometry and proteome microarray could be used to identify protein targets of AMPs and changes in protein expression due to the peptide entry into the bacterial cell.

These and similar studies would help us improve our understanding of the key structural determinants and their relationship with peptide antimicrobial and haemolytic effects. Moreover, they would aid the rational design of peptidomimetics that could address the growing problem of antibiotic resistance.

7 References

1. Aminov R. A Brief History of the Antibiotic Era: Lessons Learned and Challenges for the Future. Front Microbiol. 2010;1.
2. Valent P, Groner B, Schumacher U, Superti-Furga G, Busslinger M, Kralovics R, et al. Paul Ehrlich (1854-1915) and His Contributions to the Foundation and Birth of Translational Medicine. J Innate Immun. 2016;8(2):111-20.
3. Hutchings MI, Truman AW, Wilkinson B. Antibiotics: past, present and future. Curr Opin Microbiol. 2019;51:72-80.
4. Frith J. Syphilis - its early history and treatment until penicillin, and the debate on its origins. J Mil Veterans Health. 2012;20(4):49-58.
5. Gould K. Antibiotics: from prehistory to the present day. J Antimicrob Chemother. 2016;71(3):572-5.
6. Fleming A. On the Antibacterial Action of Cultures of a Penicillium, with Special Reference to their Use in the Isolation of B. influenzæ. Br J Exp Pathol. 1929;10(3):226-36.
7. Butler MS, Gigante V, Sati H, Paulin S, Al-Sulaiman L, Rex JH, et al. Analysis of the Clinical Pipeline of Treatments for Drug-Resistant Bacterial Infections: Despite Progress, More Action Is Needed. Antimicrob Agents Chemother. 2022;66(3):e01991-21.
8. Brown DG, Wobst HJ. A Decade of FDA-Approved Drugs (2010-2019): Trends and Future Directions. J Med Chem. 2021;64(5):2312-38.
9. Thaller MC, Migliore L, Marquez C, Tapia W, Cedeño V, Rossolini GM, et al. Tracking acquired antibiotic resistance in commensal bacteria of Galápagos land iguanas: no man, no resistance. PLoS One. 2010;5(2):e8989.
10. Davis CE, Anandan J. The Evolution of R Factor. N Engl J Med. 1970;282(3):117-22.
11. Knapp CW, Dolfing J, Ehlert PAI, Graham DW. Evidence of Increasing Antibiotic Resistance Gene Abundances in Archived Soils since 1940. Environ Sci Technol. 2010;44(2):580-7.
12. Barlow M, Hall BG. Phylogenetic analysis shows that the OXA beta-lactamase genes have been on plasmids for millions of years. J Mol Evol. 2002;55(3):314-21.
13. D'Costa VM, King CE, Kalan L, Morar M, Sung WWL, Schwarz C, et al. Antibiotic resistance is ancient. Nature. 2011;477(7365):457-61.
14. Bhullar K, Waglechner N, Pawlowski A, Koteva K, Banks ED, Johnston MD, et al. Antibiotic Resistance Is Prevalent in an Isolated Cave Microbiome. PLoS One. 2012;7(4):e34953.
15. Larsson DGJ, Flach C-F. Antibiotic resistance in the environment. Nat Rev Microbiol. 2022;20(5):257-69.
16. Murray CJL, Ikuta KS, Sharara F, Swetschinski L, Robles Aguilar G, Gray A, et al. Global burden of bacterial antimicrobial resistance in 2019: a systematic analysis. Lancet. 2022;399(10325):629-55.
17. Avent ML, Rogers BA, Cheng AC, Paterson DL. Current use of aminoglycosides: indications, pharmacokinetics and monitoring for toxicity. Intern Med J. 2011;41(6):441-9.
18. Ordooei Javan A, Shokouhi S, Sahraei Z. A review on colistin nephrotoxicity. Eur J Clin Pharmacol. 2015;71(7):801-10.
19. WHO. Fifty-first World Health Assembly; Resolutions and Decisions Annexes [Internet]. 1998. [cited 2023 Feb 23]. Available from: https://apps.who.int/iris/bitstream/handle/10665/258896/WHA51-1998-REC-1-eng.pdf?sequence=1.
20. WHO. Global Strategy for Containment of Antimicrobial Resistance [Internet]. 2001. [cited 2023 Feb 23]. Available from: https://apps.who.int/iris/bitstream/handle/10665/66860/WHO_CDS_CSR_DRS_2001.2.pdf;jsessionid=56174BEE91D506855B57B8E65E40C755?sequence=1.
21. WHO. Global action plan on antimicrobial resistance [Internet]. 2015. [cited 2023 Feb 23]. Available from: https://apps.who.int/iris/rest/bitstreams/864486/retrieve.
22. Assambly. UG. Political Declaration of the High-Level Meeting of the General Assembly on Antimicrobial Resistance : draft resolution / submitted by the President of the General Assembly [Internet]. 2016. [cited 2023 Feb 23]. Available from: https://digitallibrary.un.org/record/842813.

23. IACG. No time to wait: securing the future from drug-resistant infections. 2019. [cited 2023 Feb 23]. Available from: https://www.who.int/docs/default-source/documents/no-time-to-wait-securing-the-future-from-drug-resistant-infections-en.pdf.
24. FAO. Antimicrobial resistance: Now is the time for collective action [Internet]. 2022. [cited 2023 Feb 23]. Available from: https://www.fao.org/newsroom/detail/antimicrobial-resistance-now-is-the-time-for-collective-action/en.
25. Food and Agriculture Organisation of the United Nations. Antimicrobial Resistance [Internet]. 2023. [cited 2023 Feb 23]. Available from: https://www.fao.org/antimicrobial-resistance/quadripartite/the-platform/en/.
26. GARDP. The Global Antibiotic Research & Development Partnership [Internet]. 2023. [cited 2023 February 23]. Available from: https://gardp.org/.
27. CARB-X. Annual report 2020-2021 [Internet]. [cited 2023 Feb 23]. Available from: https://carb-x.org/wp-content/uploads/2021/10/CarbX_AR_20-21.pdf.
28. Ryser S, Tenorio E, Estellés A, Kauvar LM. Human antibody repertoire frequently includes antibodies to a bacterial biofilm associated protein. PLoS One. 2019;14(7):e0219256.
29. Sieber SA, Marahiel MA. Learning from nature's drug factories: nonribosomal synthesis of macrocyclic peptides. J Bacteriol. 2003;185(24):7036-43.
30. Debono M, Abbott BJ, Molloy RM, Fukuda DS, Hunt AH, Daupert VM, et al. Enzymatic and chemical modifications of lipopeptide antibiotic A21978C: the synthesis and evaluation of daptomycin (LY146032). J Antibiot. 1988;41(8):1093-105.
31. Kleijn LHJ, Martin NI. The Cyclic Lipopeptide Antibiotics. In: Fisher JF, Mobashery S, Miller MJ, editors. Antibacterials: Volume II. Cham: Springer International Publishing; 2018. p. 27-53.
32. Strieker M, Marahiel MA. The structural diversity of acidic lipopeptide antibiotics. Chembiochem. 2009;10(4):607-16.
33. Jung D, Rozek A, Okon M, Hancock RE. Structural transitions as determinants of the action of the calcium-dependent antibiotic daptomycin. Chem Biol. 2004;11(7):949-57.
34. Hover BM, Kim S-H, Katz M, Charlop-Powers Z, Owen JG, Ternei MA, et al. Culture-independent discovery of the malacidins as calcium-dependent antibiotics with activity against multidrug-resistant Gram-positive pathogens. Nat Microbiol. 2018;3(4):415-22.
35. Debono M, Barnhart M, Carrell CB, Hoffmann JA, Occolowitz JL, Abbott BJ, et al. A21978C, a complex of new acidic peptide antibiotics: isolation, chemistry, and mass spectral structure elucidation. J Antibiot. 1987;40(6):761-77.
36. Miao V, Coëffet-LeGal M-F, Brian P, Brost R, Penn J, Whiting A, et al. Daptomycin biosynthesis in Streptomyces roseosporus: cloning and analysis of the gene cluster and revision of peptide stereochemistry. Microbiology. 2005;151(5):1507-23.
37. Eisenstein BI, Oleson FB, Jr., Baltz RH. Daptomycin: From the Mountain to the Clinic, with Essential Help from Francis Tally, MD. Clin Infect Dis. 2010;50(Supplement_1):S10-S5.
38. Ball LJ, Goult CM, Donarski JA, Micklefield J, Ramesh V. NMR structure determination and calcium binding effects of lipopeptide antibiotic daptomycin. Org Biomol Chem. 2004;2(13):1872-8.
39. Rotondi KS, Gierasch LM. A well-defined amphipathic conformation for the calcium-free cyclic lipopeptide antibiotic, daptomycin, in aqueous solution. Biopolymers. 2005;80(2-3):374-85.
40. Muraih JK, Pearson A, Silverman J, Palmer M. Oligomerization of daptomycin on membranes. Biochim Biophys Acta. 2011;1808(4):1154-60.
41. Silverman JA, Perlmutter NG, Shapiro HM. Correlation of daptomycin bactericidal activity and membrane depolarization in Staphylococcus aureus. Antimicrob Agents Chemother. 2003;47(8):2538-44.
42. Hachmann A-B, Angert ER, Helmann JD. Genetic analysis of factors affecting susceptibility of Bacillus subtilis to daptomycin. Antimicrob Agents Chemother. 2009;53(4):1598-609.
43. Pogliano J, Pogliano N, Silverman JA. Daptomycin-mediated reorganization of membrane architecture causes mislocalization of essential cell division proteins. J Bacteriol. 2012;194(17):4494-504.

44. Müller A, Wenzel M, Strahl H, Grein F, Saaki TNV, Kohl B, et al. Daptomycin inhibits cell envelope synthesis by interfering with fluid membrane microdomains. Proc Natl Acad Sci U S A. 2016;113(45):E7077-e86.
45. Grein F, Müller A, Scherer KM, Liu X, Ludwig KC, Klöckner A, et al. Ca(2+)-Daptomycin targets cell wall biosynthesis by forming a tripartite complex with undecaprenyl-coupled intermediates and membrane lipids. Nat Commun. 2020;11(1):1455.
46. Kotsogianni I, Wood TM, Alexander FM, Cochrane SA, Martin NI. Binding Studies Reveal Phospholipid Specificity and Its Role in the Calcium-Dependent Mechanism of Action of Daptomycin. ACS Infect Dis. 2021;7(9):2612-9.
47. Parenti F, Beretta G, Berti M, Arioli V. Teichomycins, new antibiotics from Actinoplanes teichomyceticus Nov. Sp. I. Description of the producer strain, fermentation studies and biological properties. J Antibiot. 1978;31(4):276-83.
48. Scholar E. Teicoplanin. In: Enna SJ, Bylund DB, editors. xPharm: The Comprehensive Pharmacology Reference. New York: Elsevier; 2007. p. 1-5.
49. Barna JCJ, Williams DH, Stone DJM, Leung TWC, Doddrell DM. Structure elucidation of the teicoplanin antibiotics. J Am Chem Soc. 1984;106(17):4895-902.
50. Economou NJ, Zentner IJ, Lazo E, Jakoncic J, Stojanoff V, Weeks SD, et al. Structure of the complex between teicoplanin and a bacterial cell-wall peptide: use of a carrier-protein approach. Acta Crystallogr D Biol Crystallogr. 2013;69(Pt 4):520-33.
51. Reynolds PE, Somner EA. Comparison of the target sites and mechanisms of action of glycopeptide and lipoglycodepsipeptide antibiotics. Drugs Exp Clin Res. 1990;16(8):385-9.
52. Beauregard DA, Williams DH, Gwynn MN, Knowles DJ. Dimerization and membrane anchors in extracellular targeting of vancomycin group antibiotics. Antimicrob Agents Chemother. 1995;39(3):781-5.
53. EMA. Targocid and associated names [Internet]. 2013. [cited 2023 Feb 23]. Available from: https://www.ema.europa.eu/en/medicines/human/referrals/targocid-associated-names.
54. Campoli-Richards DM, Brogden RN, Faulds D. Teicoplanin. A review of its antibacterial activity, pharmacokinetic properties and therapeutic potential. Drugs. 1990;40(3):449-86.
55. Svetitsky S, Leibovici L, Paul M. Comparative efficacy and safety of vancomycin versus teicoplanin: systematic review and meta-analysis. Antimicrob Agents Chemother. 2009;53(10):4069-79.
56. Malabarba A, Ciabatti R. Glycopeptide derivatives. Curr Med Chem. 2001;8(14):1759-73.
57. Allen NE, Nicas TI. Mechanism of action of oritavancin and related glycopeptide antibiotics. FEMS Microbiol Rev. 2003;26(5):511-32.
58. Guskey MT, Tsuji BT. A Comparative Review of the Lipoglycopeptides: Oritavancin, Dalbavancin, and Telavancin. Pharmacotherapy. 2010;30(1):80-94.
59. Leadbetter MR, Adams SM, Bazzini B, Fatheree PR, Karr DE, Krause KM, et al. Hydrophobic vancomycin derivatives with improved ADME properties: discovery of telavancin (TD-6424). J Antibiot. 2004;57(5):326-36.
60. Blaskovich MAT, Hansford KA, Butler MS, Jia Z, Mark AE, Cooper MA. Developments in Glycopeptide Antibiotics. ACS Infect Dis. 2018;4(5):715-35.
61. Higgins Deborah L, Chang R, Debabov Dmitri V, Leung J, Wu T, Krause Kevin M, et al. Telavancin, a Multifunctional Lipoglycopeptide, Disrupts both Cell Wall Synthesis and Cell Membrane Integrity in Methicillin-Resistant Staphylococcus aureus. Antimicrob Agents Chemother. 2005;49(3):1127-34.
62. Lunde CS, Hartouni SR, Janc JW, Mammen M, Humphrey PP, Benton BM. Telavancin disrupts the functional integrity of the bacterial membrane through targeted interaction with the cell wall precursor lipid II. Antimicrob Agents Chemother. 2009;53(8):3375-83.
63. FDA. VIBATIV® (telavancin) – Highlights of prescribing information. 2016. [cited 2023 Feb 23]. Available from: https://www.accessdata.fda.gov/drugsatfda_docs/label/2016/022110s012lbl.pdf.
64. Shaw JP, Seroogy J, Kaniga K, Higgins DL, Kitt M, Barriere S. Pharmacokinetics, serum inhibitory and bactericidal activity, and safety of telavancin in healthy subjects. Antimicrob Agents Chemother. 2005;49(1):195-201.

65. Leonard SN, Rybak MJ. Telavancin: An Antimicrobial with a Multifunctional Mechanism of Action for the Treatment of Serious Gram-Positive Infections. Pharmacotherapy. 2008;28(4):458-68.
66. Cooper RD, Snyder NJ, Zweifel MJ, Staszak MA, Wilkie SC, Nicas TI, et al. Reductive alkylation of glycopeptide antibiotics: synthesis and antibacterial activity. J Antibiot. 1996;49(6):575-81.
67. van Groesen E, Innocenti P, Martin NI. Recent Advances in the Development of Semisynthetic Glycopeptide Antibiotics: 2014–2022. ACS Infect Dis. 2022;8(8):1381-407.
68. Brade KD, Rybak JM, Rybak MJ. Oritavancin: A New Lipoglycopeptide Antibiotic in the Treatment of Gram-Positive Infections. Infect Dis Ther. 2016;5(1):1-15.
69. Kim SJ, Cegelski L, Stueber D, Singh M, Dietrich E, Tanaka KSE, et al. Oritavancin Exhibits Dual Mode of Action to Inhibit Cell-Wall Biosynthesis in Staphylococcus aureus. J Mol Biol. 2008;377(1):281-93.
70. Münch D, Engels I, Müller A, Reder-Christ K, Falkenstein-Paul H, Bierbaum G, et al. Structural Variations of the Cell Wall Precursor Lipid II and Their Influence on Binding and Activity of the Lipoglycopeptide Antibiotic Oritavancin. Antimicrob Agents Chemother. 2015;59(2):772-81.
71. Patti GJ, Kim SJ, Yu TY, Dietrich E, Tanaka KS, Parr TR, Jr., et al. Vancomycin and oritavancin have different modes of action in Enterococcus faecium. J Mol Biol. 2009;392(5):1178-91.
72. Markham A. Oritavancin: First Global Approval. Drugs. 2014;74(15):1823-8.
73. Arhin FF, Belley A, McKay G, Beaulieu S, Sarmiento I, Parr TR, Jr., et al. Assessment of oritavancin serum protein binding across species. Antimicrob Agents Chemother. 2010;54(8):3481-3.
74. Zhanel GG, Calic D, Schweizer F, Zelenitsky S, Adam H, Lagacé-Wiens PR, et al. New lipoglycopeptides: a comparative review of dalbavancin, oritavancin and telavancin. Drugs. 2010;70(7):859-86.
75. Yushchuk O, Vior NM, Andreo-Vidal A, Berini F, Rückert C, Busche T, et al. Genomic-Led Discovery of a Novel Glycopeptide Antibiotic by Nonomuraea coxensis DSM 45129. ACS Chem Biol. 2021;16(5):915-28.
76. Goldstein BP, Selva E, Gastaldo L, Berti M, Pallanza R, Ripamonti F, et al. A40926, a new glycopeptide antibiotic with anti-Neisseria activity. Antimicrob Agents Chemother. 1987;31(12):1961-6.
77. Economou NJ, Nahoum V, Weeks SD, Grasty KC, Zentner IJ, Townsend TM, et al. A Carrier Protein Strategy Yields the Structure of Dalbavancin. J Am Chem Soc. 2012;134(10):4637-45.
78. Jones RN, Sader HS, Flamm RK. Update of dalbavancin spectrum and potency in the USA: report from the SENTRY Antimicrobial Surveillance Program (2011). Diagn Microbiol Infect Dis. 2013;75(3):304-7.
79. Taylor K, Williamson J, Luther V, Stone T, Johnson J, Gruss Z, et al. Evaluating the Use of Dalbavancin for Off-Label Indications. Infect Dis Rep. 2022;14(2):266-72.
80. Leighton A, Gottlieb AB, Dorr MB, Jabes D, Mosconi G, VanSaders C, et al. Tolerability, pharmacokinetics, and serum bactericidal activity of intravenous dalbavancin in healthy volunteers. Antimicrob Agents Chemother. 2004;48(3):940-5.
81. Johnson BA, Anker H, Meleney FL. Bacitracin: a new antibiotic produced by a member of the *B. subtilis* group. Science. 1945;102(2650):376-7.
82. MELENEY FL, JOHNSON B. Bacitracin therapy: the first hundred cases of surgical infections treated locally with the antibiotic. J Am Med Assoc. 1947;133(10):675-80.
83. Nakano MM, Zuber P. Molecular biology of antibiotic production in Bacillus. Crit Rev Biotechnol. 1990;10(3):223-40.
84. Ming LJ, Epperson JD. Metal binding and structure-activity relationship of the metalloantibiotic peptide bacitracin. J Inorg Biochem. 2002;91(1):46-58.
85. Kopp F, Marahiel MA. Macrocyclization strategies in polyketide and nonribosomal peptide biosynthesis. Nat Prod Rep. 2007;24(4):735-49.
86. Porath J. Structure of Bacitracin A. Nature. 1953;172(4384):871-.
87. Ikai Y, Oka H, Hayakawa J, Matsumoto M, Saito M, Harada K, et al. Total structures and antimicrobial activity of bacitracin minor components. J Antibiot. 1995;48(3):233-42.

88. Hirotsu Y, Shiba T, Kaneko T. Synthetic studies of bacitracin. IV. Synthesis of thiazoline peptides by iminoether coupling method. Bull Chem Soc Jpn. 1967;40(12):2945-9.
89. Siewert G, Strominger JL. Bacitracin: an inhibitor of the dephosphorylation of lipid pyrophosphate, an intermediate in the biosynthesis of the peptidoglycan of bacterial cell walls. Proc Natl Acad Sci U S A. 1967;57(3):767-73.
90. Stone KJ, Strominger JL. Mechanism of Action of Bacitracin: Complexation with Metal Ion and C55-Isoprenyl Pyrophosphate. Proc Natl Acad Sci U S A. 1971;68(12):3223-7.
91. Storm DR. Mechanism of bacitracin action: a specific lipid-peptide interaction. Ann N Y Acad Sci. 1974;235(0):387-98.
92. Benedict RG, Langlykke AF. Antibiotic activity of Bacillus polymyxa. J Bacteriol. 1947;54(1):24.
93. Stansly PG, Shepherd RG, White HJ. Polymyxin: a new chemotherapeutic agent. Bull Johns Hopkins Hosp. 1947;81 1:43-54.
94. Ainsworth GC, Brown AM, Brownlee G. Aerosporin, an antibiotic produced by Bacillus aerosporus Greer. Nature. 1947;159(4060):263.
95. Velkov T, Thompson PE, Azad MAK, Roberts KD, Bergen PJ. History, Chemistry and Antibacterial Spectrum. Adv Exp Med Biol. 2019;1145:15-36.
96. Ledger EVK, Sabnis A, Edwards AM. Polymyxin and lipopeptide antibiotics: membrane-targeting drugs of last resort. Microbiology. 2022;168(2).
97. Clifford HE, Stewart GT. Intraventricular administration of a new derivative of Polymyxin B in meningitis due to Ps. pyocyanea. Lancet. 1961;278(7195):177-80.
98. Kwa A, Kasiakou SK, Tam VH, Falagas ME. Polymyxin B: similarities to and differences from colistin (polymyxin E). Expert Rev Anti Infect Ther. 2007;5(5):811-21.
99. Schwartz BS, Warren MR, Barkley FA, Landis L. Microbiological and pharmacological studies of colistin sulfate and sodium colistinmethanesulfonate. Antibiot Annu. 1959;7:41-60.
100. Dubos RJ. Studies on a bactericidal agent extracted from a soil Bacullus: I. Preparation of the agent. Its activity *in vitro*. J Exp Med. 1939;70(1):1-10.
101. Dubos RJ. Studies on a bactericidal agent extracted from a soil Bacullus: II. Protective effect of the bactericidal agent against experimental pneumococcus infections in mice. J Exp Med. 1939;70(1):11-7.
102. Hotchkiss RD, Dubos RJ. Fractionation of the bactericidal agent from cultures of a soil bacillus. J Biol Chem. 1940;132(2):791-2.
103. Hotchkiss RD, Dubos RJ. Bactericidal fractions from an aerobic sporulating bacillus. J Biol Chem. 1940;136(3):803-4.
104. Herrell WE, Heilman D. Experimental and clinical studies on gramicidin. J Clin Invest. 1941;20(5):583-91.
105. Gause GF, Brazhnikova MG. Gramicidin S and its use in the Treatment of Infected Wounds. Nature. 1944;154(3918):703-.
106. Okada T, Yoshizumi H, Terashima Y. A Lethal Toxic Substance for Brewing Yeast in Wheat and Barley. Agric Biol Chem. 1970;34(7):1084-94.
107. Balls AK, Hale WS, Harris TH. A crystalline protein obtained from a lipoprotein of wheat flour. Cereal Chem. 1942;19:279-88.
108. Zeya HI, Spitznagel JK. Antibacterial and enzymatic basic proteins from leukocyte lysosomes: separation and identification. Science. 1963;142(3595):1085-7.
109. Zeya HI, Spitznagel JK. Cationic proteins of polymorphonuclear leukocyte lysosomes. I. Resolution of antibacterial and enzymatic activities. J Bacteriol. 1966;91(2):750-4.
110. Zeya HI, Spitznagel JK. Arginine-rich proteins of polymorphonuclear leukocyte lysosomes: antimicrobial specificity and biochemical heterogeneity. J Exp Med. 1968;127(5):927-41.
111. Patterson-Delafield J, Martinez RJ, Lehrer RI. Microbicidal cationic proteins in rabbit alveolar macrophages: a potential host defense mechanism. Infect Immun. 1980;30(1):180-92.
112. Patterson-Delafield J, Szklarek D, Martinez RJ, Lehrer RI. Microbicidal cationic proteins of rabbit alveolar macrophages: amino acid composition and functional attributes. Infect Immun. 1981;31(2):723-31.

113. Selsted ME, Harwig SS, Ganz T, Schilling JW, Lehrer RI. Primary structures of three human neutrophil defensins. J Clin Invest. 1985;76(4):1436-9.
114. Ganz T, Selsted ME, Szklarek D, Harwig SS, Daher K, Bainton DF, et al. Defensins. Natural peptide antibiotics of human neutrophils. J Clin Invest. 1985;76(4):1427-35.
115. Hultmark D, Steiner H, Rasmuson T, Boman HG. Insect immunity. Purification and properties of three inducible bactericidal proteins from hemolymph of immunized pupae of Hyalophora cecropia. Eur J Biochem. 1980;106(1):7-16.
116. Steiner H, Hultmark D, Engström Å, Bennich H, Boman HG. Sequence and specificity of two antibacterial proteins involved in insect immunity. Nature. 1981;292(5820):246-8.
117. Simmaco M, Mignogna G, Barra D, Bossa F. Antimicrobial peptides from skin secretions of Rana esculenta. Molecular cloning of cDNAs encoding esculentin and brevinins and isolation of new active peptides. J Biol Chem. 1994;269(16):11956-61.
118. Zasloff M. Antimicrobial peptides of multicellular organisms. Nature. 2002;415:389.
119. Csordás A, Michl H. Isolierung und Strukturaufklärung eines hämolytisch wirkenden Polypeptides aus dem Abwehrsekret europäischer Unken. Monatsh Chem. 1970;101(1):182-9.
120. Anastasi A, Erspamer V, Bucci M. Isolation and structure of bombesin and alytesin, two analogous active peptides from the skin of the european amphibians Bombina and Alytes. Experientia. 1971;27(2):166-7.
121. Zasloff M. Magainins, a class of antimicrobial peptides from Xenopus skin: isolation, characterization of two active forms, and partial cDNA sequence of a precursor. Proc Natl Acad Sci U S A. 1987;84(15):5449-53.
122. Ramachander Turaga VN. Peptaibols: Antimicrobial Peptides from Fungi. In: Singh J, Meshram V, Gupta M, editors. Bioactive Natural products in Drug Discovery. Singapore: Springer Singapore; 2020. p. 713-30.
123. Nawrot R, Barylski J, Nowicki G, Broniarczyk J, Buchwald W, Goździcka-Józefiak A. Plant antimicrobial peptides. Folia Microbiol. 2014;59(3):181-96.
124. Moretta A, Scieuzo C, Petrone AM, Salvia R, Manniello MD, Franco A, et al. Antimicrobial Peptides: A New Hope in Biomedical and Pharmaceutical Fields. Front Cell Infect Microbiol. 2021;11.
125. Koo HB, Seo J. Antimicrobial peptides under clinical investigation. J Pept Sci. 2019;111(5):e24122.
126. Hancock RE, Chapple DS. Peptide antibiotics. Antimicrob Agents Chemother. 1999;43(6):1317-23.
127. Mootz HD, Schwarzer D, Marahiel MA. Ways of Assembling Complex Natural Products on Modular Nonribosomal Peptide Synthetases. ChemBioChem. 2002;3(6):490-504.
128. Faulkner DJ. Marine natural products. Nat Prod Rep. 2002;19(1):1-49.
129. Arnison PG, Bibb MJ, Bierbaum G, Bowers AA, Bugni TS, Bulaj G, et al. Ribosomally synthesized and post-translationally modified peptide natural products: overview and recommendations for a universal nomenclature. Nat Prod Rep. 2013;30(1):108-60.
130. McIntosh JA, Donia MS, Schmidt EW. Ribosomal peptide natural products: bridging the ribosomal and nonribosomal worlds. Nat Prod Rep. 2009;26(4):537-59.
131. Sivonen K, Leikoski N, Fewer DP, Jokela J. Cyanobactins-ribosomal cyclic peptides produced by cyanobacteria. Appl Microbiol Biotechnol. 2010;86(5):1213-25.
132. Duquesne S, Destoumieux-Garzón D, Peduzzi J, Rebuffat S. Microcins, gene-encoded antibacterial peptides from enterobacteria. Nat Prod Rep. 2007;24(4):708-34.
133. Terlau H, Olivera BM. Conus Venoms: A Rich Source of Novel Ion Channel-Targeted Peptides. Physiol Rev. 2004;84(1):41-68.
134. Jennings C, West J, Waine C, Craik D, Anderson M. Biosynthesis and insecticidal properties of plant cyclotides: The cyclic knotted proteins from Oldenlandia affinis. Proc Natl Acad Sci U S A. 2001;98(19):10614-9.
135. Hallen HE, Luo H, Scott-Craig JS, Walton JD. Gene family encoding the major toxins of lethal Amanita mushrooms. Proc Natl Acad Sci U S A. 2007;104(48):19097-101.
136. Zhang Q-Y, Yan Z-B, Meng Y-M, Hong X-Y, Shao G, Ma J-J, et al. Antimicrobial peptides: mechanism of action, activity and clinical potential. Mil Med Res. 2021;8(1):48.

137. Wang G. Chapter One - Unifying the classification of antimicrobial peptides in the antimicrobial peptide database. In: Hicks LM, editor. Methods Enzymol. 663: Academic Press; 2022. p. 1-18.
138. Brogden KA. Antimicrobial peptides: pore formers or metabolic inhibitors in bacteria? Nat Rev Microbiol. 2005;3(3):238-50.
139. Koehbach J, Craik DJ. The Vast Structural Diversity of Antimicrobial Peptides. Trends Pharmacol Sci. 2019;40(7):517-28.
140. Amiss AS, Henriques ST, Lawrence N. Antimicrobial peptides provide wider coverage for targeting drug-resistant bacterial pathogens. Peptide Science. 2022;114(2):e24246.
141. Giangaspero A, Sandri L, Tossi A. Amphipathic α helical antimicrobial peptides. Eur J Biochem. 2001;268(21):5589-600.
142. Terwilliger TC, Eisenberg D. The structure of melittin. I. Structure determination and partial refinement. J Biol Chem. 1982;257(11):6010-5.
143. Holak TA, Engström A, Kraulis PJ, Lindeberg G, Bennich H, Jones TA, et al. The solution conformation of the antibacterial peptide cecropin A: a nuclear magnetic resonance and dynamical simulated annealing study. Biochemistry. 1988;27(20):7620-9.
144. Turner J, Cho Y, Dinh NN, Waring AJ, Lehrer RI. Activities of LL-37, a cathelin-associated antimicrobial peptide of human neutrophils. Antimicrob Agents Chemother. 1998;42(9):2206-14.
145. Xhindoli D, Pacor S, Benincasa M, Scocchi M, Gennaro R, Tossi A. The human cathelicidin LL-37 — A pore-forming antibacterial peptide and host-cell modulator. Biochim Biophys Acta Biomembr. 2016;1858(3):546-66.
146. Uggerhøj LE, Poulsen TJ, Munk JK, Fredborg M, Sondergaard TE, Frimodt-Moller N, et al. Rational Design of Alpha-Helical Antimicrobial Peptides: Do's and Don'ts. ChemBioChem. 2015;16(2):242-53.
147. Lewies A, Du Plessis LH, Wentzel JF. Antimicrobial Peptides: the Achilles' Heel of Antibiotic Resistance? Probiotics Antimicrob Proteins. 2019;11(2):370-81.
148. Brogden KA, Ackermann M, McCray PB, Tack BF. Antimicrobial peptides in animals and their role in host defences. Int J Antimicrob Agents. 2003;22(5):465-78.
149. Panteleev PV, Bolosov IA, Balandin SV, Ovchinnikova TV. Structure and Biological Functions of β-Hairpin Antimicrobial Peptides. Acta Naturae. 2015;7(1):37-47.
150. Romeo D, Skerlavaj B, Bolognesi M, Gennaro R. Structure and bactericidal activity of an antibiotic dodecapeptide purified from bovine neutrophils. J Biol Chem. 1988;263(20):9573-5.
151. Nakamura T, Furunaka H, Miyata T, Tokunaga F, Muta T, Iwanaga S, et al. Tachyplesin, a class of antimicrobial peptide from the hemocytes of the horseshoe crab (Tachypleus tridentatus). Isolation and chemical structure. J Biol Chem. 1988;263(32):16709-13.
152. Kawano K, Yoneya T, Miyata T, Yoshikawa K, Tokunaga F, Terada Y, et al. Antimicrobial peptide, tachyplesin I, isolated from hemocytes of the horseshoe crab (Tachypleus tridentatus). NMR determination of the beta-sheet structure. J Biol Chem. 1990;265(26):15365-7.
153. Park CH, Valore EV, Waring AJ, Ganz T. Hepcidin, a urinary antimicrobial peptide synthesized in the liver. J Biol Chem. 2001;276(11):7806-10.
154. Jordan JB, Poppe L, Haniu M, Arvedson T, Syed R, Li V, et al. Hepcidin revisited, disulfide connectivity, dynamics, and structure. J Biol Chem. 2009;284(36):24155-67.
155. Bin Hafeez A, Jiang X, Bergen PJ, Zhu Y. Antimicrobial Peptides: An Update on Classifications and Databases. Int J Mol Sci. 2021;22(21).
156. Klotman ME, Chang TL. Defensins in innate antiviral immunity. Nat Rev Immunol. 2006;6(6):447-56.
157. Selsted ME, Tang YQ, Morris WL, McGuire PA, Novotny MJ, Smith W, et al. Purification, primary structures, and antibacterial activities of beta-defensins, a new family of antimicrobial peptides from bovine neutrophils. J Biol Chem. 1993;268(9):6641-8.
158. Szyk A, Wu Z, Tucker K, Yang D, Lu W, Lubkowski J. Crystal structures of human alpha-defensins HNP4, HD5, and HD6. Protein Sci. 2006;15(12):2749-60.
159. Ganz T. Defensins: antimicrobial peptides of innate immunity. Nat Rev Immunol. 2003;3(9):710-20.

160. Tang Y-Q, Yuan J, Ösapay G, Ösapay K, Tran D, Miller Christopher J, et al. A Cyclic Antimicrobial Peptide Produced in Primate Leukocytes by the Ligation of Two Truncated α-Defensins. Science. 1999;286(5439):498-502.
161. Trabi M, Schirra HJ, Craik DJ. Three-dimensional structure of RTD-1, a cyclic antimicrobial defensin from Rhesus macaque leukocytes. Biochemistry. 2001;40(14):4211-21.
162. Selsted ME, Novotny MJ, Morris WL, Tang YQ, Smith W, Cullor JS. Indolicidin, a novel bactericidal tridecapeptide amide from neutrophils. J Biol Chem. 1992;267(7):4292-5.
163. Rozek A, Friedrich CL, Hancock RE. Structure of the bovine antimicrobial peptide indolicidin bound to dodecylphosphocholine and sodium dodecyl sulfate micelles. Biochemistry. 2000;39(51):15765-74.
164. Bulet P, Dimarcq JL, Hetru C, Lagueux M, Charlet M, Hegy G, et al. A novel inducible antibacterial peptide of Drosophila carries an O-glycosylated substitution. J Biol Chem. 1993;268(20):14893-7.
165. Agerberth B, Lee JY, Bergman T, Carlquist M, Boman HG, Mutt V, et al. Amino acid sequence of PR-39. Isolation from pig intestine of a new member of the family of proline-arginine-rich antibacterial peptides. Eur J Biochem. 1991;202(3):849-54.
166. Cabiaux V, Agerberth B, Johansson J, Homblé F, Goormaghtigh E, Ruysschaert JM. Secondary structure and membrane interaction of PR-39, a Pro+Arg-rich antibacterial peptide. Eur J Biochem. 1994;224(3):1019-27.
167. Dias Rde O, Franco OL. Cysteine-stabilized αβ defensins: From a common fold to antibacterial activity. Peptides. 2015;72:64-72.
168. Cornet B, Bonmatin J-M, Hetru C, Hoffmann JA, Ptak M, Vovelle F. Refined three-dimensional solution structure of insect defensin A. Structure. 1995;3(5):435-48.
169. Lay FT, Schirra HJ, Scanlon MJ, Anderson MA, Craik DJ. The Three-dimensional Solution Structure of NaD1, a New Floral Defensin from Nicotiana alata and its Application to a Homology Model of the Crop Defense Protein alfAFP. J Mol Biol. 2003;325(1):175-88.
170. Shafee TMA, Lay FT, Phan TK, Anderson MA, Hulett MD. Convergent evolution of defensin sequence, structure and function. Cell Mol Life Sci. 2017;74(4):663-82.
171. Samyn B, Martinez-Bueno M, Devreese B, Maqueda M, Gálvez A, Valdivia E, et al. The cyclic structure of the enterococcal peptide antibiotic AS-48. FEBS Lett. 1994;352(1):87-90.
172. Scholz R, Vater J, Budiharjo A, Wang Z, He Y, Dietel K, et al. Amylocyclicin, a Novel Circular Bacteriocin Produced by Bacillus amyloliquefaciens FZB42. J Bacteriol. 2014;196(10):1842-52.
173. Craik DJ, Daly NL, Bond T, Waine C. Plant cyclotides: A unique family of cyclic and knotted proteins that defines the cyclic cystine knot structural motif. J Mol Biol. 1999;294(5):1327-36.
174. Gabrielsen C, Brede DA, Nes IF, Diep DB. Circular bacteriocins: biosynthesis and mode of action. Appl Environ Microbiol. 2014;80(22):6854-62.
175. de Veer SJ, Kan M-W, Craik DJ. Cyclotides: From Structure to Function. Chem Rev. 2019;119(24):12375-421.
176. Saether O, Craik DJ, Campbell ID, Sletten K, Juul J, Norman DG. Elucidation of the primary and three-dimensional structure of the uterotonic polypeptide kalata B1. Biochemistry. 1995;34(13):4147-58.
177. Li C, Alam K, Zhao Y, Hao J, Yang Q, Zhang Y, et al. Mining and Biosynthesis of Bioactive Lanthipeptides From Microorganisms. Front Bioeng Biotechnol. 2021;9:692466.
178. Ongey EL, Neubauer P. Lanthipeptides: chemical synthesis versus *in vivo* biosynthesis as tools for pharmaceutical production. Microbial Cell Factories. 2016;15(1):97.
179. Cheng C, Hua Z-C. Lasso Peptides: Heterologous Production and Potential Medical Application. Front Bioeng Biotechnol. 2020;8.
180. Kawulka KE, Sprules T, Diaper CM, Whittal RM, McKay RT, Mercier P, et al. Structure of Subtilosin A, a Cyclic Antimicrobial Peptide from Bacillus subtilis with Unusual Sulfur to α-Carbon Cross-Links: Formation and Reduction of α-Thio-α-Amino Acid Derivatives. Biochemistry. 2004;43(12):3385-95.
181. Mathur H, Rea MC, Cotter PD, Hill C, Ross RP. The sactibiotic subclass of bacteriocins: an update. Curr Protein Pept Sci. 2015;16(6):549-58.

182. Norris GE, Patchett ML. The glycocins: in a class of their own. Curr Opin Struct Biol. 2016;40:112-9.
183. Dürr UHN, Sudheendra US, Ramamoorthy A. LL-37, the only human member of the cathelicidin family of antimicrobial peptides. Biochim Biophys Acta Biomembr. 2006;1758(9):1408-25.
184. Kumari S, Booth V. Antimicrobial Peptide Mechanisms Studied by Whole-Cell Deuterium NMR. Int J Mol Sci. 2022;23(5).
185. Andersson DI, Hughes D, Kubicek-Sutherland JZ. Mechanisms and consequences of bacterial resistance to antimicrobial peptides. Drug Resist Updat. 2016;26:43-57.
186. Brown S, Santa Maria JP, Jr., Walker S. Wall teichoic acids of gram-positive bacteria. Annu Rev Microbiol. 2013;67:313-36.
187. Brown L, Wolf JM, Prados-Rosales R, Casadevall A. Through the wall: extracellular vesicles in Gram-positive bacteria, mycobacteria and fungi. Nat Rev Microbiol. 2015;13(10):620-30.
188. Ebbensgaard A, Mordhorst H, Aarestrup FM, Hansen EB. The Role of Outer Membrane Proteins and Lipopolysaccharides for the Sensitivity of Escherichia coli to Antimicrobial Peptides. Front Microbiol. 2018;9.
189. Zamyatina A. Aminosugar-based immunomodulator lipid A: synthetic approaches. Beilstein J Org Chem. 2018;14:25-53.
190. Weidenmaier C, Peschel A. Teichoic acids and related cell-wall glycopolymers in Gram-positive physiology and host interactions. Nat Rev Microbiol. 2008;6(4):276-87.
191. Ryu M, Park J, Yeom JH, Joo M, Lee K. Rediscovery of antimicrobial peptides as therapeutic agents. J Microbiol. 2021;59(2):113-23.
192. Mookherjee N, Anderson MA, Haagsman HP, Davidson DJ. Antimicrobial host defence peptides: functions and clinical potential. Nat Rev Drug Discov. 2020;19(5):311-32.
193. Baumann G, Mueller P. A molecular model of membrane excitability. J Supramol Struct. 1974;2(5-6):538-57.
194. Fox RO, Jr., Richards FM. A voltage-gated ion channel model inferred from the crystal structure of alamethicin at 1.5-A resolution. Nature. 1982;300(5890):325-30.
195. Rapaport D, Shai Y. Interaction of fluorescently labeled pardaxin and its analogues with lipid bilayers. J Biol Chem. 1991;266(35):23769-75.
196. Ramamoorthy A, Lee D-K, Narasimhaswamy T, Nanga RPR. Cholesterol reduces pardaxin's dynamics—a barrel-stave mechanism of membrane disruption investigated by solid-state NMR. Biochim Biophys Acta Biomembr. 2010;1798(2):223-7.
197. Cruciani RA, Barker JL, Durell SR, Raghunathan G, Guy HR, Zasloff M, et al. Magainin 2, a natural antibiotic from frog skin, forms ion channels in lipid bilayer membranes. Eur J Pharmacol. 1992;226(4):287-96.
198. Ludtke SJ, He K, Heller WT, Harroun TA, Yang L, Huang HW. Membrane pores induced by magainin. Biochemistry. 1996;35(43):13723-8.
199. Matsuzaki K, Murase O, Fujii N, Miyajima K. An antimicrobial peptide, magainin 2, induced rapid flip-flop of phospholipids coupled with pore formation and peptide translocation. Biochemistry. 1996;35(35):11361-8.
200. Teixeira V, Feio MJ, Bastos M. Role of lipids in the interaction of antimicrobial peptides with membranes. Prog Lipid Res. 2012;51(2):149-77.
201. Cheng JT, Hale JD, Elliot M, Hancock RE, Straus SK. Effect of membrane composition on antimicrobial peptides aurein 2.2 and 2.3 from Australian southern bell frogs. Biophys J. 2009;96(2):552-65.
202. Yang L, Weiss TM, Lehrer RI, Huang HW. Crystallization of antimicrobial pores in membranes: magainin and protegrin. Biophys J. 2000;79(4):2002-9.
203. Yang L, Harroun TA, Weiss TM, Ding L, Huang HW. Barrel-Stave Model or Toroidal Model? A Case Study on Melittin Pores. Biophys J. 2001;81(3):1475-85.
204. Talandashti R, Mehrnejad F, Rostamipour K, Doustdar F, Lavasanifar A. Molecular Insights into Pore Formation Mechanism, Membrane Perturbation, and Water Permeation by the Antimicrobial

Peptide Pleurocidin: A Combined All-Atom and Coarse-Grained Molecular Dynamics Simulation Study. J Phys Chem B. 2021;125(26):7163-76.
205. Pouny Y, Rapaport D, Mor A, Nicolas P, Shai Y. Interaction of antimicrobial dermaseptin and its fluorescently labeled analogues with phospholipid membranes. Biochemistry. 1992;31(49):12416-23.
206. Shai Y. Mechanism of the binding, insertion and destabilization of phospholipid bilayer membranes by alpha-helical antimicrobial and cell non-selective membrane-lytic peptides. Biochim Biophys Acta. 1999;1462(1-2):55-70.
207. Fernandez DI, Le Brun AP, Whitwell TC, Sani MA, James M, Separovic F. The antimicrobial peptide aurein 1.2 disrupts model membranes via the carpet mechanism. Phys Chem Chem Phys. 2012;14(45):15739-51.
208. Zhao H, Sood R, Jutila A, Bose S, Fimland G, Nissen-Meyer J, et al. Interaction of the antimicrobial peptide pheromone Plantaricin A with model membranes: implications for a novel mechanism of action. Biochim Biophys Acta. 2006;1758(9):1461-74.
209. Cruz VL, Ramos J, Melo MN, Martinez-Salazar J. Bacteriocin AS-48 binding to model membranes and pore formation as revealed by coarse-grained simulations. Biochim Biophys Acta. 2013;1828(11):2524-31.
210. Miteva M, Andersson M, Karshikoff A, Otting G. Molecular electroporation: a unifying concept for the description of membrane pore formation by antibacterial peptides, exemplified with NK-lysin. FEBS Lett. 1999;462(1-2):155-8.
211. Pokorny A, Birkbeck TH, Almeida PFF. Mechanism and Kinetics of δ-Lysin Interaction with Phospholipid Vesicles. Biochemistry. 2002;41(36):11044-56.
212. Pokorny A, Almeida PFF. Kinetics of Dye Efflux and Lipid Flip-Flop Induced by δ-Lysin in Phosphatidylcholine Vesicles and the Mechanism of Graded Release by Amphipathic, α-Helical Peptides. Biochemistry. 2004;43(27):8846-57.
213. Hale JD, Hancock RE. Alternative mechanisms of action of cationic antimicrobial peptides on bacteria. Expert Rev Anti Infect Ther. 2007;5(6):951-9.
214. Park CB, Kim HS, Kim SC. Mechanism of Action of the Antimicrobial Peptide Buforin II: Buforin II Kills Microorganisms by Penetrating the Cell Membrane and Inhibiting Cellular Functions. Biochem Biophys Res Commun. 1998;244(1):253-7.
215. Subbalakshmi C, Sitaram N. Mechanism of antimicrobial action of indolicidin. FEMS Microbiol Lett. 1998;160(1):91-6.
216. Hsu C-H, Chen C, Jou M-L, Lee AY-L, Lin Y-C, Yu Y-P, et al. Structural and DNA-binding studies on the bovine antimicrobial peptide, indolicidin: evidence for multiple conformations involved in binding to membranes and DNA. Nucleic Acids Res. 2005;33(13):4053-64.
217. Marchand C, Krajewski K, Lee HF, Antony S, Johnson AA, Amin R, et al. Covalent binding of the natural antimicrobial peptide indolicidin to DNA abasic sites. Nucleic Acids Res. 2006;34(18):5157-65.
218. Rintoul MaR, de Arcuri BF, Salomón RA, Farías RN, Morero RD. The antibacterial action of microcin J25: evidence for disruption of cytoplasmic membrane energization in Salmonella newport. FEMS Microbiol Lett. 2001;204(2):265-70.
219. Yuzenkova J, Delgado M, Nechaev S, Savalia D, Epshtein V, Artsimovitch I, et al. Mutations of Bacterial RNA Polymerase Leading to Resistance to Microcin J25*. J Biol Chem. 2002;277(52):50867-75.
220. Roy RN, Lomakin IB, Gagnon MG, Steitz TA. The mechanism of inhibition of protein synthesis by the proline-rich peptide oncocin. Nat Struct Mol Biol. 2015;22(6):466-9.
221. Seefeldt AC, Nguyen F, Antunes S, Pérébaskine N, Graf M, Arenz S, et al. The proline-rich antimicrobial peptide Onc112 inhibits translation by blocking and destabilizing the initiation complex. Nat Struct Mol Biol. 2015;22(6):470-5.
222. Gagnon MG, Roy RN, Lomakin IB, Florin T, Mankin AS, Steitz TA. Structures of proline-rich peptides bound to the ribosome reveal a common mechanism of protein synthesis inhibition. Nucleic Acids Res. 2016;44(5):2439-50.

223. Florin T, Maracci C, Graf M, Karki P, Klepacki D, Berninghausen O, et al. An antimicrobial peptide that inhibits translation by trapping release factors on the ribosome. Nat Struct Mol Biol. 2017;24(9):752-7.
224. Kragol G, Lovas S, Varadi G, Condie BA, Hoffmann R, Otvos L, Jr. The antibacterial peptide pyrrhocoricin inhibits the ATPase actions of DnaK and prevents chaperone-assisted protein folding. Biochemistry. 2001;40(10):3016-26.
225. Ho YH, Shah P, Chen YW, Chen CS. Systematic Analysis of Intracellular-targeting Antimicrobial Peptides, Bactenecin 7, Hybrid of Pleurocidin and Dermaseptin, Proline-Arginine-rich Peptide, and Lactoferricin B, by Using Escherichia coli Proteome Microarrays. Mol Cell Proteomics. 2016;15(6):1837-47.
226. Couto MA, Harwig SS, Lehrer RI. Selective inhibition of microbial serine proteases by eNAP-2, an antimicrobial peptide from equine neutrophils. Infect Immun. 1993;61(7):2991-4.
227. Wiedemann I, Breukink E, van Kraaij C, Kuipers OP, Bierbaum G, de Kruijff B, et al. Specific Binding of Nisin to the Peptidoglycan Precursor Lipid II Combines Pore Formation and Inhibition of Cell Wall Biosynthesis for Potent Antibiotic Activity *. J Biol Chem. 2001;276(3):1772-9.
228. Scherer Katharina M, Spille J-H, Sahl H-G, Grein F, Kubitscheck U. The Lantibiotic Nisin Induces Lipid II Aggregation, Causing Membrane Instability and Vesicle Budding. Biophys J. 2015;108(5):1114-24.
229. Sass V, Schneider T, Wilmes M, Körner C, Tossi A, Novikova N, et al. Human beta-defensin 3 inhibits cell wall biosynthesis in Staphylococci. Infect Immun. 2010;78(6):2793-800.
230. Essig A, Hofmann D, Münch D, Gayathri S, Künzler M, Kallio PT, et al. Copsin, a Novel Peptide-based Fungal Antibiotic Interfering with the Peptidoglycan Synthesis *. J Biol Chem. 2014;289(50):34953-64.
231. Brötz H, Bierbaum G, Reynolds PE, Sahl H-G. The Lantibiotic Mersacidin Inhibits Peptidoglycan Biosynthesis at the Level of Transglycosylation. Eur J Biochem. 1997;246(1):193-9.
232. Utsugi T, Schroit AJ, Connor J, Bucana CD, Fidler IJ. Elevated expression of phosphatidylserine in the outer membrane leaflet of human tumor cells and recognition by activated human blood monocytes. Cancer Res. 1991;51(11):3062-6.
233. Schröder-Borm H, Bakalova R, Andrä J. The NK-lysin derived peptide NK-2 preferentially kills cancer cells with increased surface levels of negatively charged phosphatidylserine. FEBS Lett. 2005;579(27):6128-34.
234. Preta G. New Insights Into Targeting Membrane Lipids for Cancer Therapy. Front Cell Dev Biol. 2020;8.
235. Al-Benna S, Shai Y, Jacobsen F, Steinstraesser L. Oncolytic activities of host defense peptides. Int J Mol Sci. 2011;12(11):8027-51.
236. Okumura K, Itoh A, Isogai E, Hirose K, Hosokawa Y, Abiko Y, et al. C-terminal domain of human CAP18 antimicrobial peptide induces apoptosis in oral squamous cell carcinoma SAS-H1 cells. Cancer Lett. 2004;212(2):185-94.
237. Lehmann J, Retz M, Sidhu SS, Suttmann H, Sell M, Paulsen F, et al. Antitumor activity of the antimicrobial peptide magainin II against bladder cancer cell lines. Eur Urol. 2006;50(1):141-7.
238. Parvy JP, Yu Y, Dostalova A, Kondo S, Kurjan A, Bulet P, et al. The antimicrobial peptide defensin cooperates with tumour necrosis factor to drive tumour cell death in Drosophila. Elife. 2019;8.
239. Riedl S, Leber R, Rinner B, Schaider H, Lohner K, Zweytick D. Human lactoferricin derived di-peptides deploying loop structures induce apoptosis specifically in cancer cells through targeting membranous phosphatidylserine. Biochim Biophys Acta. 2015;1848(11 Pt A):2918-31.
240. Chen J, Xu X-M, Underhill CB, Yang S, Wang L, Chen Y, et al. Tachyplesin Activates the Classic Complement Pathway to Kill Tumor Cells. Cancer Res. 2005;65(11):4614-22.
241. Hancock REW, Sahl H-G. Antimicrobial and host-defense peptides as new anti-infective therapeutic strategies. Nat Biotechnol. 2006;24(12):1551-7.
242. Silhavy TJ, Kahne D, Walker S. The bacterial cell envelope. Cold Spring Harb Perspect Biol. 2010;2(5):a000414.

243. Shagaghi N, Palombo EA, Clayton AHA, Bhave M. Antimicrobial peptides: biochemical determinants of activity and biophysical techniques of elucidating their functionality. World J Microbiol Biotechnol. 2018;34(4):62.
244. Lipke Peter N, Ovalle R. Cell Wall Architecture in Yeast: New Structure and New Challenges. J Bacteriol. 1998;180(15):3735-40.
245. Pasupuleti M, Schmidtchen A, Malmsten M. Antimicrobial peptides: key components of the innate immune system. Crit Rev Biotechnol. 2012;32(2):143-71.
246. Dathe M, Nikolenko H, Meyer J, Beyermann M, Bienert M. Optimization of the antimicrobial activity of magainin peptides by modification of charge. FEBS Lett. 2001;501(2-3):146-50.
247. Tachi T, Epand RF, Epand RM, Matsuzaki K. Position-dependent hydrophobicity of the antimicrobial magainin peptide affects the mode of peptide-lipid interactions and selective toxicity. Biochemistry. 2002;41(34):10723-31.
248. Yount NY, Bayer AS, Xiong YQ, Yeaman MR. Advances in antimicrobial peptide immunobiology. Biopolymers. 2006;84(5):435-58.
249. Misawa T, Goto C, Shibata N, Hirano M, Kikuchi Y, Naito M, et al. Rational design of novel amphipathic antimicrobial peptides focused on the distribution of cationic amino acid residues. Medchemcomm. 2019;10(6):896-900.
250. Edwards IA, Elliott AG, Kavanagh AM, Blaskovich MAT, Cooper MA. Structure-Activity and -Toxicity Relationships of the Antimicrobial Peptide Tachyplesin-1. ACS Infect Dis. 2017;3(12):917-26.
251. Fernández-Vidal M, Jayasinghe S, Ladokhin AS, White SH. Folding amphipathic helices into membranes: amphiphilicity trumps hydrophobicity. J Mol Biol. 2007;370(3):459-70.
252. Villa-Hernández O, Hernández-Orihuela L, del Carmen Rodríguez M, Zamudio-Zuñiga F, Castro-Franco R, Pando V, et al. Novel antimicrobial peptides isolated from skin secretions of the Mexican frog Hyla eximia. Protein Pept Lett. 2009;16(11):1371-8.
253. Harris F, Dennison SR, Phoenix DA. Anionic antimicrobial peptides from eukaryotic organisms. Curr Protein Pept Sci. 2009;10(6):585-606.
254. Dennison SR, Harris F, Mura M, Phoenix DA. An Atlas of Anionic Antimicrobial Peptides from Amphibians. Curr Protein Pept Sci. 2018;19(8):823-38.
255. Schittek B, Hipfel R, Sauer B, Bauer J, Kalbacher H, Stevanovic S, et al. Dermcidin: a novel human antibiotic peptide secreted by sweat glands. Nat Immunol. 2001;2(12):1133-7.
256. Lai R, Liu H, Hui Lee W, Zhang Y. An anionic antimicrobial peptide from toad Bombina maxima. Biochem Biophys Res Commun. 2002;295(4):796-9.
257. Joo H-S, Fu C-I, Otto M. Bacterial strategies of resistance to antimicrobial peptides. Philos Trans R Soc Lond B Biol Sci. 2016;371(1695):20150292.
258. Schindler BD, Kaatz GW. Multidrug efflux pumps of Gram-positive bacteria. Drug Resist Updat. 2016;27:1-13.
259. Otręebska-Machaj E, Chevalier J, Handzlik J, Szymańska E, Schabikowski J, Boyer G, et al. Efflux Pump Blockers in Gram-Negative Bacteria: The New Generation of Hydantoin Based-Modulators to Improve Antibiotic Activity. Front Microbiol. 2016;7:622-.
260. Miyoshi S-i, Shinoda S. Microbial metalloproteases and pathogenesis. Microbes Infect. 2000;2(1):91-8.
261. Sieprawska-Lupa M, Mydel P, Krawczyk K, Wójcik K, Puklo M, Lupa B, et al. Degradation of human antimicrobial peptide LL-37 by Staphylococcus aureus-derived proteinases. Antimicrob Agents Chemother. 2004;48(12):4673-9.
262. Lai Y, Villaruz AE, Li M, Cha DJ, Sturdevant DE, Otto M. The human anionic antimicrobial peptide dermcidin induces proteolytic defence mechanisms in staphylococci. Mol Microbiol. 2007;63(2):497-506.
263. Hytönen J, Haataja S, Gerlach D, Podbielski A, Finne J. The SpeB virulence factor of Streptococcus pyogenes, a multifunctional secreted and cell surface molecule with strepadhesin, laminin-binding and cysteine protease activity. Mol Microbiol. 2001;39(2):512-9.

264. Kapur V, Topouzis S, Majesky MW, Li LL, Hamrick MR, Hamill RJ, et al. A conserved Streptococcus pyogenes extracellular cysteine protease cleaves human fibronectin and degrades vitronectin. Microb Pathog. 1993;15(5):327-46.
265. Schmidtchen A, Frick IM, Andersson E, Tapper H, Björck L. Proteinases of common pathogenic bacteria degrade and inactivate the antibacterial peptide LL-37. Mol Microbiol. 2002;46(1):157-68.
266. Rasmussen M, Björck L. Proteolysis and its regulation at the surface of Streptococcus pyogenes. Mol Microbiol. 2002;43(3):537-44.
267. Nyberg P, Rasmussen M, Björck L. alpha2-Macroglobulin-proteinase complexes protect Streptococcus pyogenes from killing by the antimicrobial peptide LL-37. J Biol Chem. 2004;279(51):52820-3.
268. Schmidtchen A, Frick I-M, Björck L. Dermatan sulphate is released by proteinases of common pathogenic bacteria and inactivates antibacterial α-defensin. Mol Microbiol. 2001;39(3):708-13.
269. Park PW, Pier GB, Preston MJ, Goldberger O, Fitzgerald ML, Bernfield M. Syndecan-1 shedding is enhanced by LasA, a secreted virulence factor of Pseudomonas aeruginosa. J Biol Chem. 2000;275(5):3057-64.
270. Åkesson P, Sjöholm AG, Björck L. Protein SIC, a Novel Extracellular Protein of Streptococcus pyogenes Interfering with Complement Function. J Biol Chem. 1996;271(2):1081-8.
271. Fernie-King BA, Seilly DJ, Davies A, Lachmann PJ. Streptococcal inhibitor of complement inhibits two additional components of the mucosal innate immune system: secretory leukocyte proteinase inhibitor and lysozyme. Infect Immun. 2002;70(9):4908-16.
272. Frick IM, Akesson P, Rasmussen M, Schmidtchen A, Björck L. SIC, a secreted protein of Streptococcus pyogenes that inactivates antibacterial peptides. J Biol Chem. 2003;278(19):16561-6.
273. Peetermans M, Vanassche T, Liesenborghs L, Lijnen RH, Verhamme P. Bacterial pathogens activate plasminogen to breach tissue barriers and escape from innate immunity. Crit Rev Microbiol. 2016;42(6):866-82.
274. Braff MH, Jones AL, Skerrett SJ, Rubens CE. Staphylococcus aureus Exploits Cathelicidin Antimicrobial Peptides Produced during Early Pneumonia to Promote Staphylokinase-Dependent Fibrinolysis. J Infect Dis. 2007;195(9):1365-72.
275. Jin T, Bokarewa M, Foster T, Mitchell J, Higgins J, Tarkowski A. Staphylococcus aureus resists human defensins by production of staphylokinase, a novel bacterial evasion mechanism. J Immunol. 2004;172(2):1169-76.
276. Brinkmann V, Reichard U, Goosmann C, Fauler B, Uhlemann Y, Weiss DS, et al. Neutrophil extracellular traps kill bacteria. Science. 2004;303(5663):1532-5.
277. Papayannopoulos V. Neutrophil extracellular traps in immunity and disease. Nat Rev Immunol. 2018;18(2):134-47.
278. Bisno AL, Brito MO, Collins CM. Molecular basis of group A streptococcal virulence. Lancet Infect Dis. 2003;3(4):191-200.
279. Lauer P, Rinaudo Cira D, Soriani M, Margarit I, Maione D, Rosini R, et al. Genome Analysis Reveals Pili in Group B Streptococcus. Science. 2005;309(5731):105-.
280. Maisey HC, Quach D, Hensler ME, Liu GY, Gallo RL, Nizet V, et al. A group B streptococcal pilus protein promotes phagocyte resistance and systemic virulence. FASEB J. 2008;22(6):1715-24.
281. Fronzes R, Remaut H, Waksman G. Architectures and biogenesis of non-flagellar protein appendages in Gram-negative bacteria. EMBO J. 2008;27(17):2271-80.
282. Scott JR, Zähner D. Pili with strong attachments: Gram-positive bacteria do it differently. Mol Microbiol. 2006;62(2):320-30.
283. Nawrocki KL, Crispell EK, McBride SM. Antimicrobial Peptide Resistance Mechanisms of Gram-Positive Bacteria. Antibiotics. 2014;3(4):461-92.
284. Geiger C, Korn SM, Häsler M, Peetz O, Martin J, Kötter P, et al. LanI-Mediated Lantibiotic Immunity in Bacillus subtilis: Functional Analysis. Appl Environ Microbiol. 2019;85(11):e00534-19.
285. Chatterjee C, Paul M, Xie L, van der Donk WA. Biosynthesis and Mode of Action of Lantibiotics. Chem Rev. 2005;105(2):633-84.

286. Kuipers OP, Beerthuyzen MM, Siezen RJ, De Vos WM. Characterization of the nisin gene cluster nisABTCIPR of Lactococcus lactis. Requirement of expression of the nisA and nisI genes for development of immunity. Eur J Biochem. 1993;216(1):281-91.
287. Takala TM, Saris PEJ. C terminus of NisI provides specificity to nisin. Microbiology. 2006;152(12):3543-9.
288. Engelke G, Gutowski-Eckel Z, Kiesau P, Siegers K, Hammelmann M, Entian KD. Regulation of nisin biosynthesis and immunity in Lactococcus lactis 6F3. Appl Environ Microbiol. 1994;60(3):814-25.
289. Taylor CM, Roberts IS. Capsular polysaccharides and their role in virulence. Contrib Microbiol. 2005;12:55-66.
290. Herasimenka Y, Benincasa M, Mattiuzzo M, Cescutti P, Gennaro R, Rizzo R. Interaction of antimicrobial peptides with bacterial polysaccharides from lung pathogens. Peptides. 2005;26(7):1127-32.
291. Llobet E, Tomás JM, Bengoechea JA. Capsule polysaccharide is a bacterial decoy for antimicrobial peptides. Microbiology. 2008;154(Pt 12):3877-86.
292. Mack D, Fischer W, Krokotsch A, Leopold K, Hartmann R, Egge H, et al. The intercellular adhesin involved in biofilm accumulation of Staphylococcus epidermidis is a linear beta-1,6-linked glucosaminoglycan: purification and structural analysis. J Bacteriol. 1996;178(1):175-83.
293. Vuong C, Voyich JM, Fischer ER, Braughton KR, Whitney AR, DeLeo FR, et al. Polysaccharide intercellular adhesin (PIA) protects Staphylococcus epidermidis against major components of the human innate immune system. Cell Microbiol. 2004;6(3):269-75.
294. Beiter K, Wartha F, Hurwitz R, Normark S, Zychlinsky A, Henriques-Normark B. The capsule sensitizes Streptococcus pneumoniae to alpha-defensins human neutrophil proteins 1 to 3. Infect Immun. 2008;76(8):3710-6.
295. Wartha F, Beiter K, Albiger B, Fernebro J, Zychlinsky A, Normark S, et al. Capsule and D-alanylated lipoteichoic acids protect Streptococcus pneumoniae against neutrophil extracellular traps. Cell Microbiol. 2007;9(5):1162-71.
296. Jansen A, Szekat C, Schröder W, Wolz C, Goerke C, Lee JC, et al. Production of capsular polysaccharide does not influence Staphylococcus aureusvancomycin susceptibility. BMC Microbiol. 2013;13(1):65.
297. Kristian Sascha A, Datta V, Weidenmaier C, Kansal R, Fedtke I, Peschel A, et al. d-Alanylation of Teichoic Acids Promotes Group A Streptococcus Antimicrobial Peptide Resistance, Neutrophil Survival, and Epithelial Cell Invasion. J Bacteriol. 2005;187(19):6719-25.
298. Peschel A, Jack RW, Otto M, Collins LV, Staubitz P, Nicholson G, et al. Staphylococcus aureus resistance to human defensins and evasion of neutrophil killing via the novel virulence factor MprF is based on modification of membrane lipids with l-lysine. J Exp Med. 2001;193(9):1067-76.
299. Staubitz P, Neumann H, Schneider T, Wiedemann I, Peschel A. MprF-mediated biosynthesis of lysylphosphatidylglycerol, an important determinant in staphylococcal defensin resistance. FEMS Microbiol Lett. 2004;231(1):67-71.
300. Maloney E, Stankowska D, Zhang J, Fol M, Cheng QJ, Lun S, et al. The two-domain LysX protein of Mycobacterium tuberculosis is required for production of lysinylated phosphatidylglycerol and resistance to cationic antimicrobial peptides. PLoS Pathog. 2009;5(7):e1000534.
301. Samant S, Hsu FF, Neyfakh AA, Lee H. The Bacillus anthracis protein MprF is required for synthesis of lysylphosphatidylglycerols and for resistance to cationic antimicrobial peptides. J Bacteriol. 2009;191(4):1311-9.
302. Neuhaus FC, Baddiley J. A continuum of anionic charge: structures and functions of D-alanyl-teichoic acids in gram-positive bacteria. Microbiol Mol Biol Rev. 2003;67(4):686-723.
303. Saar-Dover R, Bitler A, Nezer R, Shmuel-Galia L, Firon A, Shimoni E, et al. D-alanylation of lipoteichoic acids confers resistance to cationic peptides in group B streptococcus by increasing the cell wall density. PLoS Pathog. 2012;8(9):e1002891.
304. Chipman DM, Sharon N. Mechanism of lysozyme action. Science. 1969;165(3892):454-65.

305. Bera A, Herbert S, Jakob A, Vollmer W, Götz F. Why are pathogenic staphylococci so lysozyme resistant? The peptidoglycan O-acetyltransferase OatA is the major determinant for lysozyme resistance of Staphylococcus aureus. Mol Microbiol. 2005;55(3):778-87.
306. Pfeffer JM, Strating H, Weadge JT, Clarke AJ. Peptidoglycan O acetylation and autolysin profile of Enterococcus faecalis in the viable but nonculturable state. J Bacteriol. 2006;188(3):902-8.
307. Aubry C, Goulard C, Nahori MA, Cayet N, Decalf J, Sachse M, et al. OatA, a peptidoglycan O-acetyltransferase involved in Listeria monocytogenes immune escape, is critical for virulence. J Infect Dis. 2011;204(5):731-40.
308. Rae CS, Geissler A, Adamson PC, Portnoy DA. Mutations of the Listeria monocytogenes peptidoglycan N-deacetylase and O-acetylase result in enhanced lysozyme sensitivity, bacteriolysis, and hyperinduction of innate immune pathways. Infect Immun. 2011;79(9):3596-606.
309. Vollmer W, Tomasz A. The pgdA gene encodes for a peptidoglycan N-acetylglucosamine deacetylase in Streptococcus pneumoniae. J Biol Chem. 2000;275(27):20496-501.
310. Deckers D, Masschalck B, Aertsen A, Callewaert L, Van Tiggelen CG, Atanassova M, et al. Periplasmic lysozyme inhibitor contributes to lysozyme resistance in Escherichia coli. Cell Mol Life Sci. 2004;61(10):1229-37.
311. Binks MJ, Fernie-King BA, Seilly DJ, Lachmann PJ, Sriprakash KS. Attribution of the various inhibitory actions of the streptococcal inhibitor of complement (SIC) to regions within the molecule. J Biol Chem. 2005;280(20):20120-5.
312. Ming X, Daeschel MA. Nisin Resistance of Foodborne Bacteria and the Specific Resistance Responses of Listeria monocytogenes Scott A. J Food Prot. 1993;56(11):944-8.
313. Maisnier-Patin S, Richard J. Cell wall changes in nisin-resistant variants of Listeria innocua grown in the presence of high nisin concentrations. FEMS Microbiol Lett. 1996;140(1):29-35.
314. Bonnet M, Rafi MM, Chikindas ML, Montville TJ. Bioenergetic mechanism for nisin resistance, induced by the acid tolerance response of Listeria monocytogenes. Appl Environ Microbiol. 2006;72(4):2556-63.
315. Du D, Wang-Kan X, Neuberger A, van Veen HW, Pos KM, Piddock LJV, et al. Multidrug efflux pumps: structure, function and regulation. Nat Rev Microbiol. 2018;16(9):523-39.
316. Costa SS, Viveiros M, Rosato AE, Melo-Cristino J, Couto I. Impact of efflux in the development of multidrug resistance phenotypes in Staphylococcus aureus. BMC Microbiol. 2015;15(1):232.
317. Hassan KA, Liu Q, Henderson PJF, Paulsen IT, Bush K. Homologs of the Acinetobacter baumannii AceI Transporter Represent a New Family of Bacterial Multidrug Efflux Systems. mBio. 2015;6(1):e01982-14.
318. Hassan KA, Liu Q, Elbourne LDH, Ahmad I, Sharples D, Naidu V, et al. Pacing across the membrane: the novel PACE family of efflux pumps is widespread in Gram-negative pathogens. Res Microbiol. 2018;169(7-8):450-4.
319. Davidson AL, Dassa E, Orelle C, Chen J. Structure, function, and evolution of bacterial ATP-binding cassette systems. Microbiol Mol Biol Rev. 2008;72(2):317-64.
320. Draper LA, Ross RP, Hill C, Cotter PD. Lantibiotic immunity. Curr Protein Pept Sci. 2008;9(1):39-49.
321. Gebhard S. ABC transporters of antimicrobial peptides in Firmicutes bacteria - phylogeny, function and regulation. Mol Microbiol. 2012;86(6):1295-317.
322. Zähner D, Zhou X, Chancey ST, Pohl J, Shafer WM, Stephens DS. Human antimicrobial peptide LL-37 induces MefE/Mel-mediated macrolide resistance in Streptococcus pneumoniae. Antimicrob Agents Chemother. 2010;54(8):3516-9.
323. Shafer WM, Qu X, Waring AJ, Lehrer RI. Modulation of Neisseria gonorrhoeae susceptibility to vertebrate antibacterial peptides due to a member of the resistance/nodulation/division efflux pump family. Proc Natl Acad Sci U S A. 1998;95(4):1829-33.
324. Tzeng YL, Ambrose KD, Zughaier S, Zhou X, Miller YK, Shafer WM, et al. Cationic antimicrobial peptide resistance in Neisseria meningitidis. J Bacteriol. 2005;187(15):5387-96.
325. Padilla E, Llobet E, Doménech-Sánchez A, Martínez-Martínez L, Bengoechea JA, Albertí S. Klebsiella pneumoniae AcrAB efflux pump contributes to antimicrobial resistance and virulence. Antimicrob Agents Chemother. 2010;54(1):177-83.

326. Bina XR, Provenzano D, Nguyen N, Bina JE. Vibrio cholerae RND family efflux systems are required for antimicrobial resistance, optimal virulence factor production, and colonization of the infant mouse small intestine. Infect Immun. 2008;76(8):3595-605.
327. Rieg S, Huth A, Kalbacher H, Kern WV. Resistance against antimicrobial peptides is independent of Escherichia coli AcrAB, Pseudomonas aeruginosa MexAB and Staphylococcus aureus NorA efflux pumps. Int J Antimicrob Agents. 2009;33(2):174-6.
328. Ohki R, Giyanto, Tateno K, Masuyama W, Moriya S, Kobayashi K, et al. The BceRS two-component regulatory system induces expression of the bacitracin transporter, BceAB, in Bacillus subtilis. Mol Microbiol. 2003;49(4):1135-44.
329. Hiron A, Falord M, Valle J, Débarbouillé M, Msadek T. Bacitracin and nisin resistance in Staphylococcus aureus: a novel pathway involving the BraS/BraR two-component system (SA2417/SA2418) and both the BraD/BraE and VraD/VraE ABC transporters. Mol Microbiol. 2011;81(3):602-22.
330. Eldholm V, Gutt B, Johnsborg O, Brückner R, Maurer P, Hakenbeck R, et al. The pneumococcal cell envelope stress-sensing system LiaFSR is activated by murein hydrolases and lipid II-interacting antibiotics. J Bacteriol. 2010;192(7):1761-73.
331. Miller SI, Kukral AM, Mekalanos JJ. A two-component regulatory system (phoP phoQ) controls Salmonella typhimurium virulence. Proc Natl Acad Sci U S A. 1989;86(13):5054-8.
332. Bader MW, Sanowar S, Daley ME, Schneider AR, Cho U, Xu W, et al. Recognition of antimicrobial peptides by a bacterial sensor kinase. Cell. 2005;122(3):461-72.
333. Gunn JS, Miller SI. PhoP-PhoQ activates transcription of pmrAB, encoding a two-component regulatory system involved in Salmonella typhimurium antimicrobial peptide resistance. J Bacteriol. 1996;178(23):6857-64.
334. Gunn JS, Lim KB, Krueger J, Kim K, Guo L, Hackett M, et al. PmrA-PmrB-regulated genes necessary for 4-aminoarabinose lipid A modification and polymyxin resistance. Mol Microbiol. 1998;27(6):1171-82.
335. Groisman EA. The pleiotropic two-component regulatory system PhoP-PhoQ. J Bacteriol. 2001;183(6):1835-42.
336. Assoni L, Milani B, Carvalho MR, Nepomuceno LN, Waz NT, Guerra MES, et al. Resistance Mechanisms to Antimicrobial Peptides in Gram-Positive Bacteria. Front Microbiol. 2020;11.
337. Gan BH, Gaynord J, Rowe SM, Deingruber T, Spring DR. The multifaceted nature of antimicrobial peptides: current synthetic chemistry approaches and future directions. Chem Soc Rev. 2021;50(13):7820-80.
338. Di L. Strategic approaches to optimizing peptide ADME properties. AAPS J. 2015;17(1):134-43.
339. Gottler LM, Ramamoorthy A. Structure, membrane orientation, mechanism, and function of pexiganan — A highly potent antimicrobial peptide designed from magainin. Biochim Biophys Acta Biomembr. 2009;1788(8):1680-6.
340. Jenssen H, Hamill P, Hancock Robert EW. Peptide Antimicrobial Agents. Clin Microbiol Rev. 2006;19(3):491-511.
341. Zhao X, Zhang M, Muhammad I, Cui Q, Zhang H, Jia Y, et al. An Antibacterial Peptide with High Resistance to Trypsin Obtained by Substituting d-Amino Acids for Trypsin Cleavage Sites. Antibiotics. 2021;10(12):1465.
342. Kumar P, Kizhakkedathu JN, Straus SK. Antimicrobial Peptides: Diversity, Mechanism of Action and Strategies to Improve the Activity and Biocompatibility *In Vivo*. Biomolecules. 2018;8(1).
343. Jia F, Wang J, Peng J, Zhao P, Kong Z, Wang K, et al. D-amino acid substitution enhances the stability of antimicrobial peptide polybia-CP. Acta Biochim Biophys Sin. 2017;49(1672-9145):916.
344. Zhao Y, Zhang M, Qiu S, Wang J, Peng J, Zhao P, et al. Antimicrobial activity and stability of the D-amino acid substituted derivatives of antimicrobial peptide polybia-MPI. AMB Express. 2016;6(1):122.
345. Kindrachuk J, Scruten E, Attah-Poku S, Bell K, Potter A, Babiuk LA, et al. Stability, toxicity, and biological activity of host defense peptide BMAP28 and its inversed and retro-inversed isomers. Biopolymers. 2011;96(1):14-24.

346. Lakshmaiah Narayana J, Golla R, Mishra B, Wang X, Lushnikova T, Zhang Y, et al. Short and Robust Anti-Infective Lipopeptides Engineered Based on the Minimal Antimicrobial Peptide KR12 of Human LL-37. ACS Infect Dis. 2021;7(6):1795-808.
347. Ting DSJ, Beuerman RW, Dua HS, Lakshminarayanan R, Mohammed I. Strategies in Translating the Therapeutic Potentials of Host Defense Peptides. Front Immunol. 2020;11.
348. Saikia K, Sravani YD, Ramakrishnan V, Chaudhary N. Highly potent antimicrobial peptides from N-terminal membrane-binding region of E. coli MreB. Sci Rep. 2017;7:42994.
349. Wang G. Post-translational Modifications of Natural Antimicrobial Peptides and Strategies for Peptide Engineering. Curr Biotechnol. 2012;1(1):72-9.
350. Dos Santos Cabrera MP, Arcisio-Miranda M, Broggio Costa ST, Konno K, Ruggiero JR, Procopio J, et al. Study of the mechanism of action of anoplin, a helical antimicrobial decapeptide with ion channel-like activity, and the role of the amidated C-terminus. J Pept Sci. 2008;14(6):661-9.
351. Irudayam SJ, Berkowitz ML. Binding and reorientation of melittin in a POPC bilayer: Computer simulations. Biochim Biophys Acta Biomembr. 2012;1818(12):2975-81.
352. Dennison SR, Phoenix DA. Influence of C-terminal amidation on the efficacy of modelin-5. Biochemistry. 2011;50(9):1514-23.
353. Mura M, Wang J, Zhou Y, Pinna M, Zvelindovsky AV, Dennison SR, et al. The effect of amidation on the behaviour of antimicrobial peptides. Eur Biophys J. 2016;45(3):195-207.
354. Dennison SR, Harris F, Bhatt T, Singh J, Phoenix DA. The effect of C-terminal amidation on the efficacy and selectivity of antimicrobial and anticancer peptides. Mol Cell Biochem. 2009;332(1-2):43-50.
355. Kuzmin DV, Emelianova AA, Kalashnikova MB, Panteleev PV, Ovchinnikova TV. Effect of N- and C-Terminal Modifications on Cytotoxic Properties of Antimicrobial Peptide Tachyplesin I. Bull Exp Biol Med. 2017;162(6):754-7.
356. Oliva R, Chino M, Pane K, Pistorio V, De Santis A, Pizzo E, et al. Exploring the role of unnatural amino acids in antimicrobial peptides. Sci Rep. 2018;8(1):8888.
357. Zhang R, Wu F, Wu L, Tian Y, Zhou B, Zhang X, et al. Novel Self-Assembled Micelles Based on Cholesterol-Modified Antimicrobial Peptide (DP7) for Safe and Effective Systemic Administration in Animal Models of Bacterial Infection. Antimicrob Agents Chemother. 2018;62(11).
358. Chen L, Shen T, Liu Y, Zhou J, Shi S, Wang Y, et al. Enhancing the antibacterial activity of antimicrobial peptide PMAP-37(F34-R) by cholesterol modification. BMC Vet Res. 2020;16(1):419.
359. Jevsevar S, Kunstelj M, Porekar VG. PEGylation of therapeutic proteins. Biotechnol J. 2010;5(1):113-28.
360. Veronese FM, Pasut G. PEGylation, successful approach to drug delivery. Drug Discov Today. 2005;10(21):1451-8.
361. Rezende SB, Oshiro KGN, Júnior NGO, Franco OL, Cardoso MH. Advances on chemically modified antimicrobial peptides for generating peptide antibiotics. Chem Commun (Camb). 2021;57(88):11578-90.
362. Imura Y, Nishida M, Matsuzaki K. Action mechanism of PEGylated magainin 2 analogue peptide. Biochim Biophys Acta. 2007;1768(10):2578-85.
363. Li Y, Clark KA, Tan Z. Methods for engineering therapeutic peptides. Chin Chem Lett. 2018;29(7):1074-8.
364. Nollmann FI, Goldbach T, Berthold N, Hoffmann R. Controlled systemic release of therapeutic peptides from PEGylated prodrugs by serum proteases. Angew Chem Int Ed Engl. 2013;52(29):7597-9.
365. Böttger R, Hoffmann R, Knappe D. Differential stability of therapeutic peptides with different proteolytic cleavage sites in blood, plasma and serum. PLoS One. 2017;12(6):e0178943.
366. Gong Y, Andina D, Nahar S, Leroux JC, Gauthier MA. Releasable and traceless PEGylation of arginine-rich antimicrobial peptides. Chem Sci. 2017;8(5):4082-6.
367. Huan Y, Kong Q, Mou H, Yi H. Antimicrobial Peptides: Classification, Design, Application and Research Progress in Multiple Fields. Front Microbiol. 2020;11.

368. Arias M, Piga KB, Hyndman ME, Vogel HJ. Improving the Activity of Trp-Rich Antimicrobial Peptides by Arg/Lys Substitutions and Changing the Length of Cationic Residues. Biomolecules. 2018;8(2).
369. Wani MC, Taylor HL, Wall ME, Coggon P, McPhail AT. Plant antitumor agents. VI. The isolation and structure of taxol, a novel antileukemic and antitumor agent from Taxus brevifolia. J Am Chem Soc. 1971;93(9):2325-7.
370. Umezawa H, Maeda K, Takeuchi T, Okami Y. New antibiotics, bleomycin A and B. J Antibiot. 1966;19(5):200-9.
371. Povirk LF. Bleomycin. In: Neidle S, Waring MJ, editors. Molecular Aspects of Anti-Cancer Drug Action. London: Macmillan Education UK; 1983. p. 157-81.
372. Nakayama K, Kawato HC, Inagaki H, Nakajima R, Kitamura A, Someya K, et al. Synthesis and Antifungal Activity of Rhodopeptin Analogues. 2. Modification of the West Amino Acid Moiety. Org Lett. 2000;2(7):977-80.
373. Roberts KD, Zhu Y, Azad MAK, Han M-L, Wang J, Wang L, et al. A synthetic lipopeptide targeting top-priority multidrug-resistant Gram-negative pathogens. Nat Commun. 2022;13(1):1625.
374. Aslan AT, Akova M, Paterson DL. Next-Generation Polymyxin Class of Antibiotics: A Ray of Hope Illuminating a Dark Road. Antibiotics (Basel). 2022;11(12).
375. Cui Z, Johnston WA, Alexandrov K. Cell-Free Approach for Non-canonical Amino Acids Incorporation Into Polypeptides. Front Bioeng Biotechnol. 2020;8.
376. Dumas A, Lercher L, Spicer CD, Davis BG. Designing logical codon reassignment - Expanding the chemistry in biology. Chem Sci. 2015;6(1):50-69.
377. Kuthning A, Durkin P, Oehm S, Hoesl MG, Budisa N, Süssmuth RD. Towards Biocontained Cell Factories: An Evolutionarily Adapted Escherichia coli Strain Produces a New-to-nature Bioactive Lantibiotic Containing Thienopyrrole-Alanine. Sci Rep. 2016;6:33447.
378. Kakkar N, Perez JG, Liu WR, Jewett MC, van der Donk WA. Incorporation of Nonproteinogenic Amino Acids in Class I and II Lantibiotics. ACS Chem Biol. 2018;13(4):951-7.
379. Piscotta FJ, Tharp JM, Liu WR, Link AJ. Expanding the chemical diversity of lasso peptide MccJ25 with genetically encoded noncanonical amino acids. Chem Commun (Camb). 2015;51(2):409-12.
380. Saravolatz LD, Pawlak J, Johnson L, Bonilla H, Saravolatz LD, 2nd, Fakih MG, et al. *In vitro* activities of LTX-109, a synthetic antimicrobial peptide, against methicillin-resistant, vancomycin-intermediate, vancomycin-resistant, daptomycin-nonsusceptible, and linezolid-nonsusceptible Staphylococcus aureus. Antimicrob Agents Chemother. 2012;56(8):4478-82.
381. Bojsen R, Torbensen R, Larsen CE, Folkesson A, Regenberg B. The synthetic amphipathic peptidomimetic LTX109 is a potent fungicide that disturbs plasma membrane integrity in a sphingolipid dependent manner. PLoS One. 2013;8(7):e69483.
382. Haug BE, Stensen W, Kalaaji M, Rekdal Ø, Svendsen JS. Synthetic Antimicrobial Peptidomimetics with Therapeutic Potential. J Med Chem. 2008;51(14):4306-14.
383. Isaksson J, Brandsdal BO, Engqvist M, Flaten GE, Svendsen JSM, Stensen W. A Synthetic Antimicrobial Peptidomimetic (LTX 109): Stereochemical Impact on Membrane Disruption. J Med Chem. 2011;54(16):5786-95.
384. NIH. ClinicalTrials.gov [cited 2023 February 23]. Available from: https://beta.clinicaltrials.gov/search?distance=50&cond=ltx-109&limit=25&page=1.
385. Gálvez A, Maqueda M, Valdivia E, Quesada A, Montoya E. Characterization and partial purification of a broad spectrum antibiotic AS-48 produced by Streptococcus faecalis. Can J Microbiol. 1986;32(10):765-71.
386. Fang XY, Chen W, Fan JT, Song R, Wang L, Gu YH, et al. Plant cyclopeptide RA-V kills human breast cancer cells by inducing mitochondria-mediated apoptosis through blocking PDK1-AKT interaction. Toxicol Appl Pharmacol. 2013;267(1):95-103.
387. Svangård E, Göransson U, Hocaoglu Z, Gullbo J, Larsson R, Claeson P, et al. Cytotoxic cyclotides from Viola tricolor. J Nat Prod. 2004;67(2):144-7.
388. Chen B, Colgrave ML, Wang C, Craik DJ. Cycloviolacin H4, a Hydrophobic Cyclotide from Viola hederaceae. J Nat Prod. 2006;69(1):23-8.

389. White KM, Rosales R, Yildiz S, Kehrer T, Miorin L, Moreno E, et al. Plitidepsin has potent preclinical efficacy against SARS-CoV-2 by targeting the host protein eEF1A. Science. 2021;371(6532):926-31.
390. de Veer SJ, Weidmann J, Craik DJ. Cyclotides as Tools in Chemical Biology. Acc Chem Res. 2017;50(7):1557-65.
391. Muratspahić E, Koehbach J, Gruber CW, Craik DJ. Harnessing cyclotides to design and develop novel peptide GPCR ligands. RSC Chem Biol. 2020;1(4):177-91.
392. Chan LY, Zhang VM, Huang YH, Waters NC, Bansal PS, Craik DJ, et al. Cyclization of the antimicrobial peptide gomesin with native chemical ligation: influences on stability and bioactivity. Chembiochem. 2013;14(5):617-24.
393. Andreev K, Martynowycz MW, Ivankin A, Huang ML, Kuzmenko I, Meron M, et al. Cyclization Improves Membrane Permeation by Antimicrobial Peptoids. Langmuir. 2016;32(48):12905-13.
394. Junkes C, Wessolowski A, Farnaud S, Evans RW, Good L, Bienert M, et al. The interaction of arginine- and tryptophan-rich cyclic hexapeptides with Escherichia coli membranes. J Pept Sci. 2008;14(4):535-43.
395. Tam JP, Wu C, Yang JL. Membranolytic selectivity of cystine-stabilized cyclic protegrins. Eur J Biochem. 2000;267(11):3289-300.
396. Yu Q, Lehrer RI, Tam JP. Engineered salt-insensitive alpha-defensins with end-to-end circularized structures. J Biol Chem. 2000;275(6):3943-9.
397. Mwangi J, Yin Y, Wang G, Yang M, Li Y, Zhang Z, et al. The antimicrobial peptide ZY4 combats multidrug-resistant Pseudomonas aeruginosa and Acinetobacter baumannii infection. Proc Natl Acad Sci U S A. 2019;116(52):26516-22.
398. Etayash H, Pletzer D, Kumar P, Straus SK, Hancock REW. Cyclic Derivative of Host-Defense Peptide IDR-1018 Improves Proteolytic Stability, Suppresses Inflammation, and Enhances *In Vivo* Activity. J Med Chem. 2020;63(17):9228-36.
399. Raaijmakers JM, De Bruijn I, Nybroe O, Ongena M. Natural functions of lipopeptides from Bacillus and Pseudomonas: more than surfactants and antibiotics. FEMS Microbiol Rev. 2010;34(6):1037-62.
400. Ongena M, Jacques P. Bacillus lipopeptides: versatile weapons for plant disease biocontrol. Trends Microbiol. 2008;16(3):115-25.
401. Théatre A, Hoste ACR, Rigolet A, Benneceur I, Bechet M, Ongena M, et al. Bacillus sp.: A Remarkable Source of Bioactive Lipopeptides. Adv Biochem Eng Biotechnol. 2022;181:123-79.
402. Hubrich F, Bösch NM, Chepkirui C, Morinaka BI, Rust M, Gugger M, et al. Ribosomally derived lipopeptides containing distinct fatty acyl moieties. Proc Natl Acad Sci U S A. 2022;119(3).
403. Rounds T, Straus SK. Lipidation of Antimicrobial Peptides as a Design Strategy for Future Alternatives to Antibiotics. Int J Mol Sci. 2020;21(24):9692.
404. Chu-Kung AF, Nguyen R, Bozzelli KN, Tirrell M. Chain length dependence of antimicrobial peptide-fatty acid conjugate activity. J Colloid Interface Sci. 2010;345(2):160-7.
405. Albada HB, Prochnow P, Bobersky S, Langklotz S, Schriek P, Bandow JE, et al. Tuning the activity of a short arg-trp antimicrobial Peptide by lipidation of a C- or N-terminal lysine side-chain. ACS Med Chem Lett. 2012;3(12):980-4.
406. Lockwood NA, Haseman JR, Tirrell MV, Mayo KH. Acylation of SC4 dodecapeptide increases bactericidal potency against Gram-positive bacteria, including drug-resistant strains. Biochem J. 2004;378(1):93-103.
407. Steigenberger J, Verleysen Y, Geudens N, Martins JC, Heerklotz H. The Optimal Lipid Chain Length of a Membrane-Permeabilizing Lipopeptide Results From the Balance of Membrane Partitioning and Local Damage. Front Microbiol. 2021;12:669709.
408. Schneider EK, Huang JX, Carbone V, Han M, Zhu Y, Nang S, et al. Plasma Protein Binding Structure–Activity Relationships Related to the N-Terminus of Daptomycin. ACS Infect Dis. 2017;3(3):249-58.

409. Lee J, Kim S, Sim JY, Lee D, Kim HH, Hwang JS, et al. A potent antibacterial activity of new short d-enantiomeric lipopeptide against multi drug resistant bacteria. Biochim Biophys Acta Biomembr. 2019;1861(1):34-42.
410. Makovitzki A, Avrahami D, Shai Y. Ultrashort antibacterial and antifungal lipopeptides. Proc Natl Acad Sci U S A. 2006;103(43):15997-6002.
411. Makovitzki A, Baram J, Shai Y. Antimicrobial Lipopolypeptides Composed of Palmitoyl Di- and Tricationic Peptides: *In Vitro* and *in Vivo* Activities, Self-Assembly to Nanostructures, and a Plausible Mode of Action. Biochemistry. 2008;47(40):10630-6.
412. Avrahami D, Shai Y. Bestowing Antifungal and Antibacterial Activities by Lipophilic Acid Conjugation to d,l-Amino Acid-Containing Antimicrobial Peptides: A Plausible Mode of Action. Biochemistry. 2003;42(50):14946-56.
413. Liu Y, Li S, Shen T, Chen L, Zhou J, Shi S, et al. N-terminal Myristoylation Enhanced the Antimicrobial Activity of Antimicrobial Peptide PMAP-36PW. Front Cell Infect Microbiol. 2020;10:450.
414. Zhong C, Zhu N, Zhu Y, Liu T, Gou S, Xie J, et al. Antimicrobial peptides conjugated with fatty acids on the side chain of D-amino acid promises antimicrobial potency against multidrug-resistant bacteria. Eur J Pharm Sci. 2020;141:105123.
415. Zhong C, Zhang F, Zhu N, Zhu Y, Yao J, Gou S, et al. Ultra-short lipopeptides against gram-positive bacteria while alleviating antimicrobial resistance. Eur J Med Chem. 2021;212:113138.
416. Siano A, Húmpola MV, Rey MC, Simonetta A, Tonarelli GG. Interaction of Acylated and Substituted Antimicrobial Peptide Analogs with Phospholipid–Polydiacetylene Vesicles. Correlation with their Biological Properties. Chem Biol Drug Des. 2011;78(1):85-93.
417. Ghosh C, Konai MM, Sarkar P, Samaddar S, Haldar J. Designing Simple Lipidated Lysines: Bifurcation Imparts Selective Antibacterial Activity. ChemMedChem. 2016;11(21):2367-71.
418. Greber KE, Dawgul M, Kamysz W, Sawicki W, Łukasiak J. Biological and surface-active properties of double-chain cationic amino acid-based surfactants. Amino Acids. 2014;46(8):1893-8.
419. Chionis K, Krikorian D, Koukkou A-I, Sakarellos-Daitsiotis M, Panou-Pomonis E. Synthesis and biological activity of lipophilic analogs of the cationic antimicrobial active peptide anoplin. J Pept Sci. 2016;22(11-12):731-6.
420. Koh J-J, Lin H, Caroline V, Chew YS, Pang LM, Aung TT, et al. N-Lipidated Peptide Dimers: Effective Antibacterial Agents against Gram-Negative Pathogens through Lipopolysaccharide Permeabilization. J Med Chem. 2015;58(16):6533-48.
421. Davies JS. The cyclization of peptides and depsipeptides. J Pept Sci. 2003;9(8):471-501.
422. Góngora-Benítez M, Tulla-Puche J, Albericio F. Multifaceted roles of disulfide bonds. Peptides as therapeutics. Chem Rev. 2014;114(2):901-26.
423. Malesevic M, Strijowski U, Bächle D, Sewald N. An improved method for the solution cyclization of peptides under pseudo-high dilution conditions. J Biotechnol. 2004;112(1):73-7.
424. Biron É, Vézina-Dawod S, Bédard F. Synthetic Strategies for Macrocyclic Peptides. Practical Medicinal Chemistry with Macrocycles 2017. p. 205-41.
425. Zaretsky S, Yudin AK. Contemporary Macrocyclization Technologies. Practical Medicinal Chemistry with Macrocycles 2017. p. 1-24.
426. El Haddadi M, Cavelier F, Vives E, Azmani A, Verducci J, Martinez J. All-L-Leu-Pro-Leu-Pro: a challenging cyclization. J Pept Sci. 2000;6(11):560-70.
427. Corey EJ, Nicolaou KC. Efficient and mild lactonization method for the synthesis of macrolides. J Am Chem Soc. 1974;96(17):5614-6.
428. Mukaiyama T, Usui M, Saigo K. The facile synthesis of lactones. Chem Lett. 1976;5(1):49-50.
429. Inanaga J, Hirata K, Saeki H, Katsuki T, Yamaguchi M. A Rapid Esterification by Means of Mixed Anhydride and Its Application to Large-ring Lactonization. Bull Chem Soc Jpn. 1979;52(7):1989-93.
430. Shiina I, Kubota M, Ibuka R. A novel and efficient macrolactonization of ω-hydroxycarboxylic acids using 2-methyl-6-nitrobenzoic anhydride (MNBA). Tetrahedron Lett. 2002;43(42):7535-9.
431. Parenty A, Moreau X, Campagne JM. Macrolactonizations in the Total Synthesis of Natural Products. Chem Rev. 2006;106(3):911-39.

432. Vigneaud Vd, Ressler C, Swan CJM, Roberts CW, Katsoyannis PG, Gordon S. The synthesis of an octapeptide amide with the hormonal activity of oxytocin. J Am Chem Soc. 1953;75(19):4879-80.
433. Live DH, Agosta WC, Cowburn D. A rapid, efficient synthesis of oxytocin and 8-arginine-vasopressin. Comparison of benzyl, p-methoxybenzyl, and p-methylbenzyl as protecting groups for cysteine. J Org Chem. 1977;42(22):3556-61.
434. Sieber P, Brugger M, Kamber B, Riniker B, Rittel W. [Human calcitonin. IV. Synthesis of calcitonin M]. Helv Chim Acta. 1968;51(8):2057-61.
435. Carugo O, Čemažar M, Zahariev S, Hudáky I, Gáspári Z, Perczel A, et al. Vicinal disulfide turns. Protein Eng Des Sel. 2003;16(9):637-9.
436. Li Y, Yan J, Zhang X, Huang K. Disulfide bonds in amyloidogenesis diseases related proteins. Proteins. 2013;81(11):1862-73.
437. Sevier CS, Kaiser CA. Formation and transfer of disulphide bonds in living cells. Nat Rev Mol Cell Biol. 2002;3(11):836-47.
438. Postma TM, Albericio F. Disulfide Formation Strategies in Peptide Synthesis. European J Org Chem. 2014;2014(17):3519-30.
439. Agouridas V, El Mahdi O, Diemer V, Cargoët M, Monbaliu J-CM, Melnyk O. Native Chemical Ligation and Extended Methods: Mechanisms, Catalysis, Scope, and Limitations. Chem rev. 2019;119(12):7328-443.
440. Dawson PE, Muir TW, Clark-Lewis I, Kent SBH. Synthesis of Proteins by Native Chemical Ligation. Science. 1994;266(5186):776-9.
441. Hayes HC, Luk LYP, Tsai Y-H. Approaches for peptide and protein cyclisation. Org Biomol Chem. 2021;19(18):3983-4001.
442. Saxon E, Armstrong JI, Bertozzi CR. A "Traceless" Staudinger Ligation for the Chemoselective Synthesis of Amide Bonds. Organic Lett. 2000;2(14):2141-3.
443. Nilsson BL, Kiessling LL, Raines RT. Staudinger Ligation: A Peptide from a Thioester and Azide. Organic Lett. 2000;2(13):1939-41.
444. Bode JW, Fox RM, Baucom KD. Chemoselective Amide Ligations by Decarboxylative Condensations of N-Alkylhydroxylamines and α-Ketoacids. Angew Chem Int Ed Engl. 2006;45(8):1248-52.
445. Zhang Y, Xu C, Lam HY, Lee CL, Li X. Protein chemical synthesis by serine and threonine ligation. Proc Natl Acad Sci U S A. 2013;110(17):6657-62.
446. Rostovtsev VV, Green LG, Fokin VV, Sharpless KB. A Stepwise Huisgen Cycloaddition Process: Copper(I)-Catalyzed Regioselective "Ligation" of Azides and Terminal Alkynes. ChemInform. 2002;33(43):45-.
447. Tornøe CW, Christensen C, Meldal M. Peptidotriazoles on Solid Phase: [1,2,3]-Triazoles by Regiospecific Copper(I)-Catalyzed 1,3-Dipolar Cycloadditions of Terminal Alkynes to Azides. J Org Chem. 2002;67(9):3057-64.
448. Sako Y, Morimoto J, Murakami H, Suga H. Ribosomal Synthesis of Bicyclic Peptides via Two Orthogonal Inter-Side-Chain Reactions. J Am Chem Soc. 2008;130(23):7232-4.
449. Wills R, Adebomi V, Raj M. Site-Selective Peptide Macrocyclization. ChemBioChem. 2021;22(1):52-62.
450. Nuijens T, Toplak A, Schmidt M, Ricci A, Cabri W. Natural Occurring and Engineered Enzymes for Peptide Ligation and Cyclization. Front Chem. 2019;7:829.
451. Jia X, Kwon S, Wang CA, Huang YH, Chan LY, Tan CC, et al. Semienzymatic cyclization of disulfide-rich peptides using Sortase A. J Biol Chem. 2014;289(10):6627-38.
452. Stanger K, Maurer T, Kaluarachchi H, Coons M, Franke Y, Hannoush RN. Backbone cyclization of a recombinant cystine-knot peptide by engineered Sortase A. FEBS Lett. 2014;588(23):4487-96.
453. Nguyen GKT, Wang S, Qiu Y, Hemu X, Lian Y, Tam JP. Butelase 1 is an Asx-specific ligase enabling peptide macrocyclization and synthesis. Nat Chem Biol. 2014;10(9):732-8.
454. Schmidt M, Toplak A, Quaedflieg PJLM, Ippel H, Richelle GJJ, Hackeng TM, et al. Omniligase-1: A Powerful Tool for Peptide Head-to-Tail Cyclization. Adv Synth Catal. 2017;359(12):2050-5.

455. Nuijens T, Toplak A, Meulenreek MBACVd, Schmidt M, Goldbach M, Janssen DB, et al. Chemo-enzymatic peptide synthesis (CEPS) using omniligases and selective peptiligases Efficient biocatalysts for assembling linear and cyclic peptides and protein conjugates. Chim Oggi. 2016;34:16-9.
456. Maron B, Rolff J, Friedman J, Hayouka Z. Antimicrobial Peptide Combination Can Hinder Resistance Evolution. Microbiol Spectr. 2022;10(4):e0097322.
457. Yan Y, Li Y, Zhang Z, Wang X, Niu Y, Zhang S, et al. Advances of peptides for antibacterial applications. Colloids Surf B Biointerfaces. 2021;202:111682.
458. Molchanova N, Hansen PR, Franzyk H. Advances in Development of Antimicrobial Peptidomimetics as Potential Drugs. Molecules. 2017;22(9):1430.
459. Ramesh S, Govender T, Kruger HG, de la Torre BG, Albericio F. Short AntiMicrobial Peptides (SAMPs) as a class of extraordinary promising therapeutic agents. J Pept Sci. 2016;22(7):438-51.
460. Hansen I, Isaksson J, Poth AG, Hansen K, Andersen AJC, Richard CSM, et al. Isolation and Characterization of Antimicrobial Peptides with Unusual Disulfide Connectivity from the Colonial Ascidian Synoicum turgens. Mar Drugs. 2020;18(1).
461. Hansen I, Lövdahl T, Simonovic D, Hansen K, Andersen AJC, Devold H, et al. Antimicrobial Activity of Small Synthetic Peptides Based on the Marine Peptide Turgencin A: Prediction of Antimicrobial Peptide Sequences in a Natural Peptide and Strategy for Optimization of Potency. Int J Mol Sci. 2020;21(15).
462. Strøm MB, Haug BE, Skar ML, Stensen W, Stiberg T, Svendsen JS. The pharmacophore of short cationic antibacterial peptides. J Med Chem. 2003;46(9):1567-70.
463. Strøm MB, Rekdal O, Svendsen JS. Antimicrobial activity of short arginine- and tryptophan-rich peptides. J Pept Sci. 2002;8(8):431-7.
464. Haug BE, Svendsen JS. The role of tryptophan in the antibacterial activity of a 15-residue bovine lactoferricin peptide. J Pept Sci. 2001;7(4):190-6.
465. Wu Z, Cui Q, Yethiraj A. Why Do Arginine and Lysine Organize Lipids Differently? Insights from Coarse-Grained and Atomistic Simulations. J Phys Chem B. 2013;117(40):12145-56.
466. Solstad RG, Li C, Isaksson J, Johansen J, Svenson J, Stensvåg K, et al. Novel Antimicrobial Peptides EeCentrocins 1, 2 and EeStrongylocin 2 from the Edible Sea Urchin Echinus esculentus Have 6-Br-Trp Post-Translational Modifications. PLoS One. 2016;11(3):e0151820.
467. Solstad RG, Johansen C, Stensvåg K, Strøm MB, Haug T. Structure-activity relationship studies of shortened analogues of the antimicrobial peptide EeCentrocin 1 from the sea urchin Echinus esculentus. J Pept Sci. 2020;26(2):e3233.
468. Paulsen MH, Karlsen EA, Ausbacher D, Anderssen T, Bayer A, Ochtrop P, et al. An amphipathic cyclic tetrapeptide scaffold containing halogenated β(2,2) -amino acids with activity against multiresistant bacteria. J Pept Sci. 2018;24(10):e3117.
469. Harms MJ, Schlessman JL, Chimenti MS, Sue GR, Damjanović A, García-Moreno B. A buried lysine that titrates with a normal pKa: role of conformational flexibility at the protein-water interface as a determinant of pKa values. Protein Sci. 2008;17(5):833-45.
470. Fitch CA, Platzer G, Okon M, Garcia-Moreno BE, McIntosh LP. Arginine: Its pKa value revisited. Protein Sci. 2015;24(5):752-61.
471. Tang M, Waring AJ, Lehrer RI, Hong M. Effects of guanidinium-phosphate hydrogen bonding on the membrane-bound structure and activity of an arginine-rich membrane peptide from solid-state NMR spectroscopy. Angew Chem Int Ed Engl. 2008;47(17):3202-5.
472. Yusufaly TI, Li Y, Singh G, Olson WK. Arginine-phosphate salt bridges between histones and DNA: intermolecular actuators that control nucleosome architecture. J Chem Phys. 2014;141(16):165102.
473. DeRouchey J, Hoover B, Rau DC. A comparison of DNA compaction by arginine and lysine peptides: a physical basis for arginine rich protamines. Biochemistry. 2013;52(17):3000-9.
474. Li L, Vorobyov I, Allen TW. The different interactions of lysine and arginine side chains with lipid membranes. J Phys Chem B. 2013;117(40):11906-20.
475. Parca L, Gherardini PF, Helmer-Citterich M, Ausiello G. Phosphate binding sites identification in protein structures. Nucleic Acids Res. 2011;39(4):1231-42.

476. Pirri G, Giuliani A, Nicoletto SF, Pizzuto L, Rinaldi AC. Lipopeptides as anti-infectives: a practical perspective. Cent Eur J Biol. 2009;4(3):258-73.
477. Ortwine JK, Kaye KS, Li J, Pogue JM. Colistin: understanding and applying recent pharmacokinetic advances. Pharmacotherapy. 2015;35(1):11-6.
478. Jensen SK, Thomsen TT, Oddo A, Franzyk H, Løbner-Olesen A, Hansen PR. Novel Cyclic Lipopeptide Antibiotics: Effects of Acyl Chain Length and Position. Int J Mol Sci. 2020;21(16).
479. Grimsey E, Collis DWP, Mikut R, Hilpert K. The effect of lipidation and glycosylation on short cationic antimicrobial peptides. Biochim Biophys Acta Biomembr. 2020;1862(8):183195.
480. Sikorska E, Stachurski O, Neubauer D, Małuch I, Wyrzykowski D, Bauer M, et al. Short arginine-rich lipopeptides: From self-assembly to antimicrobial activity. Biochim Biophys Acta Biomembr. 2018;1860(11):2242-51.
481. Chen Y, Guarnieri MT, Vasil AI, Vasil ML, Mant CT, Hodges RS. Role of peptide hydrophobicity in the mechanism of action of alpha-helical antimicrobial peptides. Antimicrob Agents Chemother. 2007;51(4):1398-406.
482. Churchward CP, Alany RG, Snyder LAS. Alternative antimicrobials: the properties of fatty acids and monoglycerides. Crit Rev Microbiol. 2018;44(5):561-70.
483. Kamysz E, Sikorska E, Jaśkiewicz M, Bauer M, Neubauer D, Bartoszewska S, et al. Lipidated Analogs of the LL-37-Derived Peptide Fragment KR12—Structural Analysis, Surface-Active Properties and Antimicrobial Activity. Int J Mol Sci. 2020;21(3):887.
484. Unger T, Oren Z, Shai Y. The effect of cyclization of magainin 2 and melittin analogues on structure, function, and model membrane interactions: implication to their mode of action. Biochemistry. 2001;40(21):6388-97.
485. Oren Z, Shai Y. Cyclization of a Cytolytic Amphipathic α-Helical Peptide and Its Diastereomer: Effect on Structure, Interaction with Model Membranes, and Biological Function. Biochemistry. 2000;39(20):6103-14.
486. Wang J, Yadav V, Smart AL, Tajiri S, Basit AW. Toward Oral Delivery of Biopharmaceuticals: An Assessment of the Gastrointestinal Stability of 17 Peptide Drugs. Mol Pharm. 2015;12(3):966-73.
487. Shinbara K, Liu W, van Neer RHP, Katoh T, Suga H. Methodologies for Backbone Macrocyclic Peptide Synthesis Compatible With Screening Technologies. Front Chem. 2020;8.
488. Blair JM, Richmond GE, Piddock LJ. Multidrug efflux pumps in Gram-negative bacteria and their role in antibiotic resistance. Future Microbiol. 2014;9(10):1165-77.
489. Blair JMA, Zeth K, Bavro VN, Sancho-Vaello E. The role of bacterial transport systems in the removal of host antimicrobial peptides in Gram-negative bacteria. FEMS Microbiol Rev. 2022;46(6).
490. Paulsen MH, Engqvist M, Ausbacher D, Strøm MB, Bayer A. Efficient and scalable synthesis of α,α-disubstituted β-amino amides. Org Biomol Chem. 2016;14(31):7570-8.
491. Cabrele C, Martinek TA, Reiser O, Berlicki Ł. Peptides Containing β-Amino Acid Patterns: Challenges and Successes in Medicinal Chemistry. J Med Chem. 2014;57(23):9718-39.
492. Yang S-T, Shin SY, Lee CW, Kim Y-C, Hahm K-S, Kim JI. Selective cytotoxicity following Arg-to-Lys substitution in tritrpticin adopting a unique amphipathic turn structure. FEBS Lett. 2003;540(1-3):229-33.
493. Wimley WC, White SH. Experimentally determined hydrophobicity scale for proteins at membrane interfaces. Nat Struct Biol. 1996;3(10):842-8.
494. Livingstone JR, Spolar RS, Record MT, Jr. Contribution to the thermodynamics of protein folding from the reduction in water-accessible nonpolar surface area. Biochemistry. 1991;30(17):4237-44.
495. Isaksson J, Brandsdal BO, Engqvist M, Flaten GE, Svendsen JS, Stensen W. A synthetic antimicrobial peptidomimetic (LTX 109): stereochemical impact on membrane disruption. J Med Chem. 2011;54(16):5786-95.
496. Grant TM, Rennison D, Krause AL, Mros S, Ferguson SA, Cook GM, et al. Stereochemical Effects on the Antimicrobial Properties of Tetrasubstituted 2,5-Diketopiperazines. ACS Med Chem Lett. 2022;13(4):632-40.

Paper I

International Journal of
Molecular Sciences

MDPI

Article

Synthesis and Antimicrobial Activity of Short Analogues of the Marine Antimicrobial Peptide Turgencin A: Effects of SAR Optimizations, Cys-Cys Cyclization and Lipopeptide Modifications

Hymonti Dey [1,†], Danijela Simonovic [2,†], Ingrid Norberg-Schulz Hagen [2], Terje Vasskog [2], Elizabeth G. Aarag Fredheim [2], Hans-Matti Blencke [1], Trude Anderssen [2], Morten B. Strøm [2,*] and Tor Haug [1,*]

[1] The Norwegian College of Fishery Science, Faculty of Biosciences, Fisheries and Economics, UiT The Arctic University of Norway, NO-9037 Tromsø, Norway
[2] Department of Pharmacy, Faculty of Health Sciences, UiT The Arctic University of Norway, NO-9037 Tromsø, Norway
* Correspondence: morten.strom@uit.no (M.B.S.); tor.haug@uit.no (T.H.)
† These authors contributed equally to this work.

Abstract: We have synthesised short analogues of the marine antimicrobial peptide Turgencin A from the colonial Arctic ascidian *Synoicum turgens*. In this study, we focused on a central, cationic 12-residue Cys-Cys loop region within the sequence. Modified (tryptophan- and arginine-enriched) linear peptides were compared with Cys-Cys cyclic derivatives, and both linear and Cys-cyclic peptides were N-terminally acylated with octanoic acid (C_8), decanoic acid (C_{10}) or dodecanoic acid (C_{12}). The highest antimicrobial potency was achieved by introducing dodecanoic acid to a cyclic Turgencin A analogue with low intrinsic hydrophobicity, and by introducing octanoic acid to a cyclic analogue displaying a higher intrinsic hydrophobicity. Among all tested synthetic Turgencin A lipopeptide analogues, the most promising candidates regarding both antimicrobial and haemolytic activity were **C_{12}-cTurg-1** and **C_8-cTurg-2**. These optimized cyclic lipopeptides displayed minimum inhibitory concentrations of 4 µg/mL against *Staphylococcus aureus*, *Escherichia coli* and the fungus *Rhodothorula* sp. Mode of action studies on bacteria showed a rapid membrane disruption and bactericidal effect of the cyclic lipopeptides. Haemolytic activity against human erythrocytes was low, indicating favorable selective targeting of bacterial cells.

Keywords: AMPs; Cys-Cys cyclic peptides; lipopeptides; short antibacterial peptides; structure–activity relationship; mechanism of action

Citation: Dey, H.; Simonovic, D.; Norberg-Schulz Hagen, I.; Vasskog, T.; Fredheim, E.G.A.; Blencke, H.-M.; Anderssen, T.; Strøm, M.B.; Haug, T. Synthesis and Antimicrobial Activity of Short Analogues of the Marine Antimicrobial Peptide Turgencin A: Effects of SAR Optimizations, Cys-Cys Cyclization and Lipopeptide Modifications. *Int. J. Mol. Sci.* **2022**, *23*, 13844. https://doi.org/10.3390/ijms232213844

Academic Editor: Oxana V. Galzitskaya

Received: 19 October 2022
Accepted: 8 November 2022
Published: 10 November 2022

1. Introduction

Antimicrobial resistance (AMR) poses a serious threat to human health worldwide. According to a recent study, an estimated 4.95 million deaths were associated with AMR globally in 2019, out of which 1.27 million deaths were directly attributable to it [1]. Due to increasing AMR, treatment of infectious diseases has become one of the greatest challenges in modern medicine [2]. One of the efforts to mitigate this threat includes the development of new antibacterial agents, which could circumvent existing resistance mechanisms by attacking new targets (i.e., having novel mechanisms of action). Although efforts have been made in this direction, progress remains rather slow [3].

Natural products have historically played an invaluable role in drug discovery and development, and most antibiotics currently in commercial use, and those being developed, are of natural origin [4]. Gene-encoded, ribosomal synthesized antimicrobial peptides (AMPs) are widespread in nature and have been identified in various species ranging from bacteria and fungi to plants, invertebrates and vertebrates (including fish, birds and

mammals) [5]. In eukaryotes, they are involved in the innate immunity as a first line of defense against infectious microorganisms. These compounds, generally small, cationic, amphipathic peptides, hold promise in the fight against AMR. Due to their non-specific mechanism of action, targeting the fundamental structure of the bacterial membrane, AMPs are thought to delay the emergence of bacterial resistance [6]. Many AMPs are shown to possess selective toxicity for microbes and a broad spectrum of antimicrobial activity, acting against both Gram-positive and Gram-negative bacteria [7]. Moreover, several studies have shown a synergistic and/or adjuvant effect of AMPs with conventional antibiotics [8,9]. Due to their favorable properties, AMPs have been successfully used as templates for the development of drug candidates with improved potency and selectivity, and several natural and synthetic peptides are currently in clinical trials [10].

The marine environment, with its vast biological diversity, is shown to be a promising source for future antibiotic discoveries, including novel AMPs [11]. We have previously isolated and characterized a 36-residue long AMP, named Turgencin A, from the Arctic marine colonial ascidian *Synoicum turgens* [12], and investigated the antimicrobial activity of its shortened linear 10-residue sequence rich in cationic residues (residues 18–27 of Turgencin A) [13] (Figure 1). In the native Turgencin A peptide, this 10-residue sequence is part of a loop region in which two cysteine residues (Cys^{17}-Cys^{26}) are crosslinked by a disulphide bond.

$$G^{1}PKTK^{5}AACKM^{10}ACKLA^{15}T\underline{C}\mathbf{GKK^{20}PGGWK^{25}}\underline{C}\mathbf{KL}CE^{30}LGCDA^{35}V\text{-}NH_2$$

Figure 1. Amino acid sequence of Turgencin A with the 12-residue loop region in bold (residues 17–28). Cys-Cys connectivity in the loop region is underlined. Disulphide connectivity in the native Turgencin A peptide is Cys8-Cys33, Cys12-Cys29 and Cys17-Cys26 [12].

In the present study, we prepared a series of 12-residue peptides (residues 17–28) encompassing this loop region. The Lys^{27} and Leu^{28} residues belonging to the original Turgencin A sequence were also included as additional cationic and lipophilic residues, respectively. Our aim was to investigate the structure–activity relationship (SAR) of a variety of modifications to the antimicrobial activity and selectivity: (1) increasing lipophilicity (by including two tryptophan residues in the PGG core sequence), (2) Lys to Arg substitutions, (3) N-terminal acylation and (4) Cys-Cys cyclization. In doing so, we wanted to gain insight into how these modifications could be best utilized to fine-tune the properties of potential novel AMP leads, increasing both their antimicrobial activity and selectivity. All peptides, like the originally isolated Turgencin A, were C-terminally amidated in order to increase the overall positive charge. Minimal inhibitory concentrations (MIC) were determined against selected Gram-positive and Gram-negative bacterial strains and fungi. Haemolytic activity (EC_{50}) was tested against human red blood cells (RBCs) and a bacterial selectivity index (SI) was calculated for each peptide. Selected peptides were investigated for their antibacterial mode of action (MoA) using luciferase and fluorescence-based assays to assess the viability and integrity of the cytoplasmic inner and outer membrane of bacterial cells.

2. Results and Discussion

2.1. Peptide Design and Synthesis

All analogues of the 12-residue loop region of Turgencin A were synthesized by Fmoc solid phase peptide synthesis (SPPS) on a fully automated microwave assisted peptide synthesizer. Standard conditions were used and coupling was completed with O-(1H-6-chlorobenzotriazole-1-yl)-1,1,3,3-tetramethyluronium hexafluorophosphate (HCTU) and *N,N*-diisopropylethylamine (DIEA) as a base. A double coupling strategy was employed to ensure efficient N-terminal acylation with octanoic (C_8), decanoic (C_{10}) and dodecanoic acid (C_{12}). Prior to Cys-Cys cyclization, the synthesized peptides were purified by preparative reversed-phase high-performance liquid chromatography (RP-HPLC). Cyclization of the peptides (by disulphide formation) was successfully carried out in distilled water (pH: 6.5) at room temperature with atmospheric O_2, or by bubbling O_2 through the aqueous solution

for one to four days. The progress of cyclization was monitored by liquid chromatography–mass spectrometry (LC–MS). The mass of the final products, obtained after lyophilization, were verified by high resolution–mass spectrometry (HR–MS) (Table S1) and the purity (>90% for all peptides) was determined by ultra-performance liquid chromatography with UV detection (UPLC-UV) (Table S2 and Figures S1–S25).

2.2. Structure–Activity Relationship (SAR) of Cyclic Trp- and Arg-Modified Peptides

The first series of Cys-Cys cyclic peptides (**cTurg-1–7**) were synthesized to investigate the effects of increasing the lipophilicity of the 12-residue loop region of Turgencin A (residues 17–28) by incorporating Trp-residues, and by replacing Lys-residues with Arg-residues (Table 1). The model peptides for these modifications were based on a previously reported series of short linear Turgencin A peptides (StAMP-peptides) demonstrating improved antimicrobial activity by introducing two additional Trp-residues [13].

The first peptide in the cTurg-series, **cTurg-1**, which contained the original Turgencin A (17–28) loop sequence was, however, inactive against all tested bacterial strains (MIC $\geq$ 256 μg/mL), except against the sensitive strain *Corynebacterium glutamicum* (MIC: 16 μg/mL). The Trp-modified peptides, **cTurg-2**, **cTurg-3** and **cTurg-4** were derived from **cTurg-1** by substituting amino acids present in the central PGG core of Turgencin A. The central PGG sequence of **cTurg-1** was modified as follows: WWG for **cTurg-2**, WGW for **cTurg-3** and PWW for **cTurg-4** (Table 1). Compared to **cTurg-1,** the Trp-enriched cyclic peptides showed considerable improvement in activity against all bacterial strains, except for **cTurg-4** against *Pseudomonas aeruginosa* (Table 1). The highest antibacterial activity was achieved against the Gram-positive strains *Bacillus subtilis* and *C. glutamicum* (MIC: 4–8 μg/mL), as well as improved potency against *Staphylococcus aureus* and *Staphylococcus epidermidis* (MIC: 16–64 μg/mL). However, the potency against the Gram-negative strains (*Escherichia coli* and *P. aeruginosa*), though better than that of **cTurg-1**, was low (MIC: 32–256 μg/mL). This reduced activity of AMPs is most likely due to the presence of a lipopolysaccharide (LPS) layer, which is the main constituent of the outer membrane of Gram-negative bacteria and which binds to AMPs, thereby inhibiting their effect [14].

The next modification included substitution of the Lys- with Arg-residues in **cTurg-2**, **cTurg-3** and **cTurg-4**, resulting in the Arg-modified peptides **cTurg-5** (WWG), **cTurg-6** (WGW) and **cTurg-7** (PWW). These modifications led to a considerable increase in antimicrobial activity for the arginine-modified peptides against the Gram-positive bacteria, *S. aureus* and *S. epidermidis* (MIC: 8–16 μg/mL), and also against the Gram-negative bacteria *E. coli* and *P. aeruginosa* (MIC: 8–32 μg/mL) (Table 1). The most potent peptide was **cTurg-6** (WGW) with a MIC of 4–16 μg/mL against the Gram-positive bacterial strains and a MIC of 8–16 μg/mL against the Gram-negative bacterial strains. Of note, **cTurg-3** (WGW), with the same central core as **cTurg-6,** was the most potent peptide among the Lys-containing peptides, except against *P. aeruginosa*. The lowest overall antimicrobial activity for both the Lys- and Arg-containing analogues was observed for the two peptides with a PWW central core and three adjacent tryptophan residues in their sequences (**cTurg-4** and **cTurg-7**). All peptides were non-haemolytic (EC_{50}: $\geq$ 849 μg/mL) except for **cTurg-7**, which had an EC_{50} value of 197 μg/mL against human RBCs.

2.3. Structure–Activity Relationship of Linear Lipopeptides

A well-established strategy for generating peptides with increased efficacy is N-terminal conjugation with aliphatic fatty acids [15,16] (Figure 2). To investigate the effects of acylation on antimicrobial activity, we decided to synthesise both linear and cyclic lipopeptide analogues of three selected peptides. Our choice of peptides for acylation was driven by the observed potencies of the previously synthesised cyclic analogues. We chose **cTurg-1** for being a mostly inactive peptide, **cTurg-2** for being the most potent peptide against *P. aeruginosa* among the Lys-containing peptides, and finally the Arg-modified peptide **cTurg-6**, which exerted the overall highest antimicrobial activity against all strains. **cTurg-2** and **cTurg-6** were also non-haemolytic (EC_{50}: >1045 μg/mL).

Table 1. Antimicrobial activity (MIC in μg/mL), haemolytic activity against human RBC (EC_{50} in μg/mL) and selectivity index (SI). Sequence modifications (Trp and Arg replacements) compared to Turgencin A are shown in bold, and sequences in parentheses denote Cys-Cys cyclic peptides. SI was calculated as the ratio between haemolytic activity (EC_{50}) and the geometric mean (GM) of the MIC values against all bacterial strains, i.e., SI = EC_{50}/GM.

		Peptide	Sequence	Mw [2]	Net Charge [3]	Rt [4]	Antimicrobial Activity (MIC) [1]										RBC Tox. (EC_{50})	SI
							Gram +				Gram −		GM	Fungi				
							Bs	Cg	Sa	Se	Ec	Pa		Ap	Ca	Rh		
Cyclic peptides		cTurg-1	(CGKKPGGWKC)KL-NH_2	1301.6	+5	3.11	256	16	>256	>256	>256	>256	161	32	128	64	nt [5]	nt
	W	cTurg-2	(CGKK**WW**GWKC)KL-NH_2	1519.9	+5	3.87	8	4	32	16	64	64	20	32	32	32	>1045	>52
		cTurg-3	(CGKK**W**G**W**WKC)KL-NH_2	1519.9	+5	3.92	4	4	32	16	32	128	18	32	32	32	849	47
		cTurg-4	(CGKKP**WW**WKC)KL-NH_2	1560.0	+5	3.97	8	4	64	32	64	256	32	32	64	32	>1065	>33
	R/W	cTurg-5	(CG**RRWW**G**W**R**R**C)**R**L-NH_2	1632.0	+5	3.98	8	4	16	8	8	16	9	32	32	32	>1101	>123
		cTurg-6	(CG**RRW**G**WW**R**R**C)**R**L-NH_2	1632.0	+5	4.02	4	4	16	8	8	16	8	32	32	32	1101	138
		cTurg-7	(CG**RRP****WWW**R**R**C)**R**L-NH_2	1672.0	+5	4.09	4	4	16	8	16	32	10	32	32	32	197	20
Linear lipopeptides		C_8-Turg-1	C_8-CGKKPGGWKC KL-NH_2	1429.8	+4	4.38	8	4	128	32	32	128	29	32	128	16	>943	>33
		C_{10}-Turg-1	C_{10}-CGKKPGGWKC KL-NH_2	1457.9	+4	4.89	4	4	16	8	16	32	10	32	64	8	>957	>95
		C_{12}-Turg-1	C_{12}-CGKKPGGWKC KL-NH_2	1486.0	+4	5.44	4	4	8	4	8	16	6	32	64	8	>971	>153
	W	C_8-Turg-2	C_8-CGKK**WW**GWKC KL-NH_2	1648.1	+4	4.97	8	4	8	8	16	16	9	32	64	32	198	22
		C_{10}-Turg-2	C_{10}-CGKK**WW**GWKC KL-NH_2	1676.2	+4	5.41	8	4	8	8	8	16	8	32	64	32	64	8
		C_{12}-Turg-2	C_{12}-CGKK**WW**GWKC KL-NH_2	1704.2	+4	5.89	8	16	16	8	16	32	14	32	64	32	55	4
	R/W	C_8-Turg-6	C_8-CG**RRW**G**WW**R**R** **R**L-NH_2	1760.2	+4	5.07	4	4	16	8	8	32	9	128	64	128	54	6
		C_{10}-Turg-6	C_{10}-CG**RRW**G**WW**R**R** **R**L-NH_2	1788.2	+4	5.51	8	16	32	16	32	64	23	128	64	128	21	1
		C_{12}-Turg-6	C_{12}-CG**RRW**G**WW**R**R** **R**L-NH_2	1816.3	+4	5.98	16	16	32	16	64	128	32	128	64	>128	39	1
Cyclic lipopeptides		C_8-cTurg-1	C_8-(CGKKPGGWKC)KL-NH_2	1427.8	+4	4.27	4	4	128	32	32	128	25	64	64	8	>942	>37
		C_{10}-cTurg-1	C_{10}-(CGKKPGGWKC)KL-NH_2	1455.9	+4	4.74	2	2	16	4	8	32	6	32	64	4	>956	>151
		C_{12}-cTurg-1	C_{12}-(CGKKPGGWKC)KL-NH_2	1483.9	+4	5.22	2	2	4	4	4	16	4	32	64	4	219	55
	W	C_8-cTurg-2	C_8-(CGKK**WW**GWKC)KL-NH_2	1646.1	+4	4.70	2	2	4	4	4	8	4	16	32	4	439	123
		C_{10}-cTurg-2	C_{10}-(CGKK**WW**GWKC)KL-NH_2	1674.1	+4	5.11	2	4	4	4	8	8	5	32	64	16	106	24
		C_{12}-cTurg-2	C_{12}-(CGKK**WW**GWKC)KL-NH_2	1702.2	+4	5.55	4	8	8	8	16	16	9	32	64	32	32	4
	R/W	C_8-cTurg-6	C_8-(CG**RRW**G**WW**R**R**C)**R**L-NH_2	1758.2	+4	4.85	4	4	8	4	8	16	6	64	64	32	30	5
		C_{10}-cTurg-6	C_{10}-(CG**RRW**G**WW**R**R**C)**R**L-NH_2	1786.2	+4	5.28	4	4	8	8	16	16	8	64	64	32	16	2
		C_{12}-cTurg-6	C_{12}-(CG**RRW**G**WW**R**R**C)**R**L-NH_2	1814.3	+4	5.72	8	8	16	8	32	32	14	64	128	64	9	1
		Polymyxin B		1301.6	+5		3.1	3.1	12.5	6.3	3.1	3.1	161	3.1	12.5	3.1	nt	nt
		Chlorhexidine		505.5	+2		1.6	0.8	1.6	1.6	1.6	6.3	20	1.0	7.8	1.0	nt	nt

[1] Microbial strains; Bs—*Bacillus subtilis*, Cg—*Corynebacterium glutamicum*, Sa—*Staphylococcus aureus*, Se—*Staphylococcus epidermidis*, Ec—*Escherichia coli*, Pa—*Pseudomonas aeruginosa*, Ap—*Aurobasidium pollulans*, Ca—*Candida albicans*, Rh—*Rhodotorula* sp. [2] Average molecular mass without including a TFA salt for each cationic charge. [3] Net charge at physiological pH (7.4). [4] Hydrophobicity measured as retention time (Rt; min) on a RP-UPLC C_{18} column using a linear acetonitrile/water gradient. [5] nt: not tested.

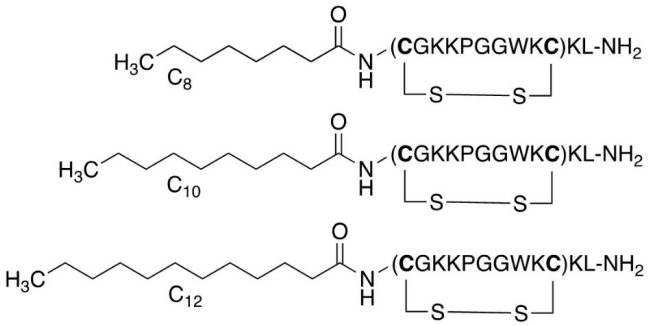

Figure 2. Lipopeptide modifications exemplified for **cTurg-1** lipopeptides containing C_8, C_{10} and C_{12} fatty acids.

Acylation was done with three aliphatic fatty acids: octanoic acid (C_8), decanoic acid (C_{10}) and dodecanoic acid (C_{12}), since these fatty acid were previously found to improve the antibacterial activity of various peptides [17]. Of note, similar, but two-residues shorter linear analogues of these peptides (based on Turgencin A residues 18–27) have been previously reported in literature, e.g., non-acylated peptides and those without the Cys-residues [13]. For the linear peptides **C_8-Turg-1**, **C_{10}-Turg-1** and **C_{12}-Turg-1** elongation of the lipid chain from 8 to 12 carbons resulted in an overall increase in antimicrobial activity (Table 1). The most potent linear lipopeptide was the longest acylated peptide **C_{12}-Turg-1** with a MIC of 4–16 μg/mL against all bacterial strains. The highest increase in antimicrobial activity following acyl chain elongation was observed against *S. aureus* with improvement in MIC from 128 to 8 μg/mL, and *P. aeruginosa* with improvement in MIC from 128 to 16 μg/mL. All three peptides **C_8-Turg-1**, **C_{10}-Turg-1** and **C_{12}-Turg-1** were non-haemolytic (EC_{50}: >943 μg/mL).

Regarding the more lipophilic peptide, **cTurg-2** (having a central WWG region), elongation of the N-terminal acyl chain of linear analogues had an opposite effect than that observed for the linear lipopeptides based on **cTurg-1** (PGG). In other words, for the lipopeptides **C_8-Turg-2**, **C_{10}-Turg-2** and **C_{12}-Turg-2**, increasing the length of the acyl chain resulted in peptides having the same or slightly reduced antimicrobial activity. One exception in this regard was the activity of **C_{10}-Turg-2** against *E. coli*, with a two-fold increased potency (MIC: 8 μg/mL) compared to **C_8-Turg-2** and **C_{12}-Turg-2** (MIC: 16 μg/mL). Thus, among the linear **Turg-2** lipopeptides, **C_8-Turg-2** and **C_{10}-Turg-2** showed the highest potency against both the Gram-positive (MIC: 4–8 μg/mL) and Gram-negative bacteria (MIC: 8–16 μg/mL). Of note, all three lipopeptides **C_8-Turg-2**, **C_{10}-Turg-2** and **C_{12}-Turg-2** showed the same antimicrobial activity against *B. subtilis* and *S. epidermidis* (MIC: 8 μg/mL). Compared to **C_8-Turg-1** and **C_{10}-Turg-1** (PGG core sequence), we observed improved antimicrobial activity for **C_8-Turg-2** and **C_{10}-Turg-2** (WWG core sequence) against *S. aureus*, *E. coli* and *P. aeruginosa*. However, **C_8-Turg-2**, **C_{10}-Turg-2** and **C_{12}-Turg-2** displayed increasingly higher haemolytic activity from EC_{50}: 198 to 55 μg/mL.

The linear lipopeptides based on the **cTurg-6** (WGW) sequence resulted in an even more noticeable reduction in antimicrobial activity following acyl chain elongation than that observed for the **C_8-Turg-2**, **C_{10}-Turg-2** and **C_{12}-Turg-2** lipopeptides. Compared to **cTurg-6**, the linear lipopeptide **C_8-Turg-6** showed a similar antibacterial effect. Further acyl chain elongation in **C_{10}-Turg-6** and **C_{12}-Turg-6** resulted in a significant decrease in potency, which was especially noticeable against *S. aureus* and the Gram-negative bacteria, *E. coli* and *P. aeruginosa* (MIC: 32–128 μg/mL). Additionally, **C_8-Turg-6**, **C_{10}-Turg-6** and **C_{12}-Turg-6** were all rather haemolytic (EC_{50}: 21–54 μg/mL). As expected, acyl chain elongation led to increased hydrophobicity for all three lipopeptide series, as monitored by their retention time on an RP-HPLC C_{18} column (Table 1).

2.4. Structure–Activity Relationship of Cyclic Lipopeptides

Our final modification included peptide cyclization of the previous series of lipopeptides by sidechain disulphide formation. In general, cyclization of the acylated peptides

resulted in some of the most potent peptides prepared and it had some unexpected effects on their haemolytic activity (Table 1). The antimicrobial activity of the cyclic lipopeptides **C_8-cTurg-1**, **C_{10}-cTurg-1** and **C_{12}-cTurg-1** was improved by increasing the acyl chain length. The latter lipopeptide, **C_{12}-cTurg-1,** was the most potent in this series with a two-fold increased antimicrobial activity against four out of six strains, compared to its linear analogue **C_{12}-Turg-1**. However, as opposed to **C_{12}-Turg-1**, the cyclic analogue **C_{12}-cTurg-1** displayed detectable haemolytic activity (EC_{50}: 219 μg/mL).

Similar to the linear lipopeptides, we observed a small reduction in antimicrobial activity following the increase in the acyl chain length for the cyclic analogues **C_8-cTurg-2**, **C_{10}-cTurg-2** and **C_{12}-cTurg-2**. Importantly, the cyclic lipopeptides in this series were more potent than their linear analogues. Moreover, this series included the overall most potent peptide prepared in this study, **C_8-cTurg-2,** with a MIC of 2–4 μg/mL against all Gram-positive bacterial test strains and *E. coli*, and a MIC of 8 μg/mL against *P. aeruginosa*. Cys-Cys sidechain cyclization had a positive effect on the overall antimicrobial activity, most likely due to the formation of a more rigid cyclic structure. Somewhat surprisingly, **C_8-cTurg-2** was considerably less haemolytic (EC_{50}: 439 μg/mL) than the linear precursor lipopeptides **C_8-, C_{10}- and C_{12}-Turg-2** (EC_{50}: 55–198 μg/mL)**.**

Cyclic lipopeptides **C_8-cTurg-6**, **C_{10}-cTurg-6** and **C_{12}-cTurg-6** were more potent than their linear analogues, but we also noticed a reduction in antimicrobial activity following the increase in the acyl chain length. Moreover, we observed an undesirable increase in haemolytic activity for this series of cyclic lipopeptides (EC_{50}: 9–30 μg/mL), which, in contrast to antimicrobial activity, increased following acyl chain elongation. These results clearly demonstrate that optimization of the peptide's activity involves a trade-off between achieving desired antimicrobial potency and minimizing unwanted toxicity against human RBCs.

2.5. SAR Summary

Our first series of cyclic peptides **cTurg-1**–**cTurg-7** demonstrated that substitution of Lys to Arg results in peptides with higher antimicrobial activity (Table 1). The cyclic Arg-modified peptides **cTurg-5**–**cTurg-7** were generally more potent than their Lys-containing counterparts **cTurg-2**–**cTurg-4**. The awareness of changes in haemolytic activity following Lys to Arg substitution is important, as shown for the Arg-modified cyclic peptide **cTurg-7** displaying weak haemolytic activity (EC_{50}: 197 μg/mL), whereas its Lys analogue, **cTurg-4,** as well as other Trp and Arg modified cyclic peptides were non-haemolytic (EC_{50}: $\geq$ 849 μg/mL).

For the linear lipopeptides **C_8-**, **C_{10}-** and **C_{12}-Turg-1**, as well as the cyclic lipopeptides **C_8-**, **C_{10}-** and **C_{12}-cTurg-1**, an increase in the number of carbons in the acyl chain resulted in increased potency of the corresponding analogues. A reverse trend was observed for both linear **C_8-**, **C_{10}-**, **C_{12}-Turg-2** and cyclic **C_8-**, **C_{10}-**, **C_{12}-cTurg-2** lipopeptides, as chain elongation beyond C_8 resulted in analogues with mostly unchanged potency (C_{10}-analogues), or even a two- to four-fold decrease in potency (C_{12}-analogues). A similar observation was made for the linear **C_8-**, **C_{10}-**, **C_{12}-Turg-6** and cyclic **C_8-**, **C_{10}-**, **C_{12}-cTurg-6** lipopeptides, where the greatest decrease in potency was observed against *E. coli* (MIC: from 8 μg/mL to 64 μg/mL). The sequences of the linear and cyclic **C_8-**, **C_{10}-**, **C_{12}-Turg-2/c-Turg-2** and **C_8-**, **C_{10}-**, **C_{12}-Turg-6/c-Turg-6** lipopeptides were more hydrophobic than that of **C_8-**, **C_{10}-**, **C_{12}-Turg-1/c-Turg-1**, due to their tryptophan-rich core sequence, which could, in part, explain the observed trend. As for the **C_8-**, **C_{10}-**, **C_{12}- Turg-1/c-Turg-1** lipopeptides, it remains unclear whether the C_{12}-chain conferred the threshold hydrophobicity, or whether this threshold could have been achieved by acylation with fatty acids containing more than 12 carbons. These results suggest that there might be an upper limit regarding hydrophobicity (threshold hydrophobicity) and that its further increase could have an unfavourable effect on antimicrobial activity, and in some cases even abrogate it entirely. This may occur, as proposed in a study done by Chu-Kung et al., when the minimal bactericidal concentration of the peptide is higher than its critical miscelle concentration [18]. Furthermore, studies have demonstrated that lipopeptides containing long fatty acid chains

tend to self-assemble, resulting in reduced antimicrobial activity [19,20]. Our findings give further credence to the assumption that hydrophobicity, easily tuned by lipidation, is an important factor influencing antimicrobial activity of peptides.

The direct correlation between haemolytic activity and hydrophobicity (mirrored in the acyl chain length) of the peptides was especially prominent for the linear **C_8-, C_{10}-, C_{12}-Turg-2** and **C_8-, C_{10}-Turg 6** lipopeptides, except for **C_{12}-Turg-6,** which had a slightly reduced haemolytic activity than its analogue with **C_{10}** fatty acid chain (Table 1). This trend was not observed for **C_8-, C_{10}-Turg-1**, and its cyclic analogues, as they were all non-haemolytic. In general, cyclic lipopeptides were more haemolytic compared to their linear analogues. These results support previous findings that lipopeptides with longer acyl chains have higher haemolytic activity, most likely due to their lower membrane selectivity [21,22].

While the effect of lipidation is shown to be bidirectional, depending on the initial hydrophobicity of the peptides, among other things, intramolecular cyclization led to increased antimicrobial activity of linear lipopeptides regardless of their primary sequence. For all cyclic lipopeptides synthesized in this work, the potency was either unchanged or improved four-fold, compared to their corresponding linear analogues. It should be noted that changes in the position of the acylation may also have bearing on the potency of lipopeptides, as well as head-to-tail cyclization, two strategies that remain to be explored. Our results are in line with previous research showing that acylation and intramolecular cyclization are useful tools important for fine-tuning antimicrobial and haemolytic activity of AMPs [17].

2.6. Antifungal Activity

The synthesised peptides were screened for antifungal activity against the molds *Aurobasidium pollulans* and *Rhodotorula* sp., and the yeast *Candida albicans*. All cyclic peptides of the **cTurg-1**–**cTurg-7** series displayed almost equal antifungal activity (MIC: 32–128 μg/mL) against all three fungi tested (Table 1). Even **cTurg-1,** containing the original Turgencin A core sequence, displayed antifungal activity against all strains at concentrations below the MIC against bacteria (except for *C. glutamicum*). None of the peptides of this series stood out as more potent than the others, indicating that the amino acid substitutions in the central core sequence are not important for antifungal activity.

All linear and cyclic lipopeptides prepared in this study displayed antifungal activity. In general, their MIC values ranged from 32 to 128 μg/mL against *A. pullulans* and *C. albicans*, making it difficult to conclude any structure–activity relationship for the peptides against these strains. The activity against *Rhodothorula* sp. varied more between the different peptides with MIC values from 4 to >128 μg/mL. The cyclic lipopeptides **C_8-, C_{10}-** and **C_{12}-cTurg-1** were somewhat more potent against *Rhodothorula* sp. compared to the linear lipopeptides **C_8-, C_{10}-** and **C_{12}-Turg-1**, while the longer C_{10}/C_{12} analogues (MIC: 4 μg/mL) were slightly more potent compared to the corresponding C_8 analogues. The linear lipopeptides **C_8-, C_{10}-** and **C_{12}-Turg-2** were equally potent (MIC: 32 μg/mL) against *Rhodothorula* sp. However, among the cyclic lipopeptides, **C_8-cTurg-2** was the most potent peptide (MIC: 4 μg/mL), followed by **C_{10}-cTurg-2** (MIC: 16 μg/mL) and **C_{12}-cTurg-2** (MIC: 32 μg/mL). These results support the antibacterial data, indicating an upper limit regarding lipophilicity. Among all lipopeptides tested, **C_8-cTurg-2** was the most potent peptide against *A. pullulans* (MIC: 16 μg/mL). The linear lipopeptides **C_8-, C_{10}-** and **C_{12}-Turg-6** were overall the least potent with MIC-values of 64 to >128 μg/mL against all test strains, but with a two- to four-fold increase in potency for their cyclic versions (**C_8-, C_{10}-** and **C_{12}-cTurg-6**) against *A. pullulans* and *Rhodothorula* sp.

2.7. Selectivity Index

The selectivity index (SI) of the peptides towards bacteria over eukaryotic cells was calculated using the geometric mean (GM) of the MIC values against all bacterial test strains, according to the method by Orlov et al. [23]. The SI for each peptide was determined as the ratio of the RBC-EC_{50} value by the corresponding GM value. Larger SI values indicate greater

selectivity for microbial cells [24]. As shown in Table 1, **cTurg-6** had the highest selectivity of the cyclic peptides (**cTurg-1** to **cTurg-7**), with an SI value of 138 for all bacterial strains tested. Interestingly, two of the lipopeptides, **C_{10}-cTurg-1 and C_{12}-Turg-1,** emerged as a promising candidates for further optimization, both having SI values for bacteria above 150. In addition, **C_8-cTurg-2** showed the best selectivity profile among both cyclic and linear lipopeptides derived from the **cTurg-2** series. In general, the SI was higher against the Gram-positive bacteral strains than the Gram-negative strains. (Table S3). Overall, peptides displaying EC_{50} < 100 μg/mL were considered too haemolytic to be of interest for further exploration.

2.8. Effects on Bacterial Viability and Membrane Integrity

We used two luciferase-based assays to investigate whether the synthesized peptides had an immediate effect on bacterial viability and membrane integrity. Changes in light emission of sensor bacteria constitutively expressing the bacterial lux operon or a eukaryotic luciferase can be used as a proxy for viability and membrane integrity, respectively [25]. Light production of the viability biosensors represents metabolic activity of the bacteria. For the membrane integrity assay on the other hand, light production depends on the influx of the externally added D-luciferin, which at neural pH will not readily pass the intact plasma membrane. An initial increase in light production therefore corresponds with damage to the plasma membrane and a concomitant influx of D-luciferin, while a subsequent drop in light emission indicates diminishing ATP reserves of the dying sensor bacteria.

Here we present the results for the two most potent cyclic lipopeptides, **C_{12}-cTurg-1** and **C_8-cTurg-2,** as well as for the membrane active agent chlorhexidine (CHX) that was used for comparison (Figures 3 and 4). The results for the remaining peptides can be found in the Supporting information, Figures S26–S33. The overall results for **C_{12}-cTurg-1** and **C_8-cTurg-2** in *B. subtilis* 168 show that increasing concentrations resulted in a decrease in light emisssion (and in increasing rates), suggesting a dose-dependent effect on viability (Figure 3).

In order to confirm that the observed decrease in viability was the result of membrane damage, we used the membrane integrity assay [13,25]. The results of the membrane integrity assay for *B. subtilis* 168 show that increasing lipophilicity of the cyclic lipopeptides **C_8-, C_{10}-,** and **C_{12}-cTurg-1** caused increased membranolytic activity. A rapid and strong membrane disruptive effect was observed for the highly potent **C_{12}-cTurg-1** peptide (Figures 3 and S27). When analysing the membrane integrity effects of the cyclic lipopeptides **C_8-, C_{10}-** and **C_{12}-cTurg-2**, increasing lipophilicity was also concordant with increased membrane activity, but not to a greater extent than for the **C_8-, C_{10}-** and **C_{12}-cTurg-1** peptides. We observed a minor effect on increased lipophilicity on the membrane activity of **C_8-, C_{10}-** and **C_{12}-cTurg-2** and **C_8-, C_{10}-** and **C_{12}-cTurg-6** cyclic lipopetides, as they showed somewhat similar activity, showing a rapid decrease in light production, from concentrations 50 to 12.5 μg/mL (Figures 3 and S29). At the lowest concentration, close to the MIC value of 2 μg/mL for all tested peptides, we observed minor changes in membrane activity and viability, most likely due to the high concentration of bacterial inoculum (1000-fold greater than that used for the MIC assay). This could explain why higher concentrations of the peptides were needed to see a more pronounced effect. However, at higher concentrations, the membranolytic action for some lipopeptides was so rapid (< 3 s) that the luminescence peak could not be detected, as the signal started declining even before the first measurement was made. This phenomenon was observed for **C_{12}-cTurg-1** and **C_8-cTurg-2** (at the highest test concentrations of 25 μg/mL and 50 μg/mL), indicating a more rapid or even different mechanism for disruption of membrane integrity than that of chlorhexidine (Figure 3).

The viability and membrane integrity assay results for *E. coli* K12 were quite different from what was observed for *B. subtilis*. For both **C_{12}-cTurg-1** and **C_8-cTurg-2,** we observed a gradual, dose-dependent reduction in viability in *E. coli*, although not as prominent as for *B. subtilis*. In the membrane integrity assay, **C_{12}-cTurg-1** showed a delayed, 3.5-fold rise in luminescence at the highest test concentration (50 μg/mL) compared to chlorhexidine, with a subsequent decline in luminescence during the assay timeframe (Figure 4). A

further delayed response was observed for **C_{12}-cTurg-1** at 25 µg/mL, whereas no effect was observed at lower concentrations. **C_8-cTurg-2** gave an even further delayed rise in peak luminescence in the membrane integrity assay, but only at the highest test concentration of 50 µg/mL (Figure 4). Although **C_{12}-cTurg-1** and **C_8-cTurg-2** displayed similar MIC values of 4 µg/mL against *E. coli* (ATCC 25922) in the screening assay run for 24 h, the results from the membrane integrity assay with *E. coli* K12 indicate a different mode of membrane disruption. This might suggest that the peptides were acting on the outer LPS and inner cytoplasmic membranes of *E. coli* at different rates, resulting in their delayed action observed in both the viability and membrane integrity assays.

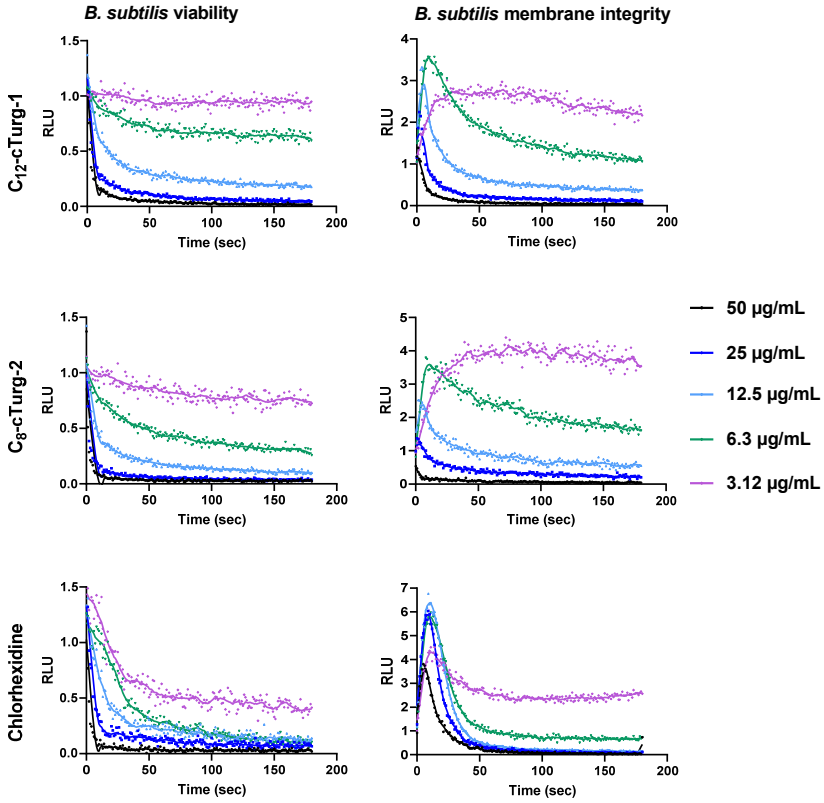

Figure 3. Effects of **C_{12}-cTurg-1**, **C_8-cTurg-2** and chlorhexidine on the kinetics of viability (**left**) and membrane integrity (**right**) in *B. subtilis* 168. Light emission normalized to the untreated water control is plotted as relative luminescence emission (RLU) over time (seconds). Kinetics of the immediate effect (within 3 min) on bacterial viability and membrane integrity, as measured by relative luminescence emission in *B. subtilis* 168 treated with increasing concentrations of the lipopeptides. Chlorhexidine served as a positive (membranolytic) control and water as a negative (untreated) control. All the graphs of this figure show a representative data set where each experiment was run at least three times independently.

2.9. Effects on E. coli Mutant Strain with an Impaired Outer Membrane

Antimicrobial activity of all synthesised cyclic peptides were determined against two additional *E. coli* strains: the hyperpermeable mutant strain NR698, and its isogenic wild type (WT) MC4100 (Table 2). The outer membrane deficiency of the mutant strain *E. coli* NR698 is based on the allele *imp*4213/*lptD*4213 constituting an in-frame deletion of the *imp* (increased membrane permeability) gene in *E. coli* [26]. It has been shown that *imp* mutations make the outer membrane more permeable to antibiotics like vancomycin, which normally does not readily cross the outer membrane barrier of *E. coli*. In addition, this mutation is also suggested to cause defects in LPS assembly [27,28]. The results from the previous screening against the laboratory strain *E. coli* ATCC 25922 are included in Table 2 for comparison and show that both the WT and mutant NR698 strains were in many cases more sensitive to the cyclic peptides than the *E. coli* ATCC 25922 laboratory strain.

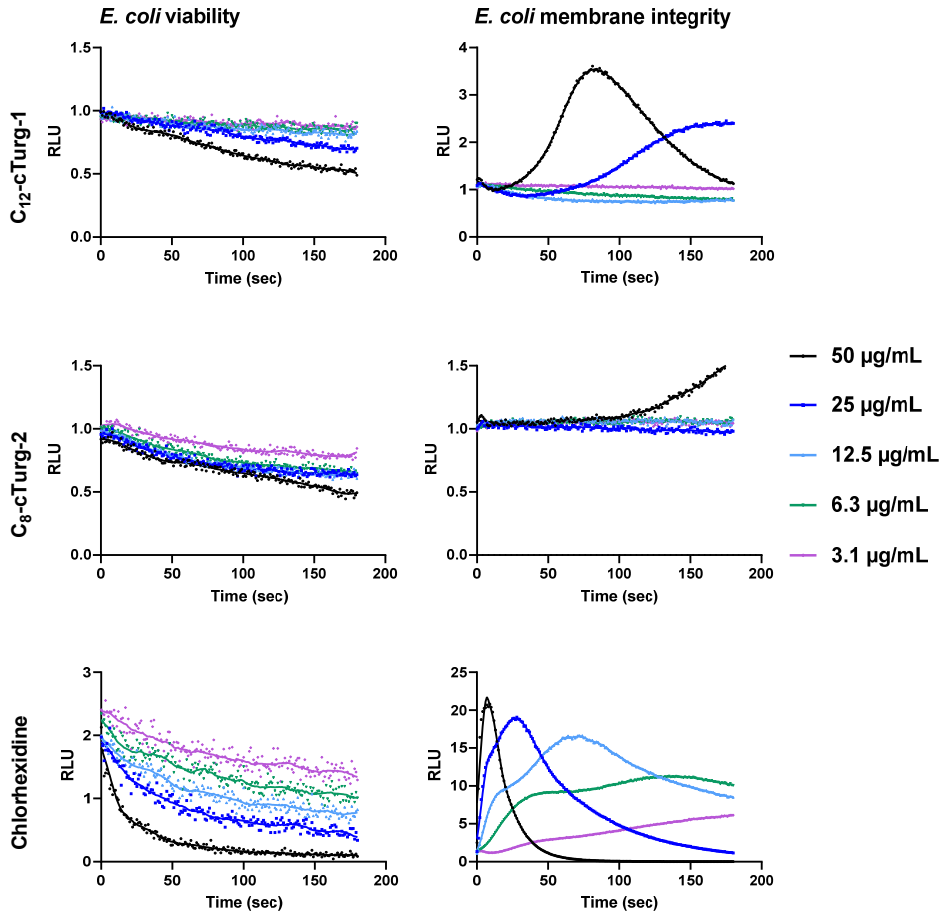

Figure 4. Effects of **C_{12}-cTurg-1**, **C_8-cTurg-2** and chlorhexidine on the kinetics of viability (**left**) and membrane integrity (**right**) in *E. coli* K12. Light emission normalized to the untreated water control is plotted as relative luminescence emission (RLU) over time (seconds). After addition of the bacterial inoculum (mixed with 1 mM D-luciferin in the membrane assay) to the wells, preloaded with lipopeptides, the light emission was measured each second for three min. Each colored line represents the total 180 s data points (mean of three independent measurements) from the assay at different concentration of the lipopeptides.

The cyclic peptide **cTurg-1,** containing the native Turgencin A core sequence, was found to be active against the mutant NR698 strain (MIC: 64 µg/mL). However, against the WT strain and the *E. coli* ATCC 25922 laboratory strain it showed no activity (Table 2). In contrast to **cTurg-1,** Trp-modified cyclic peptides **cTurg-2** to **cTurg-4** displayed increased antimicrobial activity against all three *E. coli* strains, among which the mutant NR698 was most sensitive. Thus, for these peptides, the outer membrane appeared to hinder their antimicrobial effect. For the analogous, Arg-modified cyclic peptides **cTurg-5** to **cTurg-7**, no major differences in antimicrobial activity were observed against the three *E. coli* strains (MIC: 8–16 µg/mL), making these peptides seemingly less affected by the outer LPS membrane.

With regard to the cyclic lipopeptides (Table 2), the potency against the mutant strain NR698 showed the same trend as previously described (SAR section), although with lower MIC values. In brief, according to SAR, improved potency was achieved by increasing the acyl chain length for the cyclic lipopeptides **C_8-**, **C_{10}-** and **C_{12}-cTurg-1**, while the opposite trend was observed for **C_8-**, **C_{10}-** and **C_{12}-cTurg-2** and **C_8-**, **C_{10}-** and **C_{12}-cTurg-6**. The results for the WT MC4100 strain are also in accordance with our previous SAR observations, but to a lesser degree than for the other two strains. These results clearly demonstrate that structural modifications can optimize target interactions and antibacterial potency as seen for example in **C_{12}-cTurg-1, which** displays similar high potency against all three strains (MIC: 2–4 µg/mL).

Table 2. Antimicrobial activity (MIC in μg/mL) of cyclic peptides and selected antibiotics against three strains of *E. coli* for investigation of effects concerning outer membrane permeability. In addition to the laboratory strain *E. coli* ATCC 25922, the activity against *E. coli* MC4100 (wild type, WT) and the outer membrane permeable mutant *E. coli* NR698 was measured and compared.

			***E. coli* Strains**		
		Peptide	**ATCC 25922 (from Table 1)**	**MC4100 (WT)**	**NR698 [1] (mutant)**
Cyclic peptides		cTurg-1	>256	>256	64
	W	cTurg-2	64	16	8
		cTurg-3	32	16	8
		cTurg-4	64	16	8
	R/W	cTurg-5	8	8	8
		cTurg-6	8	8	8
		cTurg-7	16	8	8
Cyclic lipopeptides		C_8-cTurg-1	32	16	8
		C_{10}-cTurg-1	8	8	4
		C_{12}-cTurg-1	4	4	2
	W	C_8-cTurg-2	4	8	2
		C_{10}-cTurg-2	8	8	4
		C_{12}-cTurg-2	16	8	8
	R/W	C_8-cTurg-6	8	8	8
		C_{10}-cTurg-6	16	8	8
		C_{12}-cTurg-6	32	16	16
Antibiotics		Polymyxin B	3.1	0.8	0.2
		Chlorhexidine	1.6	0.3	0.3
		Vancomycin	125	64	0.3
		Ampicillin	8	8	0.3
		Chloramphenicol	1.8	12.5	3.1

[1] *E. coli* MC4100 NR698 *imp*4213 (with deficient outer membrane).

In order to more closely evaluate the effect of an outer membrane on antimicrobial activity of synthesised peptides, we tested several commercially available antibiotics. Major improvement in antimicrobial activity was achieved against the mutant NR698 strain compared to the WT strain when treated with polymyxin B, vancomycin, ampicillin and chloramphenicol (Table 2). Compared to these antibiotics, several of the present cyclic peptides, such as **C_{12}-cTurg-1** and **C_8-cTurg-2**, showed similar or higher antibacterial activity against the *E. coli* ATCC 25922 and WT strains. In summary, the overall higher antibacterial activity against the mutant NR698 strain supports the hypothesis that the outer LPS membrane present in the WT strains could act as a barrier, limiting the effect of the synthesised peptides. This, in turn, may have affected the rate of bacterial membrane disruption as observed in the viability and membrane integrity studies.

2.10. Permeabilization of the Outer Membrane of E. coli

The outer membrane of Gram-negative bacteria acts as a barrier for many hydrophobic and larger hydrophilic substances (>600 Da) [29]. However, some peptides can sensitize the outer membrane and thus facilitate the entry of various hydrophobic molecules. To explore if the peptides affect the outer membrane of *E. coli* MC4100, **C_{12}-cTurg-1** and **C_8-cTurg-2** were tested for their ability to enable the entry of the hydrophobic fluorescent probe 1-*N*-phenylnapthylamine (NPN, MW of 219 Da) (Figure 5). In aqueous solutions, NPN shows very low fluorescence, which greatly increases upon interaction with the hydrophobic environment of biological membranes. Normally, the hydrophobic NPN is excluded by *E. coli* bacteria, but it can enter the bacteria once the integrity of the outer membrane is compromised. In this assay, both cyclic lipopeptides, **C_{12}-cTurg-1** and **C_8-cTurg-2**, as well as chlorhexidine, were found to increase the NPN fluorescence in a concentration-dependent manner (Figure 5), but at a slightly different rate, via membrane permeabilization. The stronger effect for **C_{12}-cTurg-1**, with almost a four-fold increase in both fluorescence and

luminescence for the concentrations of 25 to 50 µg/mL, suggests that **C_{12}-cTurg-1** disrupts both the outer and the inner membrane at a similar rate at higher concentrations (6.3–12.5 × MIC). In contrast, **C_8-cTurg-2** was found to alter the outer membrane permeability at concentrations that did not initially give any increase in luminescence in the inner membrane integrity assay (Figures 4 and 5). Thus, the observed effects indicate that the outer membrane passage of **C_8-cTurg-2** was a rate-limiting step that was most likely preventing the peptide from reaching and accumulating in the inner membrane.

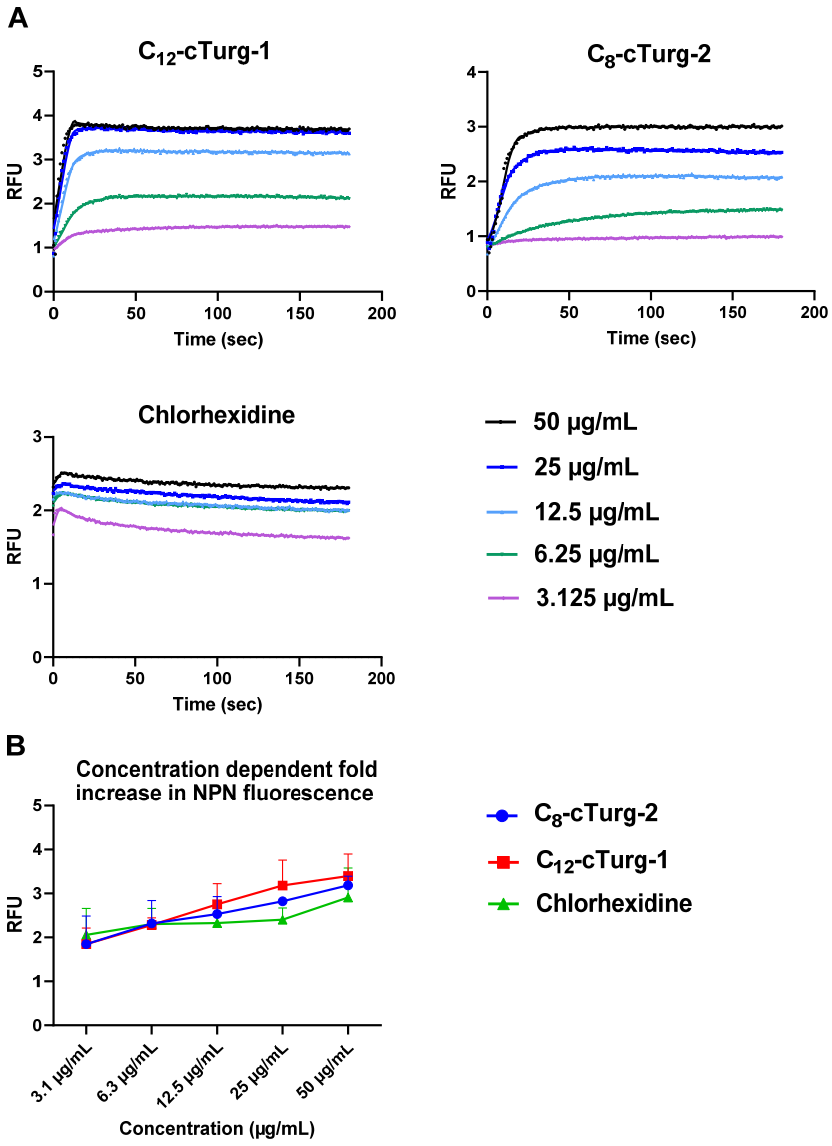

Figure 5. (**A**) Comparison of the effects of **C_{12}-cTurg-1**, **C_8-cTurg-2** and chlorhexidine on the kinetics of NPN fluorescence in *E. coli* MC4100 (WT). After addition of the bacterial inoculum (mixed with 20 µM NPN) to the wells (preloaded with lipopeptides), light emission was measured each second for 3 min. Each colored line represents the total 180 s data points from the assay at different concentrations. Each figure shows a representative data set. (**B**) *E. coli* MC4100 grown in MH media were treated with different concentrations of **C_{12}-cTurg-1**, **C_8-cTurg-2** and chlorhexidine. The permeability of the outer membrane was assessed by measuring the fluorescence of NPN after 3 min (mean of three independent measurements). In all data sets, fluorescence values were compared to bacterial cells treated with the same amount of Mill-Q water control.

2.11. Bacterial Killing Experiments

The two most potent lipopeptides (**C_{12}-cTurg-1** and **C_8-cTurg-2**) were selected for bacterial killing experiments to see whether the peptides displayed bacteriostatic or bactericidal effects on the bacterial inoculum used in the MIC assay. In this experiment, 10 µL aliquots from the wells containing peptide-treated bacteria were harvested after the MIC assay (24 h incubation), and 10-fold serially diluted and spotted on MH agar plates for colony counting. At their half-MIC concentration, slightly less colony-forming units (CFU) were formed for both *S. aureus* (ATCC 9144) and *E. coli* (ATCC 25922) in the presence of **C_{12}-cTurg-1** and **C_8-cTurg-2**, compared to the growth control (Figure 6). No CFU were observed at their MIC (or concentrations above MIC). These results show that the peptides displayed a bactericidal action on the bacterial strains tested.

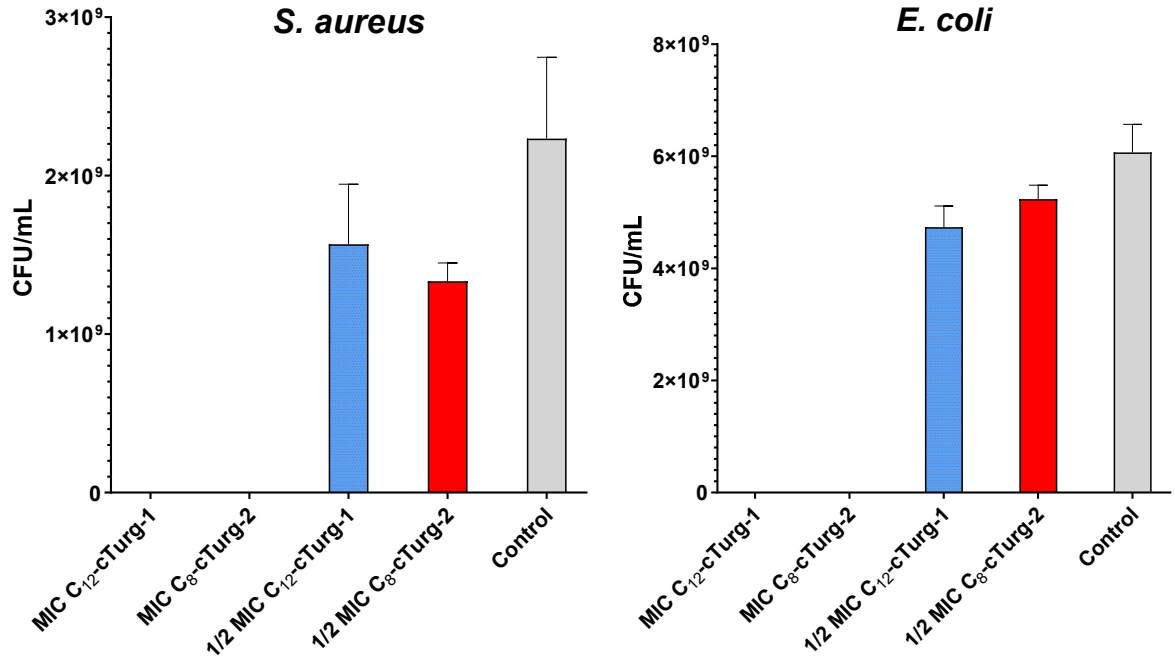

Figure 6. Bactericidal activity of **C_{12}-cTurg-1** and **C_8-cTurg-2** against *S. aureus* and *E. coli.* Colony-forming units (CFU) per mL bacterial inoculum were counted after treatment with MIC (4 µg/mL), 1/2 × MIC and no treatment (Control). Each bar presents the mean of three replicates ± SD.

3. Materials and Methods

3.1. Peptide Synthesis

All reagents and solvents were purchased from commercial sources and used as supplied. All peptides were synthesized using standard Fmoc-solid phase methodology using a Rink Amide ChemMatrix resin (loading 0.50 mmol/g). The resin was pre-swelled in *N*,*N*-dimethylformamide (DMF, 4.5 mL) for 20 min at 70 °C. The Fmoc-protected amino acids (4.0 eq.), saturated fatty acids (4.0 eq.) and O-(6-chlorobenzotriazol-1-yl)*N*,*N*,*N*′,*N*′-tetramethyl-uroniumhexafluorophosphate (HCTU, 4 eq.) were dissolved in DMF to a concentration of 0.5 M, 0.5 M and 0.6 M, respectively. *N*,*N*-Diisopropylethylamine (DIEA, 8 eq.) was dissolved in *N*-methyl-2-pyrrolidone (NMP) to a concentration of 2.0 M. Coupling steps for all amino acids except cysteine were performed under microwave conditions at 75 °C, for 10 min. To avoid racemization of Cys and Arg side-reaction due to microwave heating, Fmoc-Cys(Trt)-OH and Fmoc-Arg(Pbf)-OH were coupled at r.t. for 60 min. For the N-terminally acylated lipopeptides, the coupling reaction with HCTU was performed twice to ensure successful attachment of the acyl chain to the peptides. Following each coupling step, the resin was washed 4 times with DMF (4.5 mL) for 45 s. After the desired linear peptide was assembled, the resin was washed first with dichloromethane (DCM,

4.5 mL) for 45 s (6 times), and then with diethyl ether (3–4 times). The resin was dried on a vacuum manifold and placed in a desiccator overnight.

3.2. Fmoc Deprotection

The peptides were deprotected and cleaved from the resin using a standard cleavage cocktail consisting of trifluoracetic acid (TFA), Milli-Q ultrapure water, 1,2-ethanedithiol (EDT) and triisopropylsilane (TIS) (TFA/water/EDT/TIS; 94/2.5/2.5/1.0 (*v/v/v/v*) at room temperature. The cleavage procedure was repeated twice, each time with 10 mL of the cleavage mixture under occasional stirring. Following the first 3 h cleavage step, the resin was collapsed with a small amount of DCM, and then washed with diethyl ether. The second cleavage step was performed with the same amount of cleavage cocktail (10 mL) for an additional 1 h. After each cleavage step, as well as after addition of DCM and diethyl ether, the resin was dried under a vacuum. The collected filtrates containing the desired peptide were pooled into a round bottom flask and the solvents were evaporated, resulting in a thin, glassy film covering the walls of the flask. Precipitation of the peptides was induced by the addition of ice-cold diethyl ether, which was decanted after 24 h. This procedure was repeated twice, and the residual diethyl ether was evaporated before purification.

3.3. Peptide Purification by Preparative Reversed-Phase High-Performance Liquid Chromatography (RP-HPLC)

Crude peptide purification was performed by RP-HPLC using a preparative SunFire C_{18} OBD, 5 µm, 19 × 250 mm column (Waters, Milford, MA, USA at room temperature. The HPLC system (Waters) was equipped with a 2702 autosampler, a 2998 photodiode array (PDA) detector and an automated fraction collector. The lipopeptides were purified using a linear gradient of eluent A (water with 0.1% TFA) and eluent B (acetonitrile with 0.1% TFA), ranging from 20–60% B, over 25 min, at a flow rate of 10 mL/min. Purified fractions were collected and freeze-dried prior to further characterization.

3.4. Peptide Characterization by High-Resolution Mass Spectrometry (HRMS)

The purified peptides were characterized by HRMS using an Orbitrap Id-X Tribrid mass analyser equipped with an electrospray ionization (ESI) source (Thermo Fischer Scientific, Waltham, MA, USA), with a Vanquish UHPLC system (Waters), coupled to an Acquity Premier BEH C_{18}, 1.7 µm, 2.1 × 100 mm column (Waters). The ESI mass spectra were obtained in positive ion mode. Prior to analysis, all samples were dissolved in 1 mL of Milli-Q water. The lipopeptides were eluted with a 0.5–95.0% linear gradient of the eluent B (A: water with 0.1% formic acid, B: acetonitrile with 0.1% formic acid) over 10 min, with a flow rate of 0.5 mL/min. The injection volume was 2 µL, and the column temperature was set to 60 °C.

3.5. Purity Determination by Ultra-Performance Liquid Chromatography (UPLC)

Purity of the synthetized peptides was determined using an analytical UPLC-PDA H-class system (Waters, Milford, MA, USA). The analysis was conducted on an Acquity UPLC BEH 1.7 µm, 2.1 ×100 mm C_{18} column, using a linear gradient of eluent A (water with 0.1% TFA) and eluent B (acetonitrile with 0.1% TFA), ranging from 0.5–95.0% B, over 10 min. The flow rate was set to 0.5 mL/min and the temperature of the column was set to 60 °C. A 2996 PDA detector with a wavelength ranging from 210–400 nm was used to record the UV absorbance of the purified peptides. Retention times for each peptide were recorded as a measurement of hydrophobicity.

3.6. Cys-Cys Cyclization

The cyclization process included intramolecular disulphide formation between the sulfhydryl (SH) side chains of two cysteine residues, Cys17 and Cys26. This step was performed on a parallel reaction station, either under open air or with a continuous supply of oxygen by careful bubbling. The lipopeptides (5 mg) were dissolved in Milli-Q water

to a concentration of 250 μg/mL. The reaction proceeded at room temperature under continuous magnetic stirring. The progress of the reaction was monitored by UPLC-HRMS. Upon completion of the reaction, peptide solutions were lyophilized, and their purity determined as described above.

3.7. Antibacterial Minimum Inhibitory Concentration (MIC) Assay and Killing Assay

All cyclic and linear peptides were screened for antibacterial activity against four Gram-positive strains: *B. subtilis* (Bs, ATCC 23857), *C. glutamicum* (Cg, ATCC 13032), *S. aureus* (Sa, ATCC 9144) and *S. epidermidis* RP62A (Se, ATCC 35984), and two Gram-negative strains: *E. coli* (Ec, ATCC 25922) and *P. aeruginosa* (Pa, ATCC 27853). The activity was assessed using a broth microdilution assay according to a modified CLSI-based method [30]. Briefly, overnight bacterial cultures were grown in Mueller–Hinton (MH) broth medium (Difco Laboratories, Detroit, MI, USA) for 2 h at room temperature. The optical density (OD_{600}) was measured, and the bacterial suspensions were adjusted to 2.5–3 × 10^4 CFU/mL in MH medium. The bacterial suspension (50 μL) was distributed in 96-well plates (Nunc, Roskilde, Denmark) preloaded with two-fold dilution series (256 to 1 μg/mL) of peptide solutions (50 μL), giving a final well volume of 100 μL. The microplates were incubated in an EnVision 2103 microplate reader (PerkinElmer, Llantrisant, UK) at 35 °C, with OD_{595} recorded every hour for 24 h. MIC was defined as the lowest concentration of peptides showing an optical density less than 10% of the negative (growth) control, consisting of bacterial suspension and water. Polymyxin B sulfate (Sigma-Aldrich, St. Louis, MO, USA) and chlorhexidine acetate (CHX, Fresenius Kabi, Halden, Norway), both with concentrations ranging from 12.5 to 0.09 μg/mL, served as positive (growth inhibition) controls. All peptides were tested in triplicate.

A killing experiment was performed on selected lipopeptides by using actively growing cultures of *S. aureus* (ATCC 9144) and *E. coli* (ATCC 25922). The procedure was performed as previously described [31]. Briefly, after 24 h of peptide treatment (MIC assay, as described above), aliquots (10 μL) of 10-fold serial dilutions (in MH broth) of wells containing 1/2 , 1 and 2 × MIC of the peptides (with bacteria) were plated on MH Agar (Difco) plates. The number of colony-forming units (CFU) was determined after 24 h of incubation at 37 °C. The tests were performed in triplicate.

3.8. Antifungal MIC Assay

The synthesized peptides were screened for antifungal activity against the molds *A. pullulans* (Ap) and *Rhodotorula* sp. (Rh) (both obtained from Professor Arne Tronsmo, The Norwegian University of Life Sciences, Ås, Norway) and the yeast *C. albicans* (Ca, ATCC 10231) as previously described [13]. In short, fungal spores were grown in potato dextrose broth media (Difco) containing 2% D(+)-glucose (Merck, Darmstadt, Germany) at 25–30 °C while shaking at 200 rpm overnight. The cultures were diluted with a dextrose media containing glucose to a concentration of approx. 4 × 10^5 spores/mL. Aliquots of the cultures (50 μL) were transferred to 96 well microtiter plates preloaded with the synthetic peptides (50 μL) in two-fold serial dilutions (256 to 1 μg/mL). Polymyxin B and CHX (both with concentrations ranging from 12.5 to 0.09 μg/mL) served as positive antibiotic controls. The microtiter plates containing the fungal spores and the test peptides were incubated at room temperature for 48 h and OD_{600} was recorded using a Synergy H1 Hybrid microplate reader system (BioTek, Winooski, VT, USA). MIC was defined as the lowest peptide concentration showing an optical density less than 10% of the negative (growth) control. All experiments were performed in triplicate.

3.9. Haemolytic Activity Assay

The synthetized lipopeptides were screened for haemolytic activity against human red blood cells (RBC), in concentrations ranging from 500 to 3.9 μM, following a previously described protocol [32]. In brief, haemolysis was determined using a heparinizied (10 IU/mL) fraction of freshly drawn human blood. A second fraction of blood, which

was collected in test tubes containing ethylenediaminetetraacetic acid (EDTA, Vacutest, KIMA, Arzergrande, Italy), was used for determination of the hematocrit (hct). Plasma was removed from heparinized blood by washing three times with prewarmed phosphate-buffered saline (PBS) before being adjusted to a hematocrit of 4%. Peptides dissolved in dimethyl sulfoxide (DMSO) were further diluted with PBS to a final DMSO content of $\leq$1%. Triton X-100 (Sigma-Aldrich, St. Louis, MO, USA), used at a final concentration of 0.1%, served as a positive control for 100% haemolysis, whereas 1% DMSO in PBS buffer served as a negative control where no toxicity was detected. Duplicates of test solutions and erythrocytes, with 1% hct final concentration, were prepared in a 96-well polypropylene V-bottom plate (Nunc, Fischer scientific, Oslo, Norway). They were incubated under agitation at 37 °C and 800 rpm for 1 h. After centrifugation (5 min, 3000$\times$ *g*), 100 µL from each well were transferred to a flat-bottomed 96-well plate and absorbance was measured at 545 nm with a microplate reader (SpectraMax 190, Molecular Devices, San Jose, CA, USA). After subtracting PBS background, the percentage of haemolysis was calculated as the ratio of the absorbance in the peptide-treated and surfactant-treated samples. Three independent experiments were performed, and EC_{50} (the concentration giving 50% haemolysis) values are presented as averages.

3.10. Bacterial Biosensor Membrane Integrity Assay

A membrane integrity assay was performed using two bacterial biosensors, *B. subtilis* 168 (ATCC 23857) and *E. coli* K12 (ATCC MC1061). Both strains carry the pCSS962 plasmid that contains a eukaryotic luciferase gene (*lucGR*), which originate from the click beetle *Pyrophorus plagiophthalamus* [33]. The assay was performed as described previously [13]. Briefly, overnight cultures grown in MH media in the presence of respective antibiotics such as 5 µg/mL chloramphenicol (Merck, Darmstadt, Germany) for *B. subtilis* and both 20 µg/mL chloramphenicol and 100 µg/mL ampicillin (Sigma-Aldrich) for *E. coli*, were further diluted in fresh MH media without antibiotics and grown until they reached an OD_{600} of 0.1. D-luciferin potassium salt (Synchem Inc., Elk Grove Village, IL, USA) was added to the cell suspension at a final concentration of 1 mM. Two-fold dilutions (final assay concentration of 50–1.56 µg/mL) of peptides dissolved in Milli-Q water were prepared and added (10 µL per well) to black round-bottom 96-well microtiter plates (Nunc). Milli-Q water served as a negative control used for the normalization purpose and CHX, having known membranolytic activity, was used as a positive control. The plates were loaded into a Synergy H1 Hybrid Reader and the background luminescence was monitored before aliquots (90 µL) of the cell suspension with D-luciferin were added, one well at the time, by an automatic injector. Light emission was recorded every second for 3 min. Each study was performed at least three times independently, and the figures show a representative dataset.

3.11. Bacterial Biosensor Viability Assay

Bacterial viability, based on light production by constitutively expressed bacterial luciferase, was measured in real time according to the method described by Hansen et al. [13]. The assay was performed using *B. subtilis* 168 with chromosomally integrated *lux*ABCDE operon and *E. coli* K12 carrying the plasmid pCGLS-11 containing the *lux*CDABE operon. The assay set up was the same as for the membrane integrity assay, with the exception that *B. subtilis* 168 and *E. coli* colonies were grown in MH media supplemented with 5 µg/mL chloramphenicol and 100 µg/mL ampicillin, respectively. No D-luciferin was added to the cell suspension. Each assay was performed at least three times independently, and the figures show a representative dataset.

3.12. Screening for Activity against E. coli Mutants

MIC values were determined for all cyclic peptides against two *E. coli* strains: wild type (WT) MC4100 and the hyperpermeable variant NR698, having a deficient outer membrane. The NR698 strain, containing *lptD*4213/*imp*4213 mutation, was kindly provided by M. Grabowicz (Emory University School of Medicine, Rollins Research Center, Atlanta, GA,

USA) [28]. The assay was performed in the same way as previously described for the antibacterial MIC assay. Vancomycin hydrochloride (Hospira Enterprises BV, Almere, The Netherlands) and ampicillin: inhibitors of peptidoglycan synthesis, chloramphenicol: inhibitor of protein synthesis, and CHX and polymyxin B: membrane active compounds, were used as reference antibiotics to evaluate the permeability defects in *E. coli* NR698.

3.13. Outer Membrane Permeability Assay

The permeability of the *E. coli* outer membrane was analysed by measuring increased fluorescence as kinetics of 1-N-phenylnaphthylamine (NPN, Sigma-Aldrich) uptake following the protocol described by [34], with minor modifications. Briefly, a single colony of *E. coli* MC4100 (WT) was suspended in MH medium and incubated overnight at 37 °C with shaking (225 rpm). The culture was diluted in MH medium and adjusted to OD_{600} = 0.1 and incubated at 37 °C until it reached an OD_{600} of 0.5. The cells were centrifuged and washed twice with an assay buffer (5 mM HEPES, 5 mM glucose, pH 7.2) and resuspended in the same buffer to a final OD_{600} of 1.0. *E. coli* MC4100 cells were mixed with 20 µM NPN. The assay set up was the same as for the membrane integrity and viability assay, using black round-bottom 96-well microtiter plates (Nunc) containing 10 µL of 2-fold dilutions of peptides (500 to 31.2 µg/mL). A volume of 90 µL of cell suspension with NPN was added to each well by the automated injector of the Synergy H1 Hybrid Reader. The fluorescence was immediately measured (well by well) at an excitation wavelength of 350 nm and an emission wavelength of 420 nm every second for 3 min. The relative fluorescence was calculated by normalizing the values from each time point with the negative control (Milli-Q water). CHX was included as a positive control.

Supplementary Materials: The following supporting information can be downloaded at: https://www.mdpi.com/article/10.3390/ijms232213844/s1.

Author Contributions: D.S. and I.N.-S.H. performed the peptide synthesis; M.B.S. and T.H. performed the sequence analysis; H.D. and T.A. performed the biological activity experiments; H.D., T.A., E.G.A.F., H.-M.B., M.B.S. and T.H. conceived the biological experiments and analyzed data; D.S., I.N.-S.H., T.V. and M.B.S. conceived the MS experiments and analyzed data; H.D., D.S., I.N.-S.H., E.G.A.F., H.-M.B., M.B.S. and T.H. wrote the paper. M.B.S. and T.H. contributed to the conception of the work and supervised the project. All authors have read and agreed to the published version of the manuscript.

Funding: This work was supported by a grant (no. 217/6770) from UiT The Arctic University of Norway. The publication charges for this article have been covered by the publication fund of UiT The Arctic University of Norway.

Institutional Review Board Statement: Not applicable.

Informed Consent Statement: Not applicable.

Data Availability Statement: Not applicable.

Conflicts of Interest: The authors declare no conflict of interest.

References

1. Murray, C.J.L.; Ikuta, K.S.; Sharara, F.; Swetschinski, L.; Robles Aguilar, G.; Gray, A.; Han, C.; Bisignano, C.; Rao, P.; Wool, E.; et al. Global burden of bacterial antimicrobial resistance in 2019: A systematic analysis. *Lancet* **2022**, *399*, 629–655. [CrossRef]
2. World Health Organization. Antibiotic Resistance. Available online: https://www.who.int/news-room/fact-sheets/detail/antibiotic-resistance (accessed on 14 December 2018).
3. Boucher, H.W.; Talbot, G.H.; Benjamin, D.K., Jr.; Bradley, J.; Guidos, R.J.; Jones, R.N.; Murray, B.E.; Bonomo, R.A.; Gilbert, D.; Infectious Diseases Society of America. 10 × ′20 Progress—Development of new drugs active against Gram-negative bacilli: An update from the Infectious Diseases Society of America. *Clin. Infect. Dis.* **2013**, *56*, 1685–1694. [CrossRef] [PubMed]
4. Hutchings, M.I.; Truman, A.W.; Wilkinson, B. Antibiotics: Past, present and future. *Curr. Opin. Microbiol.* **2019**, *51*, 72–80. [CrossRef]
5. Bulet, P.; Stöcklin, R.; Menin, L. Anti-microbial peptides: From invertebrates to vertebrates. *Immunol. Rev.* **2004**, *198*, 169–184. [CrossRef]

6. Erdem Büyükkiraz, M.; Kesmen, Z. Antimicrobial peptides (AMPs): A promising class of antimicrobial compounds. *J. Appl. Microbiol.* **2022**, *132*, 1573–1596. [CrossRef] [PubMed]
7. Lei, M.; Jayaraman, A.; Deventer, J.A.V.; Lee, K. Engineering selectively targeting antimicrobial peptides. *Annu. Rev. Biomed. Eng.* **2021**, *23*, 339–357. [CrossRef]
8. Geitani, R.; Ayoub Moubareck, C.; Touqui, L.; Karam Sarkis, D. Cationic antimicrobial peptides: Alternatives and/or adjuvants to antibiotics active against methicillin-resistant *Staphylococcus aureus* and multidrug-resistant *Pseudomonas aeruginosa*. *BMC Microbiol.* **2019**, *19*, 54. [CrossRef]
9. Li, J.; Fernández-Millán, P.; Boix, E. Synergism between host defence peptides and antibiotics against bacterial infections. *Curr. Top. Med. Chem.* **2020**, *20*, 1238–1263. [CrossRef]
10. Dijksteel, G.S.; Ulrich, M.M.W.; Middelkoop, E.; Boekema, B.K.H.L. Review: Lessons learned from clinical trials using antimicrobial peptides (AMPs). *Front. Microbiol.* **2021**, *12*, 616979. [CrossRef]
11. Wu, R.; Patocka, J.; Nepovimova, E.; Oleksak, P.; Valis, M.; Wu, W.; Kuca, K. Marine invertebrate peptides: Antimicrobial peptides. *Front. Microbiol.* **2021**, *12*, 785085. [CrossRef]
12. Hansen, I.; Isaksson, J.; Poth, A.G.; Hansen, K.; Andersen, A.J.C.; Richard, C.S.M.; Blencke, H.M.; Stensvåg, K.; Craik, D.J.; Haug, T. Isolation and characterization of antimicrobial peptides with unusual disulfide connectivity from the colonial ascidian *Synoicum turgens*. *Mar. Drugs* **2020**, *18*, 51. [CrossRef] [PubMed]
13. Hansen, I.K.Ø.; Lövdahl, T.; Simonovic, D.; Hansen, K.Ø.; Andersen, A.J.C.; Devold, H.; Richard, C.S.M.; Andersen, J.H.; Strøm, M.B.; Haug, T. Antimicrobial activity of small synthetic peptides based on the marine peptide Turgencin A: Prediction of antimicrobial peptide sequences in a natural peptide and strategy for optimization of potency. *Int. J. Mol. Sci.* **2020**, *21*, 5460. [CrossRef] [PubMed]
14. Papo, N.; Shai, Y. A molecular mechanism for lipopolysaccharide protection of Gram-negative bacteria from antimicrobial peptides. *J. Biol. Chem.* **2005**, *280*, 10378–10387. [CrossRef]
15. Avrahami, D.; Shai, Y. Conjugation of a magainin analogue with lipophilic acids controls hydrophobicity, solution assembly, and cell selectivity. *Biochemistry* **2002**, *41*, 2254–2263. [CrossRef]
16. Makovitzki, A.; Avrahami, D.; Shai, Y. Ultrashort antibacterial and antifungal lipopeptides. *Proc. Natl. Acad. Sci. USA* **2006**, *103*, 15997–16002. [CrossRef]
17. Rounds, T.; Straus, S.K. Lipidation of antimicrobial peptides as a design strategy for future alternatives to antibiotics. *Int. J. Mol. Sci.* **2020**, *21*, 9692. [CrossRef] [PubMed]
18. Chu-Kung, A.F.; Nguyen, R.; Bozzelli, K.N.; Tirrell, M. Chain length dependence of antimicrobial peptide–fatty acid conjugate activity. *J. Colloid Interface Sci.* **2010**, *345*, 160–167. [CrossRef]
19. Malina, A.; Shai, Y. Conjugation of fatty acids with different lengths modulates the antibacterial and antifungal activity of a cationic biologically inactive peptide. *Biochem. J.* **2005**, *390*, 695–702. [CrossRef]
20. Kamysz, E.; Sikorska, E.; Jaśkiewicz, M.; Bauer, M.; Neubauer, D.; Bartoszewska, S.; Barańska-Rybak, W.; Kamysz, W. Lipidated analogs of the LL-37-derived peptide fragment KR12—structural analysis, surface-active properties and antimicrobial activity. *Int. J. Mol. Sci.* **2020**, *21*, 887. [CrossRef]
21. Grimsey, E.; Collis, D.W.P.; Mikut, R.; Hilpert, K. The effect of lipidation and glycosylation on short cationic antimicrobial peptides. *Biochim. Biophys. Acta* **2020**, *1862*, 183195. [CrossRef]
22. Húmpola, M.V.; Rey, M.C.; Carballeira, N.M.; Simonetta, A.C.; Tonarelli, G.G. Biological and structural effects of the conjugation of an antimicrobial decapeptide with saturated, unsaturated, methoxylated and branched fatty acids. *J. Pept. Sci.* **2017**, *23*, 45–55. [CrossRef] [PubMed]
23. Orlov, D.S.; Shamova, O.V.; Eliseev, I.E.; Zharkova, M.S.; Chakchir, O.B.; Antcheva, N.; Zachariev, S.; Panteleev, P.V.; Kokryakov, V.N.; Ovchinnikova, T.V.; et al. Redesigning Arenicin-1, an antimicrobial peptide from the marine *Polychaeta arenicola marina*, by strand rearrangement or branching, substitution of specific residues, and backbone linearization or cyclization. *Mar. Drugs* **2019**, *17*, 376. [CrossRef] [PubMed]
24. Lyu, Y.; Yang, Y.; Lyu, X.; Dong, N.; Shan, A. Antimicrobial activity, improved cell selectivity and mode of action of short PMAP-36-derived peptides against bacteria and *Candida*. *Sci. Rep.* **2016**, *6*, 27258. [CrossRef] [PubMed]
25. Virta, M.; Åkerman, K.E.O.; Saviranta, P.; Oker-Blom, C.; Karp, M.T. Real-time measurement of cell permeabilization with low-molecular-weight membranolytic agents. *J. Antimicrob. Chemother.* **1995**, *36*, 303–315. [CrossRef] [PubMed]
26. Braun, M.; Silhavy, T.J. Imp/OstA is required for cell envelope biogenesis in *Escherichia coli*. *Mol. Microbiol.* **2002**, *45*, 1289–1302. [CrossRef] [PubMed]
27. Eggert, U.S.; Ruiz, N.; Falcone, B.V.; Branstrom, A.A.; Goldman, R.C.; Silhavy, T.J.; Kahne, D. Genetic basis for activity differences between vancomycin and glycolipid derivatives of vancomycin. *Science* **2001**, *294*, 361–364. [CrossRef]
28. Ruiz, N.; Falcone, B.; Kahne, D.; Silhavy, T.J. Chemical conditionality: A genetic strategy to probe organelle assembly. *Cell* **2005**, *121*, 307–317. [CrossRef]
29. Novikova, O.D.; Solovyeva, T.F. Nonspecific porins of the outer membrane of Gram-negative bacteria: Structure and functions. *Biochem. (Mosc.) Suppl. A Membr. Cell Biol.* **2009**, *3*, 3–15. [CrossRef]
30. Igumnova, E.M.; Mishchenko, E.; Haug, T.; Blencke, H.-M.; Sollid, J.U.E.; Fredheim, E.G.A.; Lauksund, S.; Stensvåg, K.; Strøm, M.B. Synthesis and antimicrobial activity of small cationic amphipathic aminobenzamide marine natural product mimics and

evaluation of relevance against clinical isolates including ESBL–CARBA producing multi-resistant bacteria. *Bioorg. Med. Chem.* **2016**, *24*, 5884–5894. [CrossRef]
31. Solstad, R.G.; Johansen, C.; Stensvåg, K.; Strøm, M.B.; Haug, T. Structure-activity relationship studies of shortened analogues of the antimicrobial peptide EeCentrocin 1 from the sea urchin *Echinus esculentus*. *J. Pept. Sci.* **2020**, *26*, e3233. [CrossRef]
32. Paulsen, M.H.; Ausbacher, D.; Bayer, A.; Engqvist, M.; Hansen, T.; Haug, T.; Anderssen, T.; Andersen, J.H.; Sollid, J.U.E.; Strøm, M.B. Antimicrobial activity of amphipathic α,α-disubstituted β-amino amide derivatives against ESBL—CARBA producing multi-resistant bacteria; effect of halogenation, lipophilicity and cationic character. *Eur. J. Med. Chem.* **2019**, *183*, 111671. [CrossRef] [PubMed]
33. Lampinen, J.; Koivisto, L.; Wahlsten, M.; Mäntsälä, P.; Karp, M. Expression of luciferase genes from different origins in *Bacillus subtilis*. *Mol. Gen. Genet.* **1992**, *232*, 498–504. [CrossRef] [PubMed]
34. Helander, I.M.; Mattila-Sandholm, T. Fluorometric assessment of Gram-negative bacterial permeabilization. *J. Appl. Microbiol.* **2000**, *88*, 213–219. [CrossRef] [PubMed]

Supporting information

Synthesis and Antimicrobial Activity of Short Analogues of the Marine Antimicrobial Peptide Turgencin A: Effects of SAR Optimizations, Cys-Cys Cyclization And lipopeptide Modifications

Hymonti Dey [1,†], Danijela Simonovic [2,†], Ingrid Norberg-Schulz Hagen [2], Terje Vasskog [2], Elizabeth G. Aarag Fredheim [2], Hans-Matti Blencke [1], Trude Anderssen[2], Morten B. Strøm [2,*] and Tor Haug [1,*]

[1] The Norwegian College of Fishery Science, Faculty of Biosciences, Fisheries and Economics, UiT The Arctic University of Norway, NO-9037 Tromsø, Norway
[2] Department of Pharmacy, Faculty of Health Sciences, UiT The Arctic University of Norway, NO-9037 Tromsø, Norway
* Correspondence: morten.strom@uit.no (M.B.S.); tor.haug@uit.no (T.H.)
† These authors contributed equally to this work.

Contents:

Figure S27. Kinetic of the effect on viability as measured by relative luminescence in *B. subtilis* (pCGLS11) treated with different concentrations of **C_8-cTurg-1**, **C_{10}-cTurg-1**, **C_{10}-cTurg-2**, **C_{12}-cTurg-2**, **C_8-cTurg-6**, **C_{10}-cTurg-6**, and **C_{12}-cTurg-6**.

Figure S28. Kinetic of the effect on membrane integrity as measured by relative luminescence in *B. subtilis* (pCSS962) treated with different concentrations **of cTurg-1**, **cTurg-2**, **cTurg-3**, **cTurg-4**, **cTurg-5**, **cTurg-6** and **cTurg-7**.

Figure S29. Kinetic of the effect on membrane integrity as measured by relative luminescence in *B. subtilis* (pCSS962) treated with different concentrations of **C_8-cTurg-1**, **C_{10}-cTurg-1**, **C_{10}-cTurg-2**, **C_{12}-cTurg-2**, **C_8-cTurg-6**, **C_{10}-cTurg-6**, and **C_{12}-cTurg-6**.

Figure S30. Kinetic of the effect on viability as measured by relative luminescence in *E. coli* (pCGLS-11) treated with 50 μg/mL of **cTurg-1-7** and 25 μg/mL of **chlorhexidine**.

Figure S31. Kinetic of the effect on viability as measured by relative luminescence in *E. coli* (pCGLS-11) treated with different concentrations **of C_8-cTurg-1**, **C_{10}-cTurg-1**, **C_{10}-cTurg-2**, **C_{12}-cTurg-2**, **C_8-cTurg-6**, **C_{10}-cTurg-6**, and **C_{12}-cTurg-6**.

Figure S32. Kinetic of the effect on membrane integrity as measured by relative luminescence in *E. coli* (pCSS962) treated with different concentrations of cyclic peptides **cTurg-1**, **cTurg-2**, **cTurg-3**, **cTurg-4**, **cTurg-5**, **cTurg-6** and **cTurg-7**.

Figure S33. Kinetic of the effect on membrane integrity as measured by relative luminescence in *E. coli* (pCSS962) treated with different concentrations of **C_8-cTurg-1**, **C_{10}-cTurg-1**, **C_{10}-cTurg-2**, **C_{12}-cTurg-2**, **C_8-cTurg-6**, **C_{10}-cTurg-6**, and **C_{12}-cTurg-6**.

Table S1. Theoretical and measured monoisotopic mass (Da), and theoretical and observed m/z ions during HRMS of the synthesised peptides.

Table S2. Purity of synthesized peptides (%) and retention time (min), determined by UPLC using a reversed phase column.

Table S3. Selectivity index (SI) calculated as the ration between haemolytic activity (EC_{50}, in μg/mL) and the geometric mean (GM) of the MIC values (in μg/mL) against bacteria and fungi, i.e., SI = EC_{50} / GM.

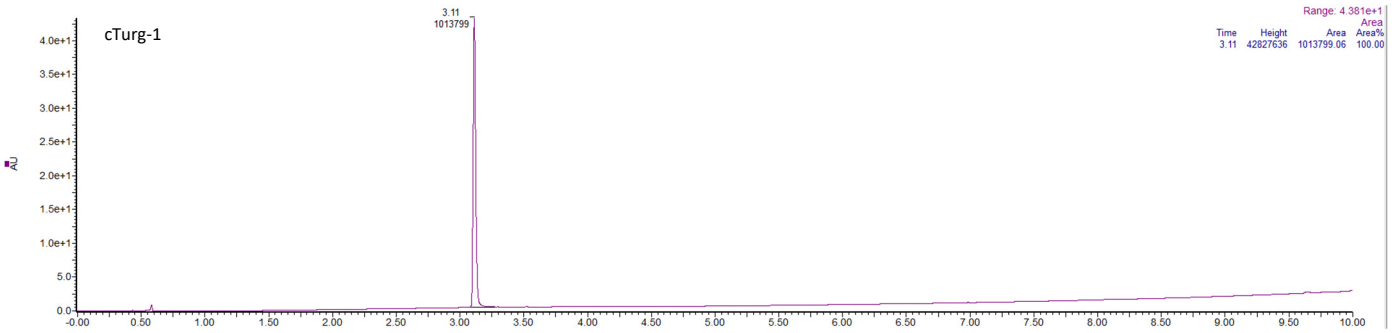

Figure S1. UPLC chromatogram of purified cyclic peptide **cTurg-1**. The peptide purity is 100 % based on the UPLC calculated area under the curves.

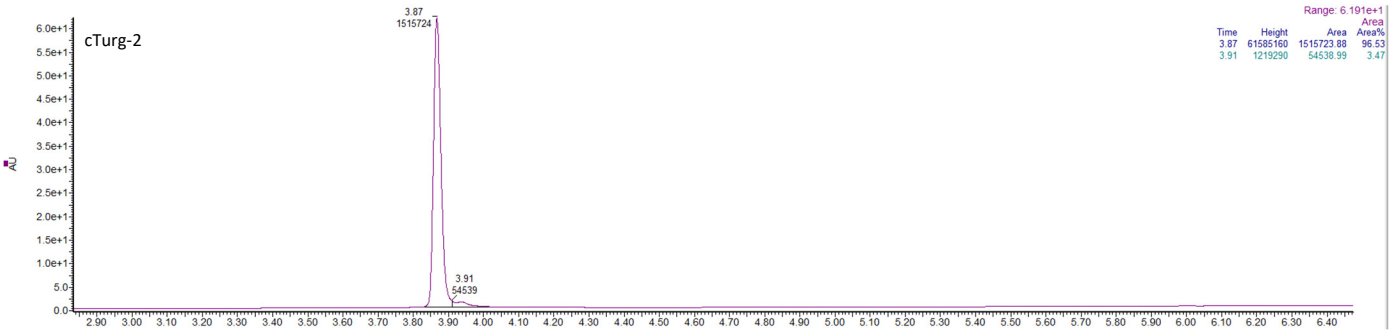

Figure S2. UPLC chromatogram of purified cyclic peptide **cTurg-2**. The peptide purity is 96.53 % based on the UPLC calculated area under the curves.

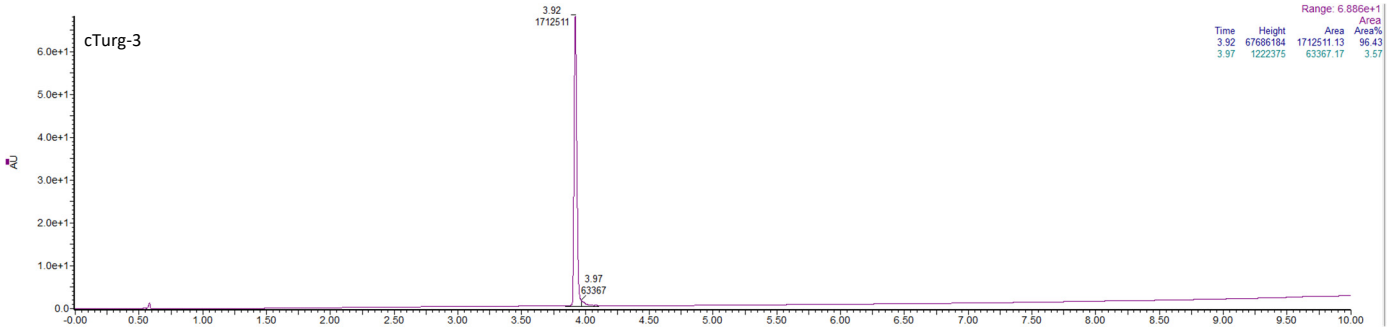

Figure S3. UPLC chromatogram of purified cyclic peptide **cTurg-3**. The peptide purity is 96.43 % based on the UPLC calculated area under the curves.

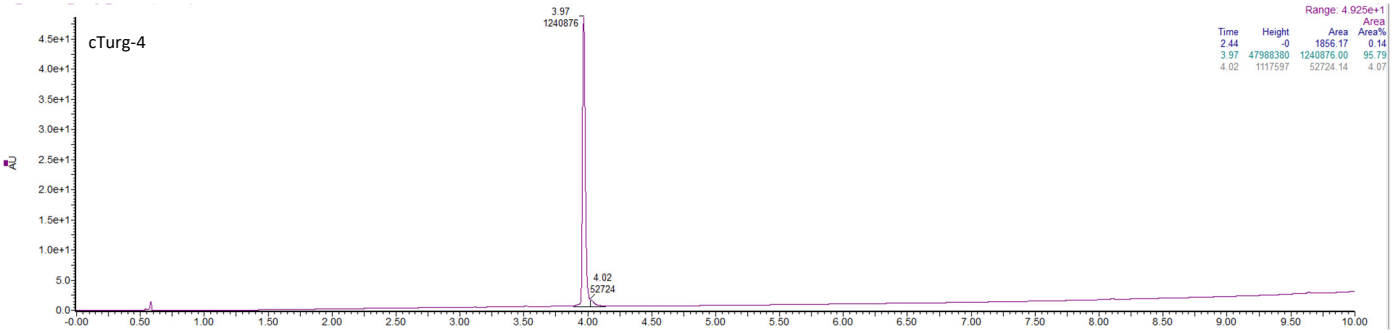

Figure S4. UPLC chromatogram of purified cyclic peptide **cTurg-4**. The peptide purity is 95.79 % based on the UPLC calculated area under the curves.

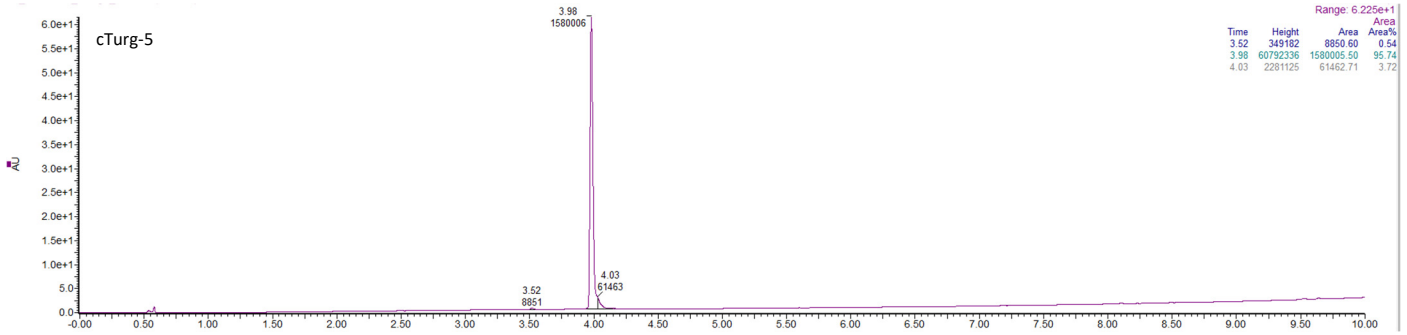

Figure S5. UPLC chromatogram of purified cyclic peptide **cTurg-5**. The peptide purity is 95.74 % based on the UPLC calculated area under the curves.

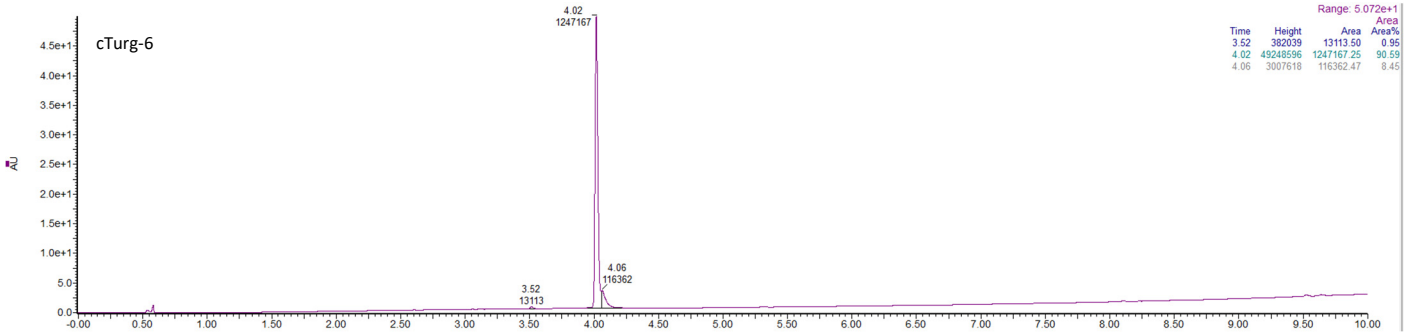

Figure S6. UPLC chromatogram of purified cyclic peptide **cTurg-6**. The peptide purity is 90.59 % based on the UPLC calculated area under the curves.

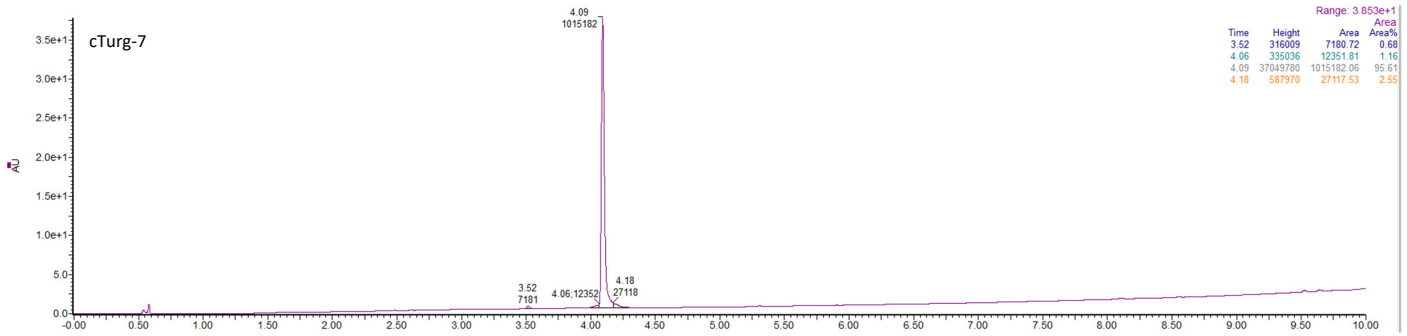

Figure S7. UPLC chromatogram of purified cyclic peptide **cTurg-7**. The peptide purity is 95.61 % based on the UPLC calculated area under the curves.

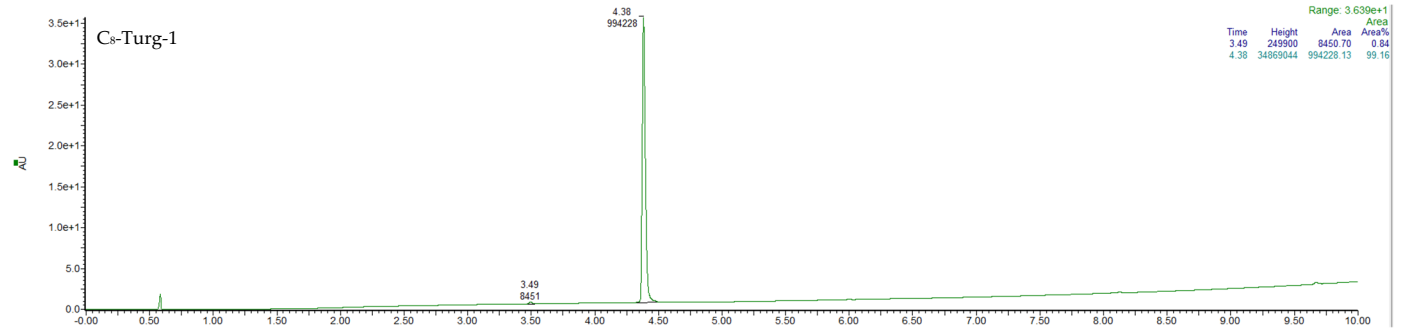

Figure S8. UPLC chromatogram of purified linear lipopeptide **C8-Turg-1**. The peptide purity is 99.16 % based on the UPLC calculated area under the curves.

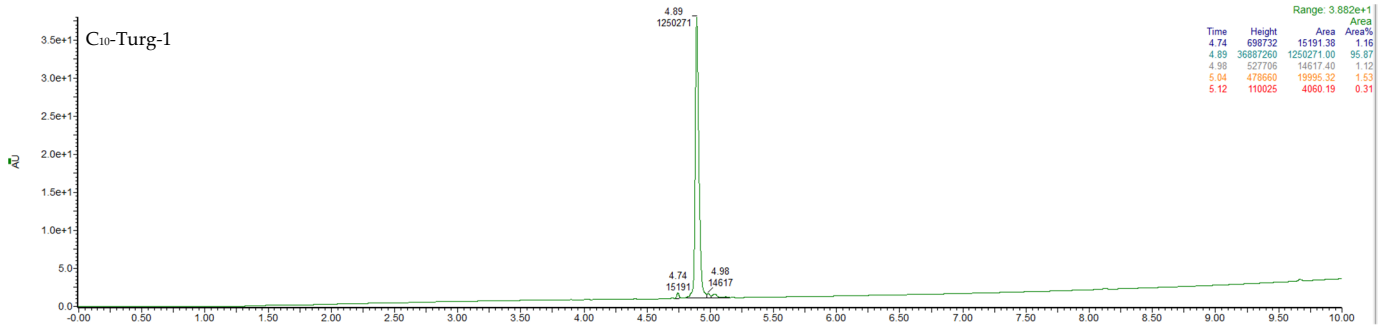

Figure S9. UPLC chromatogram of purified linear lipopeptide **C10-Turg-1**. The peptide purity is 95.87 % based on the UPLC calculated area under the curves.

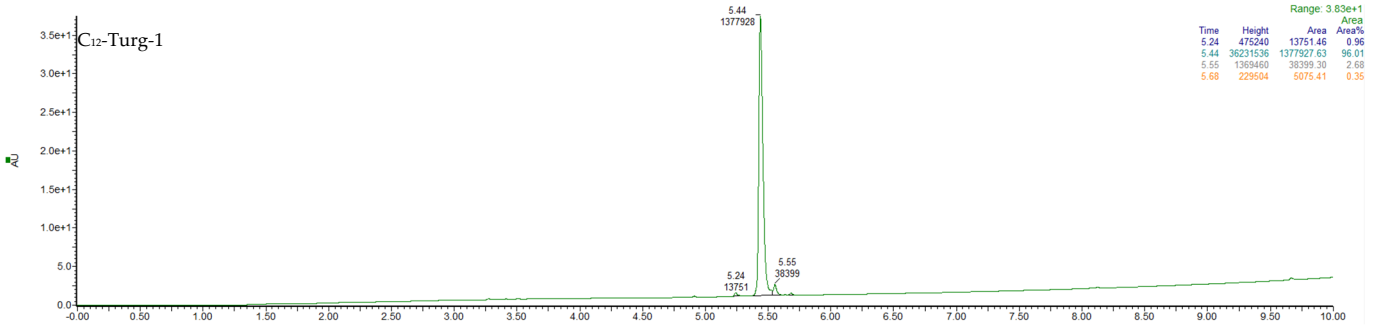

Figure S10. UPLC chromatogram of purified linear lipopeptide **C12-Turg-1**. The peptide purity is 96.01 % based on the UPLC calculated area under the curves.

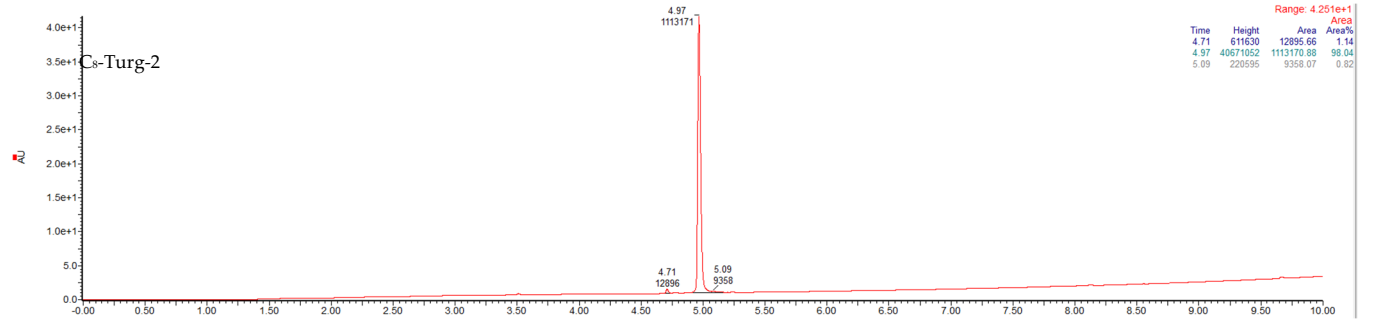

Figure S11. UPLC chromatogram of purified linear lipopeptide **C8-Turg-2**. The peptide purity is 98.04 % based on the UPLC calculated area under the curves.

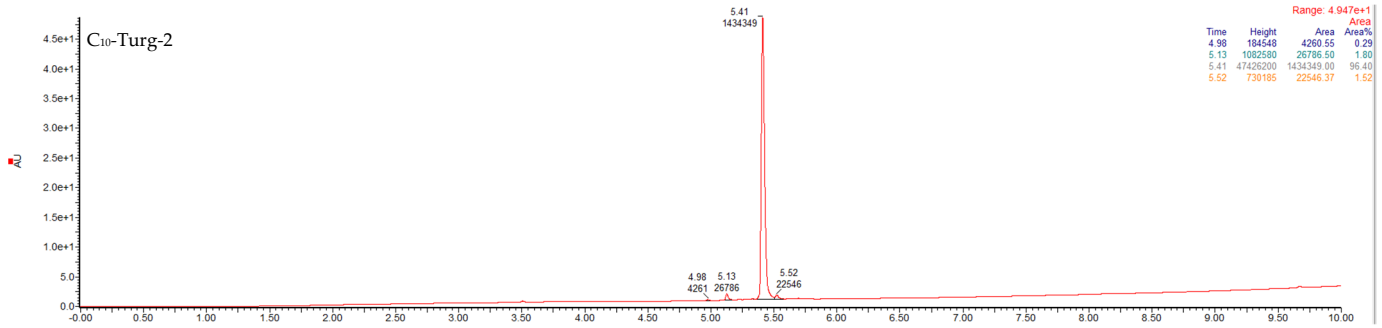

Figure S12. UPLC chromatogram of purified linear lipopeptide **C10-Turg-2**. The peptide purity is 96.40 % based on the UPLC calculated area under the curves.

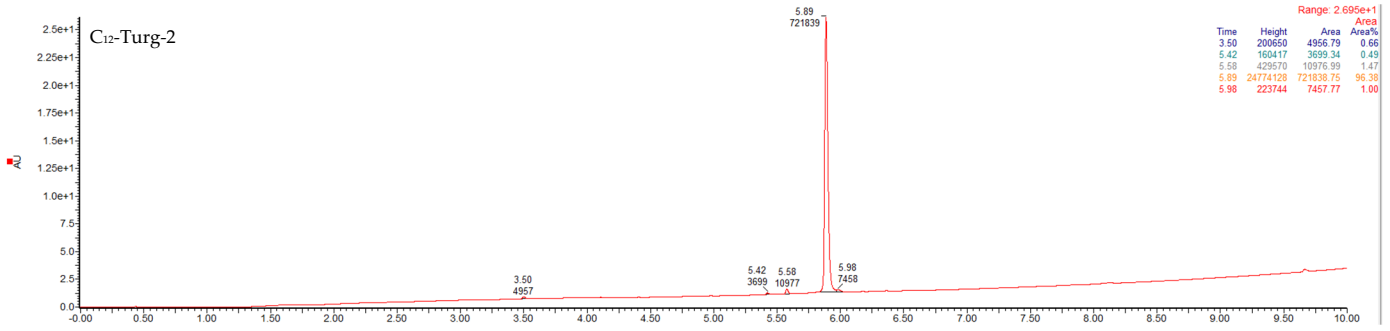

Figure S13. UPLC chromatogram of purified linear lipopeptide **C12-Turg-2**. The peptide purity is 96.38 % based on the UPLC calculated area under the curves.

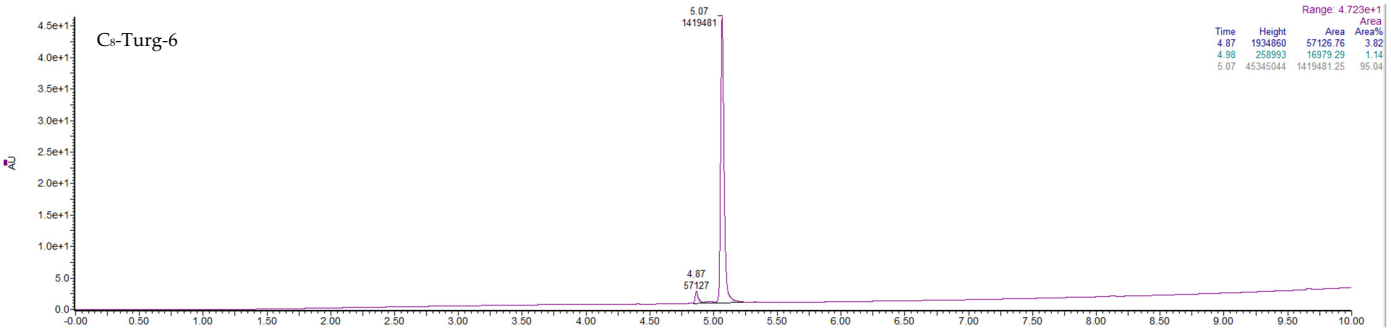

Figure S14. UPLC chromatogram of purified linear lipopeptide **C8-Turg-6**. The peptide purity is 95.04 % based on the UPLC calculated area under the curves.

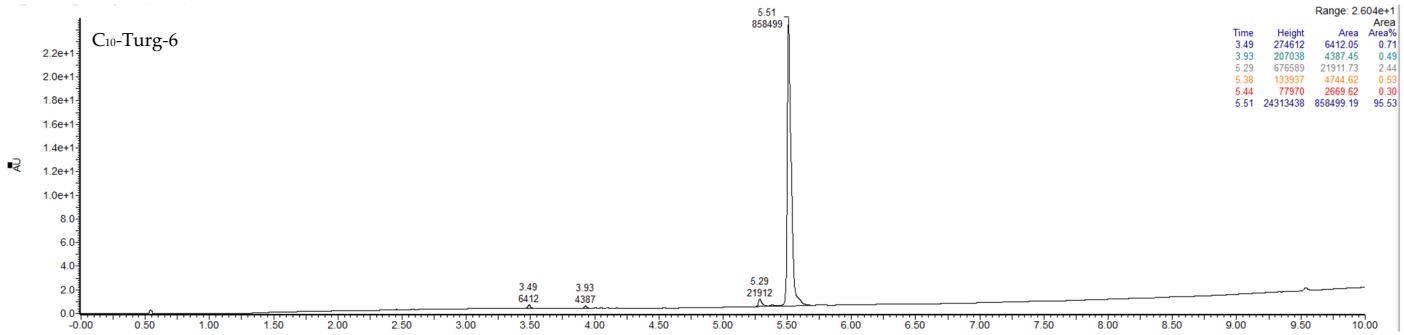

Figure S15. UPLC chromatogram of purified linear lipopeptide **C10-Turg-6**. The peptide purity is 95.53 % based on the UPLC calculated area under the curves.

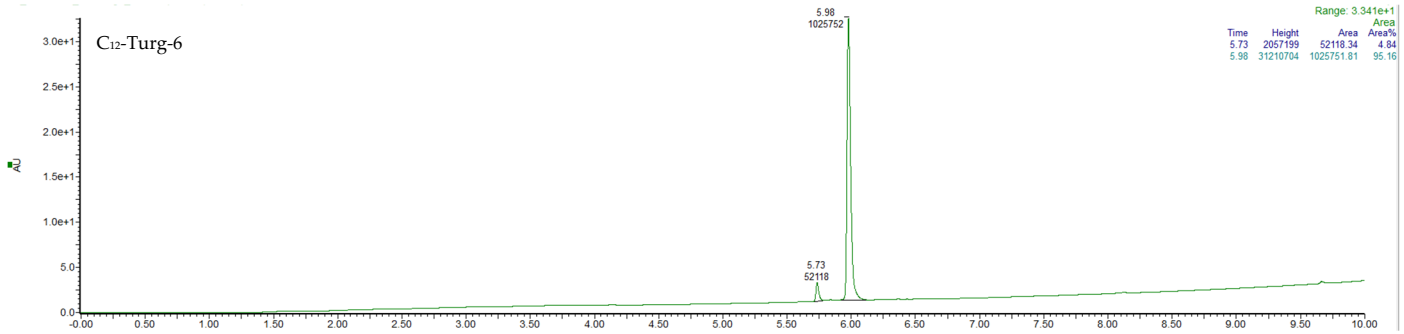

Figure S16. UPLC chromatogram of purified linear lipopeptide **C12-Turg-6**. The peptide purity is 95.16 % based on the UPLC calculated area under the curves.

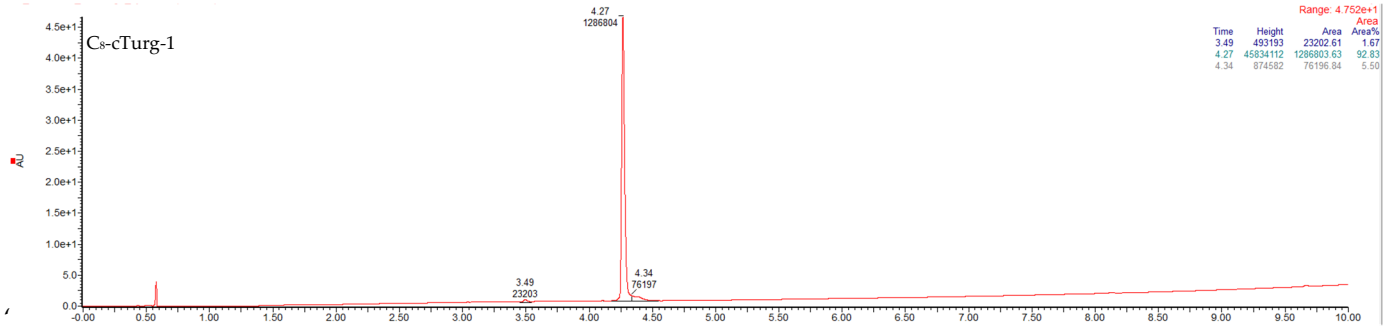

Figure S17. UPLC chromatogram of purified cyclic lipopeptide **C8-cTurg-1**. The peptide purity is 92.83 % based on the UPLC calculated area under the curves.

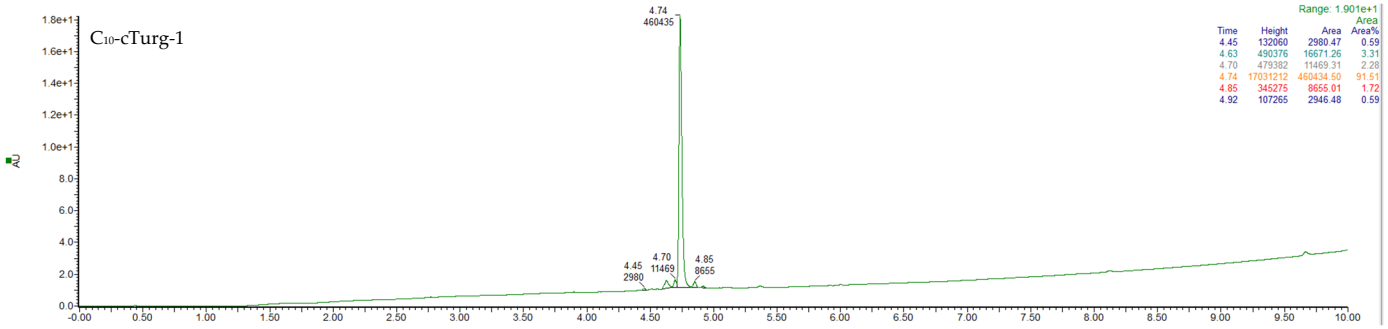

Figure S18. UPLC chromatogram of purified cyclic lipopeptide **C10-cTurg-1**. The peptide purity is 91.51 % based on the UPLC calculated area under the curves.

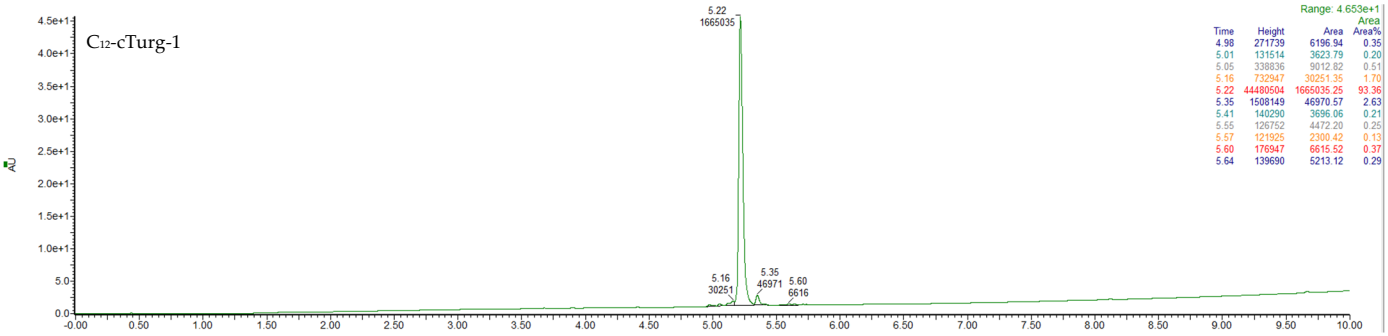

Figure S19. UPLC chromatogram of purified cyclic lipopeptide **C12-cTurg-1**. The peptide purity is 93.36 % based on the UPLC calculated area under the curves.

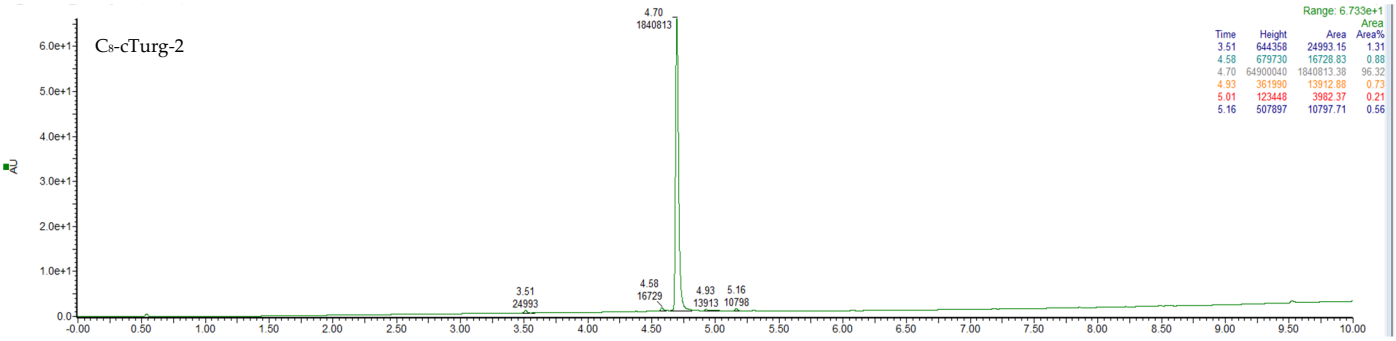

Figure S20. UPLC chromatogram of purified cyclic lipopeptide **C8-cTurg-2**. The peptide purity is 96.32 % based on the UPLC calculated area under the curves.

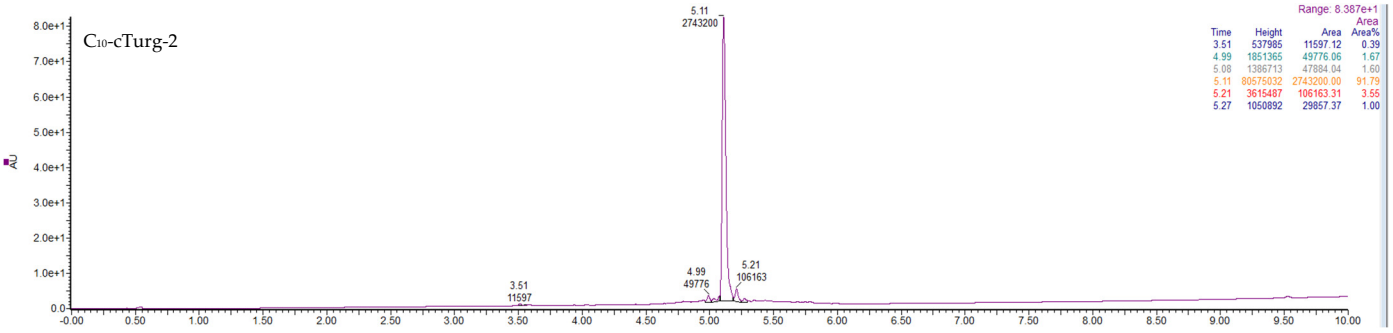

Figure S21. UPLC chromatogram of purified cyclic lipopeptide **C10-cTurg-2**. The peptide purity is 91.79 % based on the UPLC calculated area under the curves.

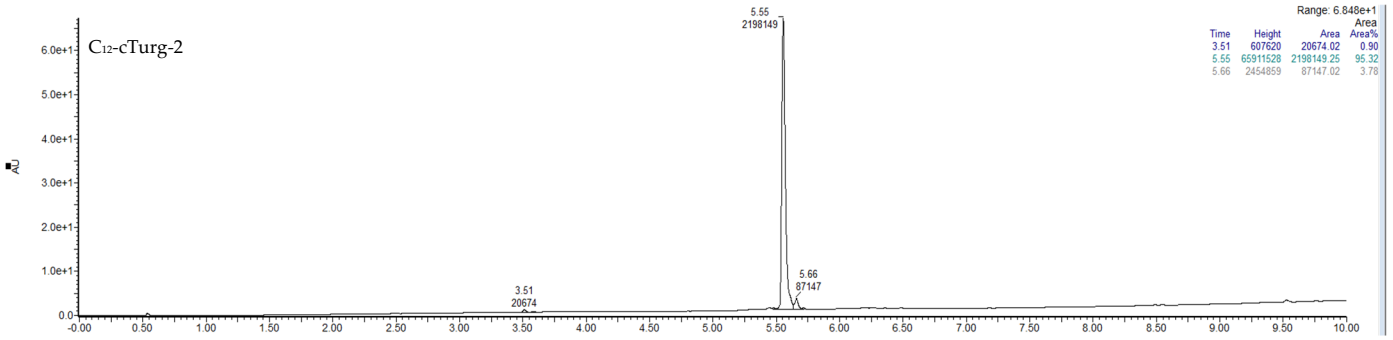

Figure S22. UPLC chromatogram of purified cyclic lipopeptide **C12-cTurg-2**. The peptide purity is 95.32 % based on the UPLC calculated area under the curves.

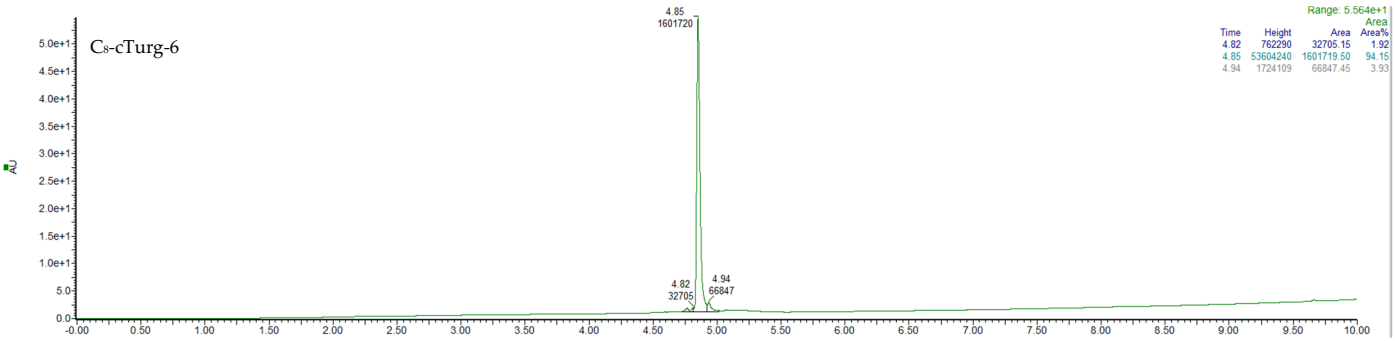

Figure S23. UPLC chromatogram of purified cyclic lipopeptide **C8-cTurg-6**. The peptide purity is 94.15 % based on the UPLC calculated area under the curves.

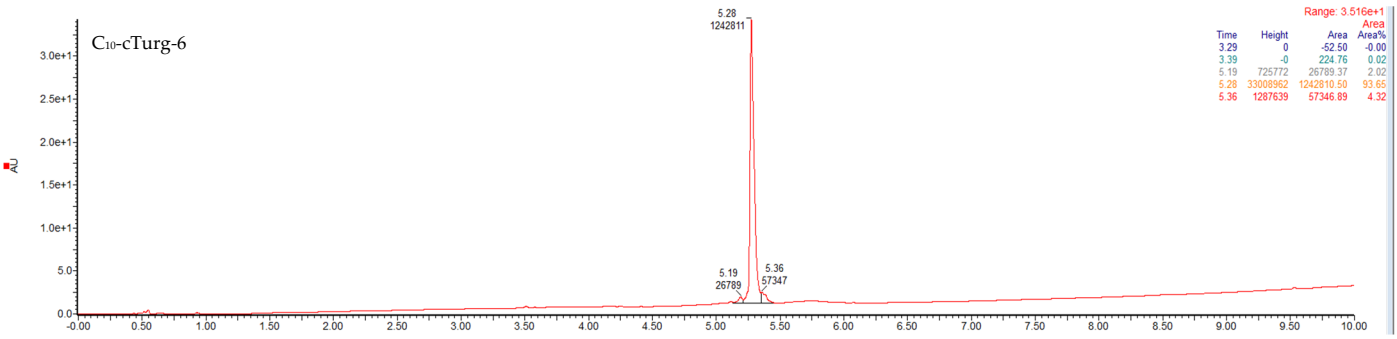

Figure S24. UPLC chromatogram of purified cyclic lipopeptide **C10-cTurg-6**. The peptide purity is 93.65 % based on the UPLC calculated area under the curves.

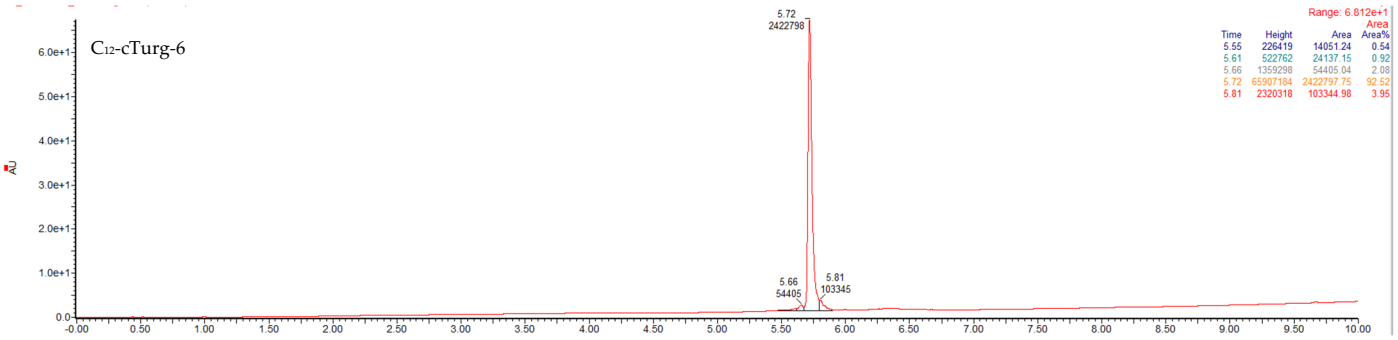

Figure S25. UPLC chromatogram of purified cyclic lipopeptide **C12-cTurg-6**. The peptide purity is 92.52 % based on the UPLC calculated area under the curves.

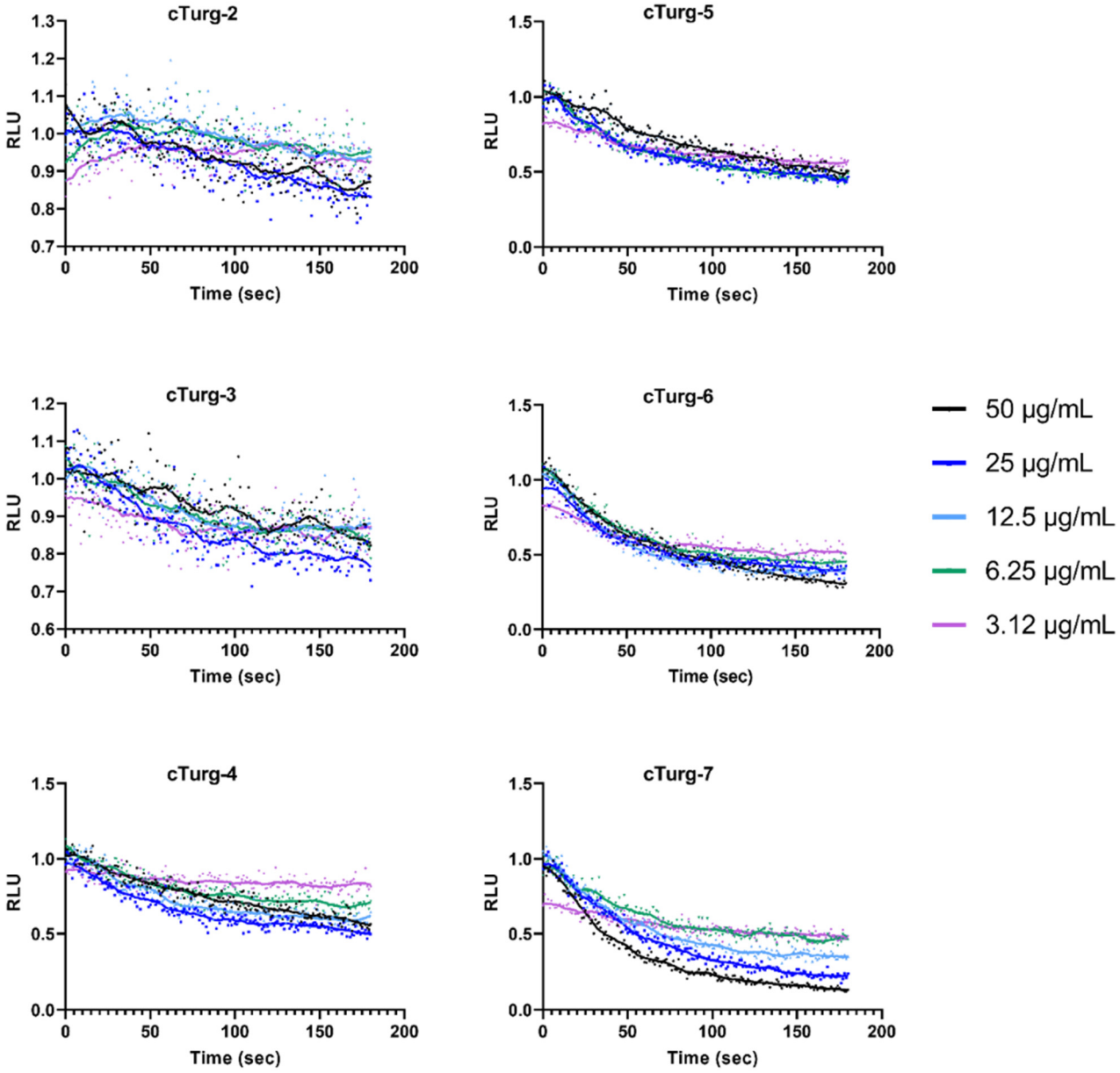

Figure S26. Kinetic of the effect on viability as measured by relative luminescence in *B. subtilis* (pCGLS11) treated with different concentrations of **cTurg-2**, **cTurg-3**, **cTurg-4**, **cTurg-5**, **cTurg-6** and **cTurg-7**.

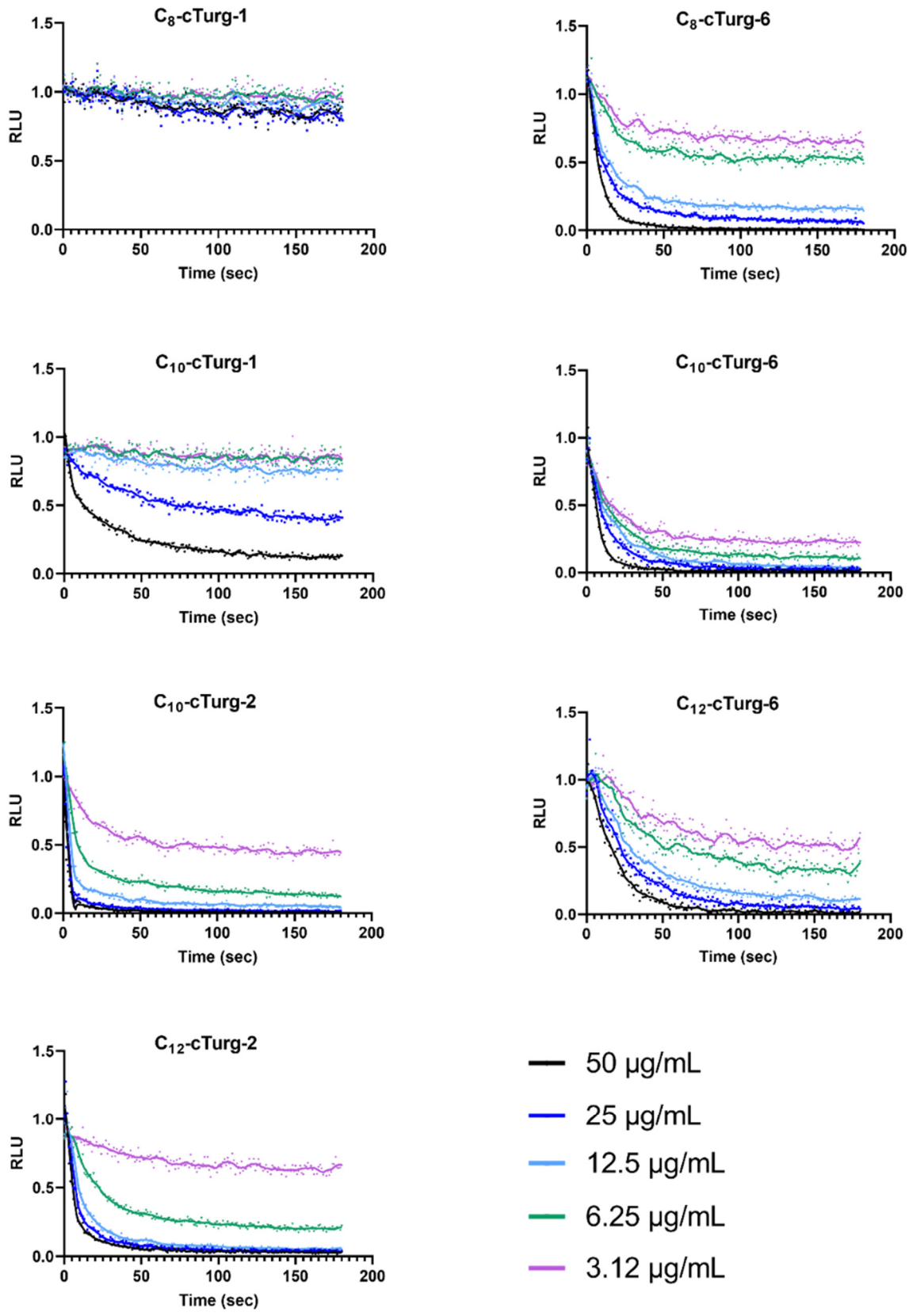

Figure S27. Kinetic of the effect on viability as measured by relative luminescence in *B. subtilis* (pCGLS11) treated with different concentrations of **C_8-cTurg-1**, **C_{10}-cTurg-1**, **C_{10}-cTurg-2**, **C_{12}-cTurg-2**, **C_8-cTurg-6**, **C_{10}-cTurg-6**, and **C_{12}-cTurg-6**.

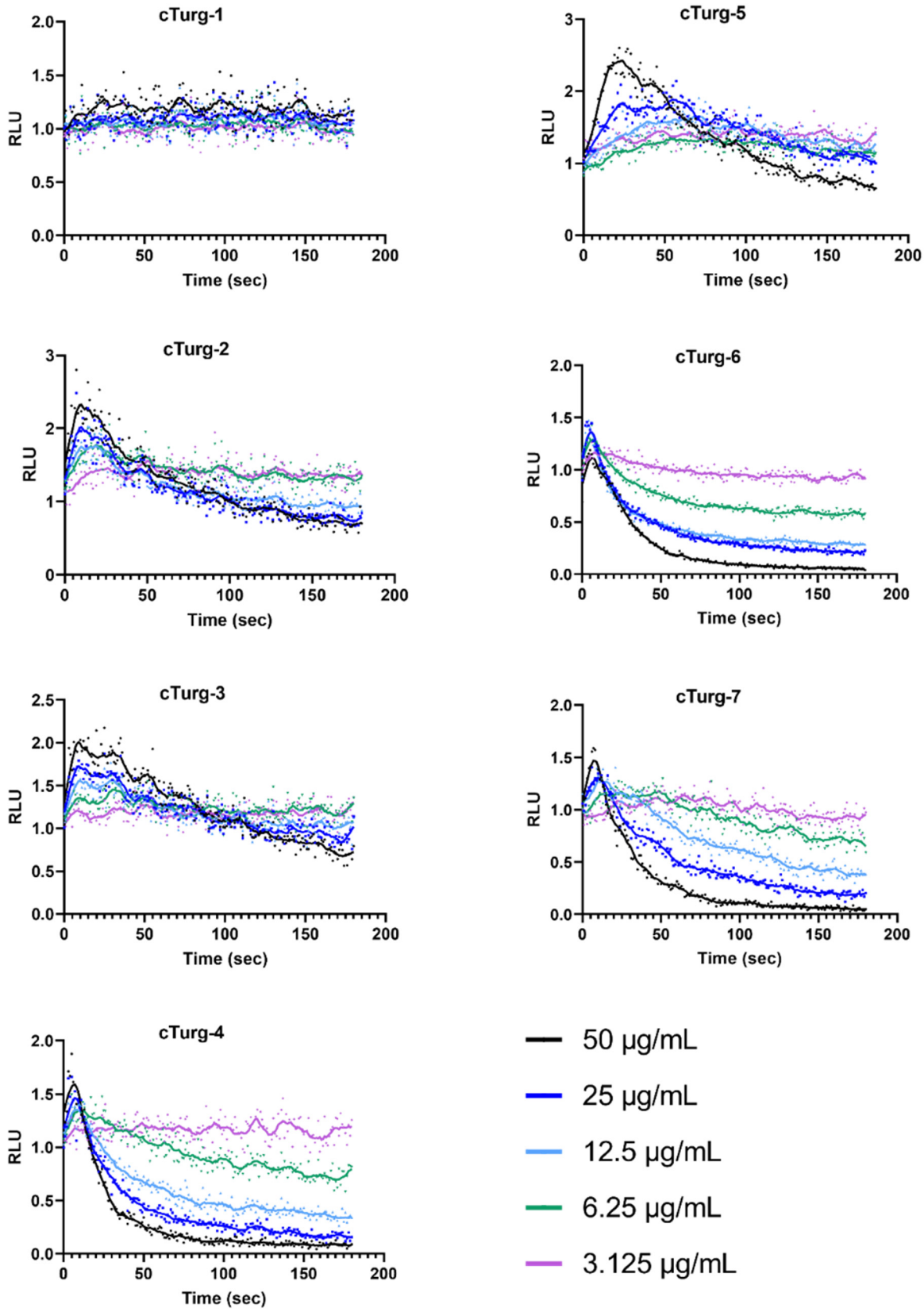

Figure S28. Kinetic of the effect on membrane integrity as measured by relative luminescence in *B. subtilis* (pCSS962) treated with different concentrations of **cTurg-1**, **cTurg-2**, **cTurg-3**, **cTurg-4**, **cTurg-5**, **cTurg-6** and **cTurg-7**.

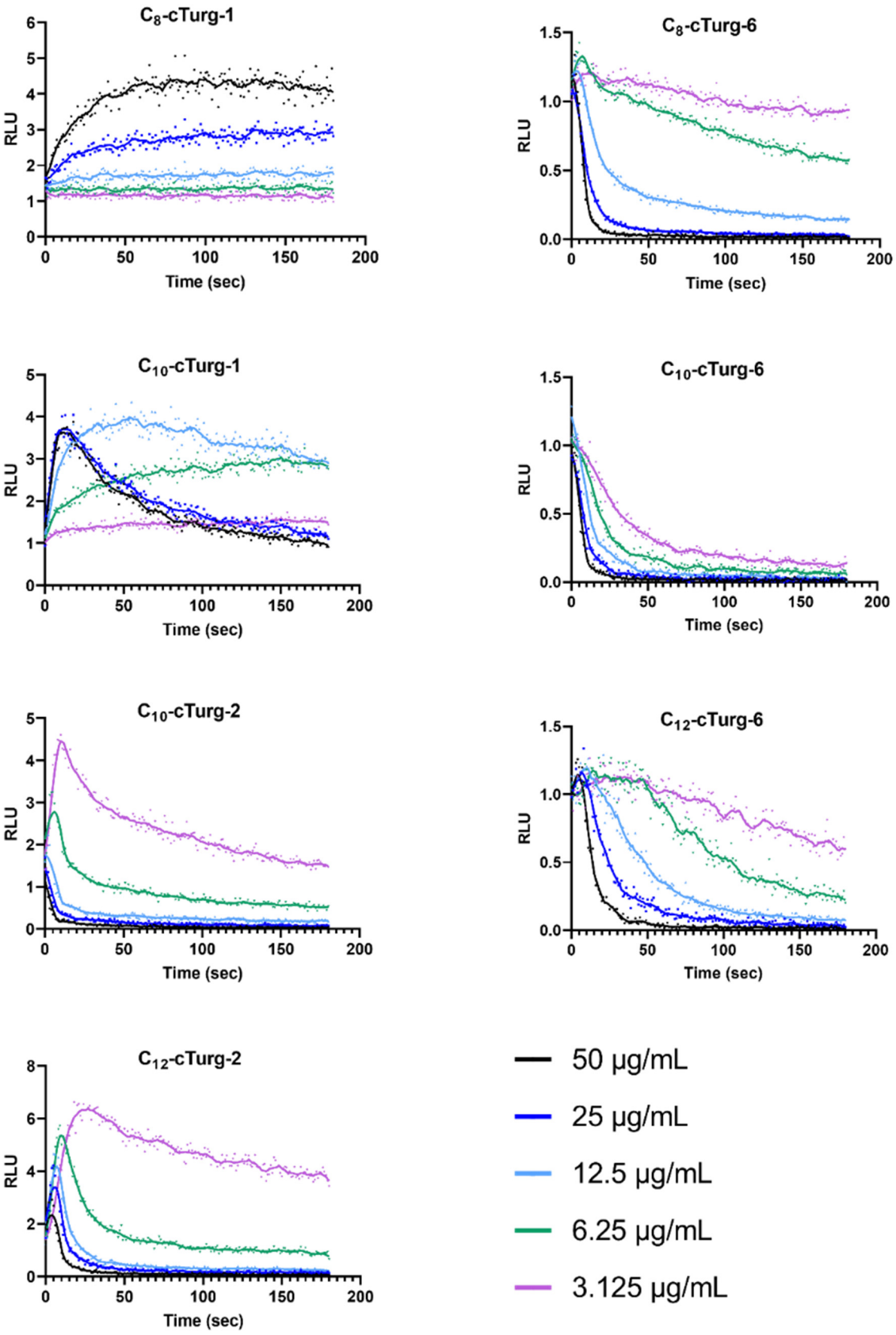

Figure S29. Kinetic of the effect on membrane integrity as measured by relative luminescence in *B. subtilis* (pCSS962) treated with different concentrations of **C8-cTurg-1**, **C10-cTurg-1**, **C10-cTurg-2**, **C12-cTurg-2**, **C8-cTurg-6**, **C10-cTurg-6**, and **C12-cTurg-6**.

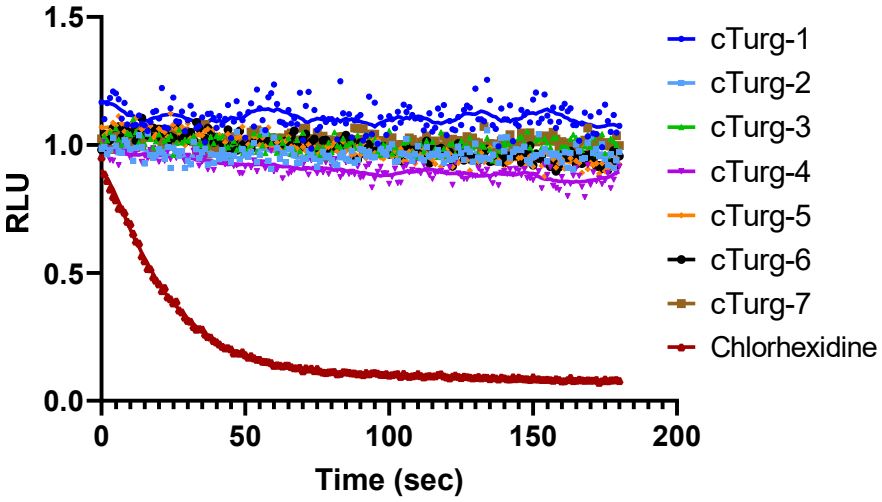

Figure S30. Kinetic of the effect on viability as measured by relative luminescence in *E. coli* (pCGLS-11) treated with 50 μg/mL of **cTurg-1-7** or 25 μg/mL of **chlorhexidine**.

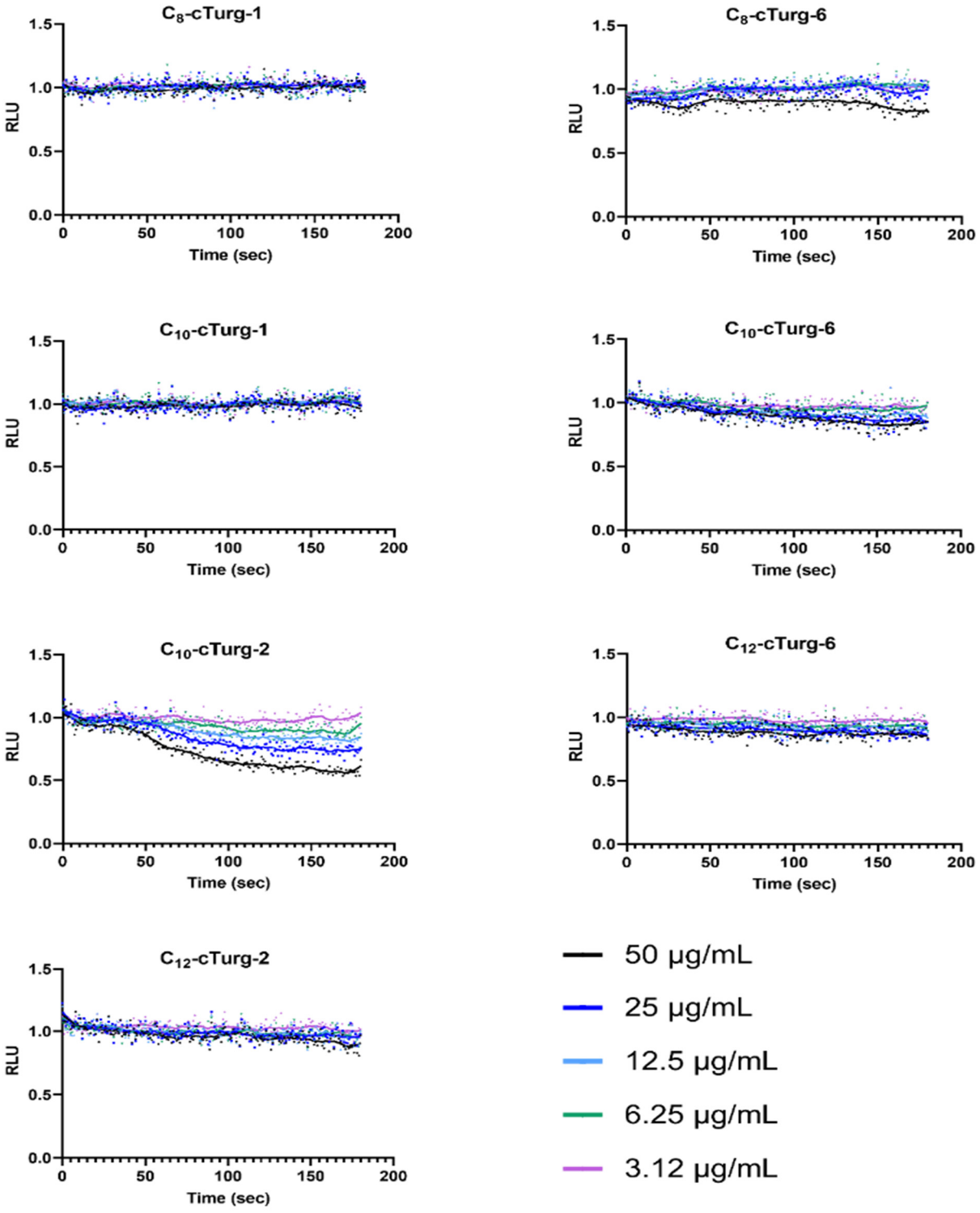

Figure S31. Kinetic of the effect on viability as measured by relative luminescence in *E. coli* (pCGLS-11) treated with different concentrations of **C8-cTurg-1**, **C10-cTurg-1**, **C10-cTurg-2**, **C12-cTurg-2**, **C8-cTurg-6**, **C10-cTurg-6**, and **C12-cTurg-6**.

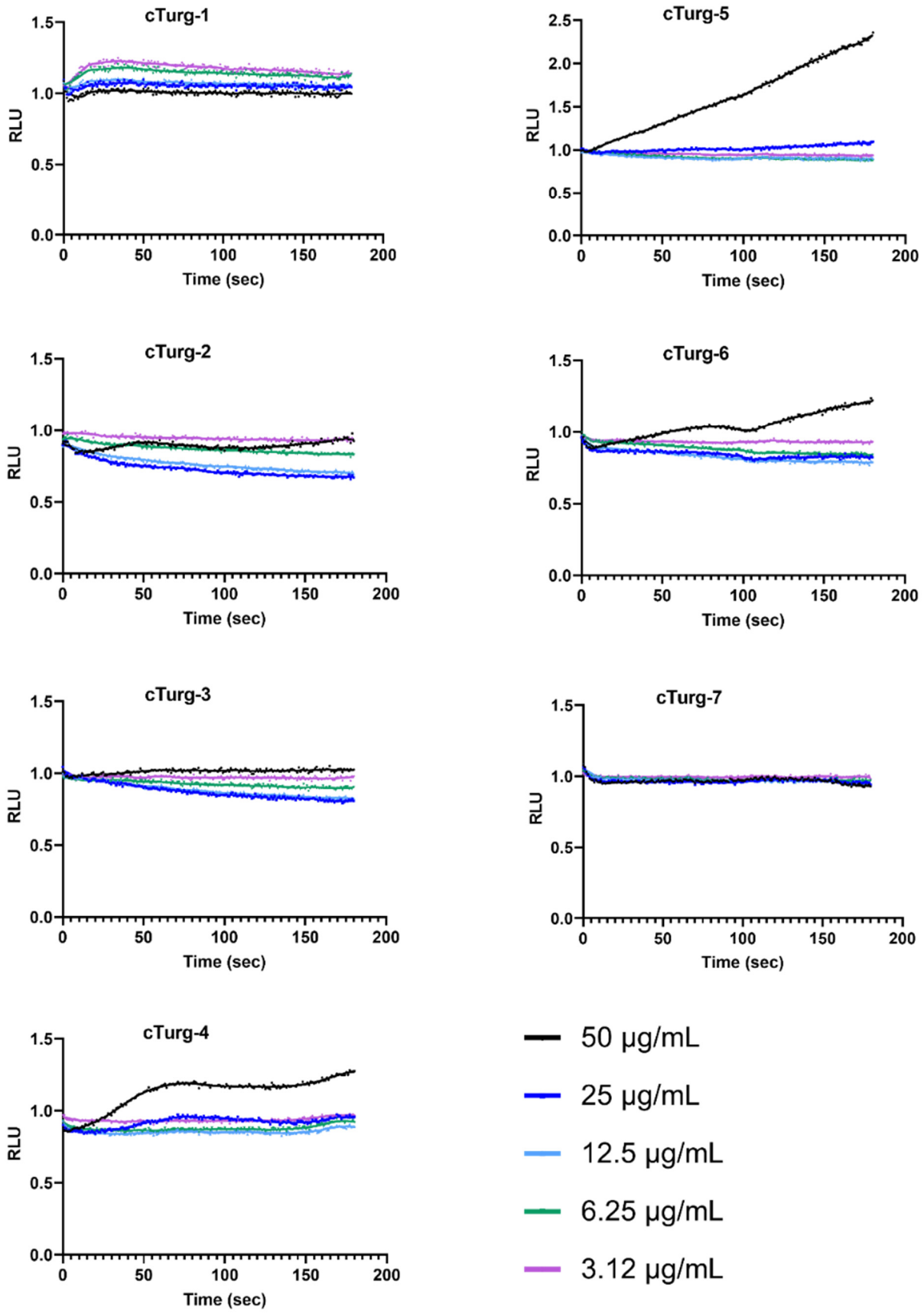

Figure S32. Kinetic of the effect on membrane integrity as measured by relative luminescence in *E. coli* (pCSS962) treated with different concentrations of cyclic peptides **cTurg-1**, **cTurg-2**, **cTurg-3**, **cTurg-4**, **cTurg-5**, **cTurg-6** and **cTurg-7**.

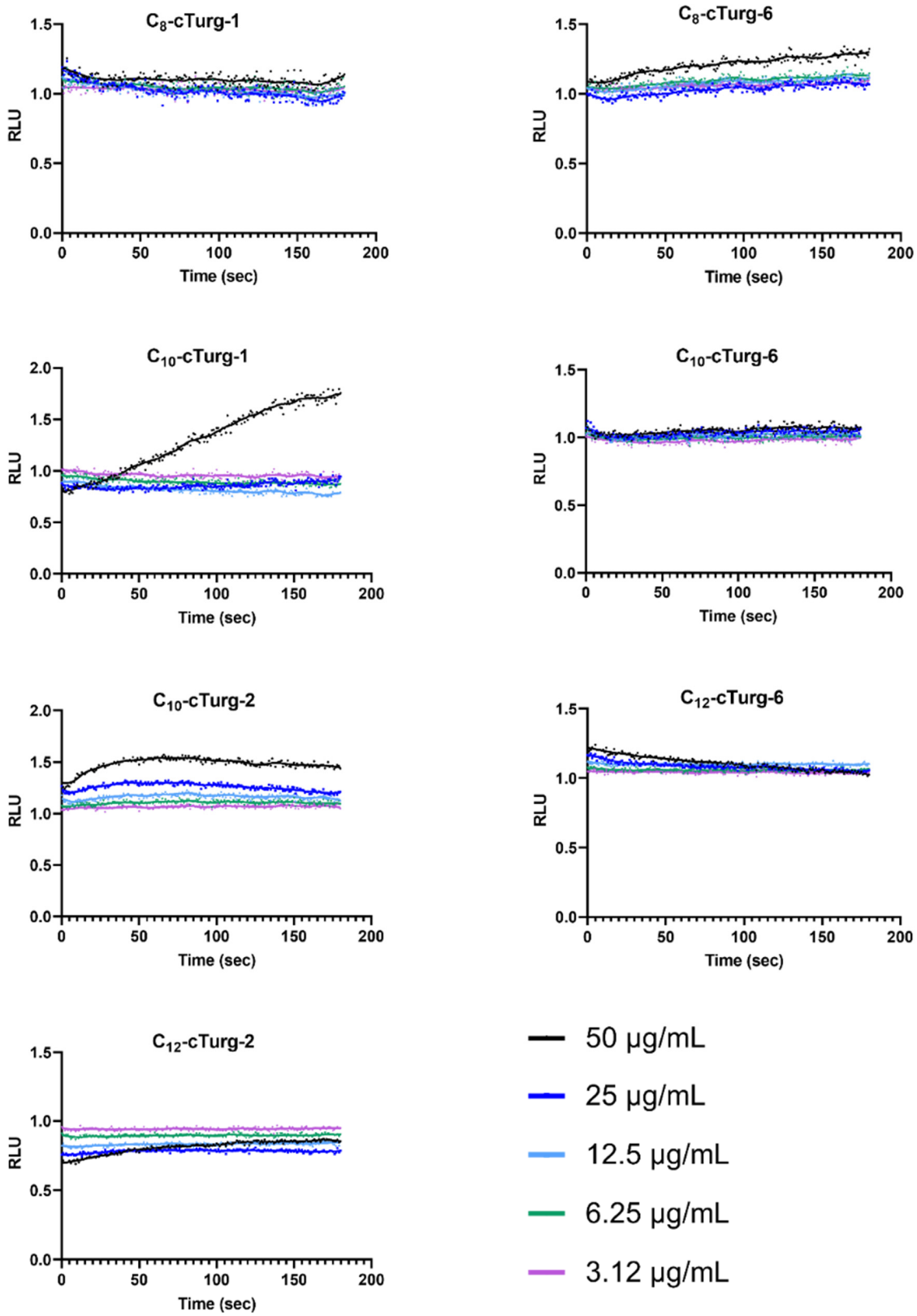

Figure S33. Kinetic of the effect on membrane integrity as measured by relative luminescence in *E. coli* (pCSS962) treated with different concentrations of **C_8-cTurg-1**, **C_{10}-cTurg-1**, **C_{10}-cTurg-2**, **C_{12}-cTurg-2**, **C_8-cTurg-6**, **C_{10}-cTurg-6**, **and C_{12}-cTurg-6**.

Table S1. Theoretical and measured monoisotopic mass (Da), and theoretical and observed m/z ions during HRMS of the synthesised peptides.

	Monoisotopic mass (Da)		$[M+2H]^{2+}$		$[M+3H]^{3+}$		$[M+4H]^{4+}$	
Peptide	Theoretical	Measured	Theoretical	Measured	Theoretical	Measured	Theoretical	Measured
cTurg-1	1300.6897	1300.6915	651.3521	651.3525	434.5705	434.5713	326.1797	326.1803
cTurg-2	1518.7741	1518.7746	760.3943	760.3944	507.2653	507.2656	380.7008	380.7009
cTurg-3	1518.7741	1518.7746	760.3943	760.3944	507.2653	507.2656	380.7008	380.7009
cTurg-4	1558.8054	1558.8061	780.4100	780.4102	520.6091	520.6094	390.7086	390.7088
cTurg-5	1630.7986	1630.7993	816.4066	816.4068	544.6068	544.6071	408.7069	408.7071
cTurg-6	1630.7987	1630.7999	816.4066	816.4068	544.6068	544.6073	408.7069	408.7074
cTurg-7	1670.8299	1670.8308	836.4222	836.4222	557.9506	557.9509	418.7148	418.7152
C_8-Turg-1	1428.8098	1428.8104	715.4122	715.4123	477.2772	477.2775	358.2097	358.2099
C_{10}-Turg-1	1456.8411	1456.8415	729.4278	729.4279	486.6210	486.6211	365.2176	365.2177
C_{12}-Turg-1	1484.8724	1484.8732	743.4435	743.4437	495.9647	495.9651	372.2254	372.2256
C_8-Turg-2	1646.8942	1646.8950	824.4544	824.4544	549.9720	549.9724	412.7308	412.7311
C_{10}-Turg-2	1674.9255	1674.9254	838.4700	838.4695	559.3158	559.3158	419.7387	419.7388
C_{12}-Turg-2	1702.9568	1702.9566	852.4857	852.4851	568.6595	568.6597	426.7465	426.7465
C_8-Turg-6	1758.9188	1758.9195	880.4667	880.4666	587.3135	587.3139	440.7370	440.7373
C_{10}-Turg-6	1786.9501	1786.9515	894.4823	894.4827	596.6573	596.6579	447.7448	447.7452
C_{12}-Turg-6	1814.9814	1814.9829	908.4980	908.4981	606.0011	606.0019	454.7526	454.7531
C_8-cTurg-1	1426.7941	1426.7948	714.4043	714.4045	476.6053	476.6056	357.7058	357.7060
C_{10}-cTurg-1	1454.8254	1454.8257	728.4200	728.4200	485.9491	485.9493	364.7136	364.7137
C_{12}-cTurg-1	1482.8567	1482.8573	742.4356	742.4358	495.2928	495.2931	371.7215	371.7216
C_8-cTurg-2	1644.8785	1644.8805	823.4465	823.4470	549.3001	549.3013	412.2269	412.2273
C_{10}-cTurg-2	1672.9098	1672.9107	837.4622	837.4621	558.6439	558.6446	419.2347	419.2349
C_{12}-cTurg-2	1700.9411	1700.9422	851.4778	851.4775	567.9876	567.9888	426.2426	426.2427
C_8-cTurg-6	1756.9031	1756.9036	879.4588	879.4586	586.6416	586.6420	440.2331	440.2333
C_{10}-cTurg-6	1784.9344	1784.9351	893.4745	893.4743	595.9854	595.9860	447.2409	447.2411
C_{12}-cTurg-6	1812.9657	1812.9685	907.4901	907.4905	605.3292	605.3303	454.2487	454.2498

Table S2. Purity of synthesized peptides (%) and retention time (min), determined by UPLC using a reversed phase column.

Peptide	Sequence	Purity [%]	Retention time [min]
cTurg-1	cyclic	100.00	3.11
cTurg-2	cyclic	96.53	3.87
cTurg-3	cyclic	96.43	3.92
cTurg-4	cyclic	95.79	3.97
cTurg-5	cyclic	95.74	3.98
cTurg-6	cyclic	90.59	4.02
cTurg-7	cyclic	95.61	4.09
C_8-Turg-1	linear	99.16	4.38
C_{10}-Turg-1	linear	95.87	4.89
C_{12}-Turg-1	linear	96.01	5.44
C_8-Turg-2	linear	98.04	4.97
C_{10}-Turg-2	linear	96.40	5.41
C_{12}-Turg-2	linear	96.38	5.89
C_8-Turg-6	linear	95.04	5.07
C_{10}-Turg-6	linear	95.53	5.51
C_{12}-Turg-6	linear	95.16	5.98
C_8-cTurg-1	cyclic	92.83	4.27
C_{10}-cTurg-1	cyclic	91.51	4.74
C_{12}-cTurg-1	cyclic	93.36	5.22
C_8-cTurg-2	cyclic	96.32	4.70
C_{10}-cTurg-2	cyclic	91.79	5.11
C_{12}-cTurg-2	cyclic	95.32	5.55
C_8-cTurg-6	cyclic	94.15	4.85
C_{10}-cTurg-6	cyclic	93.65	5.28
C_{12}-cTurg-6	cyclic	92.52	5.72

Table S3. Selectivity index (SI) calculated as the ration between haemolytic activity (EC_{50}, in µg/mL) and the geometric mean (GM) of the MIC values (in µg/mL) against bacteria and fungi, i.e., SI = EC_{50} / GM. MIC >256 were set to 256 for bacteria, MIC >128 were set to 128 for fungi, and the values for the highest tested concentration was used for haemolytic activity when calculating the SI.

			GM of MIC				Selectivity index (SI)			
		Peptide	G+	G-	Tot. bact.[1]	Fungi	G+	G-	Tot. bact.	Fungi
Cyclic peptides		**cTurg-1**	128	256	161	64	nd[2]	nd	nd	nd
	W	**cTurg-2**	11	64	20	32	92	16	52	33
		cTurg-3	10	64	18	32	89	13	47	27
		cTurg-4	16	128	32	40	67	8	33	26
	R / W	**cTurg-5**	8	11	9	32	138	97	123	34
		cTurg-6	7	11	8	32	164	97	138	34
		cTurg-7	7	23	10	32	29	9	20	6
Linear lipopeptides		**C_8-Turg-1**	19	64	29	40	50	15	33	23
		C_{10}-Turg-1	7	23	10	25	142	42	95	38
		C_{12}-Turg-1	5	11	6	25	204	86	153	38
	W	**C_8-Turg-2**	7	16	9	40	29	12	22	5
		C_{10}-Turg-2	7	11	8	40	10	6	8	2
		C_{12}-Turg-2	11	23	14	40	5	2	4	1
	R / W	**C_8-Turg-6**	7	16	9	102	8	3	6	1
		C_{10}-Turg-6	16	45	23	102	1	0	1	0
		C_{12}-Turg-6	19	91	32	91	2	0	1	0
Cyclic lipopeptides		**C_8-cTurg-1**	16	64	25	32	59	15	37	29
		C_{10}-cTurg-1	4	16	6	20	239	60	151	47
		C_{12}-cTurg-1	3	8	4	20	77	27	55	11
	W	**C_8-cTurg-2**	3	6	4	13	155	78	123	35
		C_{10}-cTurg-2	3	8	5	32	32	13	24	3
		C_{12}-cTurg-2	7	16	9	40	5	2	4	1
	R / W	**C_8-cTurg-6**	5	11	6	51	6	3	5	1
		C_{10}-cTurg-6	6	16	8	51	3	1	2	0
		C_{12}-cTurg-6	10	32	14	81	1	0	1	0

[1] GM of all bacterial test strains, [2] nd: not determined.

Paper II

Antimicrobial activity of short analogues of the marine peptide EeCentrocin 1: Synthesis of lipopeptides and head-to-tail cyclic peptides

Danijela Simonovic[1#], Hymonti Dey[2#], Natascha Johansen[1], Trude Anderssen[1], Hege Devold[2], Terje Vasskog[1], Hans-Matti Blencke[2], Elizabeth G. Aarag Fredheim[1], Tor Haug[2*], Morten B. Strøm[1*]

[1] Department of Pharmacy, Faculty of Health Sciences, UiT the Arctic University of Norway, NO-9037 Tromsø, NORWAY.

[2] The Norwegian College of Fishery Science, Faculty of Biosciences, Fisheries and Economics, UiT the Arctic University of Norway, NO-9037 Tromsø, NORWAY.

[#] Authors contributed equally.

* Corresponding authors. Correspondence: tor.haug@uit.no and morten.strom@uit.no

ABSTRACT

Keywords:
Antifungal peptides
Antimicrobial peptides
EeCentrocin 1
Head to tail cyclization
Lipopeptides
Pseudo-dilution cyclization

We have synthesised a series of 12-residue analogues of a previously reported lead peptide (**P6**) developed from the heavy chain of the marine peptide EeCentrocin 1, isolated from the sea urchin *Echinus esculentus*. We have explored ways to optimise the lead peptide by increasing its net positive charge, its lipophilicity through *N*-terminal fatty acid acylation or incorporation of a Trp residue, and by synthesising head-to-tail cyclic peptides under *pseudo-high dilution* conditions. All peptides were screened for antimicrobial and antifungal activity, and toxicity was determined against human red blood cells. The two most potent peptide analogues were the linear peptide **P6-W6R8** and its head-to-tail cyclic analogue **cP6-W6R8** displaying minimum inhibitory concentrations of 0.4 – 6.6 µM against Gram-positive and Gram-negative bacteria, and 6.2 – 13 µM against fungi. All peptides were non-haemolytic (EC_{50} > 500 µM) except for two of the lipopeptides, in which haemolytic toxicity correlated with increasing acyl chain length. Mode of action studies using bacterial biosensor strains revealed a membrane disruptive effect for both the linear and cyclic peptides. The results of our study demonstrated that relatively simple structural modifications could be successfully employed in the development of potent antimicrobial lead peptides derived from marine natural products.

(GRAPHICAL ABSTRACT):

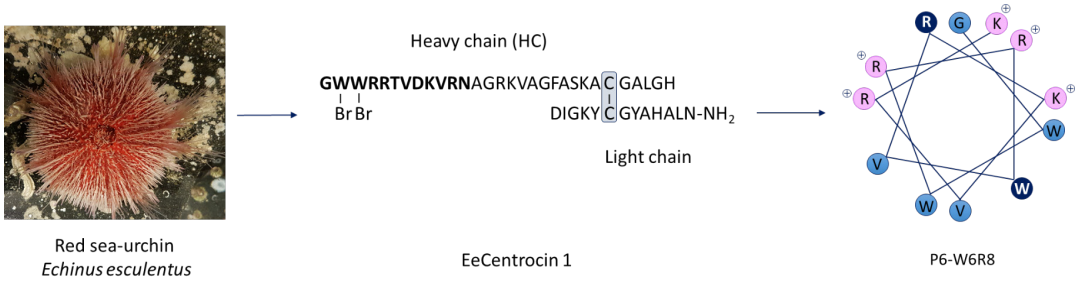

1. Introduction

The antimicrobial peptide EeCentrocin 1, isolated from the marine sea urchin *Echinus esculentus,* consists of a hetero-dimeric structure with a heavy chain (HC) essential for antimicrobial activity. (**Figure 1**) (1) To obtain a shorter *lead peptide* derived from the HC of EeCentrocin 1, a recent study explored several modifications, namely peptide truncation, substitution of the 6-bromo-Trp residues in positions 2 and 3 of the natural HC with Trp, and an alanine scan replacement strategy performed on shorter analogues of the HC. (2) The EeCentrocin 1 HC was in this way successfully truncated and modified resulting in the highly potent peptide **P6.** (**Figure 1**)

The peptide **P6** consists of the 12 *N*-terminal amino acid residues of the original *EeCentrocin 1* HC sequence and it is further modified by two amino acid replacements, Asp^8 → Ala^8 and Asn^{12} → Lys^{12}, as well as *C*-terminal amidation. The orientation of the hydrophilic and hydrophobic amino acid residues, as demonstrated by an α-helical wheel plot, indicates its amphiphilic character. (**Figure 1**) The peptide **P6** is non-haemolytic, with minimal inhibitory concentrations (MICs) against bacteria in the low micromolar range and a promising antifungal activity. (2)

In the present study we have investigated strategies to further optimise the potency of **P6** by increasing its net positive charge and lipophilicity, and by synthesising lipopeptide- and head-to-tail cyclic analogues. (**Figure 2**) The resulting peptides were screened for antimicrobial activity against the Gram-positive bacteria: *Bacillus subtilis*, *Corynebacterium glutamicum*, *Staphylococcus aureus* and *Staphylococcus epidermidis*, and the Gram-negative bacteria: *Escherichia coli* and *Pseudomonas aeruginosa*. Antifungal activity was determined against *Aureobasidium pullulans*, *Candida albicans* and *Rhodotorula* sp., whereas haemolytic activity was determined against human red blood cells (RBCs). Based on the antibacterial and haemolytic activities, the selectivity index of the peptides towards bacteria versus eukaryotic cells were calculated. Finally, mode of action studies using two bacterial biosensor strains (*B. subtilis* and *E. coli*) were performed.

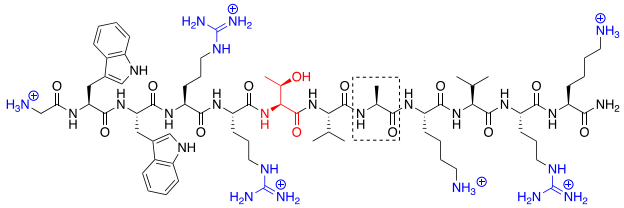

P6: Gly-Trp-Trp-Arg-Arg-Thr^{6}-Val-**Ala^{8}**-Lys-Val-Arg-Lys-NH$_2$

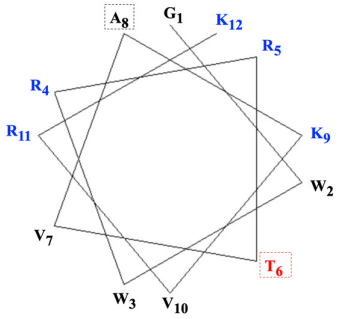

Figure 1. Structure (top) and α-helical wheel projection (bottom) of the lead peptide **P6**. The highlighted Thr^{6} residue in the α-helical lipophilic region and the Ala^{8} residue in the cationic region were both targets for the substitutions in the present study. (2)

2. Results and Discussion

2.1 Peptide Design and Synthesis

Our previously reported lead peptide **P6** is a potent antimicrobial peptide (AMP), and it is thought to adopt an amphiphilic structure upon interaction with negatively charged bacterial surfaces, as shown in an α-helix projection. (**Figure 1**) Apart from being non-haemolytic (EC_{50} >200 µM), it displayed MIC values in the low µM range (MIC: 0.9 – 28 µM) against both Gram-positive and Gram-negative bacteria, and MIC: 7 – 28 µM against fungi (**Table 1**).

The objective of the present study was to investigate if the antimicrobial potency of the lead peptide **P6** could be further improved by utilising various peptide modification strategies. This was done either by increasing its overall net charge by Ala^{8} to Lys^{8}/Arg^{8} substitution in the α-helical cationic region, or its lipophilicity by Thr^{6} to Trp^{6} substitution in the α-helical lipophilic region. In addition, we wanted to explore the effects on antimicrobial activity of acylated and head-to-tail cyclic analogues. All peptides were synthesised by Fmoc solid phase peptide synthesis (Fmoc-SPPS) on either a Rink amide ChemMatrix resin, for *N*-terminally amidated peptides, or on a preloaded 2-chlorotrityl resin for the synthesis of cyclic peptides. Head-to-tail cyclisation was performed using a modified *pseudo-high dilution* procedure reported by Malesevic *et al*. (3) Mass and purity measurements of the synthesised peptides can be found in the Supporting information, **Figures S1-S12** and **Tables S1-S2**.

A) Peptide **P6-W6R8** with increased net charge and lipophilicity

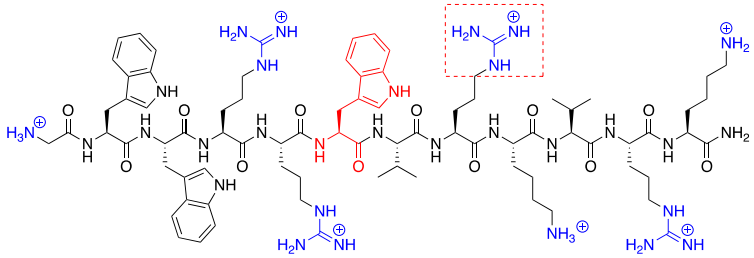

C) Cyclic peptide **cP6-W6R8**

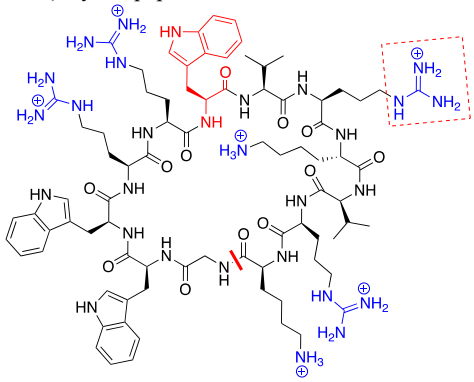

B) Lipopeptide **C$_8$-P6-R8**

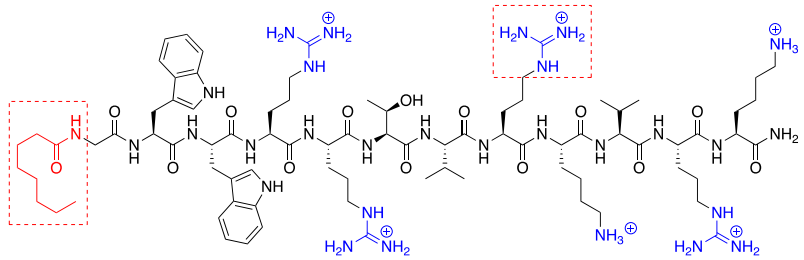

D) Cyclic peptide **cP6-W4R6,8**

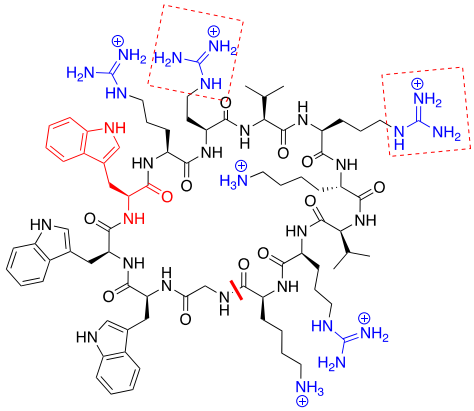

Figure 2. Optimisation strategies investigated for the antimicrobial *lead peptide* **P6**. A) Substitution of Ala^{8} with Lys^{8} or Arg^{8} (Arg^{8} marked with a red square) in the cationic region of the **P6**-amphiphilic α-helix, and subsequent Thr^{6}→Trp^{6} (residue in red) substitution in the lipophilic region of the **P6**-amphiphilic α-helix (shown is **P6-W6R8**). B) Synthesis of lipopeptides by *N*-terminal acylation with octanoic acid (shown is **C$_8$-P6R8**), decanoic acid, and dodecanoic acid. C) Head-to-tail cyclisation of a **P6** analogue (shown is **cP6-W6R8**). D) Formation of a compact lipophilic section in a head-to-tail cyclic **P6** analogue with three consecutive Trp residues (shown is **cP6-W4R6,8**). The red line shows the site of *head-to-tail* cyclisation in C) and D).

2.2 Antimicrobial Activity of Linear Peptides with Increased Net Charge and Lipophilicity

Our first strategy was to increase the net positive charge of **P6** by replacing the Ala^8 residue located in the α-helical cationic region with Lys^8, and subsequently with Arg^8. (**Figure 1** and **Table 1**) While both resulting peptides, **P6-K8** and **P6-R8** showed similar antimicrobial activity as observed for **P6**, the Arg modified peptide **P6-R8** displayed two-fold improvement in antimicrobial activity against *S. aureus.* (**Table 1**) Thus, increasing the net charge from +6 to +7 via Ala^8 to Arg^8 substitution had the greatest impact on antimicrobial activity against *S. aureus*. The observed difference in activity may be due to more favourable electrostatic and H-bond interactions between the guanidine group of Arg^8 and the bacterial membrane, as opposed to those mediated by the amino group of Lys^8.

Next, we wanted to optimise the amphipathicity of these peptides by replacing the Thr^6 residue with Trp^6 in the α-helical lipophilic region. The resulting peptides, **P6-W6K8** and **P6-W6R8** were twice as potent as their Thr-analogues against *P. aeruginosa.* A similar improvement in antimicrobial activity was also observed against *S. epidermidis* and *E. coli* for the Trp^6/Arg^8 modified peptide **P6-W6R8**. Although major improvement in antimicrobial activity of the already potent lead peptide **P6** was hard to achieve, **P6-W6R8** showed how two strategic amino acid substitutions aimed at increasing overall amphipathicity, resulted in a peptide having superior antimicrobial activity in the very low μM range (MIC: 0.8–1.6 μM) against tested Gram-positive and Gram-negative bacteria. (**Table 1**) Moreover, none of the synthesised peptides displayed any measurable haemolytic activity (EC_{50}: >500 μM).

2.3 Antimicrobial Activity of Lipopeptide Analogues

We further wanted to investigate the effects of *N*-terminal acylation with different aliphatic acyl chains on antimicrobial activity and haemolytic toxicity. The peptide **P6-R8** was selected for the *N*-acylation experiments since it was more potent than its lysine analogue, **P6-K8**. As the optimal chain length was found to be between eight and twelve carbon atoms,(C_8 to C_{12}), *N*-terminal acylation of **P6-R8** was performed with three aliphatic fatty acids: octanoic acid (C_8), decanoic acid (C_{10}) and dodecanoic acid (C_{12}), resulting in the following lipopeptides: **C_8-P6-R8**, **C_{10}-P6-R8** and **C_{12}-P6-R8.** (**Table 1**) (4) The lipopeptide with shortest acyl chain, **C_8-P6-R8** showed highest antimicrobial activity with MIC of 1.6 μM against all tested Gram-positive strains. It was, however, less potent against *E. coli* (MIC: 6.4 μM) compared to the lipopeptide analogues **C_{10}-P6-R8** and **C_{12}-P6-R8** (MIC: 3.2 μM). A peculiarity was the dramatic increase in haemolytic activity by the stepwise C_2-elongation of the acyl chain in **P6-R8**; starting from **C_8-P6-R8** that was non-haemolytic (EC_{50}: >500 μM), with **C_{10}-P6-R8** causing significant haemolysis (EC_{50}: 173 μM) and ending with the highly haemolytic peptide **C_{12}-P6-R8** (EC_{50}: 26 μM). Thus, *N*-terminal acylation with increasingly longer fatty acids had a greater impact on haemolytic activity than on the antimicrobial activity of the lipopeptides. However, compared to the previous peptides, introducing the Trp^6 residue in **P6-R8** to give **P6-W6R8,** was more beneficial than *N*-terminal acylation, as it resulted in a more potent, non-haemolytic peptide.

2.4 Antimicrobial Activity of Head-to-Tail Cyclic Peptides

Our final investigations involved studying the effects of head-to-tail cyclisation of selected linear peptides on their antimicrobial and haemolytic activity. This modification eliminates an *N*-terminal cationic amino group, thereby reducing the overall positive charge of the cyclised peptide by one unit. Furthermore, head-to-tail cyclisation is most likely to destroy any putative α-helical conformation in the linear **P6** analogues by increasing rigidity and forming a totally new structural arrangement. As described in the methods section, cyclisation was performed by means of a *pseudo-high dilution* method using two syringes and a mechanical pump. (**Figure 3**) (3) This setup allowed for a very slow addition (0.01 mL/min) of the linear protected peptide (contained in syringe 1) and a coupling reagent (contained in syringe 2), thereby creating *pseudo-high dilution* conditions. The method worked nicely in our hands and required relatively low amount of solvent (30 mL DMF in total for cyclisation of 100 μmol of linear protected peptides). (5) Also, no dimers or polymers of the peptides were isolated after the head-to-tail cyclisation procedures. The total percent yield for the cyclised peptides shown in **Table 1** ranged from 9.8% to 14.5%.

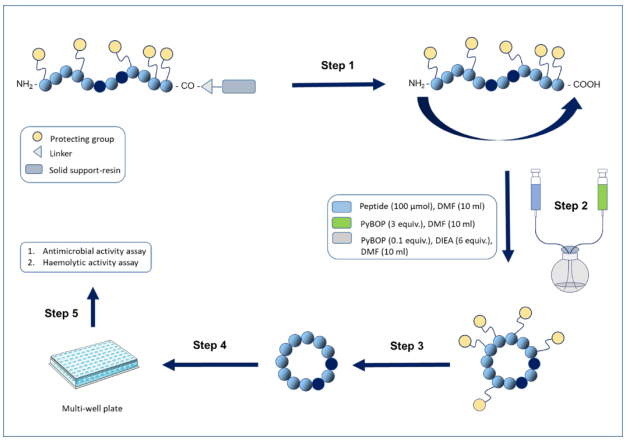

Figure 3. Strategy for preparing head-to-tail cyclic peptides using two syringes attached to a mechanical pump for creating *pseudo-high dilution conditions.*(3) Step 1: Fmoc-SPPS synthesis using a preloaded 2-Cl-Trt resin and subsequent cleavage from the resin with HFIP/DCM. Step 2: Head-to-tail cyclisation. Step 3: Deprotection of side chain protecting groups. Step 4: RP-HPLC peptide purification. Step 5: Bioactivity screening.

To optimise an amphiphilic cyclic structure (**Figure 2**), we synthesised head-to-tail cyclic peptide analogues (given in parentheses) of the starting lead peptide **P6** (**cP6**), the Arg^8 modified peptide **P6-R8** (**cP6-R8**), the highly potent Trp^6/Arg^8 modified peptide **P6-W6R8** (**cP6-W6R8**), and an analogue of the latter peptide with three consecutive Trp residues (**cP6-W4R6,8**). Our results showed that the cyclic peptide **cP6** had two- to 17-fold reduced antimicrobial activity compared to the linear lead peptide **P6** (**Table 1**), except against *C. glutamicum*. The most dramatic decrease in activity was observed against *P. aeruginosa*. This suggested that cyclisation, and thereby the reduction in overall positive charge of the peptide, along with the loss of a putative amphiphilic α-helical structure, might have

contributed to the observed reduction in antimicrobial activity.

By substituting Ala^8 for Arg^8 in **cP6**, we wanted to investigate the effect increased net charge could have on antimicrobial activity. The resultant cyclic peptide **cP6-R8** (net charge +6), was more effective against all tested strains compared to **cP6** (net charge +5), with the greatest activity observed against *C. glutamicum* (MIC: 0.1 μM), followed by *B. subtilis* (MIC: 1.7 μM) and *S. epidermidis* (MIC: 1.7 μM). Moreover, the greatest improvement in antimicrobial activity was observed for **cP6-R8** against *S. aureus*. Compared to its linear analogue **P6-R8** (+7), the cyclic peptide **cP6-R8** (+6) was almost equally effective in inhibiting the growth of *S. aureus* (MIC: 6.8 μM), *S. epidermidis* (MIC: 1.7 μM) and *E. c*oli (MIC: 3.4 μM). Against *B. subtilis* **cP6-R8** showed a small decrease in activity compared to **P6-R8**, whereas a more dramatic loss of antimicrobial activity was observed against *P. aeruginosa* (MIC 55 μM for **cP6-R8** compared to MIC: 3.2 μM for **P6-R8**). (**Table 1**)

Increasing the lipophilicity by replacing Thr^6 with Trp^6 to give **cP6-W6R8** (**Figure 3**) greatly improved antimicrobial activity compared to **cP6**, with MIC values in the range of 0.4 to 1.6 μM against Gram-positive bacteria and 3.3 to 6.6 μM against Gram-negative bacteria. Compared to its linear analogue **P6-W6R8**, the cyclic peptide **cP6-W6R8** displayed improved potency against *B. subtilis* and *C. glutamicum*, while being equally effective against *S. epidermidis*. Somewhat reduced antimicrobial activity was obtained for **cP6-W6R8** against the Gram-negative strains *E. coli* (MIC: 6.6 μM) and *P. aeruginosa* (MIC: 3.3 μM).

Finally, by switching the positions of Arg^4 and Trp^6 in **cP6-W6R8**, we synthesised a more amphiphilic cyclic analogue **cP6-W4R6,8.** (**Figure 2**) The antimicrobial activity of the resultant peptide **cP6-W4R6,8** remained unchanged against *B. subtilis* and improved 2-fold against *E. coli* compared to **cP6-W6R8** but was in general reduced 2-fold against the other four bacterial strains: *C. glutamicum*, *S. aureus*, *S. epidermidis* and *P. aeruginosa*. Although significance of having the WWW motif positioned at the *N*-terminus for the antimicrobial and biofilm activity of the linear Trp-rich peptide was reported by Zarena *et al.,* our results showed that having three adjacent Trp residues in a cyclic peptide, as in **cP6-W4R6,8**, did not cause additional increase in overall potency. (6)

The strategy of head-to-tail cyclisation revealed that additional sequence optimisations were required to achieve antimicrobial activity in the same μM range as for the linear lead peptide **P6**. Previous research has shown that head-to-tail cyclisation could be effectively used as a tool for reducing haemolysis. (7, 8) However, as both the linear peptides and their cyclic analogues were non-haemolytic, this improvement (if present) was not observed. Apart from few exceptions, cyclisation in this study mainly led to 2-fold decrease in antimicrobial activity against tested bacterial strains. It may be that structural constraints conferred by cyclisation, as well as reduction in charge, could have acted unfavourably on the peptide-membrane interactions.

All peptides showed high selectivity for bacteria compared to human RBCs except for two of the linear lipopeptides (**C_{10}-P6-R8** and **C_{12}-P6-R8**).

A selectivity index (SI) was calculated as the ratio between haemolytic activity (EC_{50}) and the geometric mean (GM) of the MIC values against all bacterial strains, i.e., SI = EC_{50}/GM. When considering the GM, the two most potent and selective peptides could be identified as **P6-W6R8** and its cyclic analogue **cP6-W6R8**, both having a GM of 1.3–1.4 μM and SI > 347. For these two peptides, as our results suggested, the amino acid sequence had much greater influence on antimicrobial activity than a linear vs. cyclic structure. Nevertheless, both peptides are considered amphiphilic, which is most likely to have contributed to their favourable antimicrobial profile. (**Figure 1** and **Figure 2)**

2.5 Antifungal Activity

All synthesised peptides were screened for antifungal activity against *A. pullulans, C. albicans*, and *Rhodotorula* sp., out of which *C. albicans* is of greatest medical importance. *A. pullulans* and the *Rhodotorula* sp. can, however, cause severe infections in immunocompromised patients and were included in this work for structure-activity relationship purpose. (**Table 1**) (9-11) Previous studies have shown that the EeCentrocin 1 HC peptide had a negligible inhibitory effect against *C. albicans* (MIC: 100 μM) while being active against *Rhodotorula* sp. (MIC: 12.5 μM). (1) The lead peptide **P6** displays, however, improved antifungal activity especially against *C. albicans* (MIC: 28 μM), and to a lesser degree against *Rhodotorula* sp. (MIC: 7.0 μM). (2) To our surprise there were only minor variations in antifungal activity with respect to differences in sequence and structure of the synthesised peptides in the present study. The linear peptides modified by either the Ala^8 to Lys^8/Arg^8 (**P6-K8** and **P6-R8**) and Thr^6 to Trp^6 substitutions (**P6-W6K8** and **P6-W6R8**) displayed (with one exception) similar antifungal activity against *A. pullulans* and *C. albicans* (MIC: 12-13 μM), but two-fold higher potency against *Rhodotorula* sp. (MIC: 6.2–6.5 μM). These analogues were overall more potent against fungi compared to **P6**.

The *N*-acylated **C_8-**, **C_{10}-** and **C_{12}-P6-R8** lipopeptides showed antifungal potency comparable to that of **P6** with MIC: 25-26 μM against *A. pullulans* and *C. albicans*, and MIC: 6.3-6.4 μM against *Rhodotorula* sp. Thus, no major variation in antifungal activity was observed by varying the acyl chain length of these lipopeptides.

The head-to-tail cyclic peptides were all equally potent against *A. pullulans* and *C. albicans* (MIC: 13–15 μM). Although still low, the antimicrobial activity of **cP6-R8**, **cP6-W6R8** and **cP6-W4R6,8** was higher against *Rhodotorula* sp., (MIC: 6.6–6.8 μM) than that of **cP6** (MIC: 15 μM). Head-to-tail cyclisation did not seem to have any major effect on antifungal activity since the potencies were comparable to those of their corresponding linear analogues. One exception was improved antifungal activity against *A. pullulans* and *C. albicans* for **cP6** compared to **P6**. However, the opposite effect was observed against *Rhodotorula* sp. in which **P6** was more potent than **cP6**. These findings highlight the need for further research with the aim of identifying the structural modifications necessary for improving the antifungal activity of these peptides.

Table 1. Antimicrobial activity of synthesised peptides against bacteria and fungi (MIC in μM), and toxicity against human RBC (EC_{50} in μM). Sequence modifications (amino acid replacements) compared to the lead peptide **P6** are shown in bold, and sequences in parentheses denote head-to-tail cyclic peptides. The selectivity index (SI) was calculated as the ratio between haemolytic activity (EC_{50}) and the geometric mean (GM) of the MIC values against all bacterial strains, i.e., SI = EC_{50}/GM.

	Peptide	Sequence	Mw[2]	Net Charge[3]	Rt[4]	Antimicrobial activity (MIC)[1]										Tox. (EC_{50})	SI
						Gram +				Gram -		GM	Fungi				
						Bs	Cg	Sa	Se	Ec	Pa		Ap	Ca	Rh	RBC	
Linear peptides	**P6**	GWWRRTVAKVRK-NH_2	1541.9	+6	3.32	0.9	0.9	28	1.8	3.5	3.5	2.8	28	28	7.0	>500	>177
	P6-K8	GWWRRTV**K**KVRK-NH_2	1599.0	+7	3.18	0.8	0.8	13	1.6	3.3	3.3	2.3	13	26	6.5	>500	>217
	P6-R8	GWWRRTV**R**KVRK-NH_2	1627.0	+7	3.20	0.8	0.8	6.4	1.6	3.2	3.2	2.0	13	13	6.4	>500	>248
	P6-W6K8	GWWRR**W**V**K**KVRK-NH_2	1684.1	+7	3.67	1.6	0.8	1.6	1.6	3.1	1.6	1.6	13	13	6.3	>500	>314
	P6-W6R8	GWWRR**W**V**R**KVRK-NH_2	1712.1	+7	3.61	1.6	0.8	1.6	0.8	1.6	1.6	1.3	12	12	6.2	>500	>394
Linear lipo-peptides	**C_8-P6-R8**	C_8-GWWRRTV**R**KVRK-NH_2	1753.2	+6	4.70	1.6	1.6	1.6	1.6	6.4	6.4	2.5	26	26	6.4	>500	>197
	C_{10}-P6-R8	C_{10}-GWWRRTV**R**KVRK-NH_2	1781.2	+6	5.16	3.2	3.2	3.2	1.6	3.2	6.3	3.2	25	26	6.3	173	54
	C_{12}-P6-R8	C_{12}-GWWRRTV**R**KVRK-NH_2	1809.3	+6	5.67	3.1	3.1	3.1	3.1	3.1	6.3	3.5	25	25	6.3	26	7
Cyclic peptides	**cP6**	c(GWWRRTV**A**KVRK)	1524.8	+5	3.36	1.9	0.9	60	15	7.5	60	9.4	15	15	15	>500	>53
	cP6-R8	c(GWWRRTV**R**KVRK)	1610.1	+6	3.20	1.7	0.1	6.8	1.7	3.4	55	2.7	14	14	6.8	>500	>187
	cP6-W6R8	c(GWWRR**W**V**R**KVRK)	1695.1	+6	3.76	0.8	0.4	1.6	0.8	6.6	3.3	1.4	13	13	6.6	>500	>347
	cP6-W4R6,8	c(GWW**W**R**R**V**R**KVRK)	1695.1	+6	3.62	0.8	0.8	3.3	1.6	3.3	6.6	2.0	13	13	6.6	>500	>244
	Oxytetracycline HCl		496.9			40	0.6	0.6	2.5	2.5	40	-[5]	-	-	-	-	-
	Polymyxin B sulfate		1189.3			0.7	0.3	5.3	2.6	0.7	1.3	-	2.6	11	1.3	-	-
	Triclosan		289.5			-	-	-	-	-	-	-	22	22	5.4	-	-

[1] Microbial strain; Bs – *Bacillus subtilis* (ATCC 23857), Cg – *Corynebacterium glutamicum* (ATCC 13032), Sa – *Staphylococcus aureus* (ATCC 9144), Se – *Staphylococcus epidermidis* RP62A (ATCC 35984), Ec – *Escherichia coli* (ATCC 25922), Pa – *Pseudomonas aeruginosa* (ATCC 27853), *Ap – Aureobasidium pullulans, Ca – Candida albicans* (ATCC 10231), *Rh – Rhodotorula* sp. [2] Average molecular mass of synthesised peptides, without including a TFA salt for each cationic charge. [3] Net charge at physiological pH (7.4). [4] Retention time (min) on RP-UPLC. ''-'': not calculated or tested.

2.6 Effects on Bacterial Viability and Membrane Integrity

Two luciferase-based biosensor assays (viability and membrane integrity) were used to investigate the mode of action of all synthesised linear and cyclic analogues on *B. subtilis* 168 and *E. coli* K12 biosensors. Bacterial luciferase is an excellent real-time sensor for bacterial viability, as endogenous production of the substrate pools, such as reduced flavin mononucleotide ($FMNH_2$) and long-chain aliphatic aldehydes, are responsible for the bioluminescence. A decrease in light production indicates loss of metabolic activity and viability. In contrast, in the membrane integrity assay the addition of exogenous substrate such as D-luciferin is required for light production by the eukaryotic luciferase gene (*LucGR*). Light emission will peak rapidly when the membrane integrity is compromised, enabling externally added substrate D-luciferin to pass through damaged membrane. The subsequent decrease in light production occurs while ATP from dying cells is consumed.

Here we present the results from the mode of actions studies of the linear peptide **P6-W6R8** and its cyclic analogue **cP6-W6R8**. The results for the remaining peptides can be found in the Supporting information, **Figures S13–S20**.

As shown in **Figure 4**, both **P6-W6R8** and **cP6-W6R8** clearly affected the viability of *B. subtilis* in a concentration-dependent manner. To further confirm that the rapid decrease in bacterial viability was caused by membrane damage, the membrane integrity assay was performed on the *B. subtilis* biosensor strain. **P6-W6R8** showed a membrane-related mode of action as light emission decreased rapidly at the two highest concentrations. In addition, for the lower concentrations a declining pattern in a dose-dependent manner was also observed. (**Figure 4**) For **cP6-W6R8**, a concentration dependent emission of light was observed, with a subsequent decline at higher concentrations. However, the effect was slightly delayed when compared to the linear peptide **P6-W6R8**. The membranolytic reference control chlorhexidine had a MIC value of 1.6 µg/mL (3.1 µM) against both *B. subtilis* and *E. coli*.

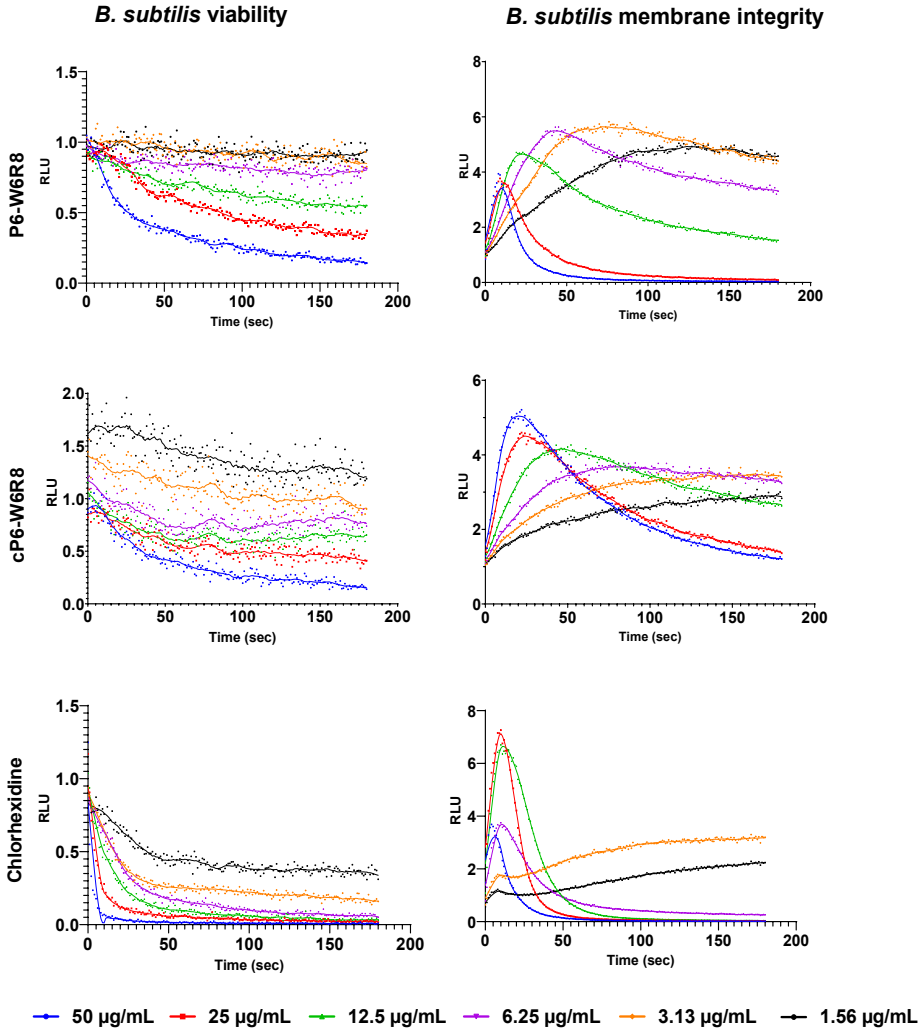

Figure 4. Immediate effects of **P6-W6R8**, **cP6-W6R8** and chlorhexidine (membranolytic control) on the kinetics of viability (left) and membrane integrity (right) in *B. subtilis* 168. Light emission normalised to the untreated water control is plotted as relative luminescence units (RLU) over time (seconds). All the graphs show a representative data set where each experiment was run at least three times independently.

While comparing the effects of **P6-W6R8** and **cP6-W6R8** on the viability and membrane integrity of the Gram-negative *E. coli*, we observed a somewhat different mode-of action. As shown in **Figure 5**, the decrease in light emission was substantially slower than that for similar concentrations in *B. subtilis*. The linear analogue **P6-W6R8** affected the membrane integrity of the *E. coli* strain and showed a concentration-dependent effect on viability. Although **cP6-W6R8** also affected the viability, a much less prominent inner membrane disruptive effect was observed as only concentrations at, or above MIC (≥12.5 µg/mL) gave rise in light emission. This might be due to its less antimicrobial activity or delayed action on the inner membrane of Gram-negative bacteria.

Results from both the membrane integrity and viability assay at concentrations below 3.13 µg/mL did not seem to reflect the MIC, as light emissions stayed unchanged throughout the assay period. However, these assays are conducted with 1000x higher bacterial concentrations than the MIC assay. In addition, the MIC assay integrates activity over a 24 h time frame, while the luminescence-based assays are only run for 3 min to elucidate immediate activity. At 50 µg/mL **cP6-W6R8** reduced viability by 35% within 3 min, while light emission from the membrane integrity assay stayed at 30x the control. Lower concentrations did not show such a strong membrane effect. This difference in light emission from the two assays is likely based on the different processes for light production. While the membrane assay is solely based on ATP as energy source and externally added D-luciferin, the viability assay integrates both ATP and reduction equivalents for light production and substrate regeneration. In this case the ATP pool does not seem to be limiting.

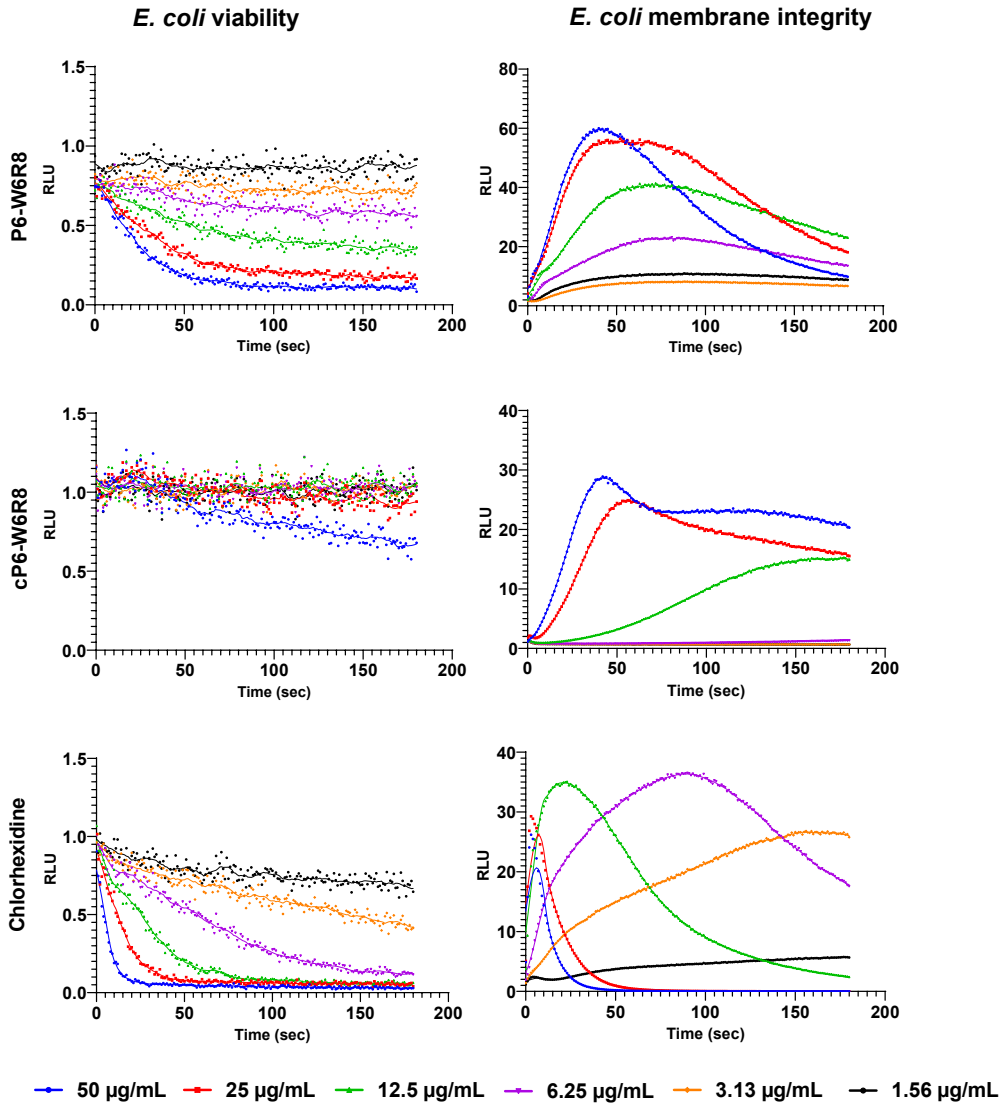

Figure 5. Immediate effects of **P6-W6R8**, **cP6-W6R8** and chlorhexidine (membranolytic control) on the kinetics of viability (left) and membrane integrity (right) in *E. coli* K12. Light emission normalised to the untreated water control is plotted as relative luminescence units (RLU) over time (seconds). All the graphs show a representative data set where each experiment was run at least three times independently.

2.7. Permeabilisation of the Outer Membrane of E. coli and P. aeruginosa

To investigate whether the delayed and reduced action on the membrane integrity might be due to the presence of the outer membrane of *E. coli* and *P. aeruginosa*, we utilised the outer membrane NPN assay. (12) The fluorescence of the lipophilic dye *N*-phenyl-1-napthylamine (NPN) can be utilised to investigate the ability of AMPs to permeabilise the outer membrane of Gram-negative bacteria. NPN emits weak fluorescence in aqueous environment and is highly fluorescent in hydrophobic environment found in lipidic membranes. NPN cannot insert into intact bacteria membranes, however, upon disruption of the outer membrane of Gram-negative bacteria by AMPs, NPN gains access to lipid layers in the outer membrane and/or in the cytoplasmic membrane and its fluorescence emission intensity increases. Both **P6-W6R8** and **cP6-W6R8** showed similar concentration-dependent increase in NPN fluorescence at concentrations from 1.56 to 25 µg/mL in *E. coli*, indicating a membrane permeabilising effect. (**Figure 6**) However, at lower concentrations, fluorescence intensities were comparatively lower for **cP6-W6R8** than for **P6-W6R8**. Similar effects were observed in *P. aeruginosa* for both **P6-W6R8** and **cP6-W6R8**. Even though both peptides displayed a membrane related (primary) mode of action, there is still possibilities that they have other mechanism at lower concentrations. It has been documented that certain cationic AMPs exhibit a concentration-dependent dual mode of action.(13, 14)

The reference control polymyxin B (PMB), a bactericidal peptide antibiotic known for its membrane disruptive properties, showed a MIC value of 0.78 µg/mL (0.7 µM) against *E. coli* and 1.56 µg/mL (1.3 µM) against *P. aeruginosa* (**Table 1**).

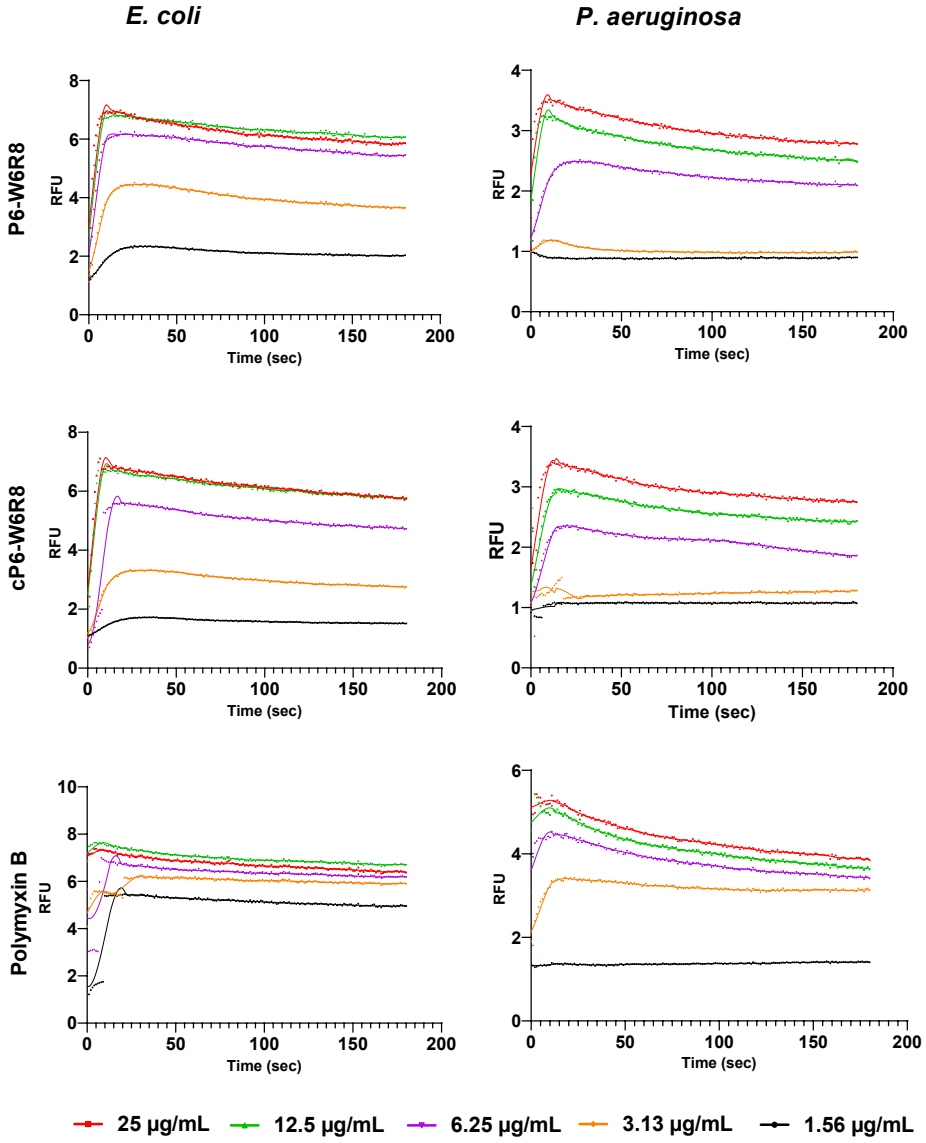

Figure 6. Comparison of the effects of **P6-W6R8**, **cP6-W6R8** and polymyxin B on the kinetics of NPN fluorescence in *E. coli* and *P. aeruginosa* strains. After addition of the bacterial inoculum (mixed with 20 µM NPN) to the wells (preloaded with lipopeptides), light emission was measured each second for 3 min. Each colored line represents the total 180 s data points from the assay at different concentrations. Each figure shows a representative data set.

3. Materials and Methods

3.1. Synthesis of Linear Peptides

Peptides were synthesised on a Biotage® Initiator+Alstra™ fully automated microwave assisted peptide synthesiser. All Fmoc-amino acids were purchased from Sigma-Aldrich. Solvents were purchased from either VWR chemicals or Sigma-Aldrich. Rink amide ChemMatrix resin was obtained from Biotage (Uppsala, Sweden).

Synthesis of the linear peptides and lipopeptides was accomplished by microwave (*mw*) assisted Fmoc solid phase peptide synthesis (Fmoc-SPPS) using Rink amide ChemMatrix resin (loading 0.50 mmol/g, scale 165 mmol). Fmoc-protected amino acids (4 equiv.) were coupled in the presence of O-(1H-6-Chlorobenzotriazole-1-yl)-1,1,3,3-tetramethyluronium-hexafluorophosphate (HCTU, 4 equiv.) and *N,N*-Diisopropylethylamine (DIEA, 8 equiv.) under *mw* irradiation at 70 °C, for 10 min, except for Fmoc-Arg(Pbf)-OH which was coupled at room temperature for 60 min. Prior to synthesis, all amino acids (0.5 M) were dissolved in *N,N*-dimethylformamide (DMF), whereas *N,N*-diisopropylethylamine (DIPEA, 2 M) was dissolved in *N*-methyl-2-pyrrolidone (NMP). A double coupling was used to ensure complete acylation of the *N*-terminal amino group with octanoic-, decanoic- and dodecanoic acid.

At each step the Fmoc group was deprotected with 20% piperidine in DMF. After the final step the resin was washed with dichloromethane (DCM) and diethyl ether and dried overnight in a desiccator. The peptide was then cleaved from the resin by two treatments of alternating washes with 10 mL trifluoracetic acid /water/triisopropylsilane (TFA:H_2O:TIS) 95:2.5:2.5 (v/v/v). The mixture was left at room temperature for 1 h with occasional stirring, followed by the second treatment lasting 2-3 h. After each treatment the resin was washed with DCM. The cleavage cocktail was removed by filtration under reduced pressure and the filtrates were combined.

Precipitation of the peptide was induced by dropwise addition of ice-cold diethyl ether to the crude product. The suspension was left overnight. The supernatant was removed the following day and the peptide pellet was resuspended in fresh diethyl ether. After diethyl ether was evaporated under reduced pressure, the final pellet was purified by reversed phase high performance liquid chromatography (RP-HPLC), and pooled fractions were freeze-dried to yield the pure peptide.

3.2. Head-to-Tail Cyclisation

For the synthesis of the cyclic peptides a preloaded H-Lys(Boc)-2-chlorotrityl resin NovaBiochem (0.75 mmol/g loading, scale 0.2 mmol) was used. Cleavage of the linear protected peptides from the resin was performed with a mixture of hexafluoropropanol-DCM (3:7, v/v, 15 mL).

Head-to-tail cyclisation was performed using a modified *microdilution* procedure previously described by Malesevic *et al*. (3) To maintain microdilution conditions during cyclisation two 10 mL syringes were used. First syringe contained linear protected tetrapeptide (1 eq., 100 µmol) predissolved in DMF (10 mL). The second syringe was filled with a solution containing (benzotriazol-1-yloxy)tripyrrolidinophosphonium hexafluorophosphate (PyBOP, 3 eq., 300 µmol) predissolved in DMF (10 mL). Both syringes were fixed to the dual-syringe programmable pump and the flow rate was set to 0.01 mL/min. This enabled simultaneous, dropwise addition of both solutions into the flask which initially contained DIEA (6 equiv., 600 µmol), PyBOP (0.1 equiv., 10 µmol) and DMF (10 mL). The reaction proceeded under constant stirring. After the cyclisation step, the reaction mixture was diluted with 5% LiCl (approx. 30 mL), prior to extraction with ethyl acetate (3 x 20 mL). The organic phase was washed with 5% LiCl solution (3 x 20 mL) and brine (1 x 20 mL), before drying over Na_2SO_4. The organic phase was filtered and concentrated under vacuum. Global deprotection was achieved using the same cleavage cocktail as previously described and following the same work-up procedure. In the final synthesis step the crude peptide was washed with diethyl ether (3 x 20 mL) and dried under vacuum prior to purification by RP-HPLC. Al peptides were >92% pure.

3.3 Antibacterial MIC Assay

All cyclic, linear and lipopeptide analogues of EeCentrocin peptides were screened for antibacterial activity against four Gram-positive strains; *B. subtilis* (Bs, ATCC 23857), *C. glutamicum* (Cg, ATCC 13032), *S. aureus* (Sa, ATCC 9144) and *S. epidermidis* RP62A (Se, ATCC 35984), and two Gram-negative strains; *E. coli* (Ec, ATCC 25922) and *P. aeruginosa* (Pa, ATCC 27853). A modified broth microdilution susceptibility assay, based on the CLSI M07-A9 protocol, was used to determine minimal inhibitory concentrations (MIC). (15) Briefly, overnight bacterial cultures were grown in Mueller-Hinton (MH) media (Difco Laboratories, USA) for 2 hours at room temperature. The bacterial inoculum was diluted to 2.5 - 3 x 10^4 cells/mL in MH medium and added in 96-well plates (Nunc, Roskilde, Denmark) preloaded with two-fold dilution series of peptide solutions in a ratio of 1:1 giving a final well volume of 100 µL. The microplates were incubated in an EnVision 2103 microplate reader (PerkinElmer, Llantrisant, UK) at 35 °C, with OD_{595} recorded every hour for 24 h. The minimal inhibitory concentration (MIC) value was defined as the lowest concentration of peptides showing an optical density less than 10% of the negative (growth) control, consisting of bacteria and MiliQ-water. Polymyxin B sulfate and Oxytetracycline HCl (both from Sigma-Aldrich, St. Louis, MO, USA) served as positive (growth inhibition) controls. All peptides were tested in three technical replicates.

3.4. Antifungal MIC Assay

The synthesised peptides were screened for antifungal activity against the molds *A. pullulans* (Ap) and *Rhodotorula* sp. (Rh) (both obtained from Professor Arne Tronsmo, The Norwegian University of Life Sciences, Ås, Norway) and the yeast *C. albicans* (Ca, ATCC 10231) as previously described. (16) In short, fungal spores were grown in potato dextrose broth media (Difco) containing 2% D(+)-glucose (Merck, Darmstadt, Germany) at 25-30 °C while shaking at 200 rpm overnight. The cultures were diluted with dextrose media containing glucose to a concentration of approx. 4 × 10^5 spores/mL. Aliquots of the cultures (50 µL) were transferred to 96 well microtiter plates preloaded with the synthetic peptides (50 µL) in two-fold serial dilutions.

Polymyxin B sulfate and Triclosan (Sigma-Aldrich, Steinheim, Germany) served as positive antibiotic controls. The microtiter plates containing the fungal spores and the test peptides were incubated at room temperature for 48 h and OD_{600} was recorded using a Synergy H1 Hybrid microplate reader system (BioTek, Winooski, VT, USA).

3.5. Haemolytic Activity Assay

The haemolytic activity of the synthesised peptides was tested according to the previously described protocol. (17) In brief, for haemolysis determination heparinized fraction (10 IU/mL) of freshly drawn blood was used. A fraction of blood which was collected in test tubes containing ethylenediaminetetraacetic acid (EDTA, Vacutest®, KIMA, Arzergrande, Italy) was used for hematocrit (hct) determination. The heparinized blood was washed 3 times with prewarmed phosphate-buffered saline (PBS) and adjusted to a final hct of 4%. Peptides were screened in concentration-range from 500 to 3.9 μM. They were initially dissolved in dimethyl sulfoxide (DMSO) and were further diluted with PBS to a final DMSO content of ≤1%. As a positive control for 100% hemolysis a solution of 1% triton X-100 was used, whereas 1% DMSO in PBS buffer served as a negative control. Duplicates of test solutions and erythrocytes (1% hct final concentration), were prepared in a 96-well polypropylene V-bottom plate (Nunc, Fischer scientific, Oslo, Norway). Following incubation under agitation at 37 °C and 800 rpm for 1 hour, and subsequent centrifugation (5 min, 3000 g), 100 µL from each well were transferred to a flat-bottomed 96-well plate. Absorbance was measured at 545 nm with a microplate reader (SpectraMax 190, Molecular Devices, San Jose, CA, USA). After subtracting PBS background, the percentage of haemolysis was calculated as the ratio of the absorbance in the peptide- and surfactant-treated samples. Three independent experiments were performed, and EC50 (the concentration giving 50% haemolysis) values are presented as averages.

3.6. Inner Membrane Integrity Biosensor Assay

The inner membrane integrity assay was performed in a real-time manner using *B. subtilis* 168 (ATCC 23857) and *E. coli* K12 (ATCC MC1061) biosensor strains, both containing the reporter plasmid pCSS962 constitutively expressing eukaryotic luciferase (*lucGR* gene). Bacterial colonies were grown overnight at RT in MH media supplemented with 5 µg/mL chloramphenicol (Merck KGaA, Darmstadt, Germany) and a mixture of 20 µg/mL chloramphenicol and 100 µg/mL ampicillin (Sigma-Aldrich, USA), respectively. Overnight cultures were further diluted and grown without antibiotics at RT for 2-3 h until they reached OD600 = 0.1. D-luciferin potassium salt (Synchem Inc., Elk Grove Village, IL, USA) was added to the bacterial cultures at a final concentration of 1 mM. Black round-bottom 96-well microtiter plates (Nunc, Roskilde, Denmark) were prepared with two-fold dilution series of the compounds (10 µL per well) at final concentrations ranging from 50 to 1.56 µg/mL. Chlorhexidine acetate (CHX, Fresenius Kabi, Halden, Norway) and Milli-Q water were used as positive and negative control, respectively. A Synergy H1 Hybrid Reader (BioTek, Winooski, VT, USA) was primed with bacterial suspension before the assay plate was loaded into the plate reader. Aliquots of 90 µL bacterial inoculum with D-luciferin were successively (well by well) injected into the test wells by an automated injector. The light (luminescence) emission, as a result of bacterial membrane disruption, was monitored every second for 3 min. Each study was performed at least three times independently, and the figures show a representative dataset.

3.7. Biosensor Viability Assay

The real-time measurement of bacterial viability was performed by using *B. subtilis* 168 and *E. coli* K12, the same strains that were used in the inner membrane integrity assay. However, in this assay *B. subtilis* 168 is carrying a constitutively expressed lux operon as a chromosomal integration in the *sac*A locus (PliaG) and *E. coli* K12 was transformed with the reporter plasmid pCGLS-11. (16) *B. subtilis* and *E. coli* cultures were prepared the same way as the membrane integrity assay in MH media supplemented with 5 µg/mL chloramphenicol and a mixture of 20 µg/mL chloramphenicol and 100 µg/mL ampicillin, respectively. The continuous light production by these biosensors was monitored in the Synergy H1 Hybrid Reader, and the respective injector was primed with bacterial suspension. Black round-bottom 96-well microtiter plates were prepared with 10 µL of each compound at the final concentration ranging from 50 to 1.56 µg/mL (two-fold dilutions), including chlorhexidine as a positive control and Milli-Q water as a negative control. An aliquot of 90 µL bacterial suspension was subsequently added by the automated injector. As a result of changes in bacterial viability, the decrease in light emission was monitored every second for 3 min. Each study was performed at least three times independently, and the figures show a representative dataset.

3.8. Outer Membrane Permeability Assay

The outer membrane integrity assay was performed in a real-time manner using *E. coli* (ATCC 25922) and *P. aeruginosa* (ATCC 27853) as test strains. Externally added *N*-phenyl-1-napthylamine (NPN, Sigma-Aldrich, USA) was used as a substrate for the fluorescence to detect light emission. *E. coli* colonies were suspended in MH media and grown overnight at RT. Overnight cultures were further diluted and grown at RT for 2-3 h until they reached OD_{600} = 0.5. NPN was added to the bacterial cultures at a final concentration of 20 µM in glucose 4-(2-hydroxyethyl)-1-piperazineethanesulfonic acid (HEPES) buffer (5 mM), and the background fluorescence was measured before the actual assay. Black round-bottom 96-well microtiter plates were prepared with two-fold dilution series of the compounds (10 µL per well) at final concentrations ranging from 50 to 1.56 µg/mL. Polymyxin B and Milli-Q water was used as a positive and negative control, respectively. A Synergy H1 Hybrid Reader was primed with bacterial suspension before the assay plate was loaded into the plate reader. Aliquots of 90 µL bacterial inoculum with NPN were successively (well by well) injected into the test wells by an automated injector. The light (fluorescence) emission, observed as a result of bacterial outer membrane disruption, was monitored every second for 3 min. Each study was performed at least three times independently, and the figures show a representative dataset.

Acknowledgments: This work was funded by a grant (no. 217/6770) from UiT The Arctic University of Norway.

References

1. Solstad RG, Li C, Isaksson J, Johansen J, Svenson J, Stensvåg K, et al. Novel Antimicrobial Peptides EeCentrocins 1, 2 and EeStrongylocin 2 from the Edible Sea Urchin Echinus esculentus Have 6-Br-Trp Post-Translational Modifications. PLOS ONE. 2016;11(3):e0151820.
2. Solstad RG, Johansen C, Stensvåg K, Strøm MB, Haug T. Structure-activity relationship studies of shortened analogues of the antimicrobial peptide EeCentrocin 1 from the sea urchin Echinus esculentus. J Pept Sci. 2020;26(2):e3233.
3. Malesevic M, Strijowski U, Bächle D, Sewald N. An improved method for the solution cyclization of peptides under pseudo-high dilution conditions. J Biotechnol. 2004;112(1):73-7.
4. Rounds T, Straus SK. Lipidation of Antimicrobial Peptides as a Design Strategy for Future Alternatives to Antibiotics. Int J Mol Sci. 2020;21(24):9692.
5. Paulsen MH, Karlsen EA, Ausbacher D, Anderssen T, Bayer A, Ochtrop P, et al. An amphipathic cyclic tetrapeptide scaffold containing halogenated β(2,2) -amino acids with activity against multiresistant bacteria. J Pept Sci. 2018;24(10):e3117.
6. Zarena D, Mishra B, Lushnikova T, Wang F, Wang G. The π Configuration of the WWW Motif of a Short Trp-Rich Peptide Is Critical for Targeting Bacterial Membranes, Disrupting Preformed Biofilms, and Killing Methicillin-Resistant Staphylococcus aureus. Biochemistry. 2017;56(31):4039-43.
7. Vernen F, Harvey PJ, Dias SA, Veiga AS, Huang Y-H, Craik DJ, et al. Characterization of Tachyplesin Peptides and Their Cyclized Analogues to Improve Antimicrobial and Anticancer Properties. Int J Mol Sci [Internet]. 2019; 20(17). Available from: https://mdpi-res.com/d_attachment/ijms/ijms-20-04184/article_deploy/ijms-20-04184-v2.pdf?version=1566889767.
8. Tam JP, Lu Y-A, Yang J-L. Marked Increase in Membranolytic Selectivity of Novel Cyclic Tachyplesins Constrained with an Antiparallel Two-β Strand Cystine Knot Framework. Biochem Biophys Res Commun. 2000;267(3):783-90.
9. Wirth F, Goldani LZ. Epidemiology of Rhodotorula: an emerging pathogen. Interdiscip Perspect Infect Dis. 2012;2012:465717.
10. Mehta SR, Johns S, Stark P, Fierer J. Successful treatment of Aureobasidium pullulans central catheter-related fungemia and septic pulmonary emboli. IDCases. 2017;10:65-7.
11. Joshi A, Singh R, Shah MS, Umesh S, Khattry N. Subcutaneous mycosis and fungemia by Aureobasidium pullulans: a rare pathogenic fungus in a post allogeneic BM transplant patient. Bone Marrow Transplant. 2010;45(1):203-4.
12. Helander IM, Mattila-Sandholm T. Fluorometric assessment of gram-negative bacterial permeabilization. J Appl Microbiol. 2000;88(2):213-9.
13. Paulsen VS, Blencke H-M, Benincasa M, Haug T, Eksteen JJ, Styrvold OB, et al. Structure-Activity Relationships of the Antimicrobial Peptide Arasin 1 — And Mode of Action Studies of the N-Terminal, Proline-Rich Region. PLOS ONE. 2013;8(1):e53326.
14. Vasilchenko AS, Rogozhin EA. Sub-inhibitory Effects of Antimicrobial Peptides. Front Microbiol. 2019;10.
15. Igumnova EM, Mishchenko E, Haug T, Blencke H-M, Sollid JUE, Fredheim EGA, et al. Synthesis and antimicrobial activity of small cationic amphipathic aminobenzamide marine natural product mimics and evaluation of relevance against clinical isolates including ESBL–CARBA producing multi-resistant bacteria. Bioorg Med Chem. 2016;24(22):5884-94.
16. Hansen I, Lövdahl T, Simonovic D, Hansen K, Andersen AJC, Devold H, et al. Antimicrobial Activity of Small Synthetic Peptides Based on the Marine Peptide Turgencin A: Prediction of Antimicrobial Peptide Sequences in a Natural Peptide and Strategy for Optimization of Potency. Int J Mol Sci. 2020;21(15).
17. Paulsen MH, Ausbacher D, Bayer A, Engqvist M, Hansen T, Haug T, et al. Antimicrobial activity of amphipathic α,α-disubstituted β-amino amide derivatives against ESBL – CARBA producing multi-resistant bacteria; effect of halogenation, lipophilicity and cationic character. Eur J Med Chem. 2019;183:111671.

Supporting information

Antimicrobial activity of short analogues of the marine peptide EeCentrocin 1: Synthesis of lipopeptides and head-to-tail cyclic peptides

Danijela Simonovic[1#], Hymonti Dey[2#], Natascha Johansen[1], Trude Anderssen[1], Hege Devold[2], Terje Vasskog[1], Hans-Matti Blencke[2], Elizabeth G. Aarag Fredheim[1], Tor Haug[2*], Morten B. Strøm[1*]

[1] Department of Pharmacy, Faculty of Health Sciences, UiT the Arctic University of Norway, NO-9037 Tromsø, NORWAY.

[2] The Norwegian College of Fishery Science, Faculty of Biosciences, Fisheries and Economics, UiT the Arctic University of Norway, NO-9037 Tromsø, NORWAY.

[#] Authors contributed equally.

* Corresponding authors. Correspondence: tor.haug@uit.no and morten.strom@uit.no

Contents:

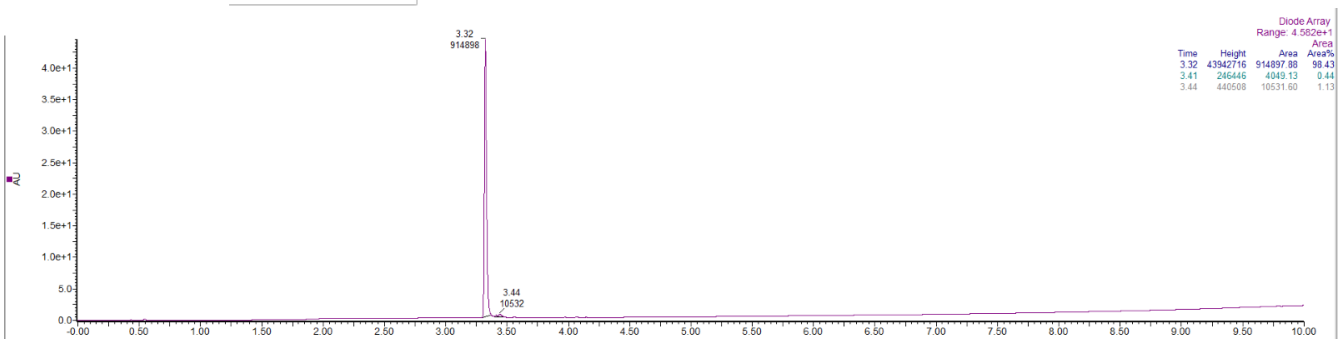

Figure S1. UPLC chromatogram of the purified cyclic peptide **P6**. The peptide purity is 98.43 % based on the UPLC calculated area under the curves.

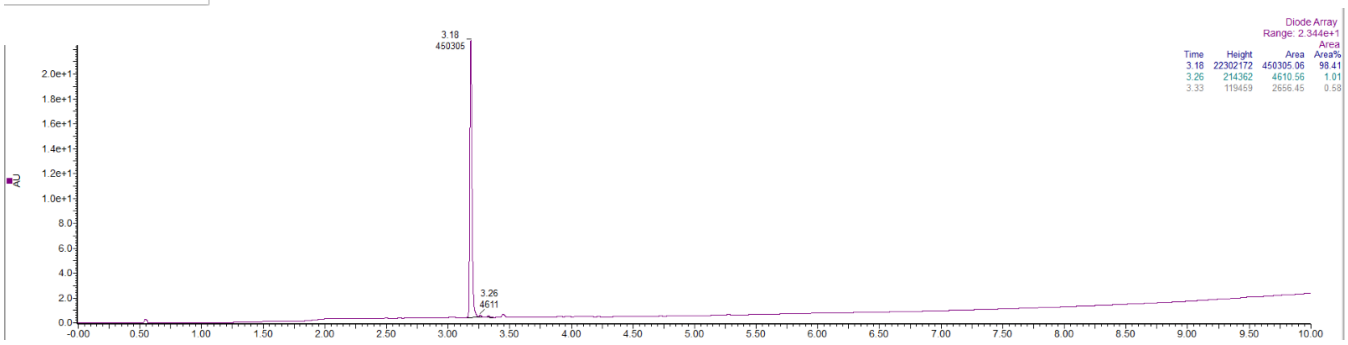

Figure S2. UPLC chromatogram of the purified cyclic peptide **P6-K8**. The peptide purity is 98.41 % based on the UPLC calculated area under the curves.

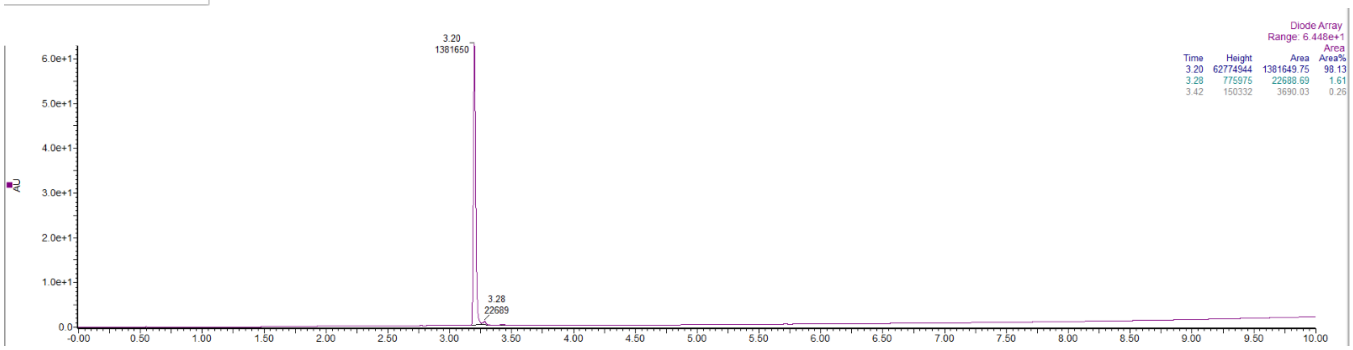

Figure S3. UPLC chromatogram of the purified cyclic peptide **P6-R8**. The peptide purity is 98.13 % based on the UPLC calculated area under the curves.

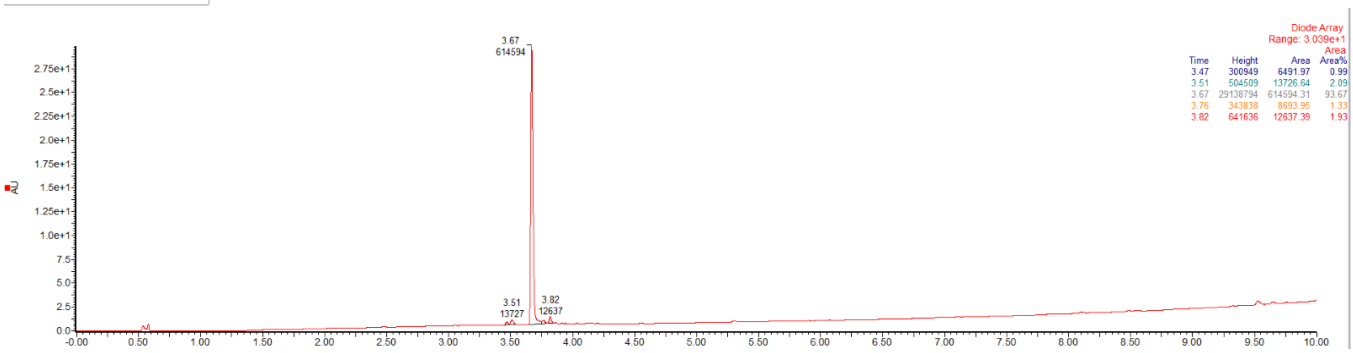

Figure S4. UPLC chromatogram of the purified cyclic peptide **P6-W6K8**. The peptide purity is 93.67 % based on the UPLC calculated area under the curves.

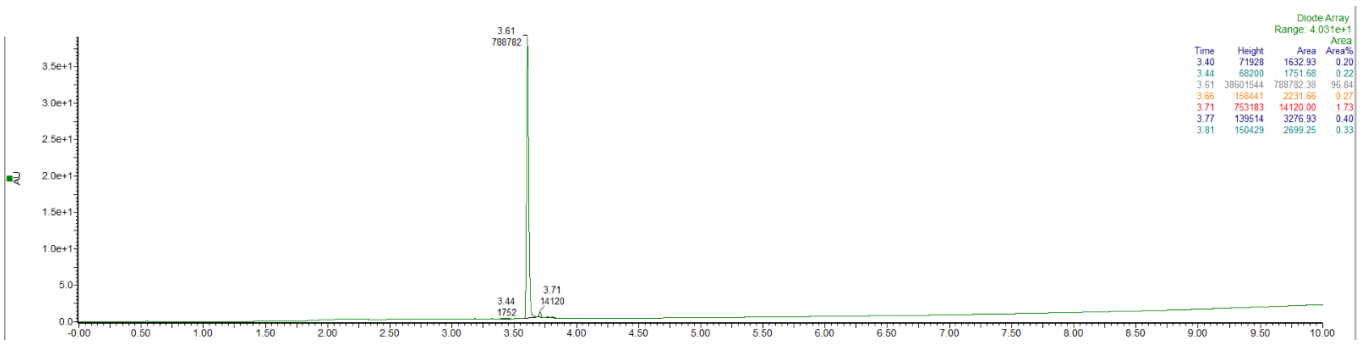

Figure S5. UPLC chromatogram of the purified cyclic peptide **P6-W6R8**. The peptide purity is 96.84 % based on the UPLC calculated area under the curves.

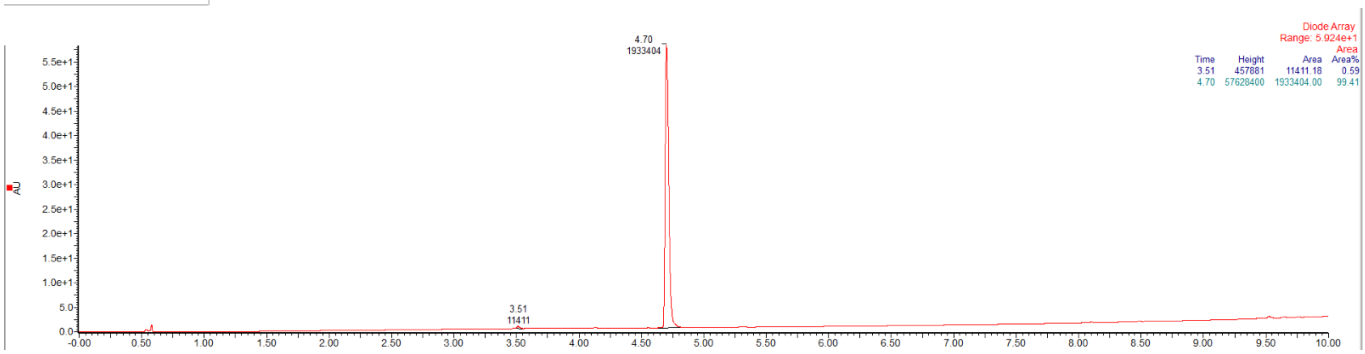

Figure S6. UPLC chromatogram of the purified cyclic peptide **C$_8$-P6-R8**. The peptide purity is 99.41 % based on the UPLC calculated area under the curves.

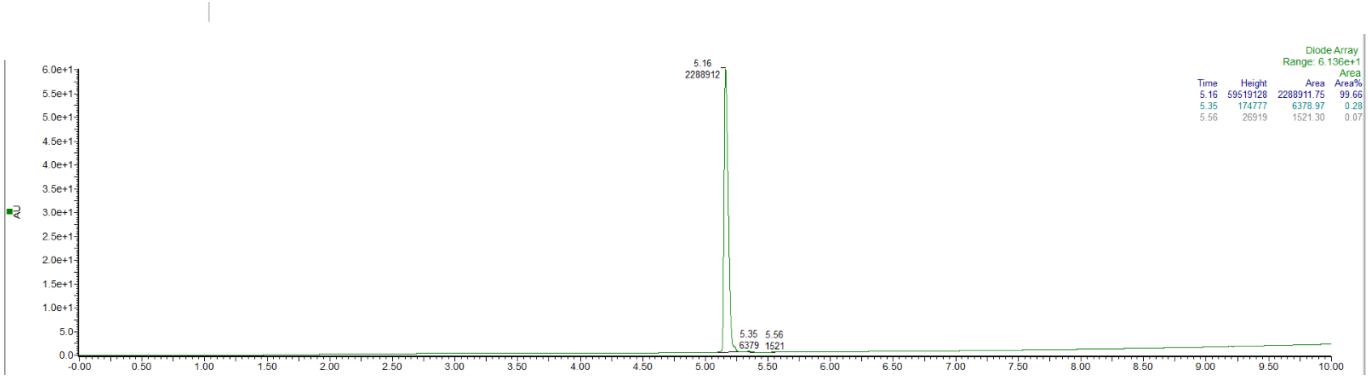

Figure S7. UPLC chromatogram of the purified cyclic peptide **C$_{10}$-P6-R8**. The peptide purity is 99.66 % based on the UPLC calculated area under the curves.

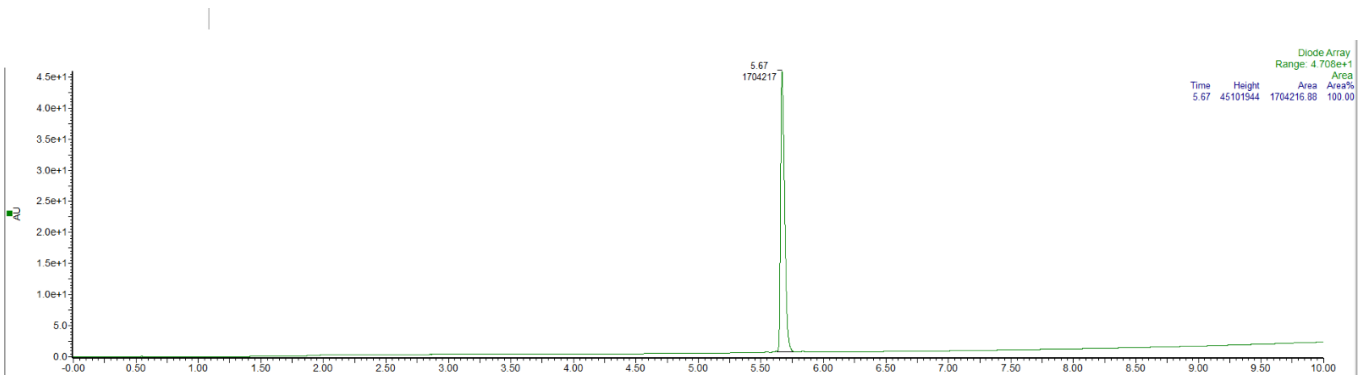

Figure S8. UPLC chromatogram of the purified cyclic peptide **C$_{12}$-P6-R8**. The peptide purity is 100 % based on the UPLC calculated area under the curves.

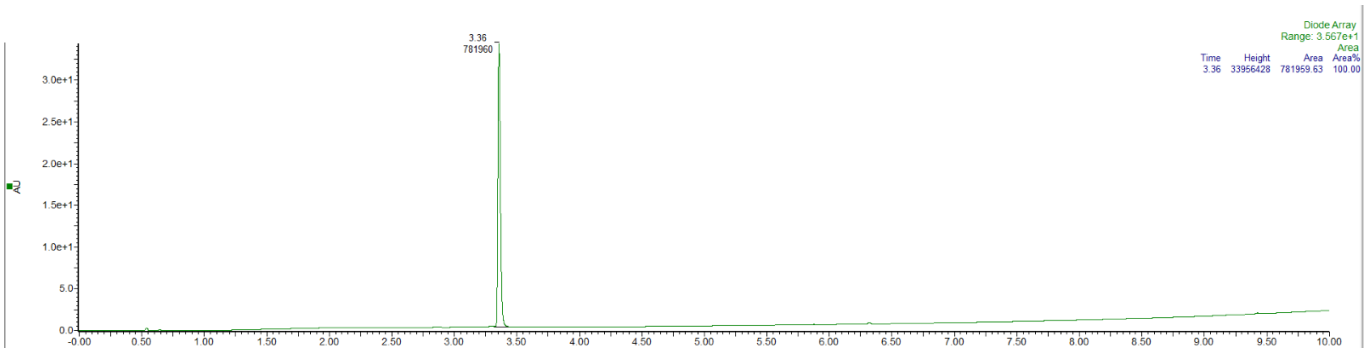

Figure S9. UPLC chromatogram of the purified cyclic peptide **cP6**. The peptide purity is 100 % based on the UPLC calculated area under the curves.

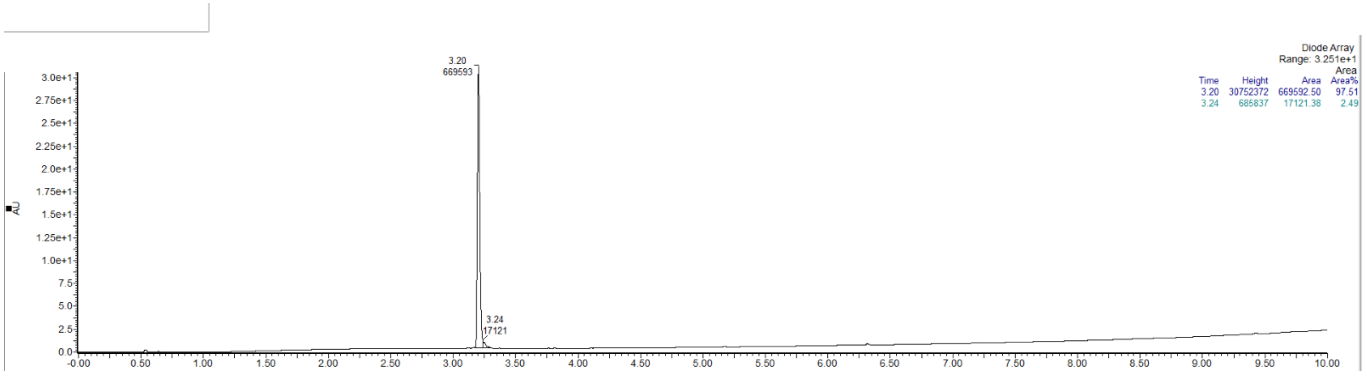

Figure S10. UPLC chromatogram of the purified cyclic peptide **cP6-R8**. The peptide purity is 97.51 % based on the UPLC calculated area under the curves.

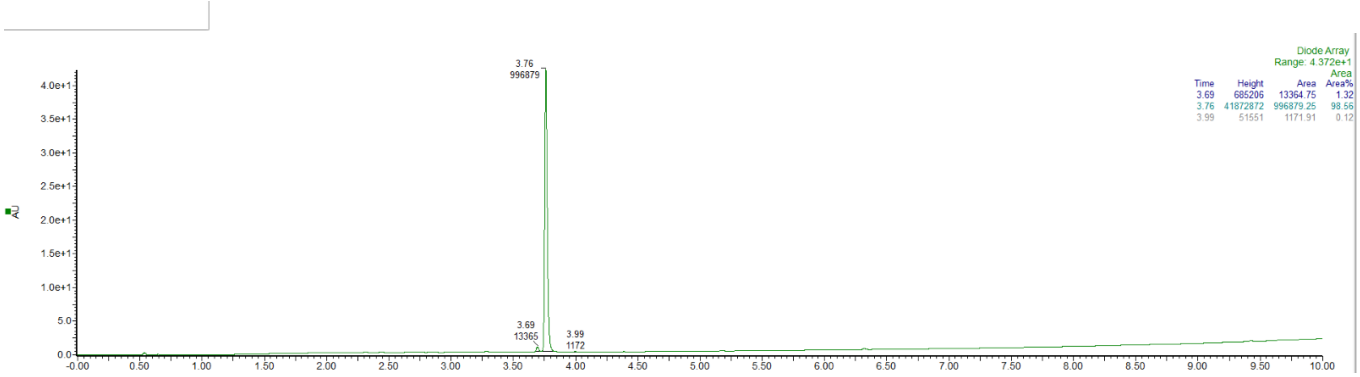

Figure S11. UPLC chromatogram of the purified cyclic peptide **cP6-W6R8**. The peptide purity is 98.56 % based on the UPLC calculated area under the curves.

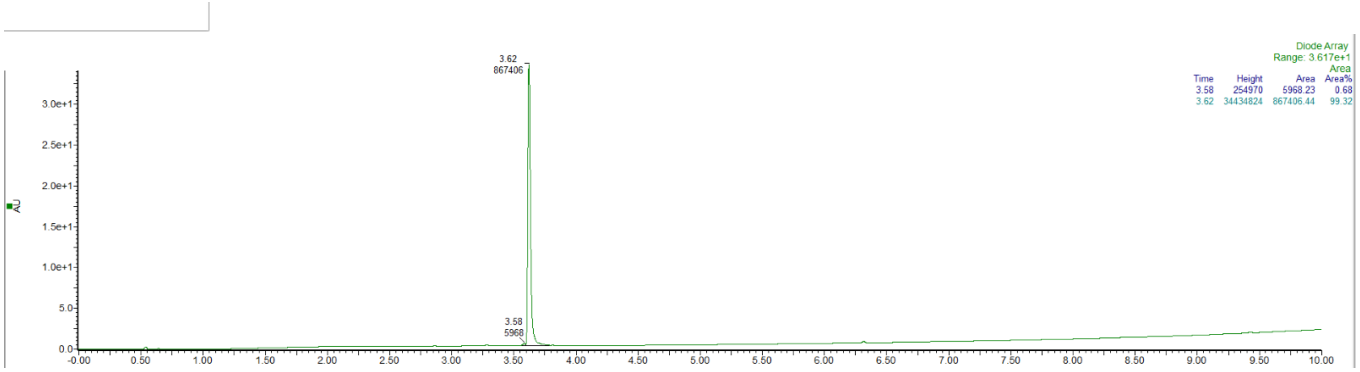

Figure S12. UPLC chromatogram of the purified cyclic peptide **cP6-W4R6,8**. The peptide purity is 99.32 % based on the UPLC calculated area under the curves.

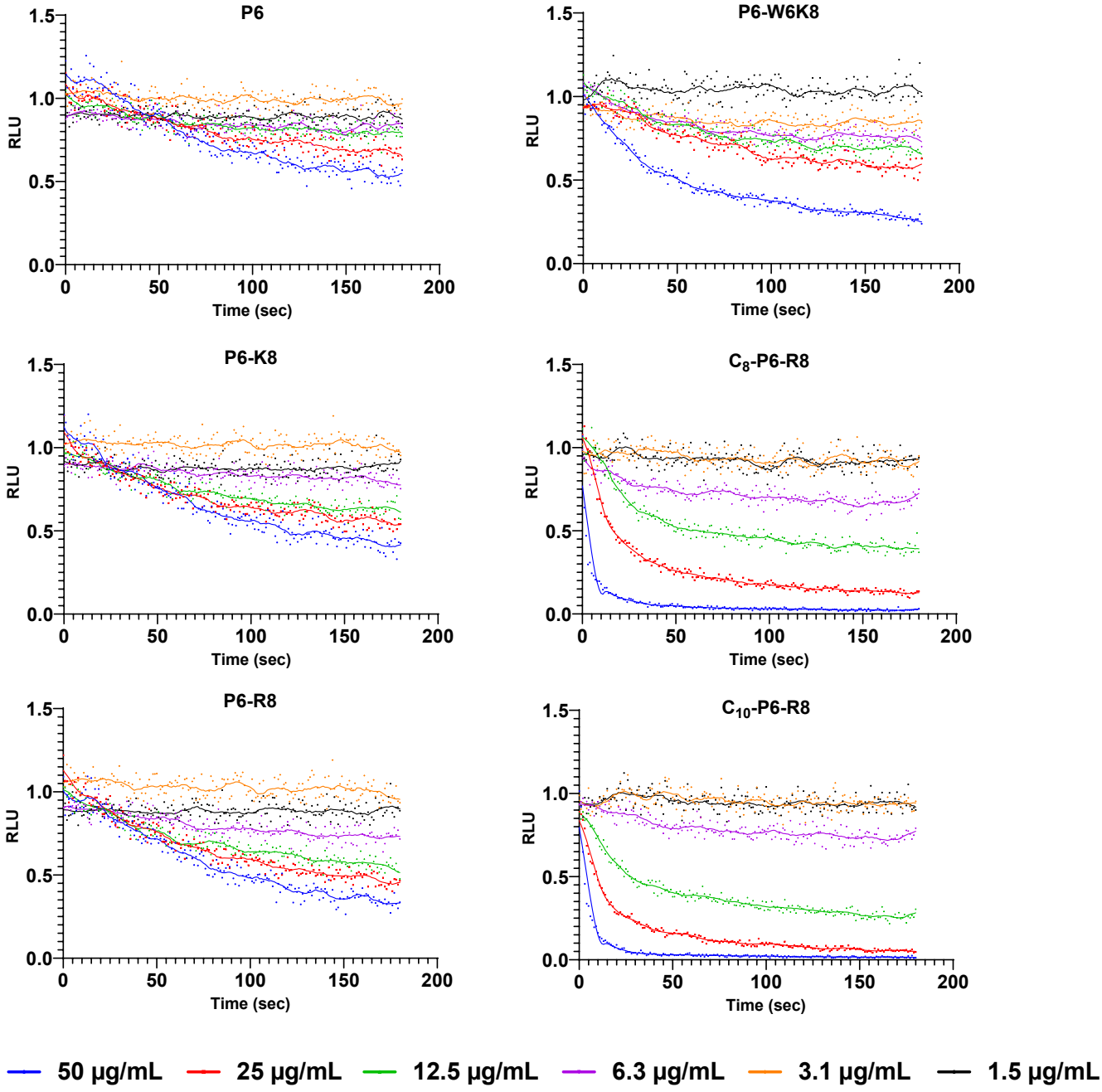

Figure S13. Kinetics of the effect on viability as measured by relative luminescence in *B. subtilis* (pCGLS11) treated with different concentrations of **P6**, **P6-K8**, **P6-R8**, **P6-W6K8**, **C_8-P6-R8** and **C_{10}-P6-R8**.

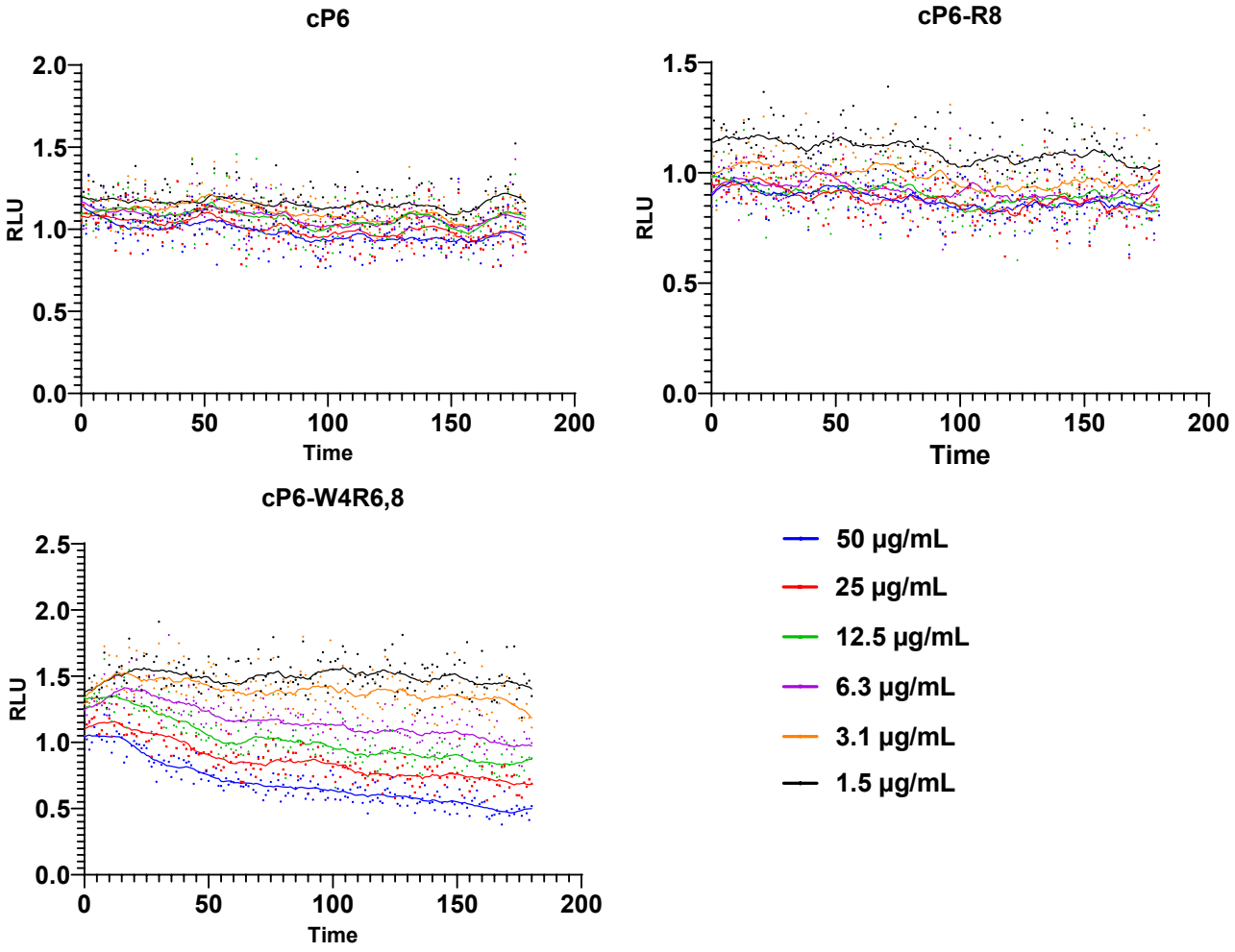

Figure S14. Kinetics of the effect on viability as measured by relative luminescence in *B. subtilis* (pCGLS11) treated with different concentrations of **cP6**, **cP6-R8** and **cP6-W4R6,8**.

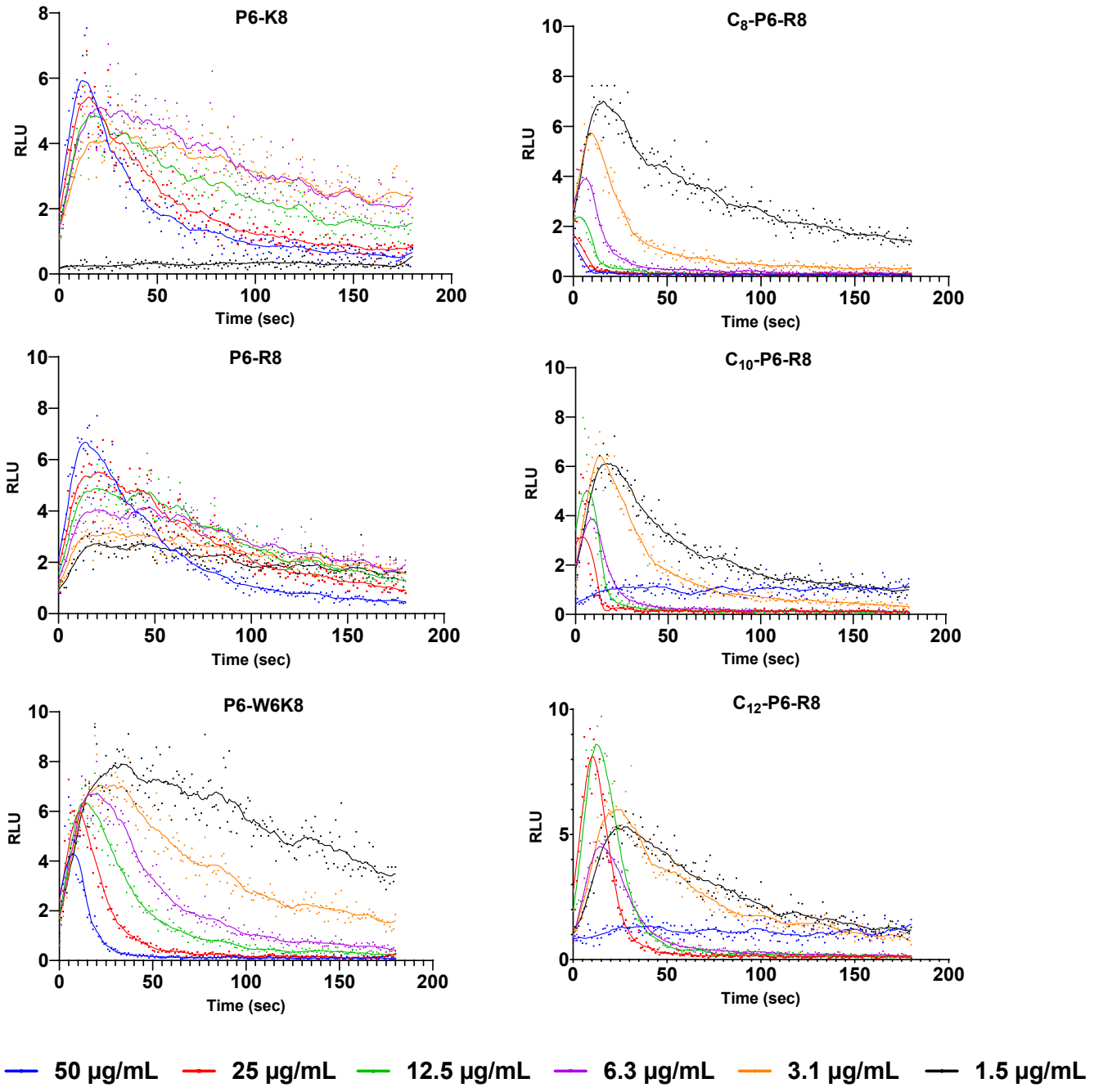

Figure S15. Kinetics of the effect on membrane integrity as measured by relative luminescence in *B. subtilis* (pCSS962) treated with different concentrations of **P6-K8**, **P6-R8**, **P6-W6K6**, **C_8-P6-R8**, **C_{10}-P6-R8** and **C_{12}-P6-R8**.

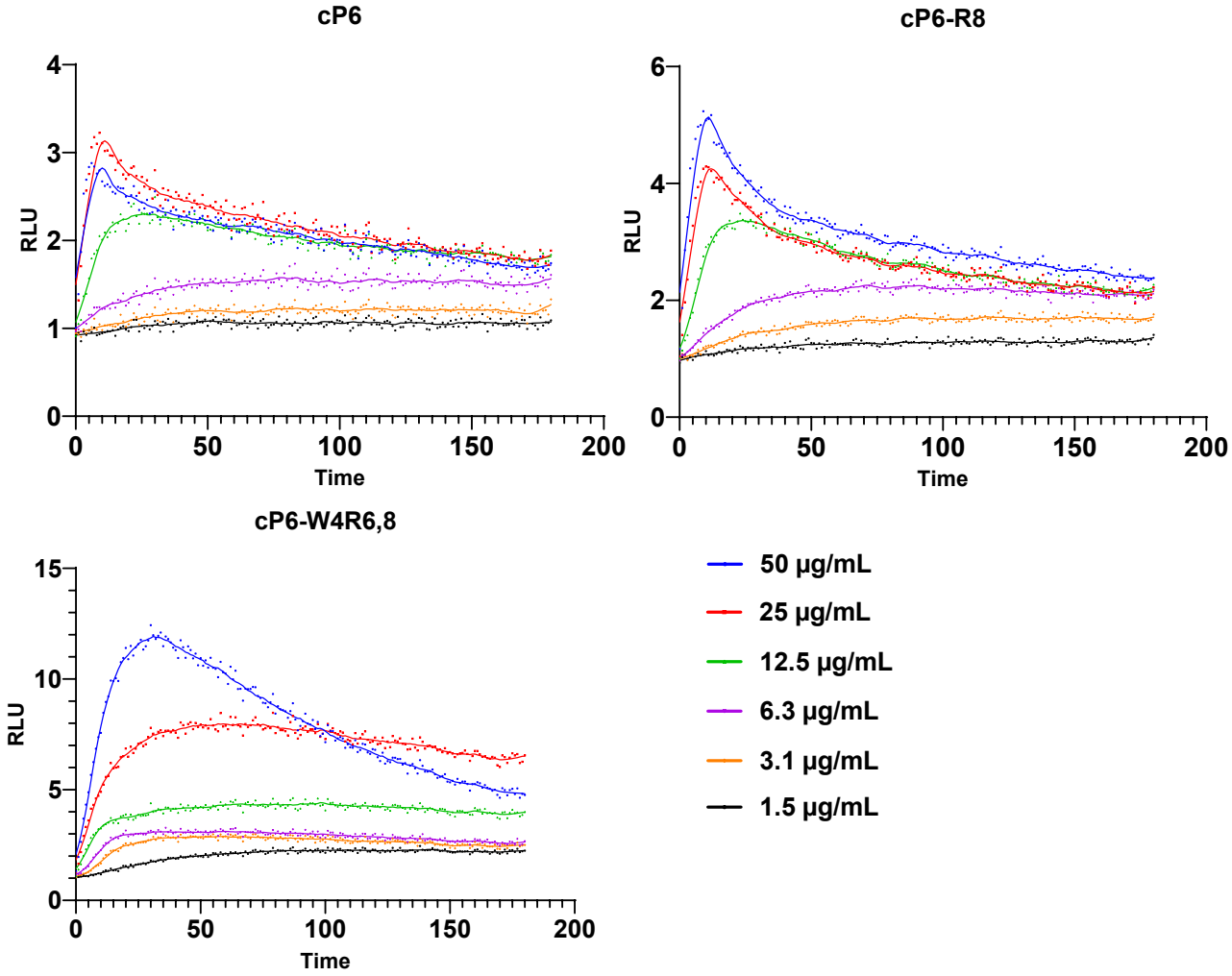

Figure S16. Kinetics of the effect on membrane integrity as measured by relative luminescence in *B. subtilis* (pCSS962) treated with different concentrations of **cP6**, **cP6-R8** and **cP6-W4R6,8**.

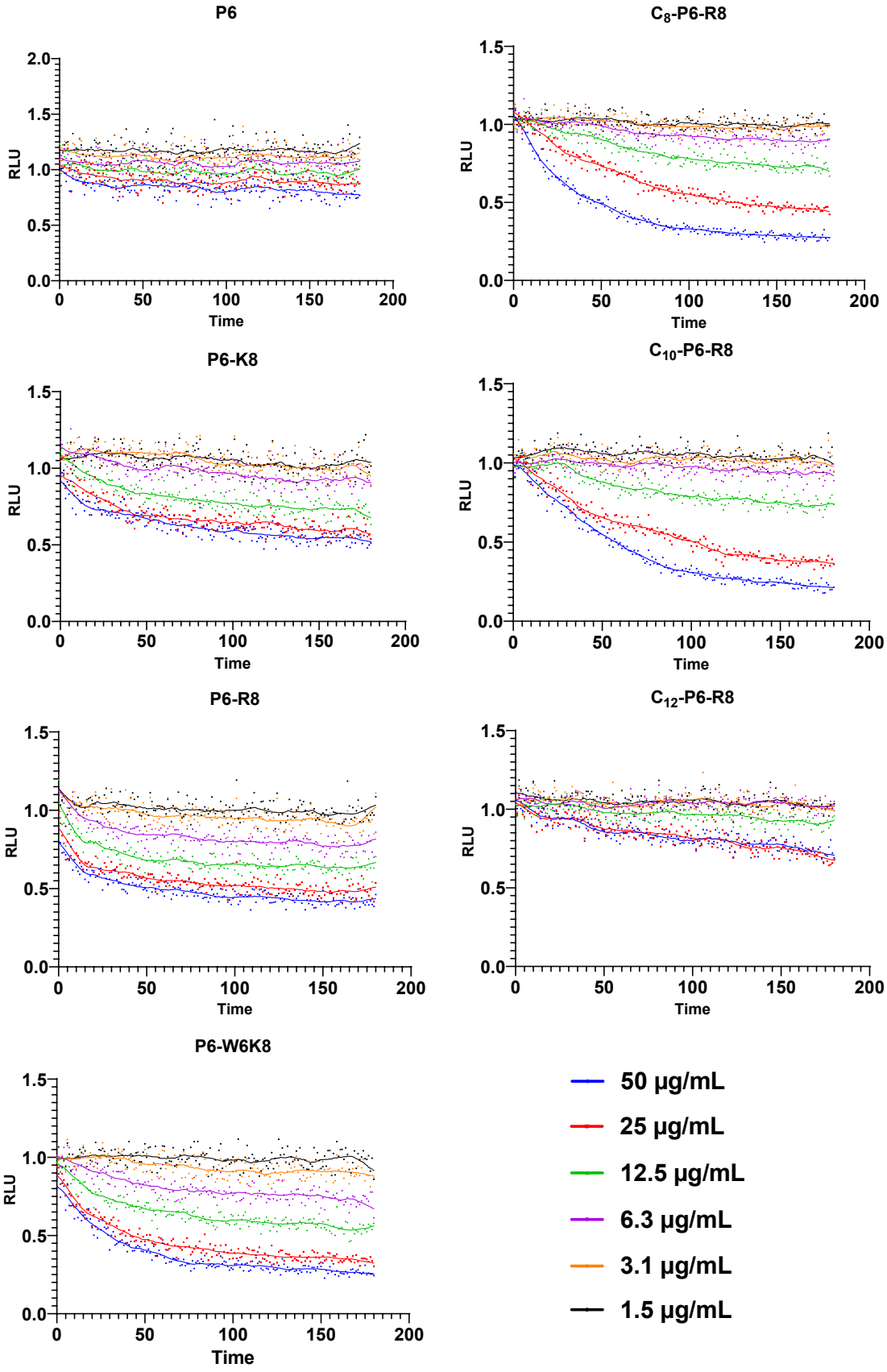

Figure S17. Kinetics of the effect on viability as measured by relative luminescence in *E. coli* (pCGLS-11) treated with different concentrations of **P6**, **P6-K8**, **P6-R8**, **P6-W6K8**, **C$_8$-P6-R8**, **C$_{10}$-P6-R8** and **C$_{12}$-P6-R8**.

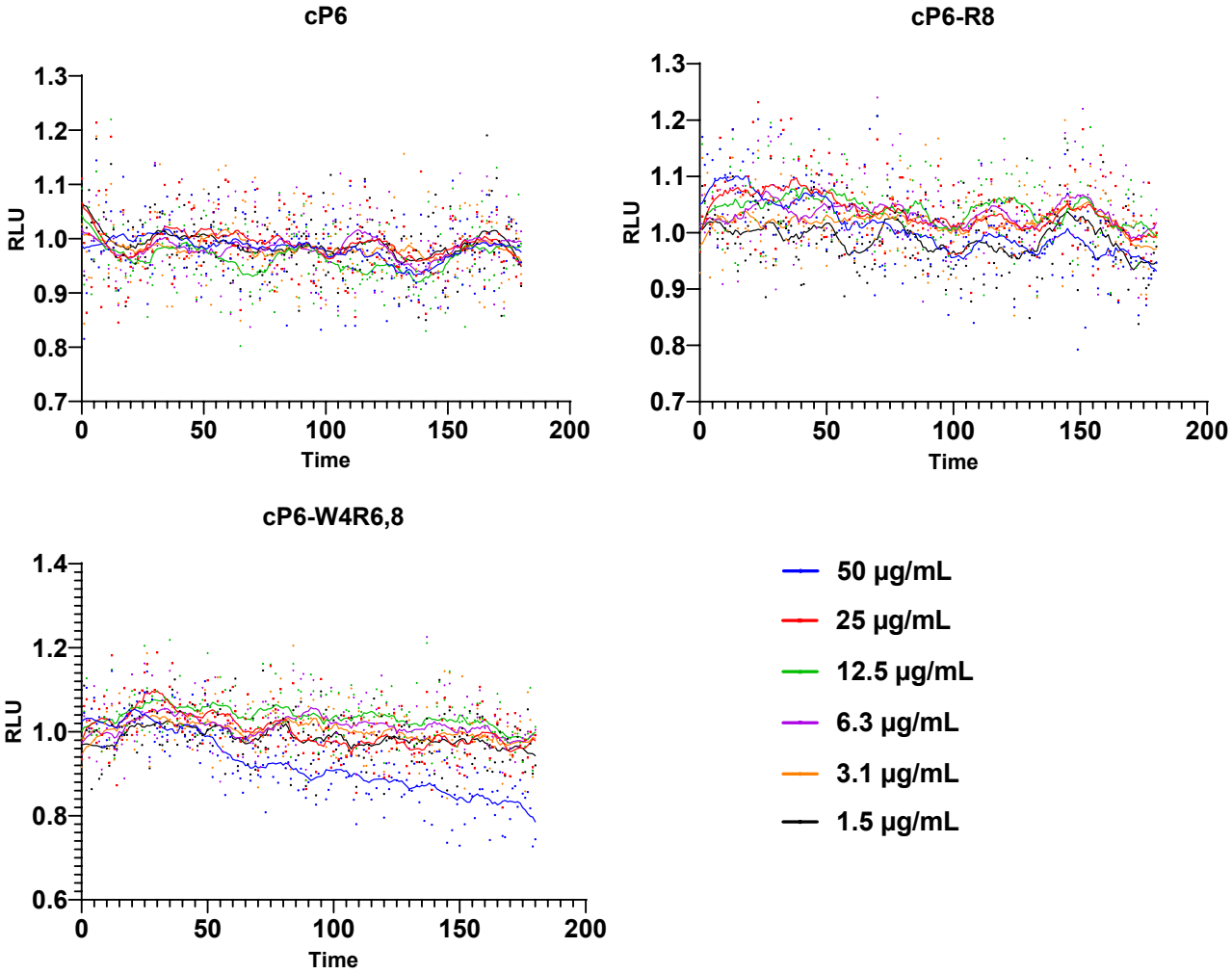

Figure S18. Kinetics of the effect on viability as measured by relative luminescence in *E. coli* (pCGLS-11) treated with different concentrations of **cP6**, **cP6-R8** and **cP6-W4R6,8**.

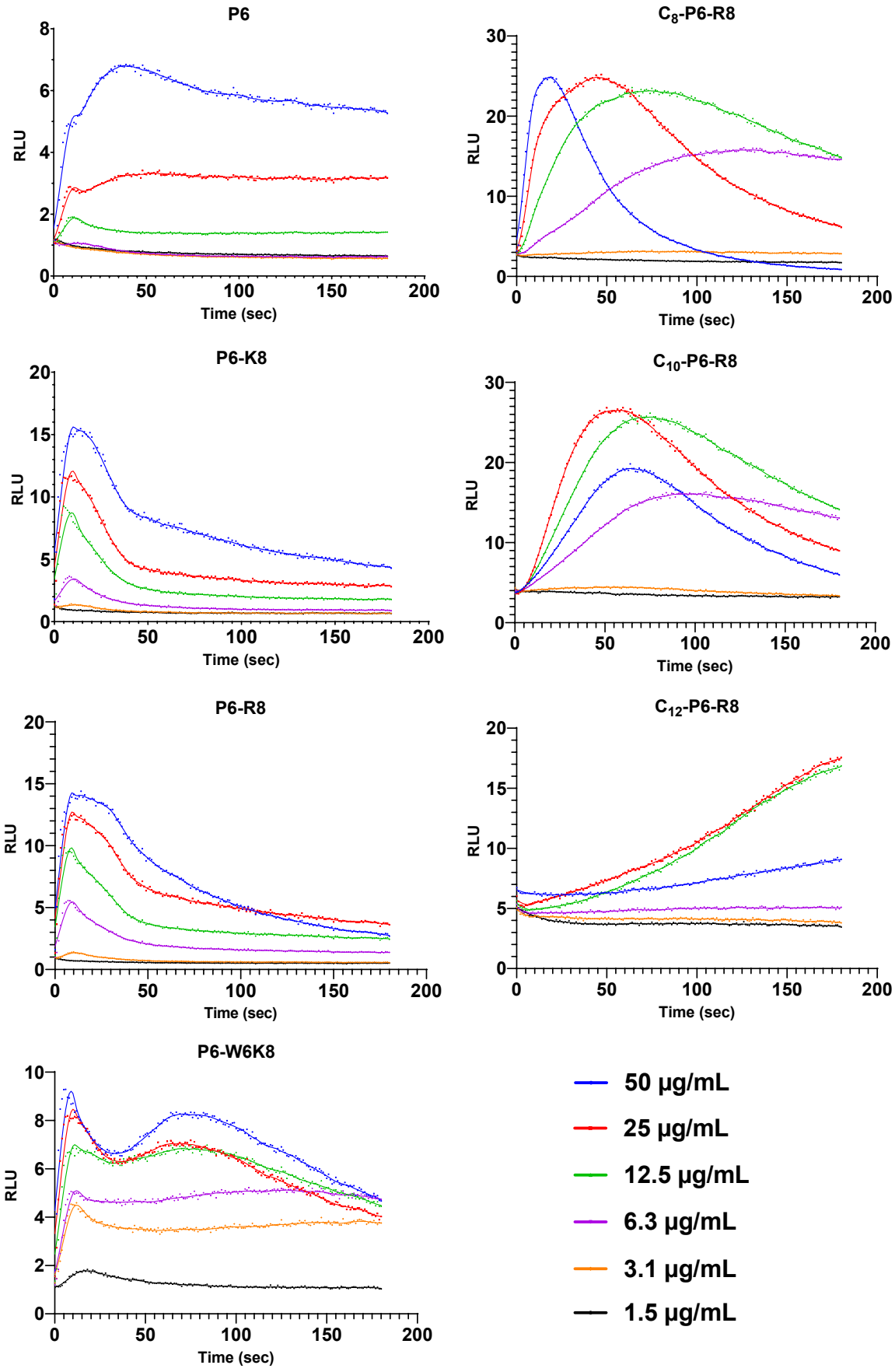

Figure S19. Kinetics of the effect on membrane integrity as measured by relative luminescence in *E. coli* (pCSS962) treated with different concentrations of **P6**, **P6-K8**, **P6-R8**, **P6-W6K8**, **C_8-P6-R8**, **C_{10}-P6-R8** and **C_{12}-P6-R8**.

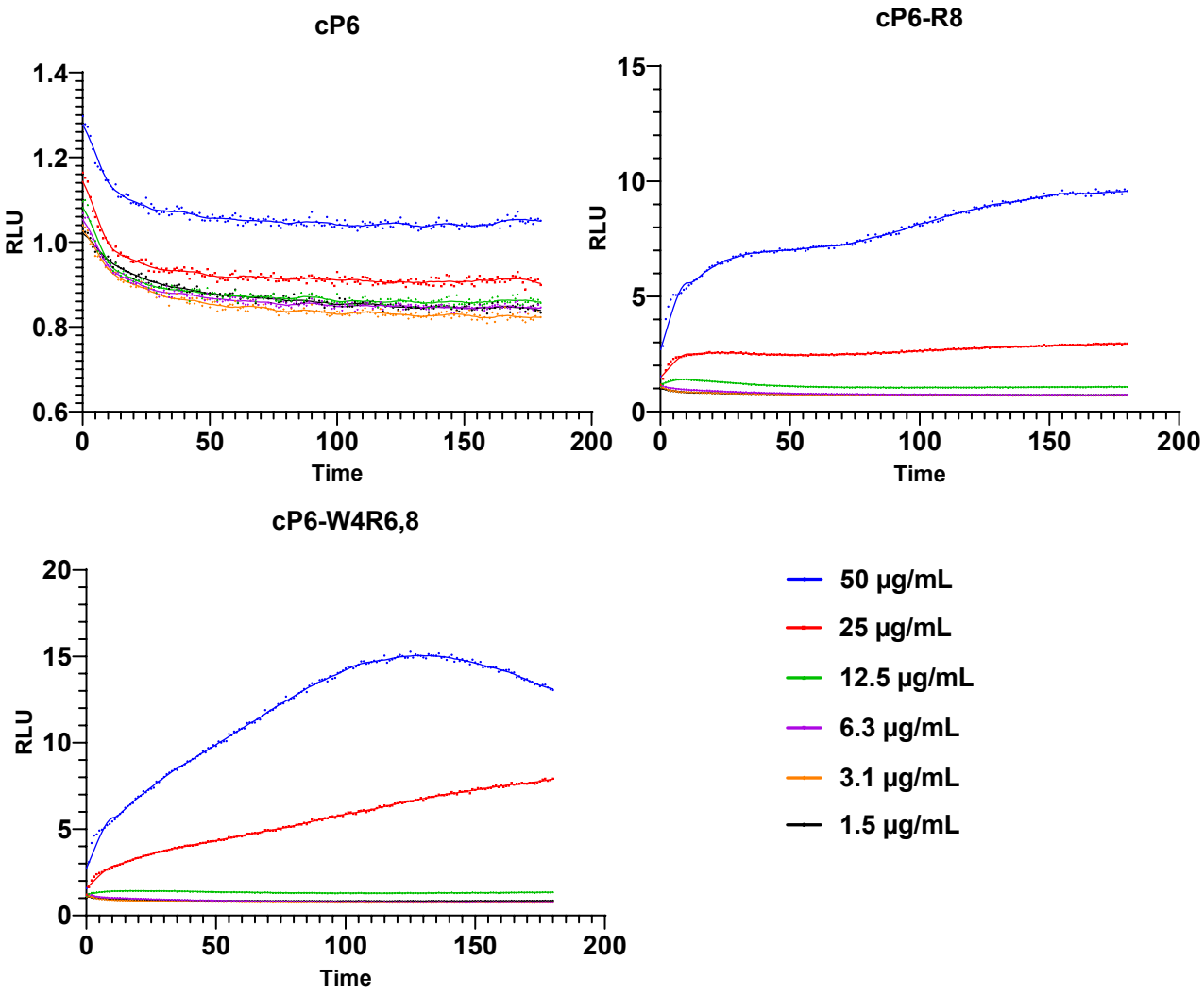

Figure S20. Kinetics of the effect on membrane integrity as measured by relative luminescence in *E. coli* (pCSS962) treated with different concentrations of **cP6**, **cP6-R8** and **cP6-W4R6,8**.

Table S1. Theoretical and observed monoisotopic mass and m/z ions (Da) during HRMS of the synthesised peptides.

	Monoisotopic mass (Da)		$[M+2H]^{2+}$		$[M+3H]^{3+}$		$[M+4H]^{4+}$	
Peptide	Theoretical	Observed	Theoretical	Observed	Theoretical	Observed	Theoretical	Observed
P6	1540.9215	1540.9226	771.4680	771.4680	514.6478	514.6481	386.2377	386.2383
P6-K8	1597.9794	1597.9802	799.9970	799.9966	533.6671	533.6673	400.5021	400.5028
P6-R8	1625.9855	1626.0196	814.0000	813.9997	543.0024	543.0026	407.5037	407.5043
P6-W6K8	1683.0110	1683.0124	842.5128	842.5123	562.0110	562.0112	421.7600	421.7611
P6-W6R8	1711.0171	1711.0173	856.5158	856.5151	571.3463	571.3465	428.7616	428.7619
C_8-P6-R8	1752.0900	1752.0911	877.0523	877.0516	585.0373	585.0376	439.0298	439.0307
C_{10}-P6-R8	1780.1213	1780.1231	891.0679	891.0677	594.3810	594.3815	446.0376	446.0387
C_{12}-P6-R8	1808.1526	1808.1545	905.0836	905.0831	603.7248	603.7253	453.0454	453.0467
cP6	1523.8950	1523.8955	762.9548	762.9548	508.9723	508.9725	381.9810	381.9813
cP6-R8	1608.9590	1608.9600	805.4868	805.4870	537.3269	537.3273	403.2470	403.2474
cP6-W6R8	1693.9906	1693.9910	848.0026	848.0023	565.6708	565.6709	424.5049	424.5053
cP6-W4R6,8	1693.9906	1693.9912	848.0026	848.0023	565.6708	565.6710	424.5049	424.5054

Table S2. Purity of the synthesised peptides (%) and retention time (min) determined by UPLC using a reversed phase column.

Peptide	Purity (%)	Retention time (min)
P6	98.43	3.32
P6-K8	98.41	3.18
P6-R8	98.13	3.20
P6-W6K8	93.67	3.67
P6-W6R8	96.84	3.61
C_8-P6R8	99.41	4.70
C_{10}-P6R8	99.66	5.16
C_{12}-P6R8	100.00	5.67
cP6	100.00	3.36
cP6-R8	97.54	3.20
cP6-W6R8	98.56	3.76
cP6-W4R6,8	99.32	3.62

Paper III

The role of amphipathicity and *L*- to *D*-amino acid substitution in a small antimicrobial cyclic tetrapeptide scaffold containing a halogenated α,α-disubstituted $\beta^{2,2}$-amino acid residue

Danijela Simonovic[a], Fredrik G. Rylandsholm[b], Martin Jakubec[b], Johan Mattias Isaksson[a,b], Hege Devold[c], Trude Anderssen[a], Annette Bayer[b], Tor Haug[c], Morten B. Strøm[a]*

[a] *Department of Pharmacy, Faculty of Health Sciences, UiT – The Arctic University of Norway, NO-9037 Tromsø, NORWAY.*
[b] *Department of Chemistry, UiT – The Arctic University of Norway, NO-9037 Tromsø, NORWAY.*
[c] *The Norwegian College of Fishery Science, Faculty of Biosciences, Fisheries and Economics, UiT – The Arctic University of Norway, NO-9037 Tromsø, NORWAY.*

ARTICLE INFO

Keywords:
Antibacterial
Antimicrobial peptides
Beta-amino acids
Cyclic peptides
Peptidomimetics
SMAMPs – synthetic mimics of antimicrobial peptides

ABSTRACT

A small library of nine cyclic tetrapeptides having cationic (Lys or Arg) and lipophilic residues were synthesised and their antimicrobial activity and haemolytic toxicity were investigated. All cyclic tetrapeptides contained a fluorinated lipophilic $\beta^{2,2}$-amino acid. Membrane-peptide interactions were studied by Surface Plasmon Resonance (SPR), whereas Nuclear Magnetic Resonance spectroscopy (NMR) was used for conformational studies.

By changing the order of the last two residues in the starting sequence c(Lys-$\beta^{2,2}$-Leu-Lys), effects of amphipathicity on antimicrobial activity and haemolytic toxicity were investigated. Introducing a cationic *D*-Lys/*D*-Arg residue allowed for the study of stereochemical aspects related to positioning of the cationic side chains relative to the plane of the cyclic tetrapeptide scaffold. Effects of substitution of Leu with more bulky, lipophilic Phe were also studied.

Surprisingly, many of the modifications had minimal effect on antimicrobial activity while having a substantial impact on haemolytic toxicity. The overall most potent cyclic tetrapeptide **006** c(Arg-$\beta^{2,2}$-Arg-Arg) had a minimum inhibitory concentration (MIC) of 1 – 4 ug/mL against both Gram-positive and Gram-negative bacteria, and low haemolytic toxicity (EC_{50} 279 ug/mL). SPR studies supported the bioactivity studies and revealed important differences in the way the cyclic tetrapeptides interacted with membrane models. NMR did not indicate any significant changes in backbone conformation, suggesting that the observed differences in activity could be attributed to different side chain properties.

In conclusion, changes in amphipathicity and in stereochemistry of a single cationic residue in small cyclic tetrapeptide scaffold encompassing a lipophilic $\beta^{2,2}$-amino acid, can be used as a powerful tool for reducing haemolytic toxicity while maintaining antimicrobial activity of membrane active cyclic tetrapeptides.

Keywords: Short antimicrobial peptides; AMPs; cyclic tetrapeptides; structure-activity relationship; $\beta^{2,2}$-amino acid residue.

1. Introduction

Effective antimicrobial drugs are the very core of modern medicine, enabling successful prevention and treatment of infectious diseases. However, systemic misuse and overuse of antibiotics in human medicine, as well as in animal husbandry have led to widespread antibiotic-resistance, rendering many of these drugs ineffective.

Antimicrobial peptides (AMPs), also called host defense peptides (HDPs), are compounds that widely exist in nature. They are an important part of the innate immune system of different organisms, and as such protect the host from a wide range of pathogens, including bacteria, viruses, and fungi. (1) Due to their broad-spectrum antimicrobial activity and unique mechanisms of action (predominantly membrane disruption), they are hailed as a potential alternative to conventional antibiotics. Moreover, AMPs have been regarded as a viable therapeutic option against infections caused by multidrug-resistant bacteria. (2, 3) It is believed that resistance towards AMPs is less likely to develop compared to conventional antibiotics, as it would be highly costly for the bacterium to alter the components of its membrane, which AMPs usually target. (4) Despite their potential as drug candidates, their application has been hindered by several obstacles, one of them being low selectivity for bacterial cells over mammalian cells.

Head-to-tail cyclic tetrapeptides isolated from natural sources are attractive lead compounds due to their small size and a diverse biological activity. They are found to have, among others, anticancer- (e.g., inhibitors of histone deacetylase) and antibacterial properties. (5) One interesting example is a recently discovered AMP teixobactin, a macrocyclic natural product, which contains a cyclotetradepsipeptide structural motif. This antibiotic exhibits a potent activity against several Gram-positive pathogenic bacteria. (6)

2. Peptide design and synthesis

To study more closely factors influencing selectivity of small cyclic peptidomimetics, we synthesised a series of cyclic tetrapeptides, containing a halogenated α,α-disubstituted $\beta^{2,2}$-amino acid with two 4-trifluoromethyl-benzyl substituents on the α-carbon**.** (**Figure 1**) In a previous work done by our group, this particular $\beta^{2,2}$-amino acid was incorporated in a tetrapeptide scaffold c(Lys-$\beta^{2,2}$-Xaa-Lys), where Xaa stands for one of the four residues: Lys, Gly, Ala, or Phe. (7) The resulting cyclic peptides had relatively high potency and they were active against multidrug-resistant bacterial strains. Therefore, we decided to use the same achiral lipophilic residue $\beta^{2,2}$ in a similar tetrapeptide scaffold c(Lys-$\beta^{2,2}$-Leu-Lys) which enabled us to study effects of amphipathicity and *L*- to *D*-amino acid substitution on peptide antimicrobial and haemolytic properties.

Synthesis of the Fmoc-$\beta^{2,2}$ amino acid building block

The α,α-disubstituted $\beta^{2,2}$-amino acid containing two 4-(trifluoromethyl)benzyl sidechains, termed $\beta^{2,2}$, was synthesised following the protocol described by Paulsen *et al.* (**Figure 1**) (8) In brief the initial dialkylation of methyl cyanoacetate with 1-(bromomethyl)-4-(trifluoromethyl)benzene using 1,8-diazabicyclo-[5.4.0]undec-7-ene (DBU) as a base was followed by nitrile reduction with H_2 (g)/Raney Nickel. The resulting $\beta^{2,2}$-amino ester was hydrolysed with lithium hydroxide (LiOH) pre-dissolved in water. After pH adjustment to 8, the final step included the protection of the free amine by subsequent addition of *N*-(9-fluorenylmethoxy-carbonyloxy) succinimide (Fmoc-OSu). The reactions were followed by thin layer chromatography (TLC) using Silica gel 60 F_{254} (Merck TLC plates) and visualised with either UV light (254 nm) or by immersion in potassium permanganate after light heating of the plates with a heating gun.

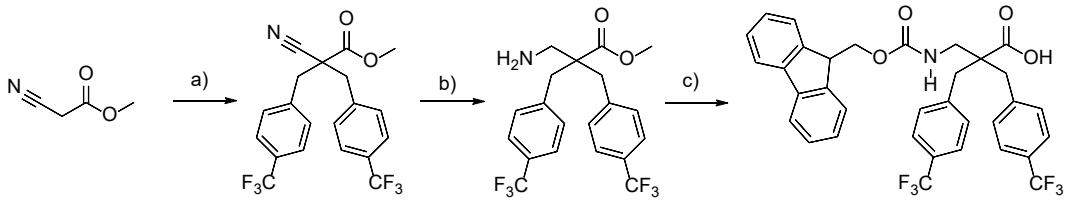

Figure 1. Synthesis of the $\beta^{2,2}$-amino acid building block by (a) $CF_3C_6H_4CH_2Br$, DBU, CH_2Cl_2, r.t.; (b) H_2 (g)/Raney-Nickel, EtOAc, 45 °C, 18 h; (c) i. LiOH, dioxane:water (4:1) reflux, 5 h, ii. aq. HCl to pH 8 then Fmoc-OSu, r.t. 18 h. (8)

Synthesis of cyclic tetrapeptides

A series of nine cyclic tetrapeptides was synthesised by Fmoc-solid phase peptide synthesis (Fmoc-SPPS) using a preloaded 2-Cl-trityl resin and microwave assisted peptide coupling. (**Figure 2**) Fully side chain protected peptides were cleaved from the resin with hexafluoroisopropanol (HFIP). Head-to-tail cyclisation was performed under *pseudo-high dilution* conditions as described by Malesevic *et al*. (9) This involved using a mechanical pump with two syringes, enabling slow addition (0.01 mL/min) of a pre-dissolved peptide, a coupling reagent PyBOP (benzotriazolyloxy-tris[pyrrolidino]-phosphonium hexafluorophosphate) and a base *N,N*-diisopropylethylamine (DIEA). Upon completion of the cyclisation reaction, the side chain protecting groups were cleaved using a trifluoroacetic acid (TFA) based cleavage cocktail, and the peptides were precipitated in diethyl ether before purification by reversed-phase high performance liquid chromatography (RP-HPLC). After lyophilisation the cyclic tetrapeptides were characterised by high-resolution mass spectrometry (HRMS) and nuclear magnetic resonance spectroscopy (NMR). Purity was determined to be >95% by reversed phase-ultra performance liquid chromatography (RP-UPLC). All peptides were tested for antimicrobial activity against the Gram-positive bacteria *Bacillus subtilis, Corynebacterium glutamicum, Staphylococcus aureus,* and *Staphylococcus epidermidis,* and the Gram-negative bacteria *Escherichia coli* and *Pseudomonas aeruginosa.* Haemolytic toxicity was determined against human red blood cells (RBCs) as a measure of toxicity.

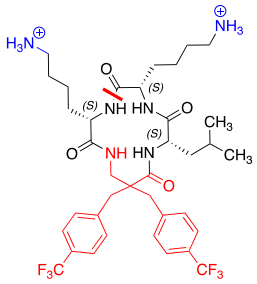

001
c(**Lys**-β^{2,2}-Leu-**Lys**)

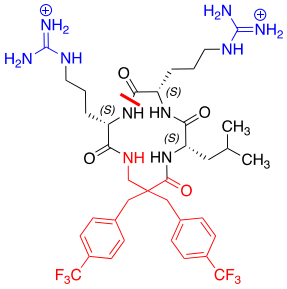

002
c(**Arg**-β^{2,2}-Leu-**Arg**)

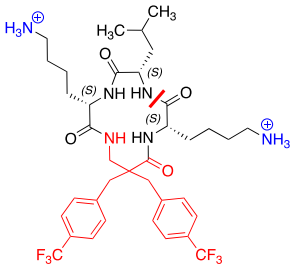

003
c(**Leu**-Lys-β^{2,2}-Lys)

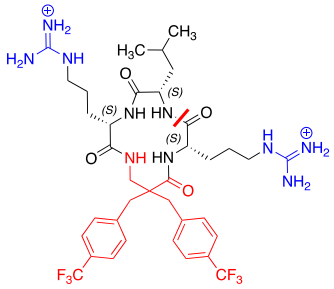

004
c(**Leu**-Arg-β^{2,2}-Arg)

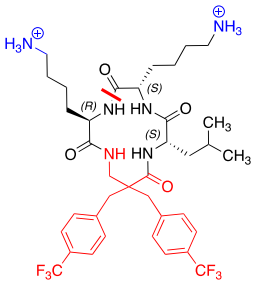

011
c(***D*-Lys**-β^{2,2}-Leu-Lys)

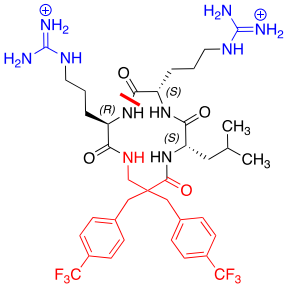

021
c(***D*-Arg**-β^{2,2}-Leu-Arg)

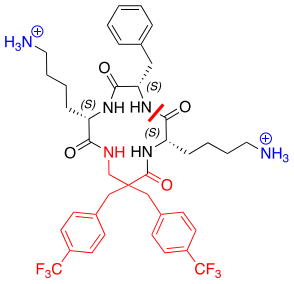

031
c(**Phe**-Lys-β^{2,2}-Lys)

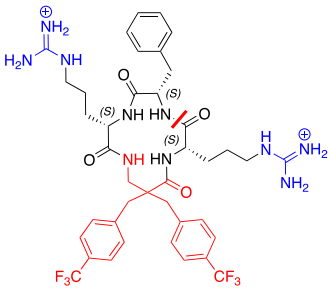

041
c(**Phe**-Arg-β^{2,2}-Arg)

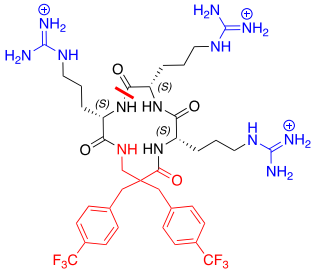

006
c(Arg-β^{2,2}-Arg-**Arg**)

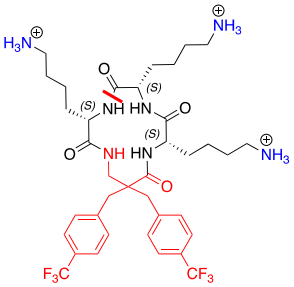

5a*
c(Lys-β^{2,2}-Lys-**Lys**)

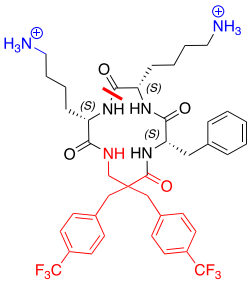

5d*
c(Lys-β^{2,2}-**Phe**-Lys)

Figure 2. Structures of the cyclic tetrapeptides screened for antimicrobial activity and haemolytic toxicity. The red line in the structures shows the site of head-to-tail cyclisation. In the peptide sequences key modifications are shown in **bold**. * Compounds synthesised by Paulsen *et al*. (7)

3. **Results and discussion**

Antimicrobial activity and haemolytic toxicity

The sequence of the first peptide synthesised in this study **001** c(**Lys**-$\beta^{2,2}$-Leu-**Lys**) was based on the previously reported highly potent cyclic tetrapeptide **5d** c(Lys-$\beta^{2,2}$-**Phe**-Lys) (MIC 0.1 – 4 μg/mL). (**Figure 2**) (7) As we initially wanted to investigate how the reduction in the overall lipophilic bulkiness affects peptides and their haemolytic properties, we synthesised the first peptide in this series **001** by substituting a Phe-residue in the sequence of **5d** with Leu. Although the cyclic tetrapeptide **001** was somewhat less potent than its parent peptide **5d**, it had good antimicrobial activity against both Gram-positive bacteria (MIC 2 – 4 μg/mL) and Gram-negative bacteria (MIC 4 – 8 μg/mL). (**Table 1**) In addition, **001** was less haemolytic (EC_{50} 105 μg/mL) than the previously reported peptide **5d** (EC_{50} 88 μg/mL). Since there was no major change in bioactivity following the substitution of a Phe-residue in **5d** with Leu, the cyclic tetrapeptide **001** became a suitable model peptide for our further investigations.

To study the effect of different cationic groups, the Lys-residues in the sequence of **001** were replaced by Arg, resulting in **002** c(**Arg**-$\beta^{2,2}$-Leu-**Arg**). The cyclic tetrapeptide **002** displayed similar antimicrobial activity to **001** against both Gram-positive (MIC 2 – 4 μg/mL) and Gram-negative (MIC 4 – 8 μg/mL) bacteria, but surprisingly **002** was considerably more haemolytic (EC_{50} 33 μg/mL). Thus, the cationic guanidine groups in **002** were clearly unfavourable with respect to RBC toxicity when compared to the primary amines of the Lys-residues in **001**.

In the next two cyclic tetrapeptides, **003** c(**Leu**-Lys-$\beta^{2,2}$-Lys) and **004** c(**Leu**-Arg-$\beta^{2,2}$-Arg), the amphipathicity was interrupted compared to the amphipathic peptides **001** and **002.** (**Figure 1**) Both cyclic tetrapeptides **003** and **004** had a sequence of alternating cationic and lipophilic residues, in which **003** contained two cationic Lys-residues, whereas **004** contained two cationic Arg-residues. Our results showed that antimicrobial activity against Gram-positive bacteria was slightly reduced for the Lys-containing non-amphipathic peptide **003** (MIC 2 – 8 μg/mL) but maintained for the Arg-containing non-amphipathic peptide **004** (MIC 2 – 4 μg/mL). A major reduction in antimicrobial activity was, however, observed for **003** against Gram-negative bacteria (MIC 32 – 64 μg/mL), and for **004** (MIC 8 – 32 μg/mL). This reduction was especially prominent against *P. aeruginosa*. Interestingly, haemolytic toxicity was considerably reduced for both peptides, with **003** being non-haemolytic (EC_{50} >492 μg/mL), whereas **004** exhibited low haemolytic toxicity (EC_{50} 215 μg/mL). Thus, interruption of amphipathicity had in general little effect on antimicrobial activity against Gram-positive bacteria, while activity against Gram-negative bacteria, as well as haemolytic toxicity, were considerably reduced.

To assess the cell selectivity of the peptides, a selectivity index was calculated as the ratio of the haemolytic toxicity (EC_{50}) to the geometric mean (GM_{Tot}) of the MIC values against all bacterial strains (i.e., $SI = EC_{50}/GM_{Tot}$). (**Table 1**) By interrupting amphipathicity, the selectivity for bacteria compared to mammalian RBCs increased, namely non-amphipathic cyclic tetrapeptides **003** and **004** displayed approx. SI: 50, whereas the SI for their amphipathic counterparts **001** (SI: 30) and **002** (SI: 9) were considerably lower.

To investigate the effects of changes in stereochemistry, a *D*-Lys analogue of **001** and a *D*-Arg analogue of **002** were synthesised. As shown in **Figure 2**, incorporation of a single *D*-residue resulted in **011** c(***D*-Lys**-$\beta^{2,2}$-Leu-Lys) and **021** c(***D*-Arg**-$\beta^{2,2}$-Leu-Arg) having the side chains of their two cationic residues pointing below and above the plane of the cyclic tetrapeptide scaffold. Although no major change in antimicrobial activity was observed compared to their corresponding all-*L* analogues, the striking difference was again observed regarding their toxicity towards human RBCs. Namely, both

D-Lys analogue **011** (EC_{50} 426 μg/mL, SI: 75) and *D*-Arg analogue **021** (EC_{50} 181 μg/mL, SI: 64) were considerably less haemolytic than their all-*L* analogues, and thus had high SI values.

To further study the effects of increasing overall bulkiness, we decided to use the two cyclic tetrapeptides **003** c(**Leu**-Lys-$\beta^{2,2}$-Lys) and **004** c(**Leu**-Arg-$\beta^{2,2}$-Arg) with interrupted amphipathicity as templates, since both peptides showed more favourable haemolytic properties than their amphipathic counterparts **001** and **002**. This was achieved by Leu to Phe substitution in the sequences of **003** and **004**, resulting in **031** c(**Phe**-Lys-$\beta^{2,2}$-Lys) and **041** c(**Phe**-Arg-$\beta^{2,2}$-Arg), respectively. It can be noted that **031** was also a non-amphipathic analogue of the previously reported cyclic tetrapeptide **5d** c(Lys-$\beta^{2,2}$-**Phe**-Lys). (**Figure 2**) (7)

For both the Phe-containing cyclic tetrapeptides **031** and **041**, this structural change resulted in a generally improved antimicrobial activity compared to their respective Leu-analogues, **003** and **004**. The non-amphipathic cyclic tetrapeptide **031** displayed MIC 1 – 8 μg/mL against Gram-positive bacteria, while **041** had MIC values in the range of 0.3 – 2 μg/mL. (**Table 1**) For these Phe-analogues, compared to **003** and **004**, improved antimicrobial activity was also obtained against Gram-negative bacteria, **031** (MIC 16 – 32 μg/mL) and **041** (MIC 4 – 16 μg/mL). Thus, for both peptides **031** and **041** substitution of Leu with Phe was shown to be beneficial regarding their antimicrobial potency.

As for haemolytic toxicity, the Lys containing cyclic tetrapeptide **031** remained non-haemolytic (EC_{50} >509 μg/mL), which resulted in a very high SI: 90. However, for the Arg containing cyclic tetrapeptide **041** this modification had an unfavourable effect on its haemolytic properties, as it was nearly 2-fold more haemolytic **041** (EC_{50} 116 μg/mL) than **004** (EC_{50} 215 μg/mL). Still, **041** had an acceptable high SI: 56 due to its high antimicrobial activity against Gram-positive bacteria and *E. coli*.

When compared to its previously reported amphipathic analogue **5d**, the cyclic tetrapeptide **031** was less potent, especially against Gram-negative bacteria. These two analogues differed more with respect to haemolytic toxicity, namely the non-amphipathic cyclic tetrapeptide **031** was non-haemolytic (EC_{50} >509 μg/mL), whereas **5d** was reported to be highly haemolytic (EC_{50} 88 μg/mL). (7) Thus, interruption of amphipathicity may be a promising strategy for reducing haemolytic toxicity of such short cyclic peptides.

The overall most potent analogue prepared in this study was the cyclic tetrapeptide **006** c(Arg-$\beta^{2,2}$-Arg-**Arg**). It exhibited very high antimicrobial activity against both Gram-positive (MIC 1 – 2 μg/mL) and Gram-negative bacteria (MIC 2 – 4 μg/mL). In addition, this analogue, which had three Arg-residues and a net charge of +3, was shown to have very low haemolytic toxicity (EC_{50} 279 μg/mL) and was thereby the most selective cyclic tetrapeptide prepared with SI: 176. Compared to the previously synthesised analogue **5a** c(Lys-$\beta^{2,2}$-Lys-**Lys**), with three Lys-residues, **006** was equally potent against Gram-positive bacteria while being more potent against Gram-negative bacteria. (7) Despite having the same net charge (+3) and lipophilic $\beta^{2,2}$-residue, there was a difference in RBC toxicity, with **006** being more haemolytic (EC_{50} 279 μg/mL) than **5a** (EC_{50} >500 μg/mL). These results confirmed the general pattern in which Lys-containing cyclic tetrapeptides were less haemolytic than their Arg-containing analogues.

In summary, the results of this study indicate that changes in stereochemistry of one cationic residue, as well as amphipathicity, in the above-described tetrapeptide scaffold, could serve as useful strategies in reducing haemolytic toxicity of resultant peptides. In addition, substitution of Leu with bulkier Phe-residue could improve antimicrobial activity, although its effect on haemolytic toxicity may vary.

Table 1. Antimicrobial activity (MIC in µg/mL), haemolytic toxicity against human RBCs (EC_{50} in µg/mL) and selectivity index (SI). The SI was calculated as the ratio between haemolytic toxicity (EC_{50}) and the geometric mean (GM_{Tot}) of the MIC values against all bacterial strains, i.e., $SI = EC_{50} / GM_{Tot}$. In the peptide sequences key modifications are shown in bold.

					Gram-positive bacteria[1,5]				Gram-negative bacteria		RBC	GM_{Tot}	SI
Entry	**Sequence**	**Mw[2]**	**Charge[3]**	**Rt[4]**	***Bs***	***Cg***	***Sa***	***Se***	***Ec***	***Pa***	**[ug/mL]**	**G+, G-**	**RBC/GM_{Tot}**
001	c(**Lys**-β[2,2]-Leu-**Lys**)	756.8	+2	6.23	2	2	4	4	4	8	105	3.6	30
002	c(**Arg**-β[2,2]-Leu-**Arg**)	812.9	+2	6.38	2	2	4	4	4	8	33	3.6	9
003	c(**Leu**-Lys-β[2,2]-Lys)	756.8	+2	5.30	4	2	8	8	32	64	>492	10.1	49
004	c(**Leu**-Arg-β[2,2]-Arg)	812.9	+2	5.46	2	2	4	2	8	32	215	4.5	48
011	c(***D*-Lys**-β[2,2]-Leu-Lys)	756.8	+2	6.07	4	2	8	8	8	8	426	5.7	75
021	c(***D*-Arg**-β[2,2]-Leu-Arg)	812.9	+2	6.18	1	4	2	2	4	8	181	2.8	64
031	c(**Phe**-Lys-β[2,2]-Lys)	790.9	+2	5.33	2	1	8	4	16	32	>509	5.7	90
041	c(**Phe**-Arg-β[2,2]-Arg)	846.9	+2	5.47	1	0.3	2	2	4	16	116	2.1	56
006	c(Arg-β[2,2]-Arg-**Arg**)	855.9	+3	5.08	1	2	1	1	2	4	279	1.6	176
5a*	c(Lys-β[2,2]-Lys-**Lys**)	771.8	+3	-	-	2	1	-	8	8	>500	-	-
5d*	c(Lys-β[2,2]-**Phe**-Lys)	790.8	+2	-	-	0.1	2	-	4	2	88	-	-
Polymyxin B[2]*		1301.6	+5		3.1	3.1	12.5	6.3	3.1	3.1	-	-	-
Chlorhexidine[2]*		505.5	+2		1.6	0.8	1.6	1.6	1.6	6.3	-	-	-

[1] Microbial strains; Bs – *Bacillus subtilis*, Cg – *Corynebacterium glutamicum*, Sa – *Staphylococcus aureus*, Se – *Staphylococcus epidermidis,* Ec – *Escherichia coli*, Pa – *Pseudomonas aeruginosa.* [2] Average molecular mass without including a TFA salt for each cationic charge. [3] Net charge at physiological pH (7.4). [4] Lipophilicity measured as retention time (Rt; min) on a RP-UPLC C_{18} column using a linear acetonitrile/water gradient. ''-'' : not tested/not calculated. * Original MIC and RBC values can be found in Paulsen *et al*.(7) [2]* Original MIC values for Polymyxin B and Chlorhexidine can be found in Dey *et al*. (10)

Retention time as with antimicrobial activity and haemolytic toxicity

Next, we wanted to ascertain if there was a correlation between retention time (Rt) values with both antimicrobial activity (GM_{Tot}) and haemolytic toxicity of the synthesised cyclic tetrapeptides. (**Figure 3**) As shown in **Figure 3**, the Arg cyclic tetrapeptides (orange line in **Figure 3**), which eluted later, were more potent and haemolytic than the cyclic Lys tetrapeptides (blue line in **Figure 3**).

Both Lys-containing peptide **001** and its Arg-analogue **002** had MIC values in the same range. However, the latter, **002** had a longer Rt and was thereby seemingly more lipophilic than **001,** what might explain the observed higher haemolytic toxicity of **002**.

The two non-amphipathic Lys analogues, Leu-containing **003** and Phe-containing **031** displayed close to identical retention times, but as mentioned previously, the analogue with a bulkier Phe-residue, **031** was in general more potent against tested bacterial strains. As both peptides were non-haemolytic, a correlation with their corresponding Rt values could not be determined.

Similarly, the non-amphipathic Arg-analogues, Leu-containing **004** and Phe-containing **041** had similar Rt, however, the latter **041** had slightly higher antimicrobial potency with increased haemolytic toxicity. Our data suggest that even minute difference in Rt values, and therefore in relative hydrophobicity (as observed for **003/031** and **004/041**), could serve as an indicator of significant changes in peptide antimicrobial and haemolytic properties.

The substitution of *L*-Lys in **001** with *D*-Lys, resulted in a diastereomer **011** with slightly lower potency and reduced haemolytic toxicity. Much greater reduction in haemolytic toxicity was observed for Arg-containing diastereomer **021**, which had very similar potency to its *L*-Arg analogue **002**. Both *D*-Lys and *D*-Arg containing tetrapeptides had slightly shorter retention times, which could be correlated with lower haemolytic toxicity and greater selectivity. Of note, **002** had the longest Rt of all synthesised tetrapeptides.

The most potent, hydrophilic tetrapeptide containing three Arg-residues, **006** had the shortest retention time of all synthesised analogues, indicating its more hydrophilic character. It had low haemolytic toxicity (EC_{50} 279 µg/mL) and the highest selectivity of all synthesised peptides (SI: 176). Compared to its Lys-analogue **5a**, it was more haemolytic, but with improved activity against Gram-negative bacteria.

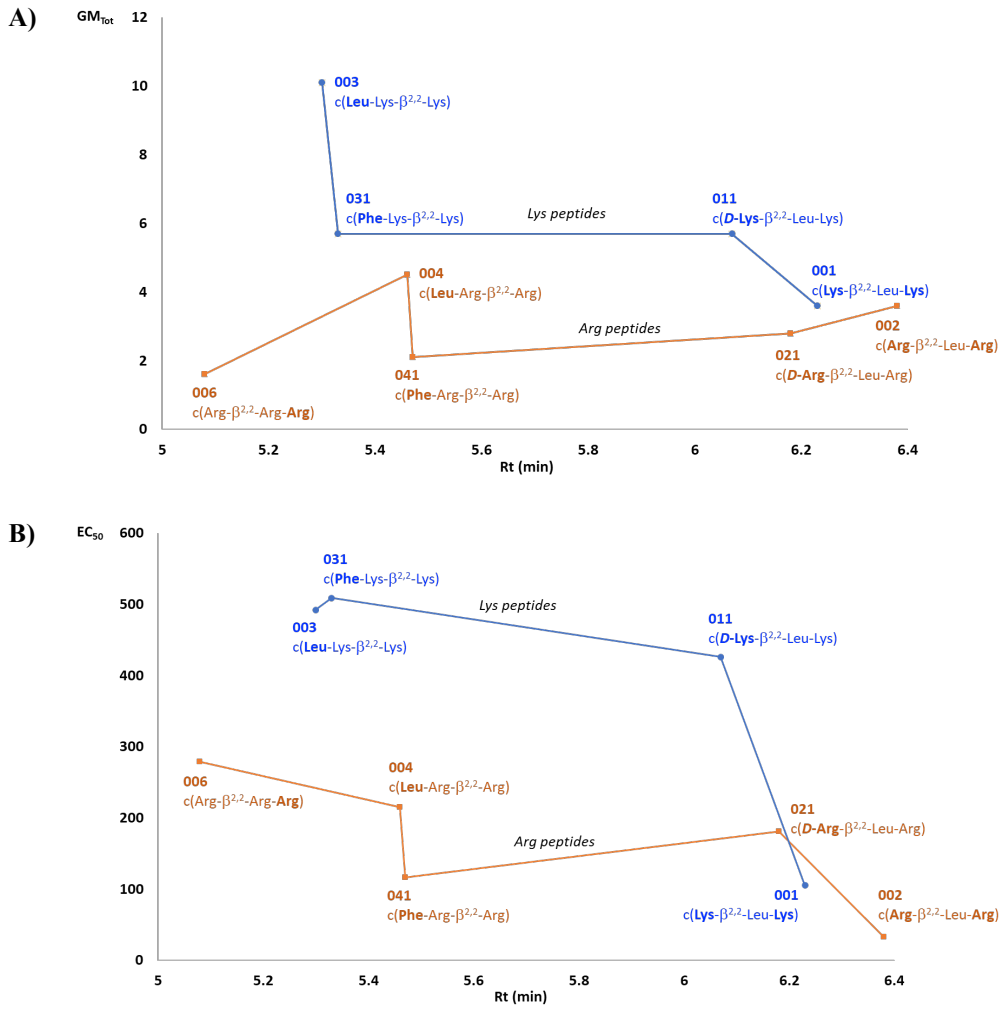

Figure 3. Comparison of retention time (Rt) with **A)** geometric mean (GM_{Tot}) of antimicrobial activity and **B)** haemolytic toxicity (EC_{50}) for Lys (blue) and Arg (orange) cyclic tetrapeptides.

Conformational analysis by NMR

In general, cyclic tetrapeptides with 12-membered backbone have a high ring strain, which makes them notoriously hard to synthesise. (11) However, introduction of a thirteenth atom into the ring structure by using a $\beta^{2,2}$-amino acid residue, alleviates some of the strain, making the synthesis of such small cycles easier, and the ring structure accordingly more flexible. It is also important to note that different cyclic tetrapeptides will also have very similar backbone conformations. In the present work five peptides **001** c(**Lys**-$\beta^{2,2}$-Leu-**Lys**), **002** c(**Arg**-$\beta^{2,2}$-Leu-**Arg**), **003** c(**Leu**-Lys-$\beta^{2,2}$-Lys), **011** c(***D***-**Lys**-$\beta^{2,2}$-Leu-Lys), and **021** c(***D***-**Arg**-$\beta^{2,2}$-Leu-Arg) were selected for conformational analysis by NMR to investigate the extent to which the observed effects of changes in sequence and stereochemistry were accompanied by induced changes in the backbone conformation. For simplicity of comparison in the conformational analysis, the amino acids in the cyclic tetrapeptides were numbered according to **Figure 4**, with the $\beta^{2,2}$-amino acid always being the fourth amino acid residue.

Figure 4. Amino acid sequence numbering for backbone analysis by NMR.

Secondary chemical shifts are a well-documented method for predicting secondary structure of peptides and proteins. (12-15) By comparing the experimental chemical shifts of the backbone to random coil chemical shifts from the literature, it is possible to estimate the α-helix-, β-sheet-, or random coil character of each residue. (14-16) Positive values indicate an α-helical character, negative numbers indicate β-sheet character, while values close to zero indicate random coil.

However, due to the tetrapeptides being cyclic and including a non-native amino acid residue, we had to make certain modifications to the procedure. The predicted random coil chemical shifts are estimated from random coil values of peptides with only native amino acids in linear peptides. (16) Therefore, we have treated the cyclic tetrapeptides as linear peptides for this analysis. Additionally, it is known that aromatic residues have a long-range effect on chemical shifts, especially on protons. (13) To mimic this effect from the $\beta^{2,2}$-amino acid, we have flanked amino acids 1-3 with two phenylalanines on each side (H_2N-F-F-X_1-X_2-X_3-F-F-Ac). With these modifications, as well as the small sample size of the tetrapeptides, we note that the secondary structure cannot be accurately divided into α-, β-, or random coil character by this method. We can, however, use it to accurately compare the cyclic tetrapeptides, to investigate if there are any clear deviations in the backbone conformation.

Using the secondary chemical shift values as a probe for structural change, our results showed that changes in the sequence and/or stereochemistry of the cyclic tetrapeptides did not induce any consistent and significant changes to the backbone conformation. (**Figure 5**) No major backbone conformational shift was identified by secondary chemical shifts as a response to the different sequence and/or stereochemistry of the studied peptides – a result which is consistent with the expected rigidity of the tetrapeptide ring.

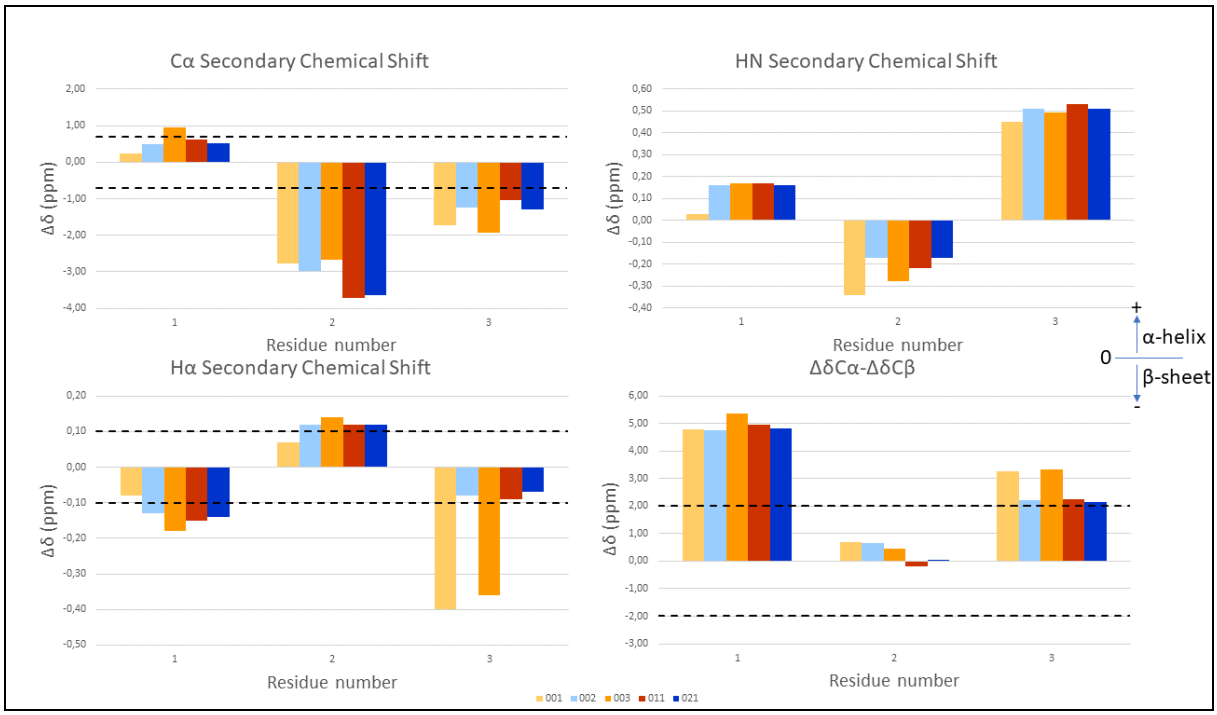

Figure 5. Comparison of the secondary chemical shift of the five peptides **001** c(**Lys**-$\beta^{2,2}$-Leu-**Lys**), **002** c(**Arg**-$\beta^{2,2}$-Leu-**Arg**), **003** c(**Leu**-Lys-$\beta^{2,2}$-Lys), **011** c(***D*-Lys**-$\beta^{2,2}$-Leu-Lys), and **021** c(***D*-Arg**-$\beta^{2,2}$-Leu-Arg) by residue. The chemical shift analysis was performed by using random coil values by Kjaergaard *et al*. (16) with corresponding correction values. Dashed lines indicate cut-off values for the identification of secondary structure elements, as defined by Wishart *et al*. (17) The figure was based on the analysis of Farina *et al*. (12) The Arg containing peptides **002** and **021** are listed in hues of blue, while the Lys containing peptides **001**, **003**, and **011** are in hues of orange. A positive Δδ indicates α-helix, a negative value indicates β-sheet, while values close to zero indicate random coil.

Cross-relaxation rates and coupling constants were used as direct secondary probes for conformational change in order not to fully rely on chemical shifts models based on native proteins. The NOE build-ups were extracted from NOESY experiments for the Arg containing cyclic tetrapeptides (**002** and **021**). However, for the Lys containing cyclic tetrapeptides (**001**, **003**, and **011**), ROESY had to be used due to intermediate tumbling rates of these peptides. The spectra were analysed in TopSpin Dynamics Center. Experiments with increasing mixing times were recorded, and integrals from the linear phase were used (typically 200 ms for NOESY, and 100 ms for ROESY). All integrals were referenced to the ortho aromatic protons of the $\beta^{2,2}$-amino acid residue, defined as a reference distance of 2.46 Å, and cross-checked against the ortho aromatic protons of the other benzene ring, as well as the stereotopic geminal α-protons of the same amino acid (defined as 1.75 Å). (18) As seen in **Figure 6**, the calculated NOE distances showed that the backbone conformation did not change significantly between the different peptides, neither as a response to the order of amino acids nor by the introduction of a *D*-amino acid residue into the sequence.

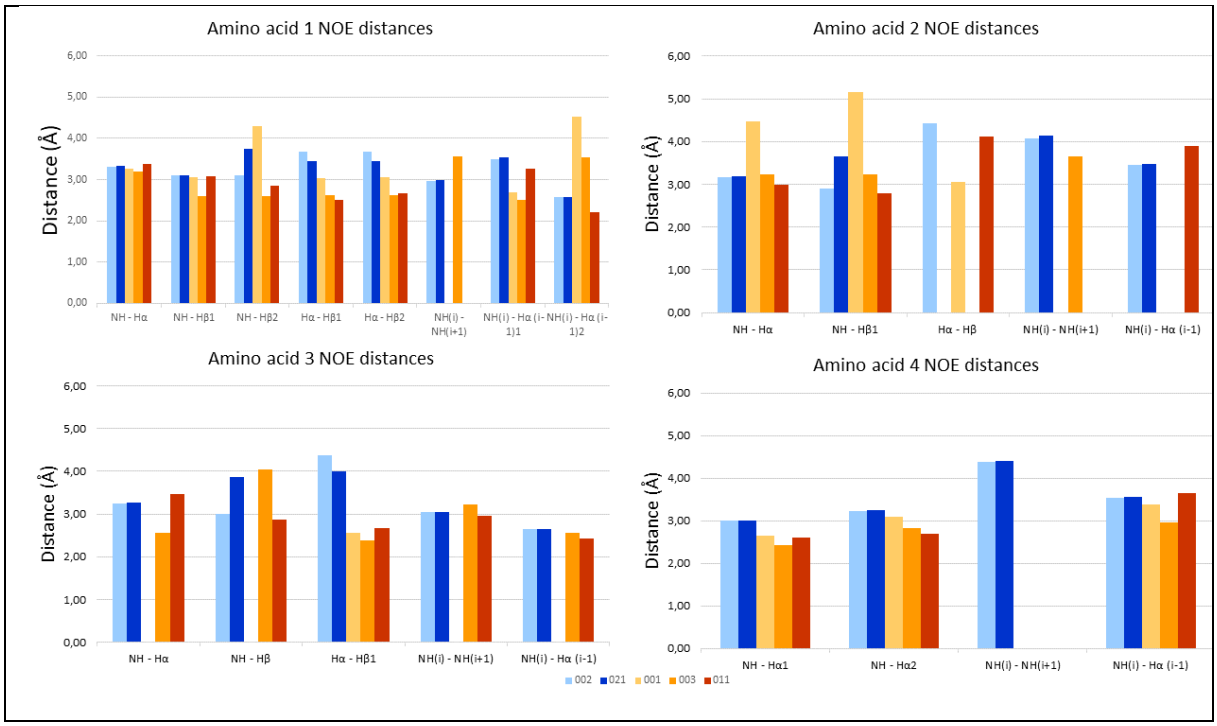

Figure 6. ^{1}H-^{1}H distances of the backbone found by Nuclear Overhauser Effect (NOE) analysis. The Arg containing peptides **002** and **021** are listed in hues of blue, while the Lys containing peptides **001**, **003**, and **011** are in hues of orange.

The ^{1}H-^{1}H J-coupling constants were analysed, both through 1D ^{1}H NMR coupling patterns and E.COSY. Water suppression and overlap made some couplings difficult to assess in 1D ^{1}H NMR, while the splitting pattern in E.COSY were unresolved for some of the signals. The coupling constants that could be extracted were mostly consistent between the five peptides, and in agreement with the secondary chemical shifts and cross-relaxation rates, showing no significant changes in backbone conformation between the peptides. (**Table 2**)

Table 2. ^{1}H-^{1}H J-coupling constants, as measured by 1D ^{1}H NMR. The residues follow the same numbering system as with the rest of the conformation assignment. The linewidth of **002** was too broad to get any measurements, most likely due to aggregation.

1D ^{1}H coupling constants (Hz)											
	1			2			3			4	
	NH - Hα	Hα - Hβ1	Hα - Hβ2	NH - Hα	Hα - Hβ1	Hα - Hβ2	NH - Hα	Hα - Hβ1	Hα - Hβ2	NH - Hα1	NH - Hα2
001	5.47	7.10	9.63	8.89	7.32	9.48	8.12	5.44	10.40	8.84	3.64
003	4.95	2.48	8.11	7.52	8.07	8.31	7.46	4.58	11.61	8.72	3.41
011	4.95	2.31	9.29	9.56	6.55	10.38	6.22	4.56	7.59	9.49	2.95
021	4.99	7.50	9.50	9.68	8.71	6.97	6.56	5.70	9.19	9.26	2.75

In conclusion, secondary chemical shifts, NOE distances, and J-coupling constants did not indicate any major changes in backbone conformation between the peptides. Thus, we can be confident that the side chains of the amino acids point in the expected directions when comparing peptide for peptide, as discussed in the SAR section above.

Interaction studies with SPR

Next, we tested the ability of the cyclic tetrapeptides to interact with lipid vesicles by surface plasmon resonance (SPR). For this, we used dimyristoylphosphatidylcholine (DMPC) vesicles without and with 10% (w/w) *E. coli* O111:B4 lipopolysaccharides (LPS). Pure DMPC vesicles represent a general zwitterionic bilayer of the human cell plasma membrane, while LPS-loaded vesicles mimic the outer membrane of Gram-negative bacteria. (19) By using a method developed by Figuera *et al.* and modified by Jakubec *et al.* we were able to measure the lipid partitioning (K_P) and dissociation rate (k_{off}) of individual cyclic tetrapeptides into the lipid bilayer. (20, 21) K_P is calculated as the ratio of the peptide concentration in lipid environment over peptide concentration in water (K_P = [$peptide_{lipid}$] / [$peptide_{H2O}$]). Thus, higher K_P indicates a preference of the cyclic tetrapeptides for the lipid environment, whereas k_{off} represents the dissociation speed, where higher speed indicates a faster release from the lipid bilayer, that is, low retention.

The most lipophilic peptide and with highest preference for the DMPC lipid environment was the *D*-Arg cyclic tetrapeptide **021** c(***D*-Arg**-$\beta^{2,2}$-Leu-Arg), with more than four times higher K_P than the *L*-Arg variant **002** c(**Arg**-$\beta^{2,2}$-Leu-**Arg**). (**Figure 7a** [full bars]) This radical change in lipophilicity could not be explained by changes in the backbone structure, as shown by NMR. However, it is possible that a simple change in stereochemistry by *L*- to *D*-amino acid substitution allowed for a more favourable orientation of these cationic side chains. Similar improvement, albeit with smaller changes, was also observed for the Lys variants, **011** c(***D*-Lys**-$\beta^{2,2}$-Leu-Lys) and **001** c(**Lys**-$\beta^{2,2}$-Leu-**Lys**), suggesting similar changes in charge distribution caused by cationic side chain orientation.

An interesting observation was the overall decrease in K_P of most cyclic tetrapeptides in the presence of LPS. (**Figure 7a** [empty bars]) LPS contains the fatty acid component lipid A, which has a negatively charged phospholipid headgroup and long oligosaccharide chains. (22) One of the roles of LPS in bacteria is the sequestration of potentially harmful compounds before they can reach the inner cytoplasmic membrane. (23) Thus, lower K_P for LPS-loaded vesicles can be viewed as a positive feature, indicating more efficient translocation of the cyclic tetrapeptides through the outer membrane. This could be recognised from the partitioning of the cyclic tetrapeptides **002** c(**Arg**-$\beta^{2,2}$-Leu-**Arg**) and **003** c(**Leu**-Lys-$\beta^{2,2}$-Lys). Both cyclic tetrapeptides had very similar K_P for DMPC vesicles. However, when LPS was present, the K_P of **003** was only slightly changed, whereas the K_P of **002** was reduced by more than a half. These observations suggested that the cyclic tetrapeptide **003** may be sequestered in the outer membrane and thus unable to reach its target, what in turn could explain the loss of activity against Gram-negative bacteria. In comparison, the more potent cyclic tetrapeptide **002** seemed able to cross the LPS bilayer unaffected. (**Figure 7a** [empty bars])

Contrary to K_P, the dissociation rate k_{off} was not affected by the presence of LPS as we measured bulk changes of dissociation. (**Figure 7b**) The fact that there was no change in k_{off} for DMPC:LPS mixtures, indicated that dissociation from LPS was much faster than from DMPC. Thus, it is the lipid environment, not the LPS, which commands k_{off} and it is responsible for major retention of the cyclic tetrapeptides in the vesicles. This retention of peptides in the bilayer can be a major source of disruption, directly reflected in the haemolytic toxicity of peptides. The cyclic tetrapeptide with the slowest dissociation rate, **002** was also the most haemolytic with EC_{50} 33 μg/mL, while the cyclic tetrapeptides with high k_{off} rate, i.e., low retention, **003**, **011** and **031** had lowest haemolytic toxicity.

In addition, SPR showed that peptides **002** and **041** had a significant deviation from the binding model for both types of vesicles. (**Figure 8**) This deviation suggested a cooperative mode of binding and possible interaction between monomers of the cyclic tetrapeptides themselves, such as formation of micelles or aggregation. (24) Similar deviation, although on a much smaller scale, was observed for peptides **001**, **004** and **021**. However, these changes were too small to be conclusive. Nevertheless, all

five cyclic tetrapeptides in these deviation models had very good antimicrobial activity, but some were also haemolytic. This, again points to a bigger bilayer disruption when this cooperation is present.

According to SPR results, the ideal antimicrobial cyclic tetrapeptide should have a good combination of high partitioning into the lipid bilayer with high enough k_{off} rate, which is still damaging to bacteria, but that does not negatively affect human RBCs.

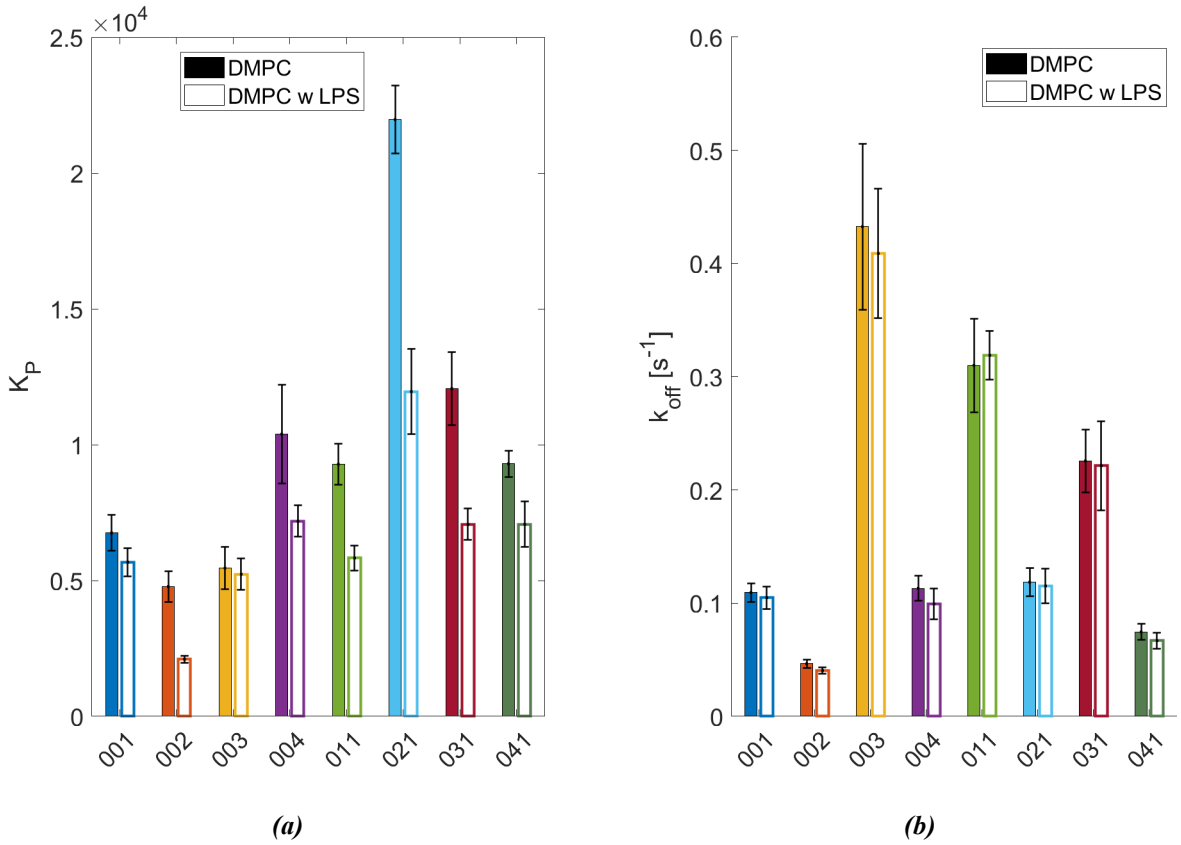

(a) *(b)*

Figure 7. Results from SPR analysis of the cyclic tetrapeptides. Partitioning constant K_P **(a)** and dissociation rate k_{off} **(b)** of the cyclic tetrapeptides towards DMPC vesicles without and with 10% (w/w) LPS marked by full and empty bars, respectively.

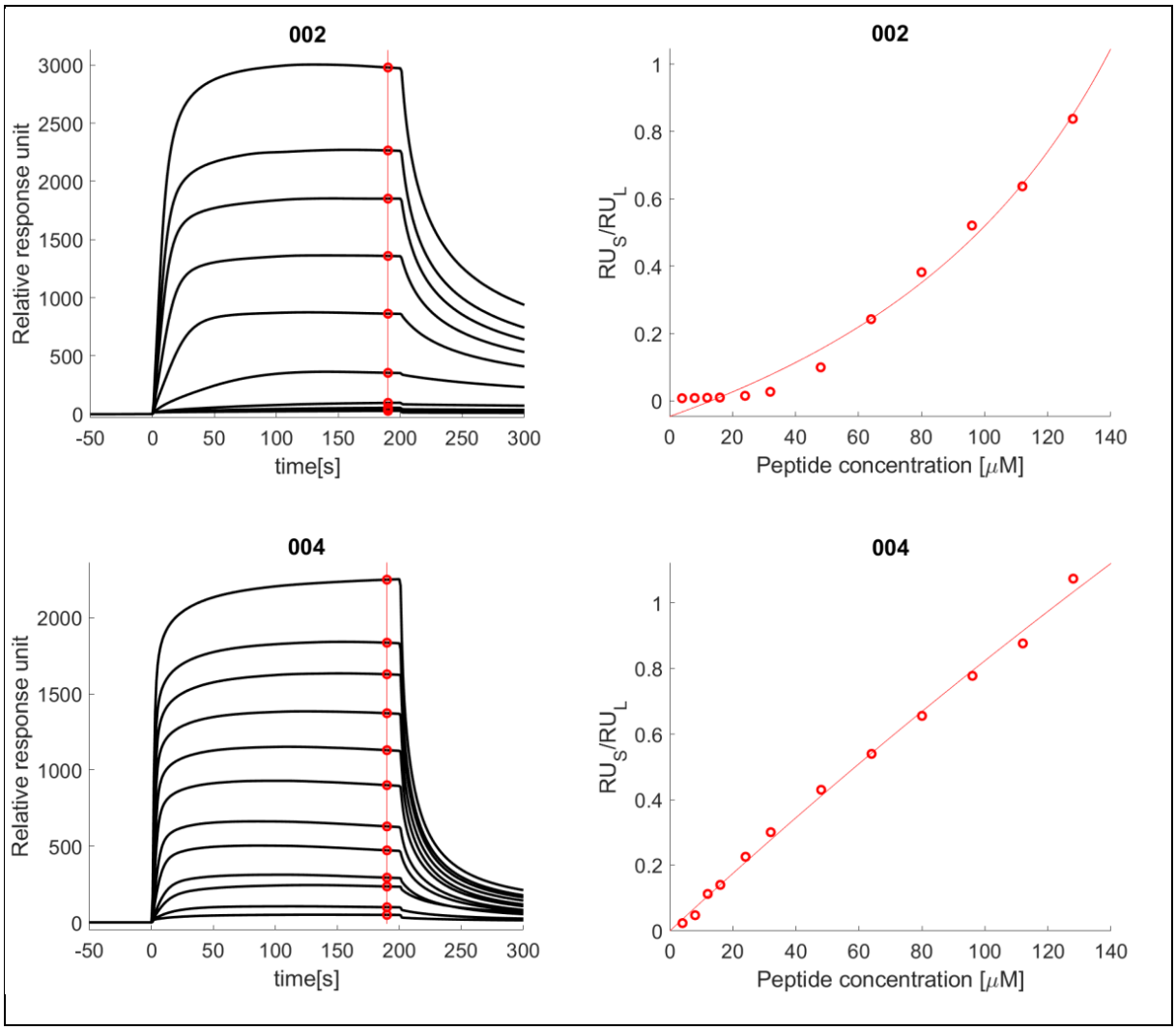

Figure 8. Example of cooperative (**002)** and noncooperative (**004)** binding towards DMPC vesicles. SPR traces of cyclic tetrapeptides are shown on the left (concentration from 4 to 128 μM) and K_P fitting on the right side.

4. Methods and materials

Chemicals

All reagents and solvents were purchased from commercial sources and used as supplied.

General protocol for linear peptide synthesis

The stepwise assembly of the linear peptides was performed using microwave assisted Fmoc solid phase peptide synthesis method at 0.22 mmol scale on preloaded 2-chlorotritylchloride resin (0.75 mmol/g for the resin with preloaded Lys, 0.54 mmol/g for the resin with preloaded Arg). The Fmoc group was removed with 20% piperidine in DMF. Peptide couplings were performed using the appropriate amino acid (3 equiv.), HCTU (3 equiv.) and DIPEA (6 equiv.). Prior to synthesis, all amino acids were dissolved in DMF (0.5M), whereas DIPEA was dissolved in NMP (2M). Microwave heating (75°C, 15 min) was applied during coupling of all amino acids, except for arginine, where coupling was done at room temperature for 60 min to avoid side reactions.

Cyclisation method

Upon completion of the synthesis, cleavage of the linear protected tetrapeptides from the 2-Chlorotrityl chloride resin was performed with the mixture of hexafluoropropanol-dichloromethane (HFIP:DCM, 3:7, v/v, 15 mL) for 45 min under slow stirring conditions, followed by two more cleavage rounds, each lasting 10 min. The collected peptide solution was evaporated under reduced pressure. Head-to-tail cyclisation was performed using modified procedure previously described by Malesevic *et al*. (9) To maintain microdilution conditions during cyclisation two 10 mL syringes were used. First syringe contained linear protected tetrapeptide (100 µmol) pre-dissolved in *N,N*-dimethylformamide (DMF, 10 mL). The second syringe was filled with a solution containing PyBOP (300 µmol), pre-dissolved in DMF (10 mL). Both syringes were fixed to the dual-syringe programmable pump and the flow rate was set to 0.01 mL/min. This enabled simultaneous, dropwise addition of both solutions into the flask which initially contained *N,N*-diisopropylethylamine (DIEA) (600 µmol), PyBOP (10 µmol) and DMF (10 mL). The reaction proceeded under constant stirring. Dimerisation was not observed using HRMS, although such observation was made in previous cyclisation attempts with much greater volumes of DMF. (7) After the cyclisation step, the reaction mixture was diluted with water (approx. 20 mL) prior to extraction with ethylacetate (2 x 10 mL). The organic phase was washed with 5% LiCl solution (3 x 20 mL) and brine (1 x 10 mL), before drying over Na_2SO_4. The organic phase was filtered and concentrated under vacuum. Upon addition of the cleavage cocktail containing TFA:TIS:H_2O (95:2.5:2.5, 5 mL) to the cyclic protected peptide, reaction mixture was left to stir for 3 hours prior to evaporation under reduced pressure. The crude peptide was washed with diethyl ether (3 x 20 mL) and again dried under vacuum prior to purification by RP-HPLC.

Peptide Purification by Preparative Reversed-Phase High-Performance Liquid Chromatography (RP-HPLC)

Purification of crude peptides was performed by RP-HPLC using a preparative SunFire C_{18} OBD, 5 µm, 19 × 250 mm column (Waters, Milford, MA, USA) at room temperature. The HPLC system (Waters) was equipped with a 2998 photodiode array (PDA) detector, a 2702 autosampler and an automated fraction collector. The peptides were purified using a linear gradient of eluent A (water with 0.1% TFA) and eluent B (acetonitrile with 0.1% TFA), ranging from 20–60% B, over 25 min. The flow rate was set at 10 mL/min. Purified fractions were collected and freeze-dried prior to further characterisation.

Purity Determination by Ultra-Performance Liquid Chromatography (UPLC)

The purity of the synthesised peptides was determined by an analytical UPLC-PDA H-class system (Waters, Milford, MA, USA). The analysis was performed on an Acquity UPLC BEH 1.7 µm, 2.1 ×100 mm C18 column, with a linear gradient of eluent A (water with 0.1% TFA) and eluent B (acetonitrile with 0.1% TFA), from 0.5–95.0% B over 10 min. The flow rate and the temperature of the column were set at 0.5 mL/min and 60 °C, respectively. A 2996 PDA detector was used to record the UV absorbance of the purified peptides at the wavelength range of 210–400 nm.

Peptide Characterisation by High-Resolution Mass Spectrometry (HRMS)

The characterisation of the purified peptides was performed by HRMS, using an Orbitrap Id-X Tribrid mass analyser equipped with an electrospray ionisation (ESI) source (Thermo Fischer Scientific, Waltham, MA, USA), with a Vanquish UHPLC system (Waters), coupled to an Acquity Premier BEH C_{18}, 1.7 µm, 2.1 × 100 mm column (Waters). Mass spectral acquisition was performed in positive ion mode. All samples were dissolved in 1 mL of Milli-Q water prior to analysis. The UHPLC was operated in a linear gradient with mobile phases A (water with 0.1% formic acid) and B (acetonitrile with 0.1% formic acid) from 0.5% – 95.0% B over 10 min, with a flow rate of 0.5 mL/min. The injection volume was 2 µL, and the column temperature was set to 60 °C.

Peptide Characterisation by Nuclear Magnetic Resonance spectroscopy (NMR)

The purified peptides were characterised by NMR using a Bruker Avance III HD spectrometer equipped with an inverse TCI probe cryogenically enhanced for ^{1}H, ^{13}C and ^{2}H operating at 600 MHz for proton. Experiments for assignment and verification were acquired in DMSO-d6, while experiments for conformation analysis were acquired in H_2O:D_2O 95:5 and D_2O. All experiments were acquired at 298 K, using standard pulse sequences from TopSpin 3.7.pl2, including 1H, 13C, HSQC, HMBC, H2BC, DQF-COSY, ROESY, NOESY, E.COSY and selective IPAP HSQMBC-TOCSY. Versions with presat or excitation sculpting, gradient selection and adiabatic pulses were used when applicable.

(3*S*,6*S*,9*S*)-3,6-Bis(4-aminobutyl)-9-isobutyl-12,12-bis(4-(trifluoromethyl)benzyl)-1,4,7,10-tetraazacyclotridecane-2,5,8,11-tetraone x TFA (001)

^{1}H NMR (600 MHz, DMSO-d_6) δ 8.39 (d, J = 8.3 Hz, 1H), 7.90 (d, J = 6.4 Hz, 1H), 7.69 (d, J = 8.2 Hz, 2H), 7.58 (d, J = 8.1 Hz, 4H), 7.54 (d, J = 8.7 Hz, 1H), 7.27 (d, J = 8.0 Hz, 2H), 6.46 (dd, J = 8.4, 3.2 Hz, 1H), 4.26 – 4.10 (m, 2H), 4.00 – 3.80 (m, 1H), 3.37 (dd, J = 13.4, 8.4 Hz, 1H), 3.15 (s, 1H), 3.09 (d, J = 14.2 Hz, 1H), 2.95 (d, J = 13.6 Hz, 2H), 2.81 – 2.71 (m, 4H), 2.66 (d, J = 13.8 Hz, 1H), 1.98 (dtd, J = 18.0, 9.1, 7.9, 4.7 Hz, 1H), 1.68 (tdt, J = 19.4, 9.7, 5.1 Hz, 1H), 1.61 (q, J = 7.7 Hz, 1H), 1.58 – 1.47 (m, 4H), 1.39 (ddd, J = 14.0, 8.8, 5.5 Hz, 1H), 1.35 – 1.18 (m, 3H), 0.91 (d, J = 6.6 Hz, 3H), 0.88 (d, J = 6.6 Hz, 3H).

^{13}C NMR (151 MHz, DMSO-d_6) δ 173.77, 172.37, 171.49, 170.48, 141.88, 141.58, 131.43, 130.92, 127.25 (q, J = 31.4 Hz), 127.17 (d, J = 31.4 Hz), 124.87 (q, J = 3.5 Hz), 124.73 (q, J = 3.4 Hz), 124.41 (q, J = 271.8 Hz), 124.36 (q, J = 271.8 Hz), 116.06, 54.55, 53.80, 52.73, 51.24, 42.84, 35.62, 30.46, 28.94, 26.52, 26.44, 24.33, 22.87, 22.66, 22.32, 21.43.

HRMS-ESI: $C_{37}H_{51}F_6N_6O_4^+$ $[M + H]^+$ calcd: 757,3871, found: 757,3872, UPLC purity 98%.

1,1'-(((3*S*,6*S*,9*S*)-9-Isobutyl-2,5,8,11-tetraoxo-12,12-bis(4-(trifluoromethyl)benzyl)-1,4,7,10-tetraazacyclotridecane-3,6-diyl)bis(propane-3,1-diyl))diguanidine x TFA (002)

^{1}H NMR (600 MHz, DMSO-d_6) δ 8.53 (d, J = 8.1 Hz, 1H), 7.99 (d, J = 6.3 Hz, 1H), 7.69 (d, J = 7.9 Hz, 3H), 7.64 (t, J = 5.4 Hz, 1H), 7.61 (d, J = 8.1 Hz, 2H), 7.57 (d, J = 8.2 Hz, 2H), 7.33 (s, 2H), 7.26 (d, J = 8.0 Hz, 2H), 6.92 (s, 4H), 6.48 (dd, J = 8.8, 3.0 Hz, 1H), 4.20 (q, J = 8.2 Hz, 1H), 4.16 (dt, J = 10.4, 5.9 Hz, 1H), 3.90 (ddd, J = 10.0, 7.9, 4.5 Hz, 1H), 3.40 (dd, J = 13.4, 8.6 Hz, 1H), 3.19 (d, J = 14.2

Hz, 1H), 3.16 – 3.04 (m, 5H), 2.99 (d, J = 13.7 Hz, 1H), 2.93 (dd, J = 13.3, 3.0 Hz, 1H), 2.62 (d, J = 13.7 Hz, 1H), 2.06 – 1.94 (m, 0H), 1.70 (dtd, J = 19.2, 9.7, 4.8 Hz, 2H), 1.64 – 1.57 (m, 2H), 1.56 – 1.33 (m, 2H), 0.91 (d, J = 6.6 Hz, 2H), 0.89 (d, J = 6.5 Hz, 2H).
^{13}C NMR (151 MHz, DMSO-d_6) δ 173.91, 172.61, 171.49, 170.24, 156.73, 141.92, 141.62, 131.52, 130.92, 127.25 (q, J = 31.9 Hz), 127.16 (q, J = 31.4 Hz), 124.83 (q, J = 3.5 Hz), 124.71 (q, J = 3.4 Hz), 124.44 (q, J = 271.7 Hz), 124.37 (q, J = 271.8 Hz), 54.62, 53.63, 52.89, 51.33, 40.32, 40.15, 40.06, 38.79, 38.31, 28.17, 26.45, 25.57, 25.11, 24.35, 22.84, 21.43.
HRMS-ESI: $C_{37}H_{51}F_6N_{10}O_4^+$ $[M + H]^+$ calcd: 813,3994, found: 813,3994, UPLC purity 100%.

(3*S*,6*S*,9*S*)-3,9-Bis(4-aminobutyl)-6-isobutyl-12,12-bis(4-(trifluoromethyl)benzyl)-1,4,7,10-tetraazacyclotridecane-2,5,8,11-tetraone x TFA (003)
^{1}H NMR (600 MHz, DMSO-d_6) δ 8.48 (d, J = 8.4 Hz, 1H), 8.13 (d, J = 5.9 Hz, 1H), 7.77 (t, J = 5.8 Hz, 3H), 7.70 (d, J = 8.2 Hz, 5H), 7.59 (d, J = 8.0 Hz, 2H), 7.56 (d, J = 8.1 Hz, 2H), 7.25 (d, J = 8.0 Hz, 2H), 6.44 (dd, J = 8.5, 3.1 Hz, 1H), 4.32 (td, J = 8.7, 6.3 Hz, 1H), 4.08 (dt, J = 9.1, 6.2 Hz, 1H), 3.92 (ddd, J = 10.3, 8.4, 4.3 Hz, 1H), 3.32 (dd, J = 13.3, 8.5 Hz, 1H), 3.20 – 3.12 (m, 2H), 2.96 – 2.92 (m, 1H), 2.90 (d, J = 14.1 Hz, 1H), 2.64 (d, J = 13.8 Hz, 1H), 1.96 (dtt, J = 13.6, 9.2, 3.7 Hz, 1H), 1.75 (dtd, J = 14.5, 9.4, 5.5 Hz, 1H), 1.67 (ddq, J = 19.3, 9.3, 5.5 Hz, 2H), 1.41 – 1.33 (m, 0H), 1.33 – 1.21 (m, 3H), 0.90 (d, J = 5.8 Hz, 2H), 0.87 (d, J = 5.8 Hz, 3H).
^{13}C NMR (151 MHz, DMSO-d_6) δ 173.96, 171.72, 171.65, 170.58, 141.84, 141.53, 131.51, 130.88, 127.27 (q, J = 31.7 Hz), 127.12 (q, J = 31.7 Hz), 124.89 (q, J = 3.8 Hz), 124.77 (q, J = 3.9 Hz), 124.40 (q, J = 272.2 Hz), 124.35 (q, J = 272.2 Hz), 56.44, 52.62, 52.56, 51.26, 42.71, 40.15, 40.06, 38.91, 38.71, 38.62, 35.34, 29.04, 28.92, 26.56, 26.50, 24.62, 22.77, 22.64, 22.45, 22.09.
HRMS-ESI: $C_{37}H_{51}F_6N_6O_4^+$ $[M + H]^+$ calcd: 757,3871, found: 757,3872, UPLC purity 97%.

1,1'-(((2*S*,5*S*,8*S*)-5-Isobutyl-3,6,9,13-tetraoxo-12,12-bis(4-(trifluoromethyl)benzyl)-1,4,7,10-tetraazacyclotridecane-2,8-diyl)bis(propane-3,1-diyl))diguanidine x TFA (004)
^{1}H NMR (600 MHz, DMSO-d_6) δ 8.62 (d, J = 8.1 Hz, 1H), 8.31 (d, J = 5.4 Hz, 1H), 7.77 (t, J = 5.5 Hz, 1H), 7.71 (d, J = 8.1 Hz, 2H), 7.65 (d, J = 7.5 Hz, 2H), 7.63 (s, 1H), 7.57 (d, J = 8.1 Hz, 2H), 7.45 (d, J = 9.1 Hz, 1H), 7.23 (d, J = 8.0 Hz, 2H), 6.46 (dd, J = 8.9, 2.9 Hz, 1H), 4.34 (q, J = 8.5 Hz, 1H), 4.06 (td, J = 7.8, 5.3 Hz, 1H), 3.86 (ddd, J = 10.9, 8.1, 4.3 Hz, 1H), 3.24 (d, J = 13.9 Hz, 1H), 3.22 – 3.06 (m, 4H), 3.00 (d, J = 13.7 Hz, 1H), 2.92 – 2.86 (m, 1H), 1.99 (tq, J = 10.5, 5.0 Hz, 1H), 1.84 – 1.68 (m, 3H), 1.67 – 1.57 (m, 1H), 1.56 – 1.35 (m, 4H), 0.91 (d, J = 6.0 Hz, 2H), 0.88 (d, J = 5.9 Hz, 3H).
^{13}C NMR (151 MHz, DMSO-d_6) δ 174.27, 171.70, 171.65, 170.19, 156.85, 156.69, 141.84, 141.58, 131.71, 130.86, 127.28 (q, J = 31.8 Hz), 127.13 (q, J = 31.9 Hz), 124.84 (q, J = 3.9 Hz), 124.72 (q, J = 4.0 Hz), 124.46 (q, J = 271.8 Hz), 124.37 (q, J = 271.9 Hz), 56.50, 52.90, 52.21, 51.47, 41.71, 40.32, 40.28, 39.17, 36.22, 26.56, 26.25, 25.64, 25.37, 24.57, 22.44, 22.14.
HRMS-ESI: $C_{37}H_{51}F_6N_{10}O_4^+$ $[M + H]^+$ calcd: 813,3994, found: 813,3994, UPLC purity 98%.

(3*R*,6*S*,9*S*)-3,6-Bis(4-aminobutyl)-9-isobutyl-12,12-bis(4-(trifluoromethyl)benzyl)-1,4,7,10-tetraazacyclotridecane-2,5,8,11-tetraone x TFA (011)
^{1}H NMR (600 MHz, DMSO-d_6) δ 8.66 (d, J = 6.8 Hz, 1H), 7.95 (d, J = 6.3 Hz, 1H), 7.69 (d, J = 8.3 Hz, 2H), 7.65 (d, J = 8.6 Hz, 2H), 7.64 (b, 6H), 7.57 (d, J = 8.1 Hz, 2H), 7.34 (d, J = 9.1 Hz, 1H), 7.25 (d, J = 8.0 Hz, 2H), 6.55 (dd, J = 7.7, 4.0 Hz, 1H), 4.25 (q, J = 7.9 Hz, 1H), 4.07 (dt, J = 9.6, 6.2 Hz, 1H), 4.01 (ddd, J = 9.5, 6.7, 5.1 Hz, 1H), 3.32 (dd, J = 13.6, 7.7 Hz, 1H), 3.12 (d, J = 13.6 Hz, 1H), 3.10 (d, J = 13.6 Hz, 1H), 2.99 (d, J = 13.4 Hz, 1H), 2.98 (d, J = 13.6 Hz, 1H), 2.81 – 2.69 (m, 4H), 1.69 (td, J = 10.6, 5.4 Hz, 1H), 1.65 – 1.61 (m, 1H), 1.61 – 1.43 (m, 7H), 1.38 (m, 3H), 1.29-1.20 (m, 1H), 1.20 – 1.12 (m, 1H), 0.92 (d, J = 6.4 Hz, 3H), 0.88 (d, J = 6.5 Hz, 3H).

^{13}C NMR (151 MHz, DMSO-d_6) δ 173.49, 172.53, 171.82, 171.05, 141.85, 141.35, 131.87, 130.94, 127.32 (q, J=32.2 Hz), 127.12 (q, J=32.2 Hz), 124.75 (q, J=3.9 Hz), 124.67 (q, J=3.9 Hz), 124.45 (q, J=272.3 Hz), 124.35 (q, J=272.3 Hz), 55.14, 54.55, 51.98, 51.60, 40.06, 39.18, 38.70, 38.60 (2C), 38.01, 30.72, 29.74, 26.87, 26.57, 24.25, 22.69, 22.64, 22.14, 21.62.
HRMS-ESI: $C_{37}H_{51}F_6N_6O_4^+$ [M + H]$^+$ calcd: 757,3871, found: 757,3874, UPLC purity 100%.

1,1'-(((3*R*,6*S*,9*S*)-9-Isobutyl-2,5,8,11-tetraoxo-12,12-bis(4-(trifluoromethyl)benzyl)-1,4,7,10-tetraazacyclotridecane-3,6-diyl)bis(propane-3,1-diyl))diguanidine x TFA (021)
^{1}H NMR (600 MHz, DMSO-d_6) δ 8.67 (d, J = 6.8 Hz, 1H), 7.98 (d, J = 6.2 Hz, 1H), 7.69 (d, J = 8.3 Hz, 2H), 7.65 (d, J = 8.2 Hz, 2H), 7.57 (d, J = 8.2 Hz, 2H), 7.54 (s, 1H), 7.41 (d, J = 9.1 Hz, 1H), 7.25 (d, J = 8.0 Hz, 2H), 6.60 (dd, J = 7.6, 4.1 Hz, 1H), 4.27 (td, J = 8.7, 6.6 Hz, 1H), 4.06 (ddt, J = 18.1, 8.9, 6.4 Hz, 2H), 3.32 (dd, J = 13.6, 7.7 Hz, 1H), 3.16 – 3.04 (m, 6H), 2.99 (td, J = 12.2, 7.1 Hz, 2H), 2.53 (d, J = 13.0 Hz, 1H), 1.73 (td, J = 7.5, 4.5 Hz, 1H), 1.66 – 1.46 (m, 7H), 1.39 (dt, J = 13.5, 7.0 Hz, 2H), 1.37 – 1.28 (m, 1H), 0.92 (d, J = 6.5 Hz, 3H), 0.88 (d, J = 6.4 Hz, 3H).
^{13}C NMR (151 MHz, DMSO-d_6) δ 173.52, 172.81, 171.66, 170.94, 156.65, 156.60, 141.85, 141.36, 131.86, 130.94, 127.29 (q, J = 31.8 Hz), 127.16 (q, J = 31.8 Hz), 124.46 (q, J = 271.9 Hz), 124.76 (q, J = 3.3 Hz), 124.67 (q, J = 2.5 Hz), 55.08, 54.35, 51.90, 51.59, 40.37, 40.29, 40.23, 39.16, 38.64, 38.04, 28.29, 27.47, 25.44, 25.04, 24.25, 22.63, 21.67.
HRMS-ESI: $C_{37}H_{51}F_6N_{10}O_4^+$ [M + H]$^+$ calcd: 813,3994, found: 813,3995, UPLC purity 99%.

(3*S*,6*S*,9*S*)-3,9-Bis(4-aminobutyl)-6-benzyl-12,12-bis(4-(trifluoromethyl)benzyl)-1,4,7,10-tetraazacyclotridecane-2,5,8,11-tetraone x TFA (031)
^{1}H NMR (600 MHz, DMSO-d_6) δ 8.22 (d, J = 5.3 Hz, 1H), 7.71 (d, J = 8.2 Hz, 2H), 7.65 (d, J = 8.1 Hz, 2H), 7.56 (t, J = 6.7 Hz, 2H), 7.28 (t, J = 7.4 Hz, 2H), 7.23 (d, J = 8.0 Hz, 2H), 7.21 (t, J = 7.8 Hz, 1H), 7.19 (d, J = 8.5 Hz, 2H), 6.46 (d, J = 8.3 Hz, 1H), 4.52 (q, J = 8.6 Hz, 1H), 3.93 (q, J = 7.4 Hz, 1H), 3.70 (dt, J = 11.3, 4.7 Hz, 1H), 3.36 (dd, J = 13.3, 8.8 Hz, 1H), 3.21 (d, J = 13.9 Hz, 1H), 3.17 (d, J = 13.7 Hz, 1H), 3.01 – 2.92 (m, 2H), 2.89 (d, J = 12.8 Hz, 1H), 2.84 (dd, J = 13.6, 8.6 Hz, 1H), 2.77 – 2.66 (m, 4H), 1.96 – 1.87 (m, 1H), 1.75 – 1.64 (m, 2H), 1.64 – 1.53 (m, 1H), 1.55 – 1.39 (m, 4H), 1.29 – 1.22 (m, 1H), 1.14 – 0.99 (m, 3H).
^{13}C NMR (151 MHz, DMSO-d_6) δ 174.04, 171.25, 170.84, 170.24, 141.81, 141.53, 137.12, 131.76, 130.86, 129.09, 128.14, 127.26 (q, J = 31.9 Hz), 127.07 (q, J = 31.8 Hz), 124.82 (q, J = 3.3 Hz), 124.70 (q, J = 3.3 Hz), 124.46 (q, J = 271.8 Hz), 124.37 (q, J = 271.8 Hz), 56.77, 54.60, 53.34, 51.43, 41.56, 38.69, 38.62, 37.27, 36.35, 29.05, 28.24, 26.64, 26.62, 22.57, 22.48.
HRMS-ESI: $C_{40}H_{49}F_6N_6O_4^+$ [M + H]$^+$ calcd: 791,3714, found: 791,3717, UPLC purity 100%.

1,1'-(((2*S*,5*S*,8*S*)-5-Benzyl-3,6,9,13-tetraoxo-12,12-bis(4-(trifluoromethyl)benzyl)-1,4,7,10-tetraazacyclotridecane-2,8-diyl)bis(propane-3,1-diyl))diguanidine x TFA (041)
^{1}H NMR (600 MHz, DMSO-d_6) δ 1H NMR (600 MHz, DMSO) δ 8.67 (d, J = 7.5 Hz, 1H), 8.38 (d, J = 4.9 Hz, 1H), 7.73 (s, 4H), 7.55 (d, J = 8.2 Hz, 2H), 7.53 (d, J = 5.5 Hz, 1H), 7.43 (d, J = 9.4 Hz, 1H), 7.42 – 7.39 (m, 1H), 7.27 (dd, J = 8.5, 6.6 Hz, 2H), 7.21 (d, J = 8.1 Hz, 2H), 7.19 (t, J = 8.0 Hz, 1H), 7.18 (d, J = 8.2 Hz, 2H), 6.50 (dd, J = 9.3, 2.7 Hz, 1H), 4.52 (dt, J = 9.7, 8.1 Hz, 1H), 3.94 (td, J = 8.0, 4.8 Hz, 1H), 3.60 (td, J = 8.6, 4.1 Hz, 1H), 3.29 (d, J = 13.8 Hz, 1H), 3.17 (d, J = 13.6 Hz, 1H), 3.14 – 3.07 (m, 3H), 3.02 (tt, J = 13.7, 6.5 Hz, 2H), 2.93 (dd, J = 13.5, 8.2 Hz, 1H), 2.86 – 2.78 (m, 2H), 2.38 (d, J = 13.4 Hz, 1H), 1.95 (td, J = 14.3, 4.2 Hz, 1H), 1.83 – 1.63 (m, 3H), 1.52 (tt, J = 13.4, 7.4 Hz, 1H), 1.37 (ddd, J = 20.7, 13.1, 7.2 Hz, 1H), 1.19 (tt, J = 12.5, 6.3 Hz, 1H), 1.10 (ddt, J = 18.6, 12.5, 6.5 Hz, 1H).
^{13}C NMR (151 MHz, DMSO-d_6) δ 174.38, 171.39, 170.81, 169.82, 156.70, 156.57, 141.82, 141.58, 136.99, 131.95, 130.83, 129.09, 128.17, 127.27 (q, J = 31.5 Hz), 127.07 (q, J = 31.4 Hz), 124.78 (q, J =

3.5 Hz), 124.66 (d, J = 2.8 Hz), 124.49 (q, J = 272.0 Hz), 124.35 (q, J = 271.8 Hz), 56.75, 54.33, 53.66, 51.61, 40.61, 40.47, 40.34, 37.48, 37.19, 26.41, 25.49, 25.37, 25.11.
HRMS-ESI: $C_{40}H_{49}F_6N_{10}O_4^+$ $[M + H]^+$ calcd: 847,3837, found: 847,3836, UPLC purity 99%.

1-(3-((2*S*,5*S*,8*S*)-2,8-Bis(3-guanidinopropyl)-3,6,9,13-tetraoxo-12,12-bis(4-(trifluoromethyl)benzyl)-1,4,7,10-tetraazacyclotridecan-5-yl)propyl)guanidine x TFA (006)
^{1}H NMR (600 MHz, DMSO-d_6) δ 8.62 (d, J = 8.0 Hz, 1H), 8.33 (d, J = 5.6 Hz, 1H), 7.83 (t, J = 5.5 Hz, 1H), 7.74 (t, J = 5.7 Hz, 1H), 7.70 (d, J = 8.2 Hz, 2H), 7.67 (t, J = 5.8 Hz, 1H), 7.64 (d, J = 8.1 Hz, 2H), 7.56 (d, J = 8.0 Hz, 2H), 7.52 (d, J = 8.7 Hz, 1H), 7.22 (d, J = 8.0 Hz, 2H), 6.51 (dd, J = 8.9, 3.1 Hz, 1H), 4.22 (q, J = 8.2 Hz, 1H), 4.09 (dt, J = 9.1, 6.1 Hz, 1H), 3.86 (ddd, J = 10.3, 7.9, 4.5 Hz, 1H), 3.42 (dd, J = 13.4, 8.9 Hz, 1H), 3.25 (d, J = 13.9 Hz, 1H), 3.15 (q, J = 7.1 Hz, 1H), 3.14 – 3.07 (m, 4H), 3.02 (d, J = 13.8 Hz, 1H), 2.91 – 2.85 (m, 1H), 2.06 – 1.97 (m, 1H), 1.85 – 1.78 (m, 1H), 1.77 – 1.66 (m, 2H), 1.68 – 1.58 (m, 2H), 1.59 – 1.51 (m, 1H), 1.51 – 1.34 (m, 3H).
^{13}C NMR (151 MHz, DMSO-d_6) δ 174.30, 172.15, 171.38, 170.13, 156.89, 156.79, 156.75, 141.86, 141.59, 131.63, 130.86, 127.26 (q, J = 31.9 Hz), 127.12 (q, J = 31.7 Hz), 124.82 (q, J = 3.7 Hz), 124.70 (q, J = 3.9, Hz), 124.44 (q, J = 271.9 Hz), 124.36 (q, J = 271.8 Hz), 56.25, 53.58, 53.03, 51.41, 41.82, 40.32, 40.26, 40.16, 36.24, 28.38, 26.42, 26.27, 25.61, 25.33, 25.10.
HRMS-ESI: $C_{37}H_{52}F_6N_{13}O_4^+$ $[M + H]^+$ calcd: 856,4164, found: 856,4163, UPLC purity 97%.

Bacterial Strains and Antibacterial Activity Testing

Antimicrobial activity testing was performed using the following test strains: The Gram-positive bacteria *B. subtilis* 168 (ATCC 23857), *C. glutamicum* (ATCC 13032), *S. aureus* (ATCC 9144) and *S. epidermidis* RP62A (ATCC 35984) and the Gram-negative bacteria *E. coli* (ATCC 25922) and *P. aeruginosa* (ATCC 27853). The antibacterial activity was assessed using a microdilution assay according to a modified CLSI-based method. (25) Briefly, bacterial cultures were grown overnight in Mueller–Hinton (MH) broth medium (Difco Laboratories, Detroit, MI, USA) and adjusted to 2.5–3 × 10^4 CFU/mL in MH medium. The peptides were diluted in ultrapure water to a concentration of 250 µg/mL. The suspension of actively growing bacteria (50 µL) was distributed in 96-well microplates (Nunc, Roskilde, Denmark) preloaded with 50 µL of two-fold dilutions of peptide solution. The microplates were incubated in an EnVision 2103 microplate reader (PerkinElmer, Llantrisant, UK) at 35 °C, with OD595 recorded every hour for 24 h. The minimum inhibitory concentration (MIC) was defined as the lowest concentration of peptides resulting in no bacterial growth, compared to the bacterial growth control, consisting of bacterial suspension and water. Polymyxin B sulfate (Sigma-Aldrich, St. Louis, MO, USA) and chlorhexidine acetate (Fresenius Kabi, Halden, Norway) served as positive (growth inhibition) controls, whereas media plus water served as a negative control. All peptides and controls were tested in triplicates.

Haemolytic Toxicity Assay

The synthesised tetrapeptides were screened for haemolytic toxicity against human red blood cells (RBC) in concentrations ranging from 500 to 3.9 µM, according to a previously described protocol. (10) In brief, haemolysis was determined using a heparinized (10 IU/mL) fraction of freshly drawn human blood. Another fraction of blood, which was collected in test tubes with ethylenediaminetetraacetic acid (EDTA, Vacutest, KIMA, Arzergrande, Italy), was used for determination of the haematocrit (hct). Plasma was removed from heparinized blood by washing three times with prewarmed phosphate-buffered saline (PBS) before being adjusted to a final hct of 4%. Tested peptides, which were dissolved in dimethyl sulfoxide (DMSO), were subsequently diluted with PBS to a final DMSO content of ≤1%.

A 1% solution of Triton X-100 (Sigma-Aldrich, St. Louis, MO, USA) served as a positive control for 100% haemolysis, whereas 1% DMSO in PBS buffer served as a negative control. Duplicates of test solutions and erythrocytes (1% hct final concentration) were prepared in a 96-well polypropylene V-bottom plate (Nunc, Fischer scientific, Oslo, Norway). They were incubated under agitation at 37 °C and 800 rpm for 1 h. After centrifugation (5 min, 3000 × g), 100 µL from each well was transferred to a flat-bottomed 96-well plate. Absorbance was measured at 545 nm with a microplate reader (SpectraMax 190, Molecular Devices, San Jose, CA, USA). After subtracting PBS background, the percentage of haemolysis was determined as the ratio of the absorbance in the peptide-treated and surfactant-treated samples. Three independent experiments were performed. EC_{50} values, which represent the concentration of the peptide giving 50% haemolysis, are presented as averages.

Surface Plasmon Resonance

The SPR experiments were performed using the L1 chip and T200 Biacore instrument (GEHealthcare, Chicago, IL, USA). The experiment setup, including flow rates, chip modification, immobilisation of vesicles and liposome recovery can be found at Jakubec *et al*. (21) Briefly, DMPC vesicles were prepared by the standard method from dry lipid film. (26) DMPC vesicles with 10% (w/w) LPS (from *Escherichia coli* O111:B4, Merk, Germany) were prepared by the same method with modification according to Palusińska-Szysz *et al*. (27) Vesicles were then extruded through 100 nm pore, using Avanti Lipids mini-extruder. An L1 chip was covered with extruded vesicles using flowrate of 2 µl/min for 2400 seconds. Coverage was tested by injection of 0.1 mg/ml bovine serine albumin for 1 minute at a flowrate of 30 µl/min; a change < 400 RU indicated sufficient coverage. Increasing concentration of peptides (from 4 to 128 µM) were injected onto the chip for 200 s association and 400 s dissociation using flowrate of 15 µl/min.

The results were processed using MATLAB R2022a (scripts available at https://github.com/MarJakubec) using the method presented by Figueira *et al.* and modified by Juskewitz *et al*. (20, 28) Briefly, K_P was calculated from steady state affinity using Eq (1):

$$\frac{RU_S}{RU_L} = \frac{\gamma_L K_P \frac{M_S}{M_L} [S]_W}{1 + \sigma \gamma_L K_P [S]_W} \quad \text{(Eq 1)}$$

where RU_S and RU_L are the relative responses of solute (peptides) and lipids respectively, γ_L is the molar volume of the lipids (average for mixture of DMPC and LPS), M_S and M_L are the molecular mass of solute and lipid, respectively, and $[S]_W$ is the concentration of solute in water. K_P and σ are obtained from fitting (with σ being lipid to solute ratio).

For k_{off} we have first linearised dissociation process using Eq (2) and then calculated average k_{off} values by Eq (3):

$$S_L(t) = \alpha e^{-k_{off,\alpha} t} + \beta e^{-k_{off,\beta} t} + S_{L,r} \quad \text{(Eq 2)}$$

$$k_{off} = \frac{\alpha k_{off,\alpha} + \beta k_{off,\beta}}{\alpha + \beta} \quad \text{(Eq 3)}$$

where S_L is the linearised ratio of solute and lipid, α and β are individual populations, and $S_{L,r}$ is the retained solute fraction.

Acknowledgments

This work was funded by a grant (no. 217/6770) from UiT The Arctic University of Norway.

References

1. Erdem Büyükkiraz M, Kesmen Z. Antimicrobial peptides (AMPs): A promising class of antimicrobial compounds. J Appl Microbiol. 2022;132(3):1573-96.
2. Rončević T, Puizina J, Tossi A. Antimicrobial Peptides as Anti-Infective Agents in Pre-Post-Antibiotic Era? Int J Mol Sci. 2019;20(22).
3. Amiss AS, Henriques ST, Lawrence N. Antimicrobial peptides provide wider coverage for targeting drug-resistant bacterial pathogens. Pept Sci. 2022;114(2):e24246.
4. Moretta A, Scieuzo C, Petrone AM, Salvia R, Manniello MD, Franco A, et al. Antimicrobial Peptides: A New Hope in Biomedical and Pharmaceutical Fields. Front Cell Infect Microbiol. 2021;11.
5. Chakraborty S, Tai DF, Lin YC, Chiou TW. Antitumor and antimicrobial activity of some cyclic tetrapeptides and tripeptides derived from marine bacteria. Mar Drugs. 2015;13(5):3029-45.
6. Gunjal VB, Thakare R, Chopra S, Reddy DS. Teixobactin: A Paving Stone toward a New Class of Antibiotics? J Med Chem. 2020;63(21):12171-95.
7. Paulsen MH, Karlsen EA, Ausbacher D, Anderssen T, Bayer A, Ochtrop P, et al. An amphipathic cyclic tetrapeptide scaffold containing halogenated β(2,2) -amino acids with activity against multiresistant bacteria. J Pept Sci. 2018;24(10):e3117.
8. Paulsen MH, Engqvist M, Ausbacher D, Strøm MB, Bayer A. Efficient and scalable synthesis of α,α-disubstituted β-amino amides. Org Biomol Chem. 2016;14(31):7570-8.
9. Malesevic M, Strijowski U, Bächle D, Sewald N. An improved method for the solution cyclization of peptides under pseudo-high dilution conditions. J Biotechnol. 2004;112(1):73-7.
10. Dey H, Simonovic D, Norberg-Schulz Hagen I, Vasskog T, Fredheim EGA, Blencke HM, et al. Synthesis and Antimicrobial Activity of Short Analogues of the Marine Antimicrobial Peptide Turgencin A: Effects of SAR Optimizations, Cys-Cys Cyclization and Lipopeptide Modifications. Int J Mol Sci. 2022;23(22).
11. Sarojini V, Cameron AJ, Varnava KG, Denny WA, Sanjayan G. Cyclic Tetrapeptides from Nature and Design: A Review of Synthetic Methodologies, Structure, and Function. Chem Rev. 2019;119(17):10318-59.
12. Farina B, Del Gatto A, Comegna D, Di Gaetano S, Capasso D, Isernia C, et al. Conformational studies of RGDechi peptide by natural-abundance NMR spectroscopy. J Pept Sci. 2019;25(5):e3166.
13. Schwarzinger S, Kroon GJ, Foss TR, Chung J, Wright PE, Dyson HJ. Sequence-dependent correction of random coil NMR chemical shifts. J Am Chem Soc. 2001;123(13):2970-8.
14. De Simone A, Cavalli A, Hsu S-TD, Vranken W, Vendruscolo M. Accurate Random Coil Chemical Shifts from an Analysis of Loop Regions in Native States of Proteins. J Am Chem Soc. 2009;131(45):16332-3.
15. Tamiola K, Acar B, Mulder FAA. Sequence-Specific Random Coil Chemical Shifts of Intrinsically Disordered Proteins. J Am Chem Soc. 2010;132(51):18000-3.
16. Kjaergaard M, Brander S, Poulsen FM. Random coil chemical shift for intrinsically disordered proteins: effects of temperature and pH. J Biomol NMR. 2011;49(2):139-49.
17. Wishart DS, Sykes BD, Richards FM. The chemical shift index: a fast and simple method for the assignment of protein secondary structure through NMR spectroscopy. Biochemistry. 1992;31(6):1647-51.
18. Claridge TD. High-resolution NMR techniques in organic chemistry: Elsevier; 2016.
19. Snyder DS, McIntosh TJ. The Lipopolysaccharide Barrier: Correlation of Antibiotic Susceptibility with Antibiotic Permeability and Fluorescent Probe Binding Kinetics. Biochemistry. 2000;39(38):11777-87.
20. Figueira TN, Freire JM, Cunha-Santos C, Heras M, Gonçalves J, Moscona A, et al. Quantitative analysis of molecular partition towards lipid membranes using surface plasmon resonance. Sci Rep. 2017;7(1):45647.
21. Jakubec M, Bariås E, Furse S, Govasli ML, George V, Turcu D, et al. Cholesterol-containing lipid nanodiscs promote an α-synuclein binding mode that accelerates oligomerization. FEBS J. 2021;288(6):1887-905.
22. Snyder S, Kim D, McIntosh TJ. Lipopolysaccharide Bilayer Structure: Effect of Chemotype, Core Mutations, Divalent Cations, and Temperature. Biochemistry. 1999;38(33):10758-67.
23. Savini F, Loffredo MR, Troiano C, Bobone S, Malanovic N, Eichmann TO, et al. Binding of an antimicrobial peptide to bacterial cells: Interaction with different species, strains and cellular components. Biochim Biophys Acta Biomembr. 2020;1862(8):183291.
24. Papo N, Shai Y. A Molecular Mechanism for Lipopolysaccharide Protection of Gram-negative Bacteria from Antimicrobial Peptides*. J Biol Chem. 2005;280(11):10378-87.
25. Igumnova EM, Mishchenko E, Haug T, Blencke H-M, Sollid JUE, Fredheim EGA, et al. Synthesis and antimicrobial activity of small cationic amphipathic aminobenzamide marine natural product mimics and evaluation of relevance against clinical isolates including ESBL–CARBA producing multi-resistant bacteria. Bioorg Med Chem. 2016;24(22):5884-94.
26. Lasch J, Weissig V, Brandl M. General methods: Preparation of liposomes. In: Torchilin V, Weissig V, editors. Liposomes : a practical approach. 2nd ed. Oxford: Oxford University Press; 2003. p. 3-27.

27. Palusińska-Szysz M, Zdybicka-Barabas A, Luchowski R, Reszczyńska E, Śmiałek J, Mak P, et al. Choline Supplementation Sensitizes Legionella dumoffii to Galleria mellonella Apolipophorin III. Int J Mol Sci. 2020;21(16).
28. Juskewitz E, Mishchenko E, Dubey VK, Jenssen M, Jakubec M, Rainsford P, et al. Lulworthinone: In Vitro Mode of Action Investigation of an Antibacterial Dimeric Naphthopyrone Isolated from a Marine Fungus. Mar Drugs. 2022;20(5):277.

Supporting information

The role of amphipathicity and *L*- to *D*-amino acid substitution in a small antimicrobial cyclic tetrapeptide scaffold containing a halogenated α,α- disubstituted $\beta^{2,2}$- amino acid residue

Danijela Simonovic[a], Fredrik G. Rylandsholm[b], Martin Jakubec[b], Johan Mattias Isaksson[a,b], Hege Devold[c], Trude Anderssen[a], Annette Bayer[b], Tor Haug[c], Morten B. Strøm[a]*

[a] *Department of Pharmacy, Faculty of Health Sciences, UiT – The Arctic University of Norway, NO-9037 Tromsø, Norway*
[b] *Department of Chemistry, UiT – The Arctic University of Norway, NO-9037 Tromsø, Norway*
[c] *The Norwegian College of Fishery Science, Faculty of Biosciences, Fisheries and Economics, UiT – The Arctic University of Norway, NO-9037 Tromsø, Norway*
** Correspondance: morten.strom@uit.no (M.B.S.)*

Contents:

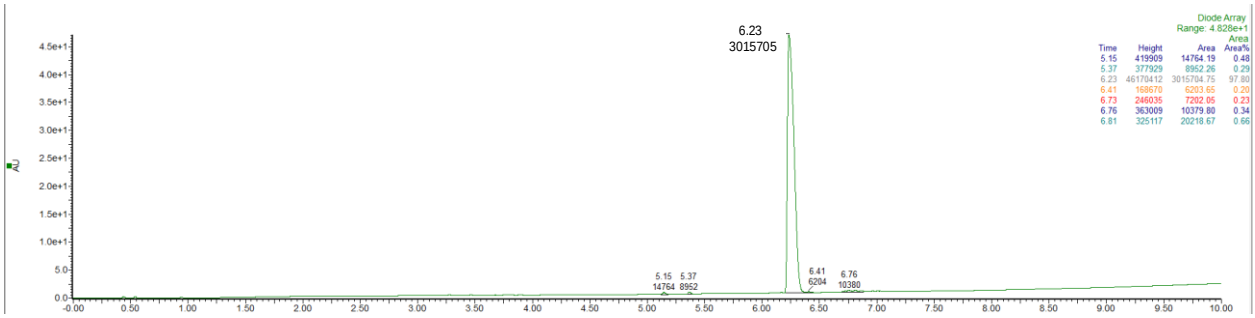

Figure S1. UPLC chromatogram of the purified cyclic peptide **001**. The peptide purity is 97.80 % based on the UPLC calculated area under the curves.

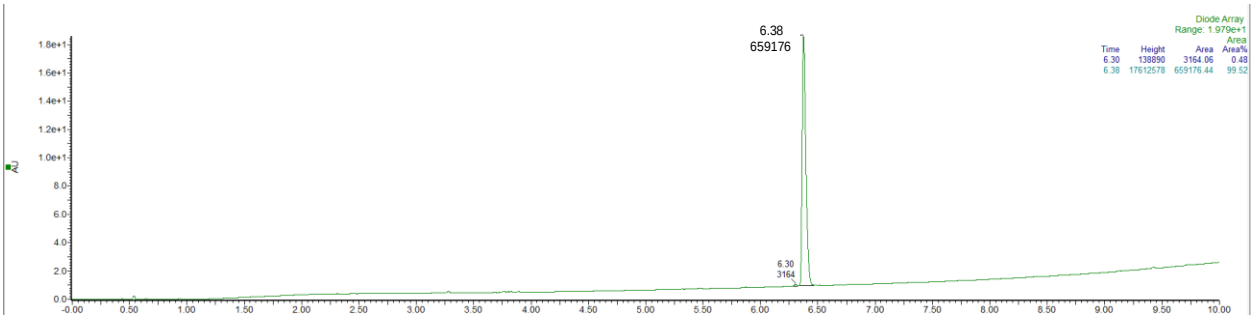

Figure S2. UPLC chromatogram of the purified cyclic peptide **002**. The peptide purity is 99.52 % based on the UPLC calculated area under the curves.

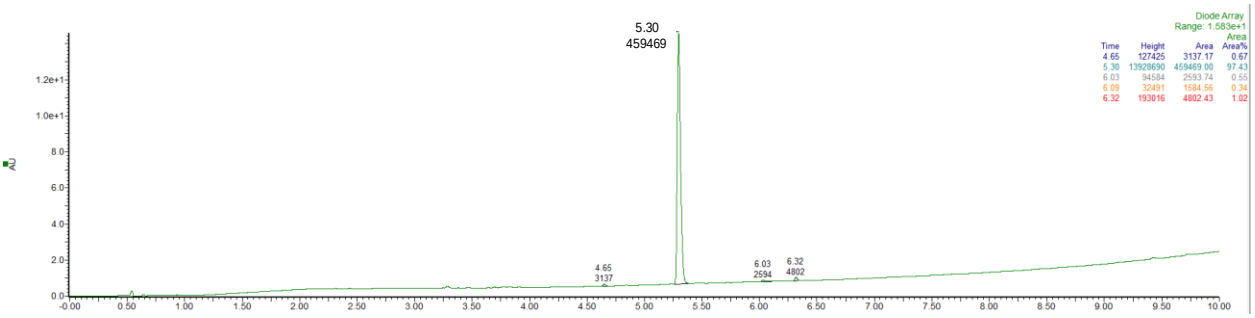

Figure S3. UPLC chromatogram of the purified cyclic peptide **003**. The peptide purity is 97.43 % based on the UPLC calculated area under the curves.

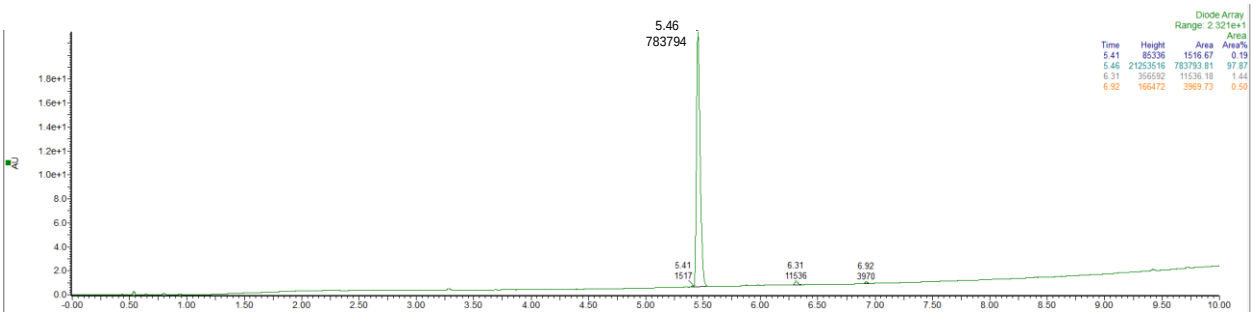

Figure S4. UPLC chromatogram of the purified cyclic peptide **004**. The peptide purity is 97.87 % based on the UPLC calculated area under the curves.

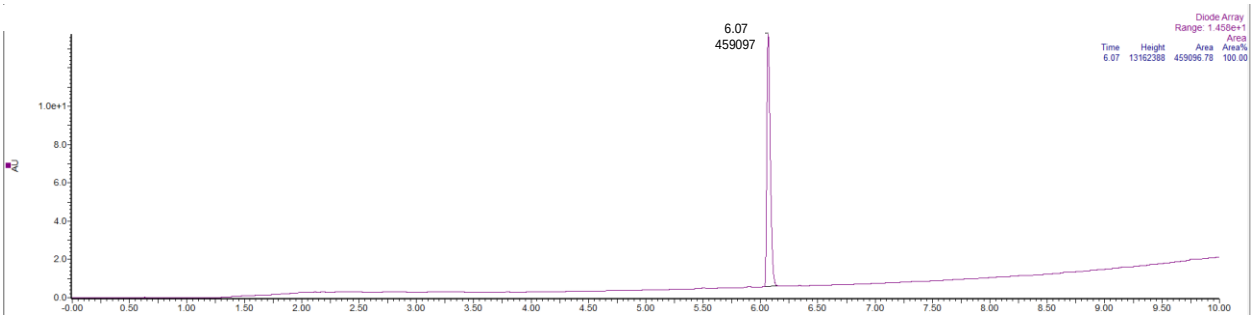

Figure S5. UPLC chromatogram of the purified cyclic peptide **011**. The peptide purity is 100.00 % based on the UPLC calculated area under the curves.

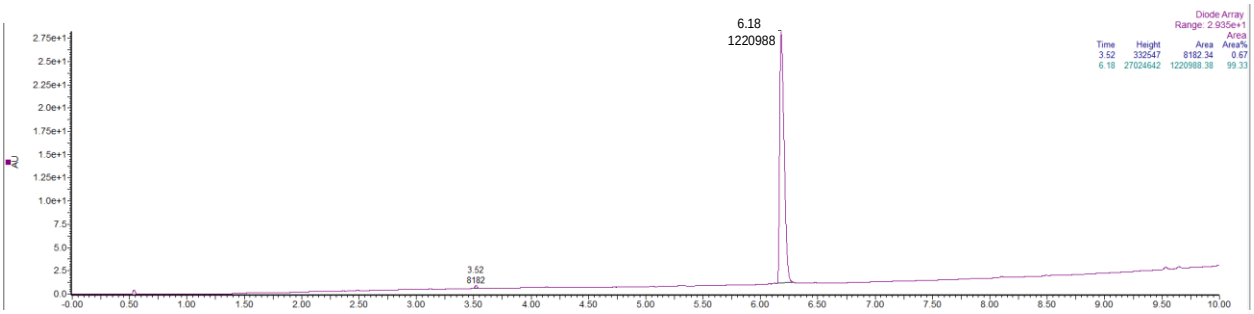

Figure S6. UPLC chromatogram of the purified cyclic peptide **021**. The peptide purity is 99.33 % based on the UPLC calculated area under the curves.

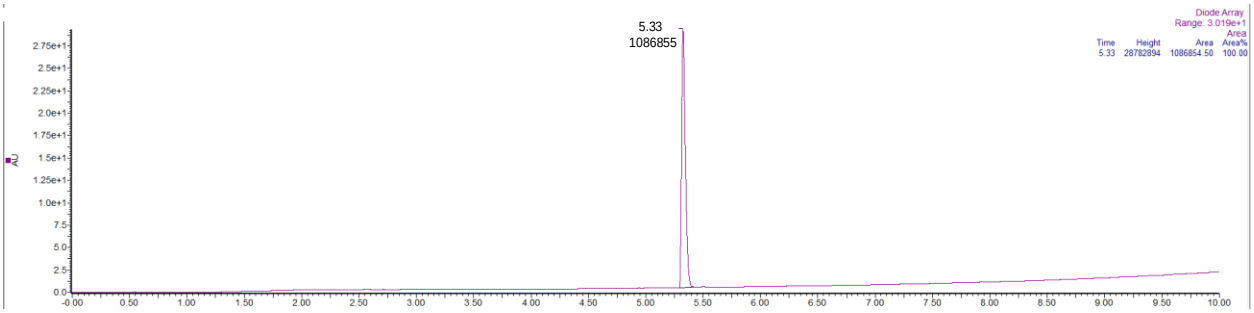

Figure S7. UPLC chromatogram of the purified cyclic peptide **031**. The peptide purity is 100.00 % based on the UPLC calculated area under the curves.

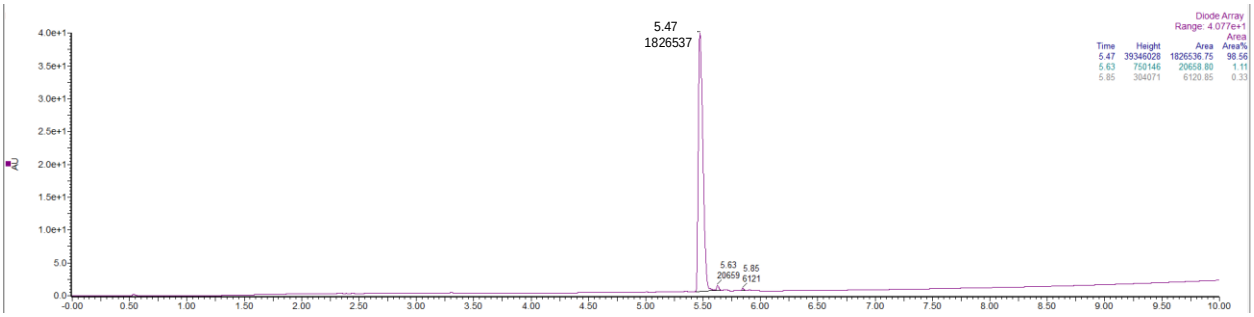

Figure S8. UPLC chromatogram of the purified cyclic peptide **041**. The peptide purity is 98.56 % based on the UPLC calculated area under the curves.

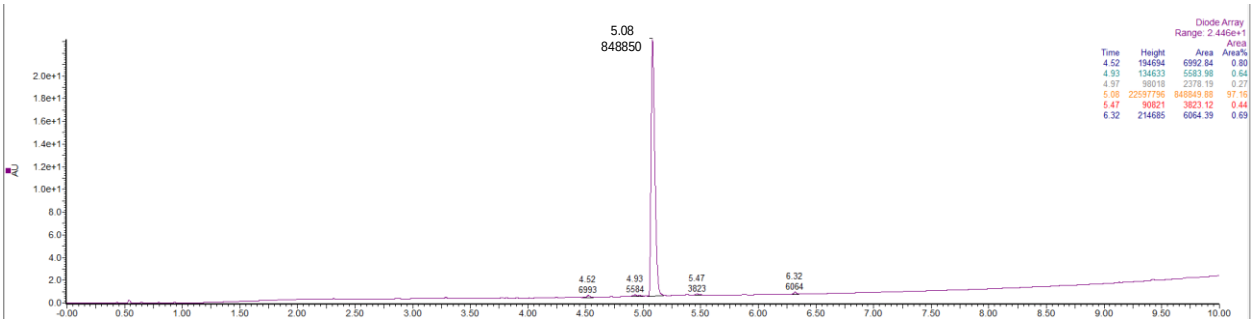

Figure S9. UPLC chromatogram of the purified cyclic peptide **006**. The peptide purity is 97.16 % based on the UPLC calculated area under the curves.

NMR spectra of selected peptides

1H NMR (600 MHz, DMSO) δ 8.39 (d, J = 8.3 Hz, 1H), 7.90 (d, J = 6.4 Hz, 1H), 7.69 (d, J = 8.2 Hz, 2H), 7.58 (d, J = 8.1 Hz, 4H), 7.54 (d, J = 8.7 Hz, 1H), 7.27 (d, J = 8.0 Hz, 2H), 6.46 (dd, J = 8.4, 3.2 Hz, 1H), 4.26 – 4.10 (m, 2H), 4.00 – 3.80 (m, 1H), 3.37 (dd, J = 13.4, 8.4 Hz, 1H), 3.15 (s, 1H), 3.09 (d, J = 14.2 Hz, 1H), 2.95 (d, J = 13.6 Hz, 2H), 2.81 – 2.71 (m, 4H), 2.66 (d, J = 13.8 Hz, 1H), 1.98 (dtd, J = 18.0, 9.1, 7.9, 4.7 Hz, 1H), 1.68 (tdt, J = 19.4, 9.7, 5.1 Hz, 1H), 1.61 (q, J = 7.7 Hz, 1H), 1.58 – 1.47 (m, 4H), 1.39 (ddd, J = 14.0, 8.8, 5.5 Hz, 1H), 1.35 – 1.18 (m, 3H), 0.91 (d, J = 6.6 Hz, 3H), 0.88 (d, J = 6.6 Hz, 3H).

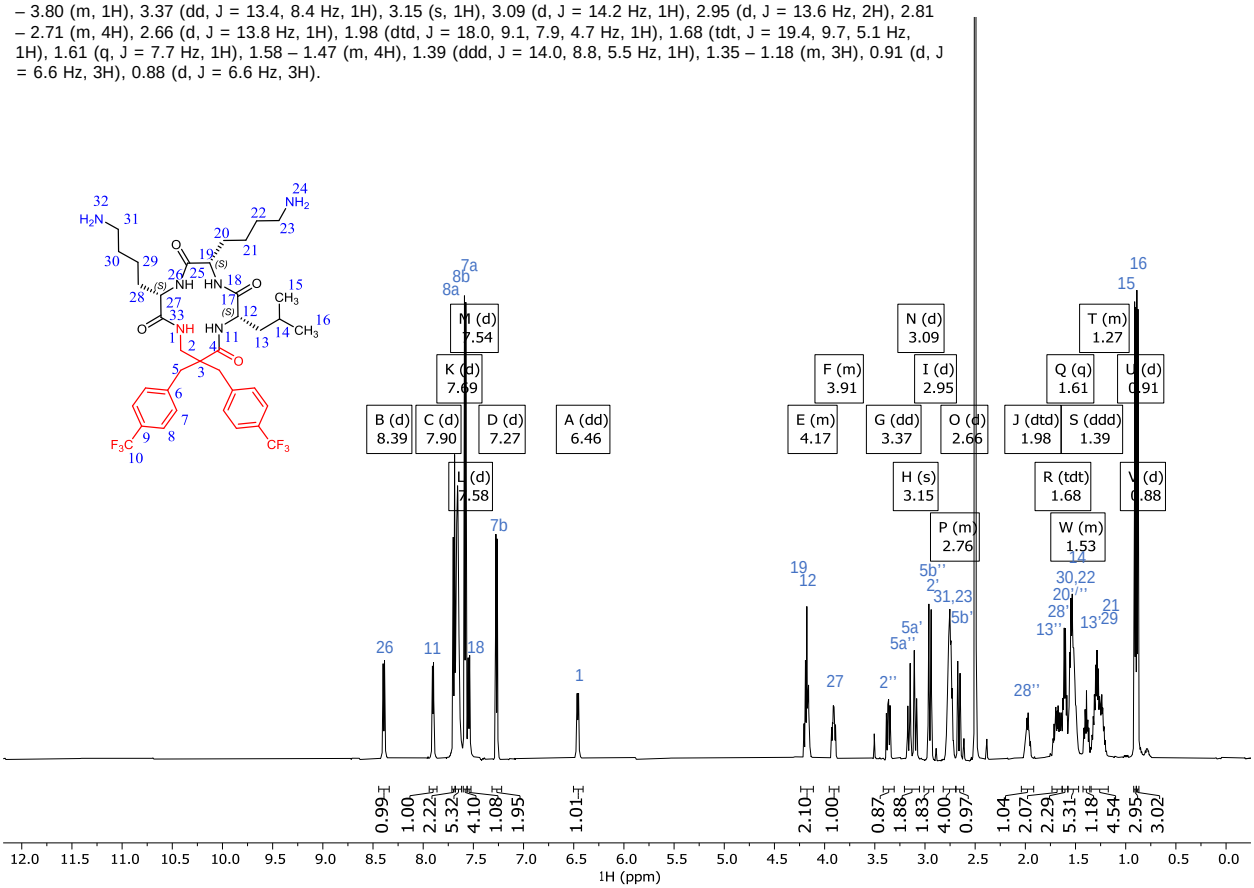

Figure S10. ^{1}H NMR spectrum of **001.**

^{13}C NMR (151 MHz, DMSO) δ 173.77, 172.37, 171.49, 170.48, 141.88, 141.58, 131.43, 130.92, 127.25 (q, *J* = 31.4 Hz), 127.17 (d, *J* = 31.4 Hz), 124.87 (q, *J* = 3.5 Hz), 124.73 (q, *J* = 3.4 Hz), 124.41 (q, *J* = 271.8 Hz), 124.36 (q, *J* = 271.8 Hz), 116.06, 54.55, 53.80, 52.73, 51.24, 42.84, 35.62, 30.46, 28.94, 26.52, 26.44, 24.33, 22.87, 22.66, 22.32, 21.43.

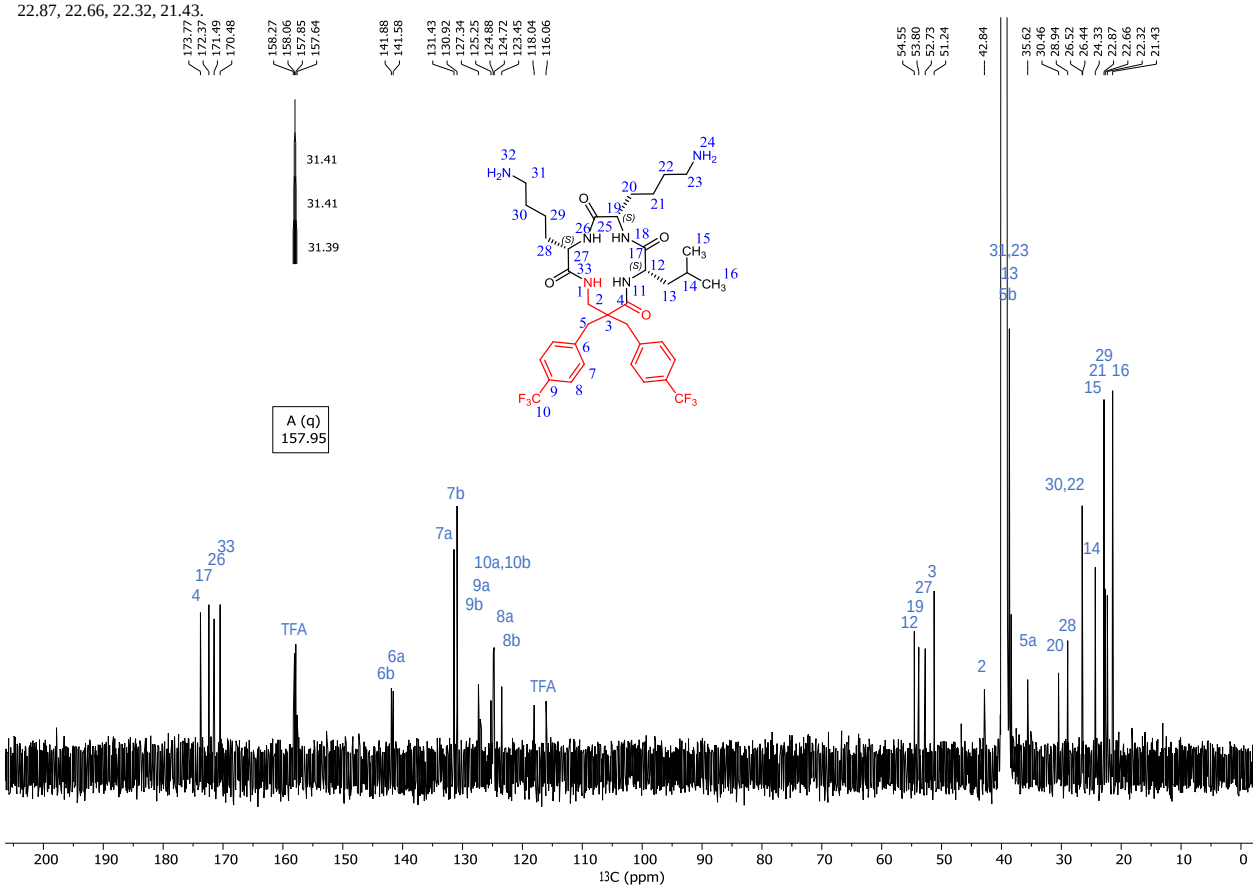

Figure S11. ^{13}C NMR spectrum of **001.**

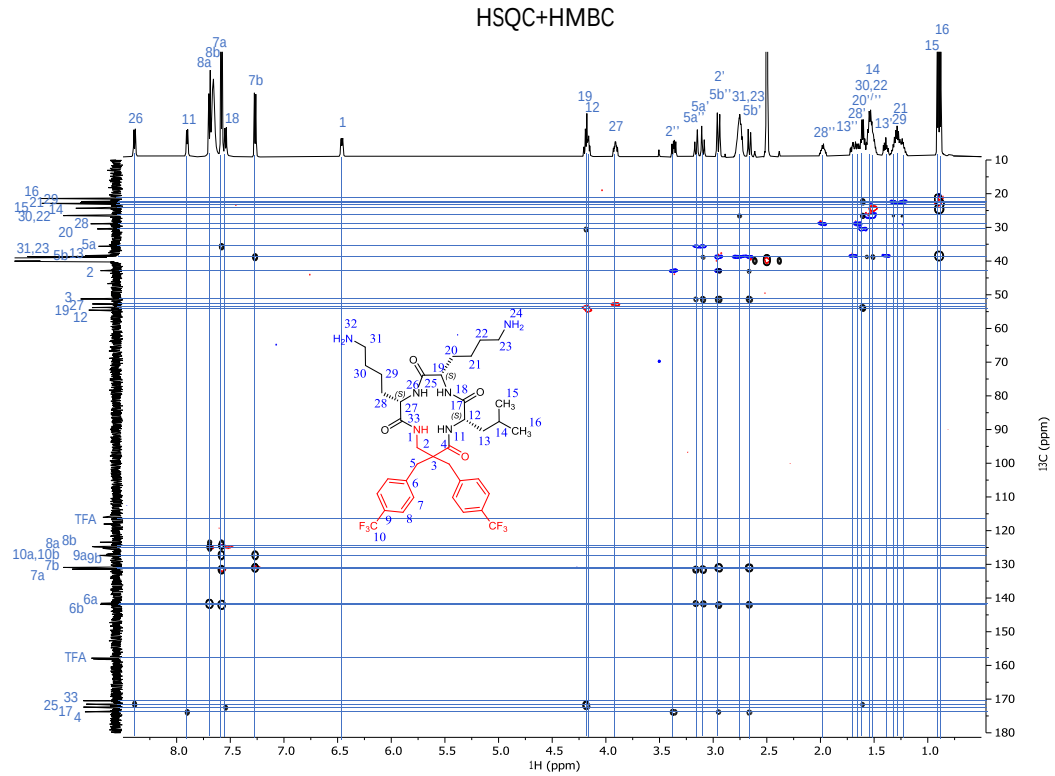

Figure S12. Superimposed HSQC (red CH, CH_3, blue CH_2) and HMBC (black) spectra of **001.**

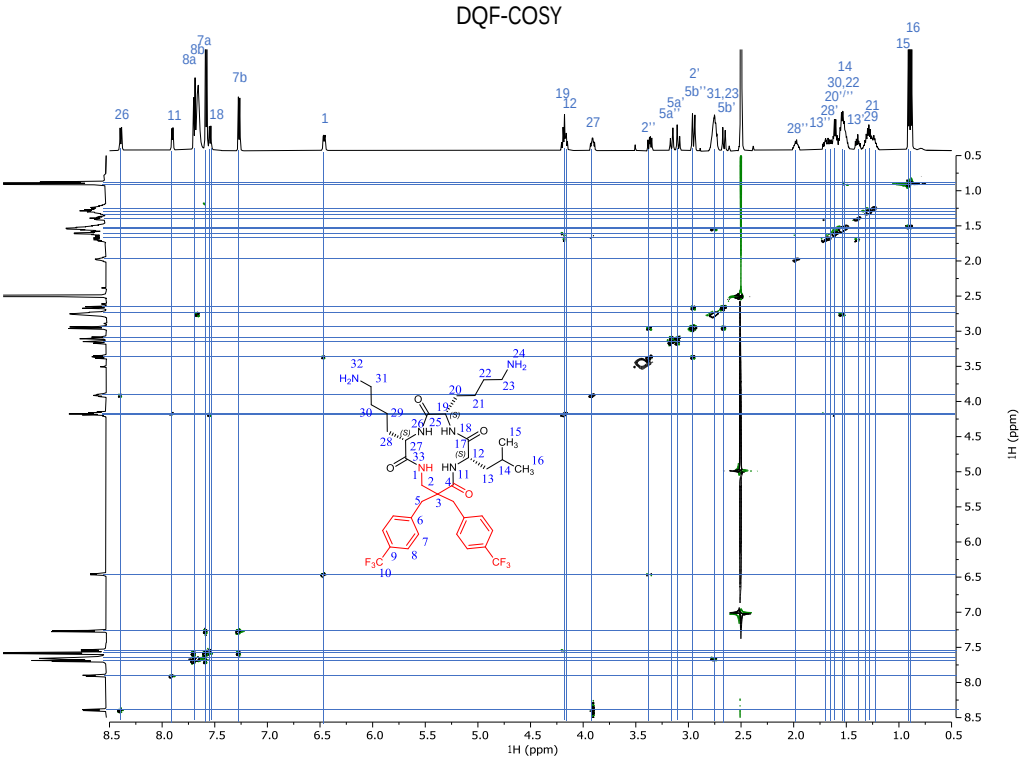

Figure S13. DQF-COSY spectrum of **001.**

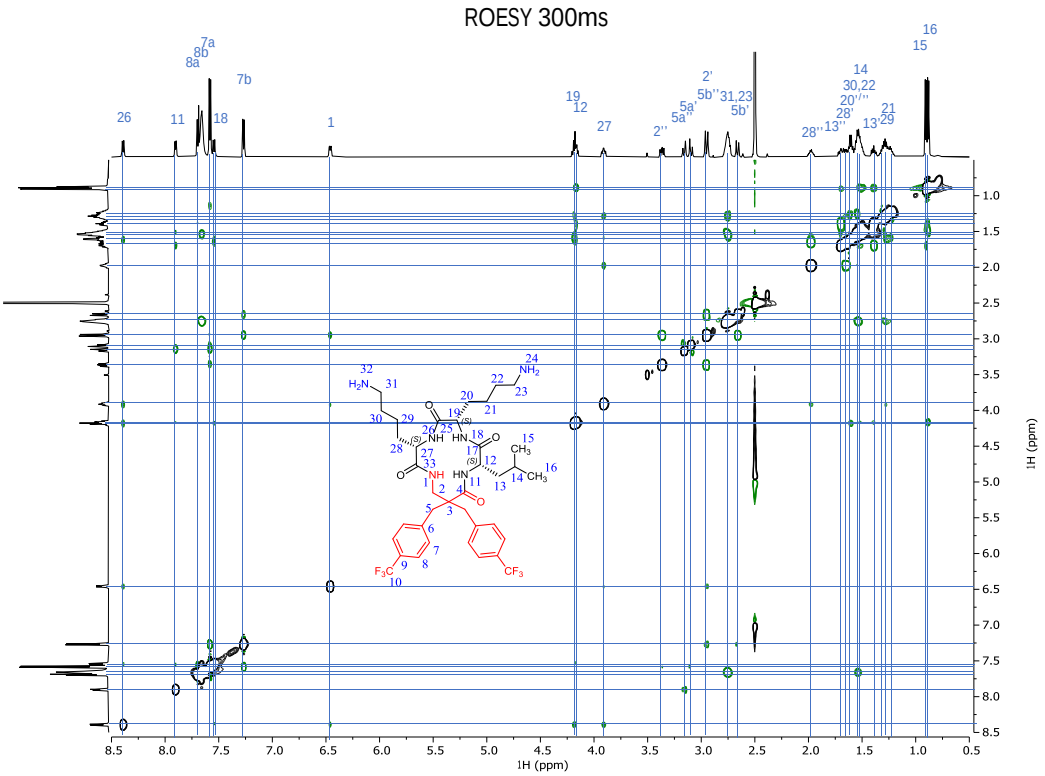

Figure S14. ROESY (300ms spinlock duration) spectrum of **001.**

^{1}H NMR (600 MHz, DMSO) δ 8.66 (d, J = 6.8 Hz, 1H), 7.95 (d, J = 6.3 Hz, 1H), 7.69 (d, J = 8.3 Hz, 2H), 7.65 (d, J = 8.6 Hz, 2H), 7.64 (b, 6H), 7.57 (d, J = 8.1 Hz, 2H), 7.34 (d, J = 9.1 Hz, 1H), 7.25 (d, J = 8.0 Hz, 2H), 6.55 (dd, J = 7.7, 4.0 Hz, 1H), 4.25 (q, J = 7.9 Hz, 1H), 4.07 (dt, J = 9.6, 6.2 Hz, 1H), 4.01 (ddd, J = 9.5, 6.7, 5.1 Hz, 1H), 3.32 (dd, J = 13.6, 7.7 Hz, 1H), 3.12 (d, J = 13.6 Hz, 1H), 3.10 (d, J = 13.6 Hz, 1H), 2.99 (d, J = 13.4 Hz, 1H), 2.98 (d, J = 13.6 Hz, 1H), 2.81 – 2.69 (m, 4H), 1.69 (td, J = 10.6, 5.4 Hz, 1H), 1.65 – 1.61 (m, 1H), 1.61 – 1.43 (m, 7H), 1.38 (m, 3H), 1.29-1.20 (m, 1H), 1.20 – 1.12 (m, 1H), 0.92 (d, J = 6.4 Hz, 3H), 0.88 (d, J = 6.5 Hz, 3H).

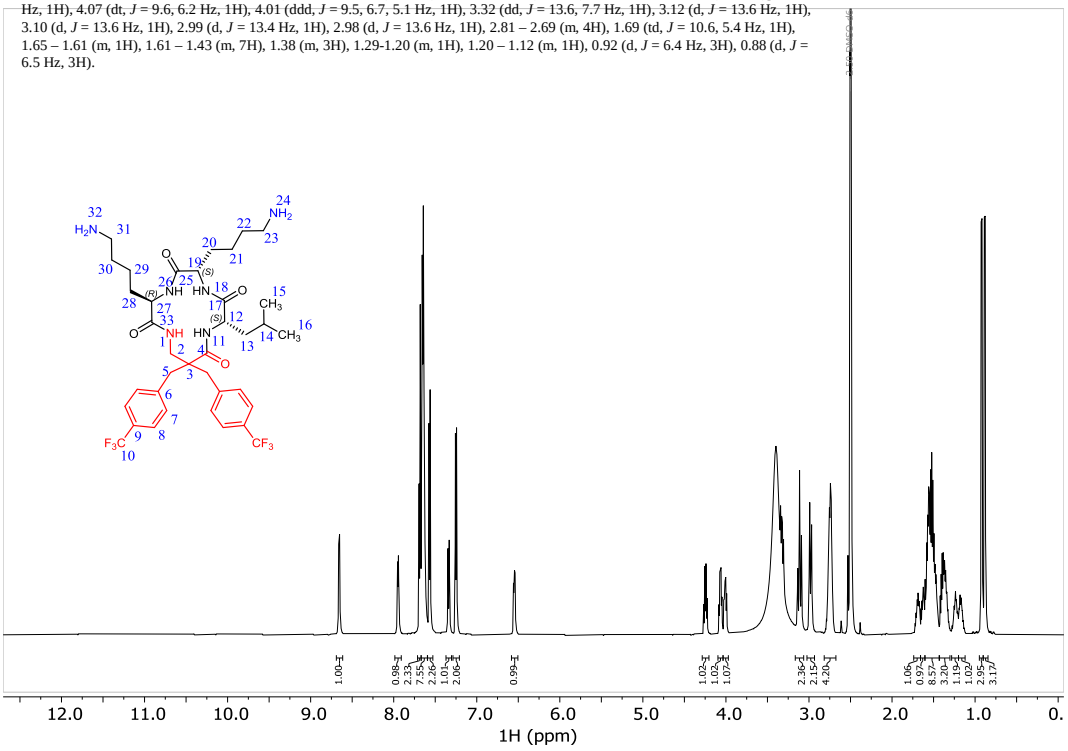

Figure S15. ^{1}H NMR spectrum of **011.**

^{13}C NMR (151 MHz, DMSO) δ 173.49, 172.53, 171.82, 171.05, 141.85, 141.35, 131.87, 130.94, 127.32 (q, J=32.2 Hz), 127.12 (q, J=32.2 Hz), 124.75 (q, J=3.9 Hz), 124.67 (q, J=3.9 Hz), 124.45 (q, J=272.3 Hz), 124.35 (q, J=272.3 Hz), 55.14, 54.55, 51.98, 51.60, 40.06, 39.18, 38.70, 38.60 (2C), 38.01, 30.72, 29.74, 26.87, 26.57, 24.25, 22.69, 22.64, 22.14, 21.62.

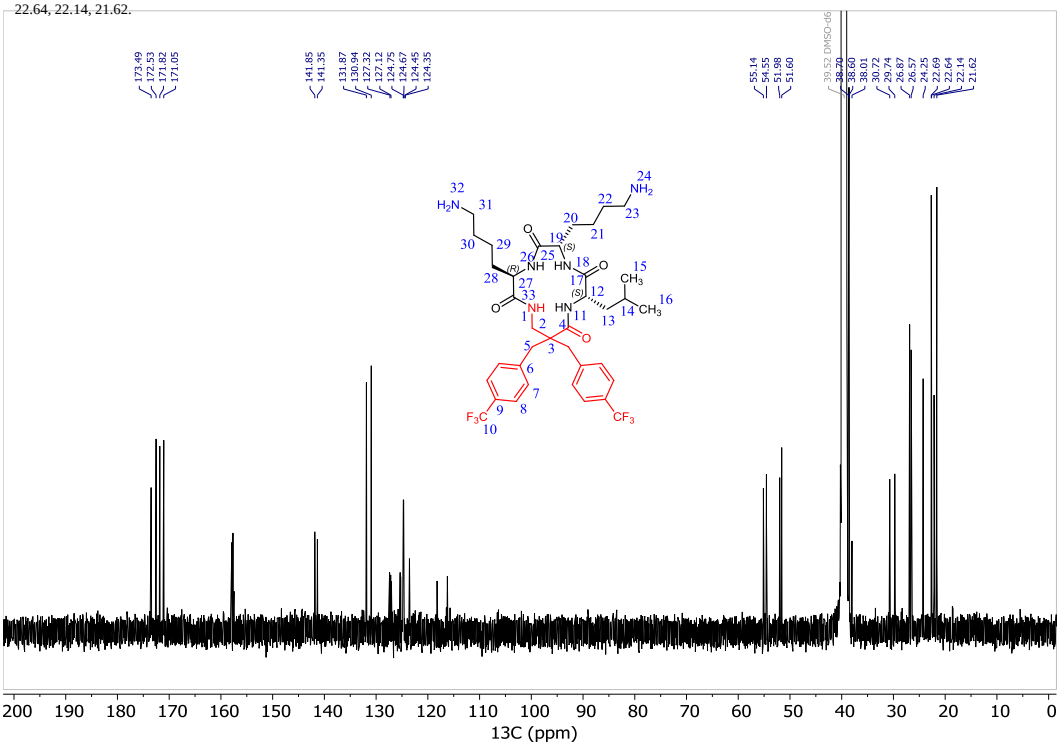

Figure S16. ^{13}C NMR spectrum of **011.**

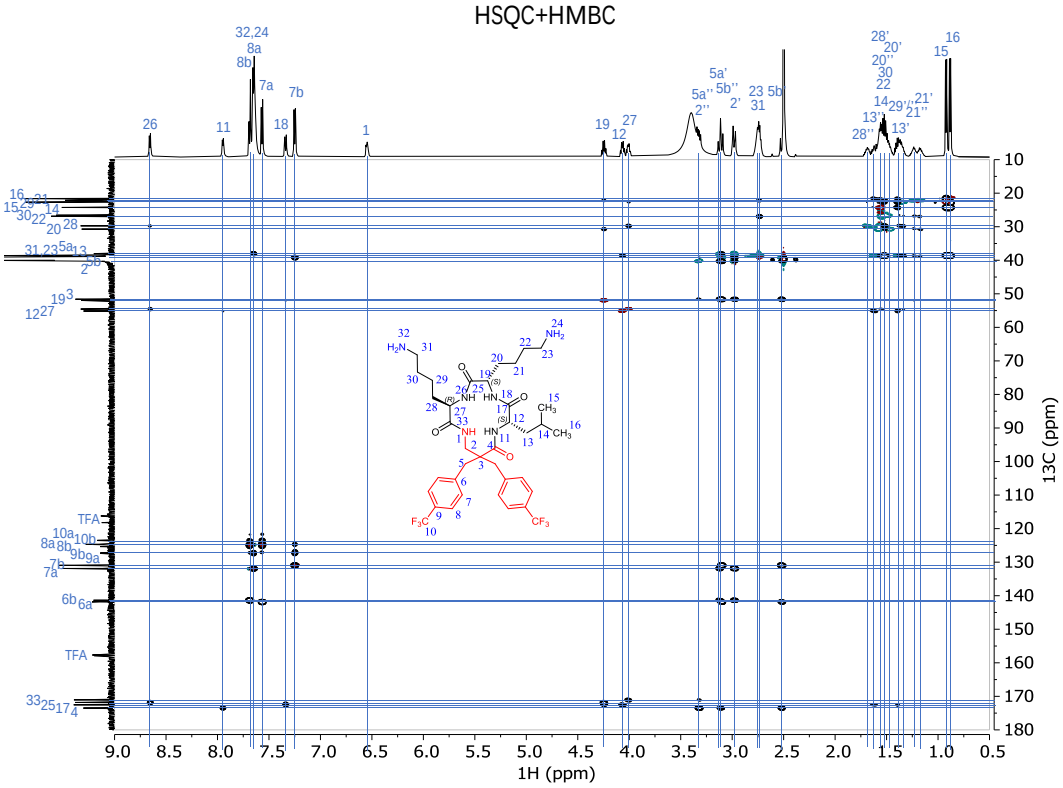

Figure S17. Superimposed HSQC (red CH, CH_3, blue CH_2) and HMBC (black) spectra of **011.**

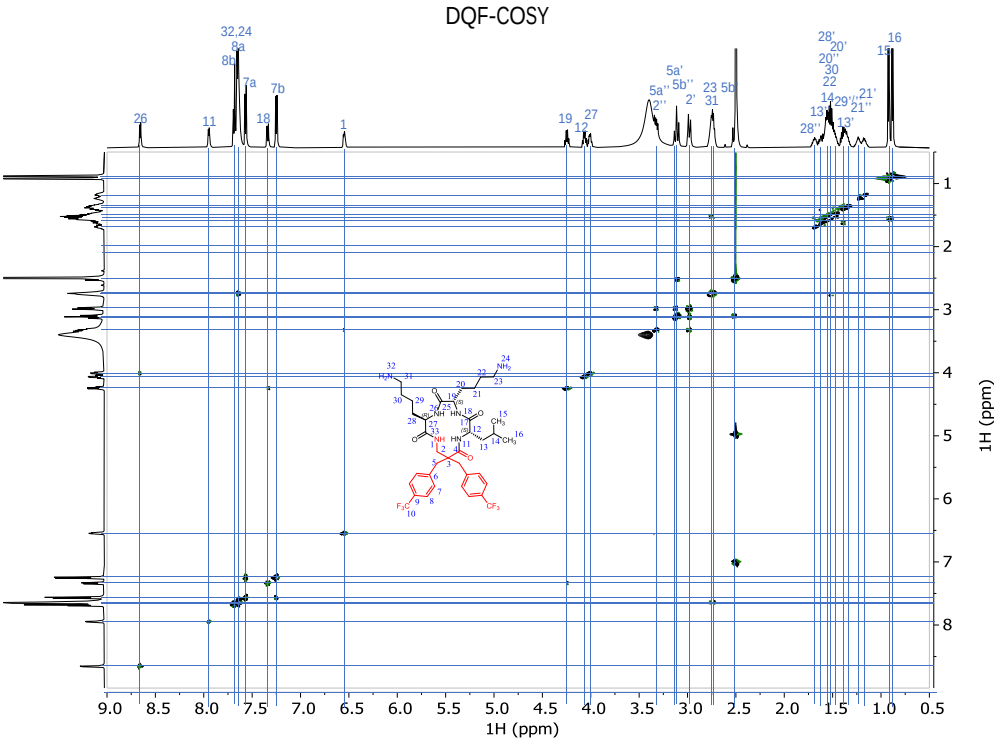

Figure S18. DQF-COSY spectrum of **011.**

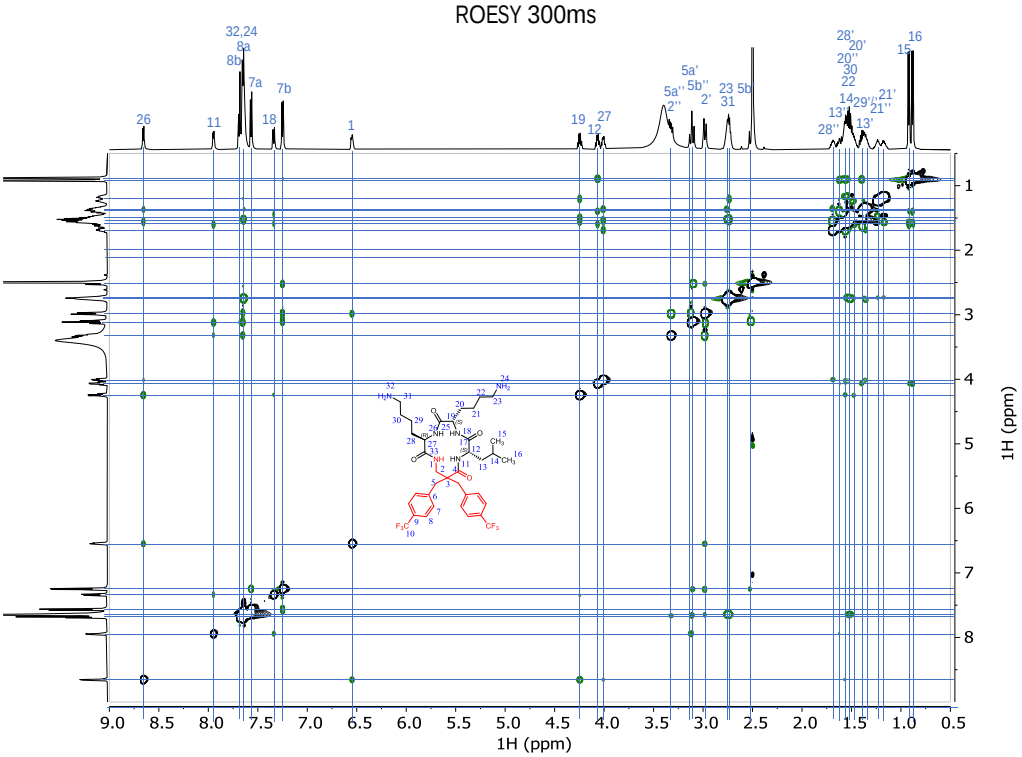

Figure S19. ROESY (300ms spinlock duration) spectrum of **011.**

^{1}H NMR (600 MHz, DMSO) δ 8.48 (d, *J* = 8.4 Hz, 1H), 8.13 (d, *J* = 5.9 Hz, 1H), 7.77 (t, *J* = 5.8 Hz, 3H), 7.70 (d, *J* = 8.2 Hz, 5H), 7.59 (d, *J* = 8.0 Hz, 2H), 7.56 (d, *J* = 8.1 Hz, 2H), 7.25 (d, *J* = 8.0 Hz, 2H), 6.44 (dd, *J* = 8.5, 3.1 Hz, 1H), 4.32 (td, *J* = 8.7, 6.3 Hz, 1H), 4.08 (dt, *J* = 9.1, 6.2 Hz, 1H), 3.92 (ddd, *J* = 10.3, 8.4, 4.3 Hz, 1H), 3.32 (dd, *J* = 13.3, 8.5 Hz, 1H), 3.20 – 3.12 (m, 2H), 2.96 – 2.92 (m, 1H), 2.90 (d, *J* = 14.1 Hz, 1H), 2.64 (d, *J* = 13.8 Hz, 1H), 1.96 (dtt, *J* = 13.6, 9.2, 3.7 Hz, 1H), 1.75 (dtd, *J* = 14.5, 9.4, 5.5 Hz, 1H), 1.67 (ddq, *J* = 19.3, 9.3, 5.5 Hz, 2H), 1.41 – 1.33 (m, 0H), 1.33 – 1.21 (m, 3H), 0.90 (d, *J* = 5.8 Hz, 2H), 0.87 (d, *J* = 5.8 Hz, 3H).

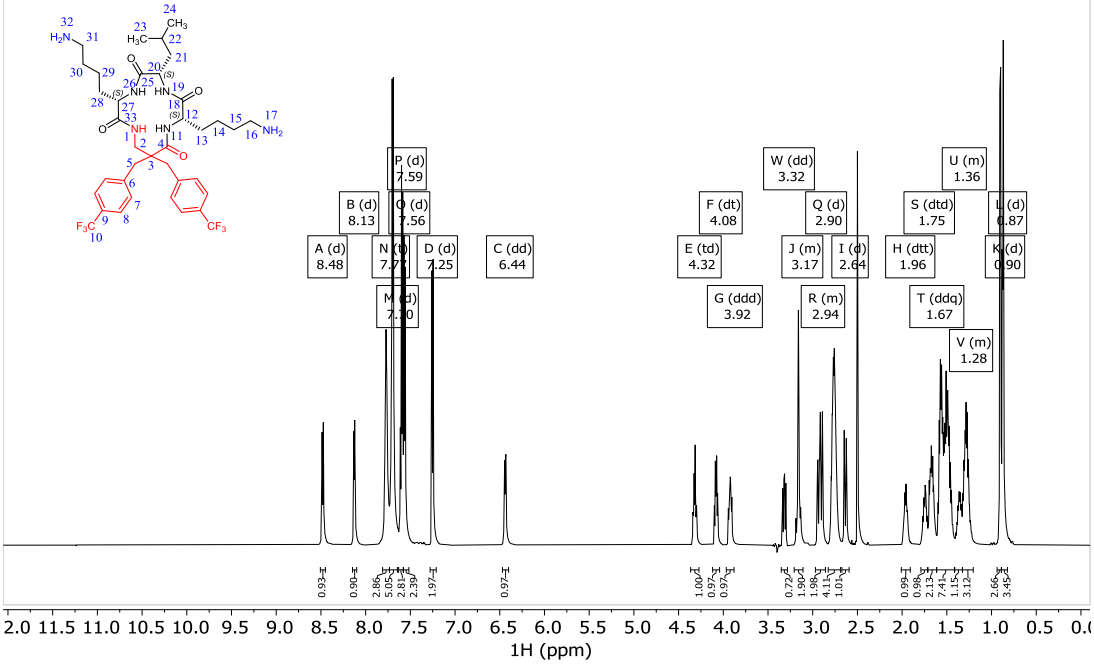

Figure S20. ^{1}H NMR spectrum of **003.**

^{13}C NMR (151 MHz, DMSO) δ 173.96, 171.72, 171.65, 170.58, 141.84, 141.53, 131.51, 130.88, 127.27 (q, *J* = 31.7 Hz), 127.12 (q, *J* = 31.7 Hz), 124.89 (q, *J* = 3.8 Hz), 124.77 (q, *J* = 3.9 Hz), 124.40 (q, *J* = 272.2 Hz), 124.35 (q, *J* = 272.2 Hz), 56.44, 52.62, 52.56, 51.26, 42.71, 40.15, 40.06, 38.91, 38.71, 38.62, 35.34, 29.04, 28.92, 26.56, 26.50, 24.62, 22.77, 22.64, 22.45, 22.09.

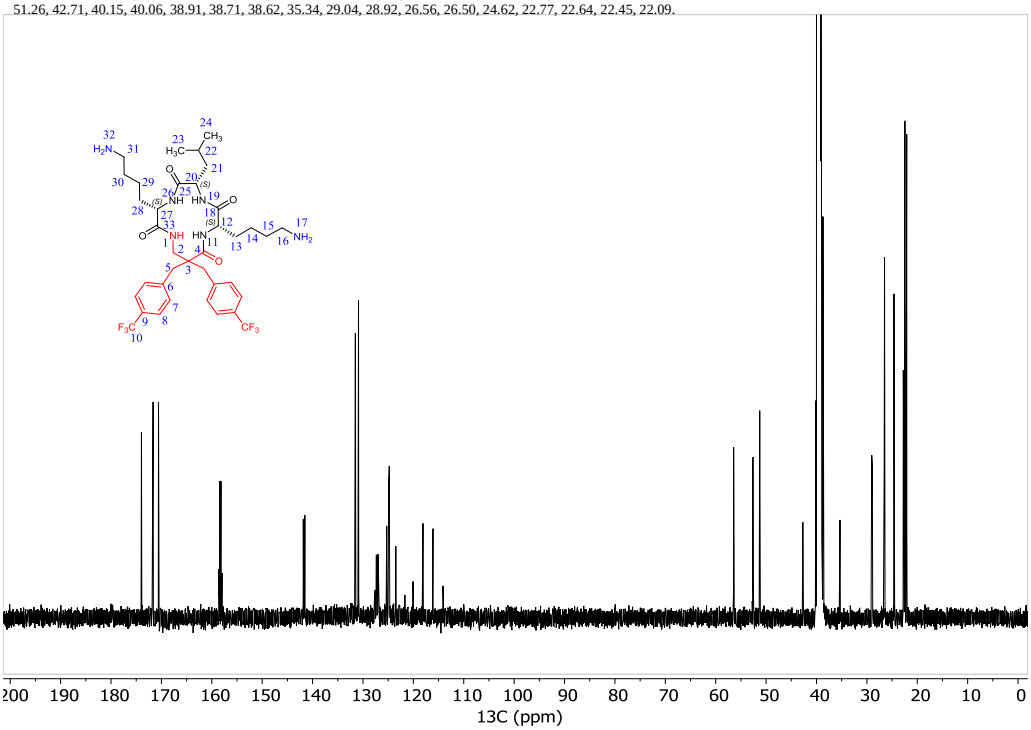

Figure S21. ^{13}C NMR spectrum of **003.**

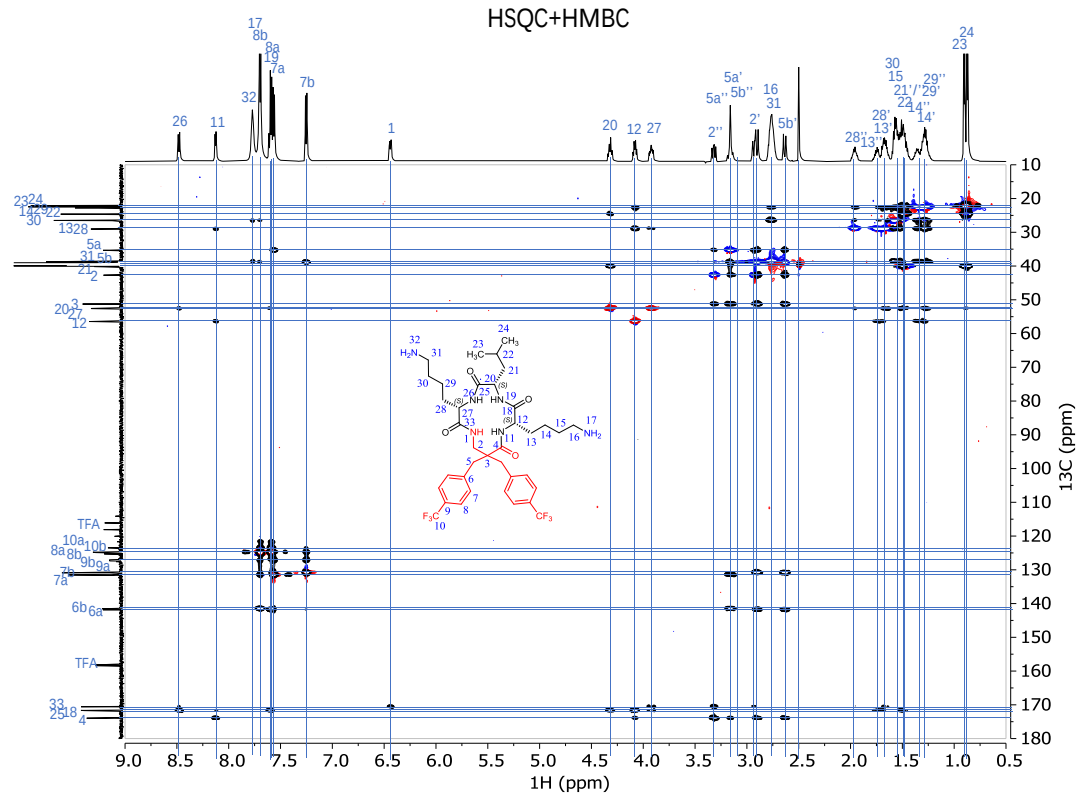

Figure S22. Superimposed HSQC (red CH, CH_3, blue CH_2) and HMBC (black) spectra of **003.**

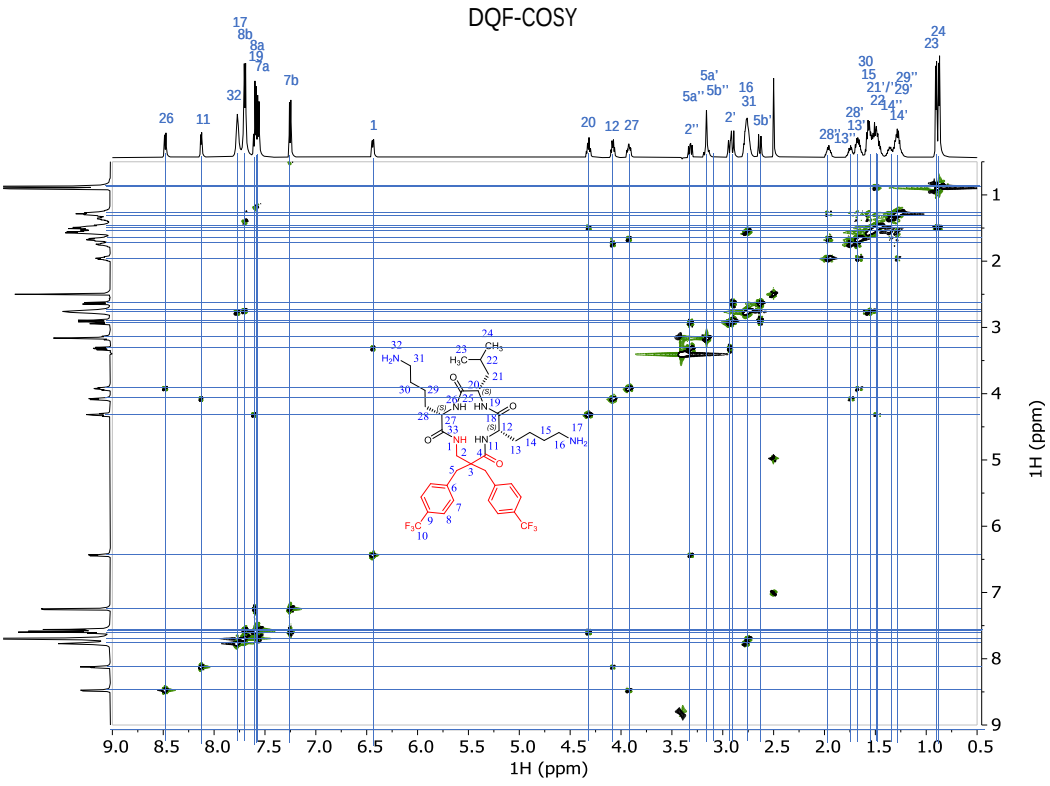

Figure S23. DQF-COSY spectrum of **003.**

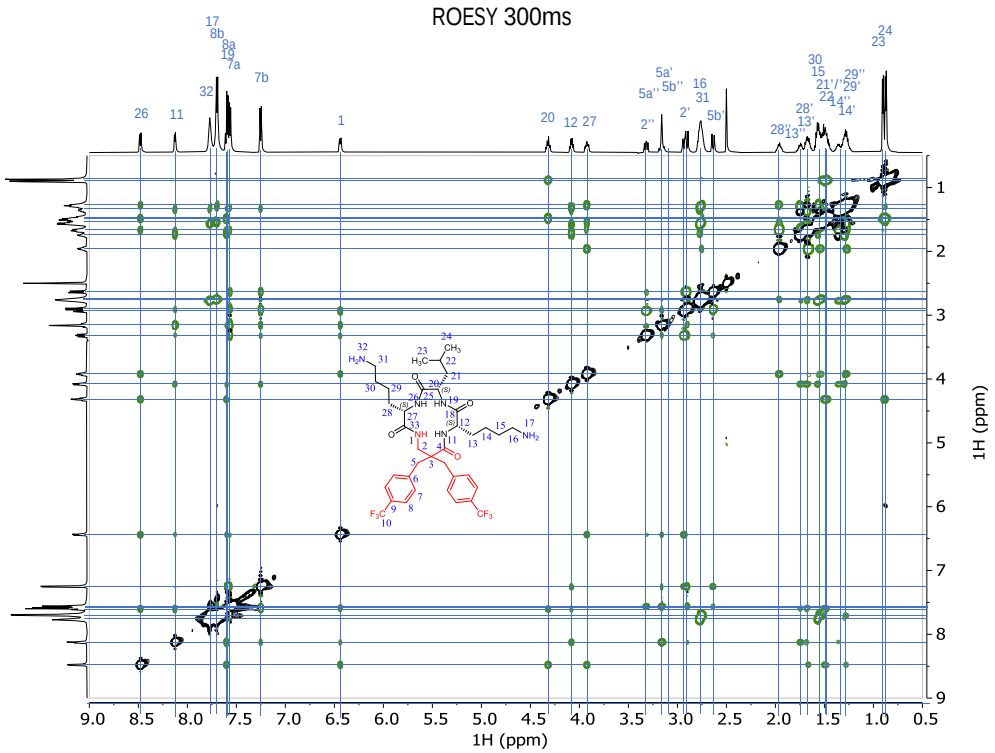

Figure S24. ROESY (300ms spinlock duration) spectrum of **003.**

^{1}H NMR (600 MHz, DMSO) δ 8.53 (d, *J* = 8.1 Hz, 1H), 7.99 (d, *J* = 6.3 Hz, 1H), 7.69 (d, *J* = 7.9 Hz, 3H), 7.64 (t, *J* = 5.4 Hz, 1H), 7.61 (d, *J* = 8.1 Hz, 2H), 7.57 (d, *J* = 8.2 Hz, 2H), 7.33 (s, 2H), 7.26 (d, *J* = 8.0 Hz, 2H), 6.92 (s, 4H), 6.48 (dd, *J* = 8.8, 3.0 Hz, 1H), 4.20 (q, *J* = 8.2 Hz, 1H), 4.16 (dt, *J* = 10.4, 5.9 Hz, 1H), 3.90 (ddd, *J* = 10.0, 7.9, 4.5 Hz, 1H), 3.40 (dd, *J* = 13.4, 8.6 Hz, 1H), 3.19 (d, *J* = 14.2 Hz, 1H), 3.16 – 3.04 (m, 5H), 2.99 (d, *J* = 13.7 Hz, 1H), 2.93 (dd, *J* = 13.3, 3.0 Hz, 1H), 2.62 (d, *J* = 13.7 Hz, 1H), 2.06 – 1.94 (m, 0H), 1.70 (dtd, *J* = 19.2, 9.7, 4.8 Hz, 2H), 1.64 – 1.57 (m, 2H), 1.56 – 1.33 (m, 2H), 0.91 (d, *J* = 6.6 Hz, 2H), 0.89 (d, *J* = 6.5 Hz, 2H).

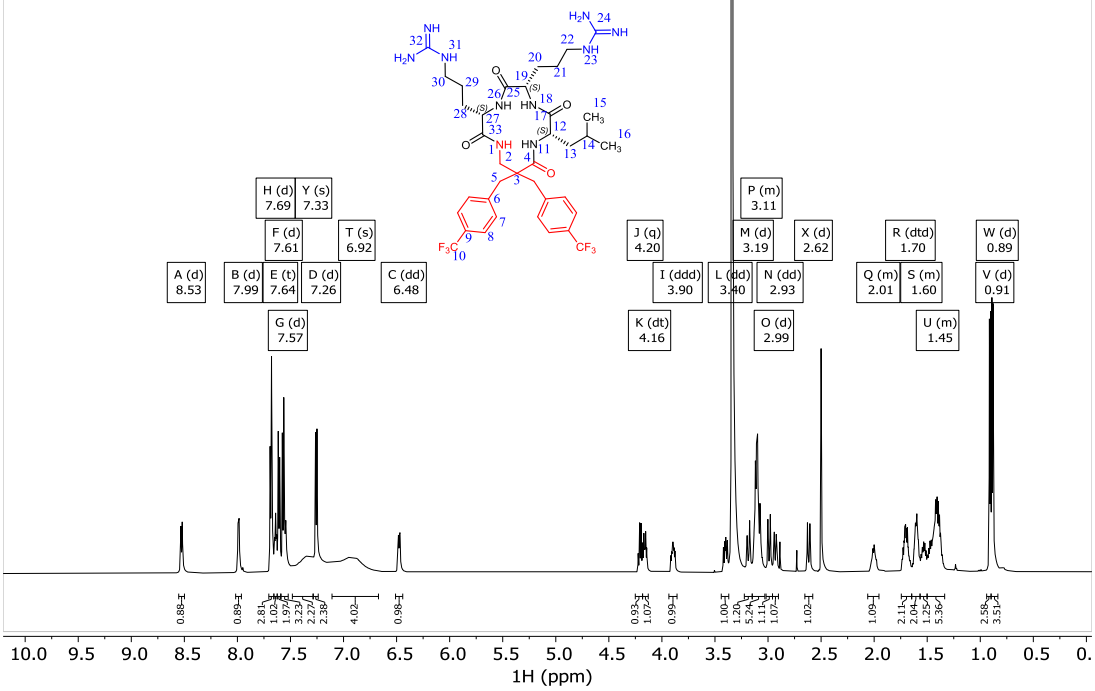

Figure S25. ^{1}H NMR spectrum of **002.**

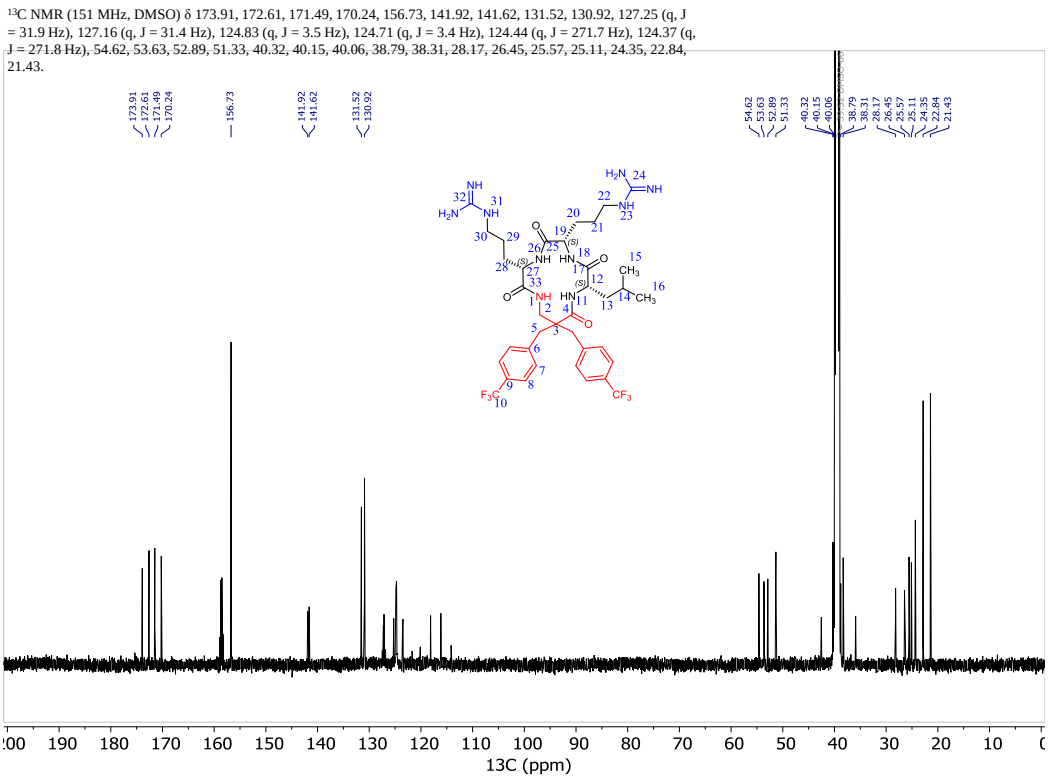

Figure S26. ^{13}C NMR spectrum of **002.**

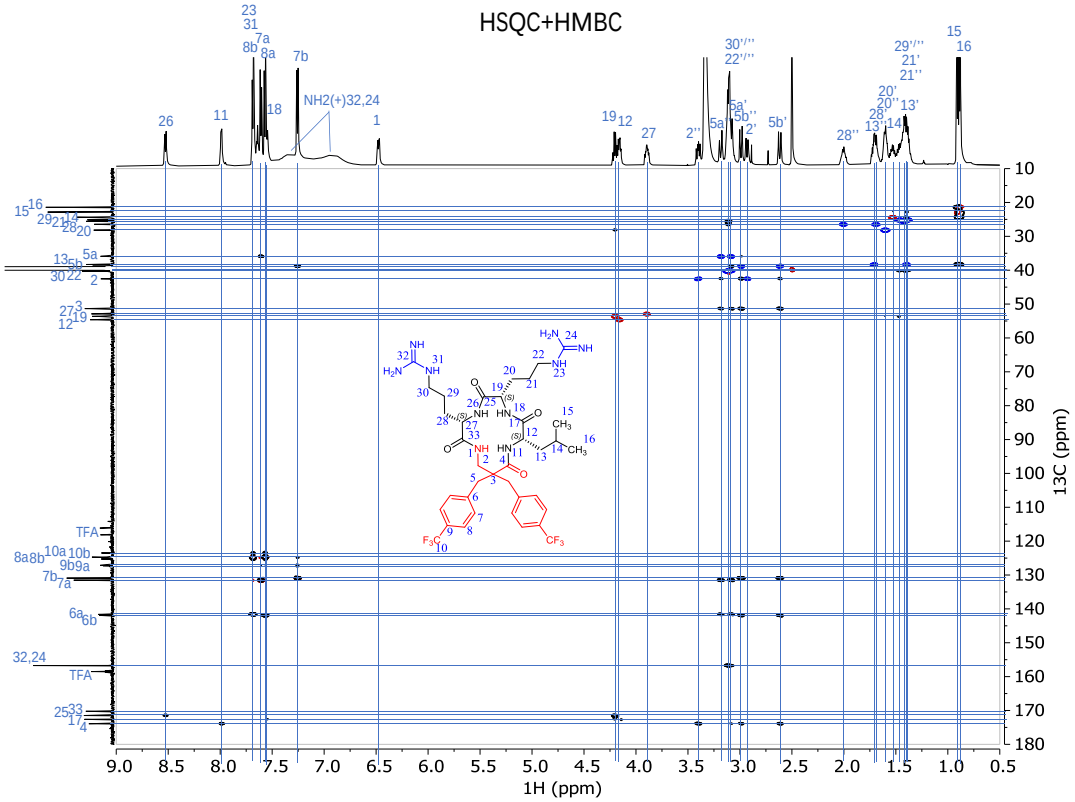

Figure S27. Superimposed HSQC (red CH, CH_3, blue CH_2) and HMBC (black) spectra of **002.**

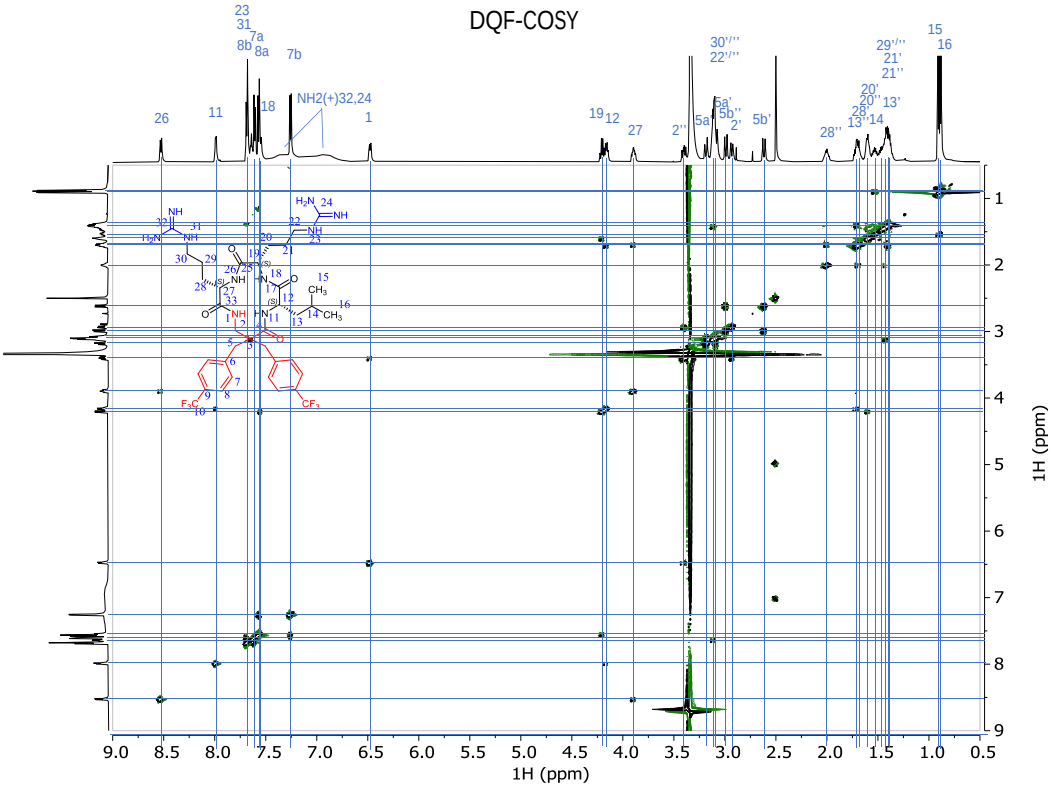

Figure S28. DQF-COSY spectrum of **002.**

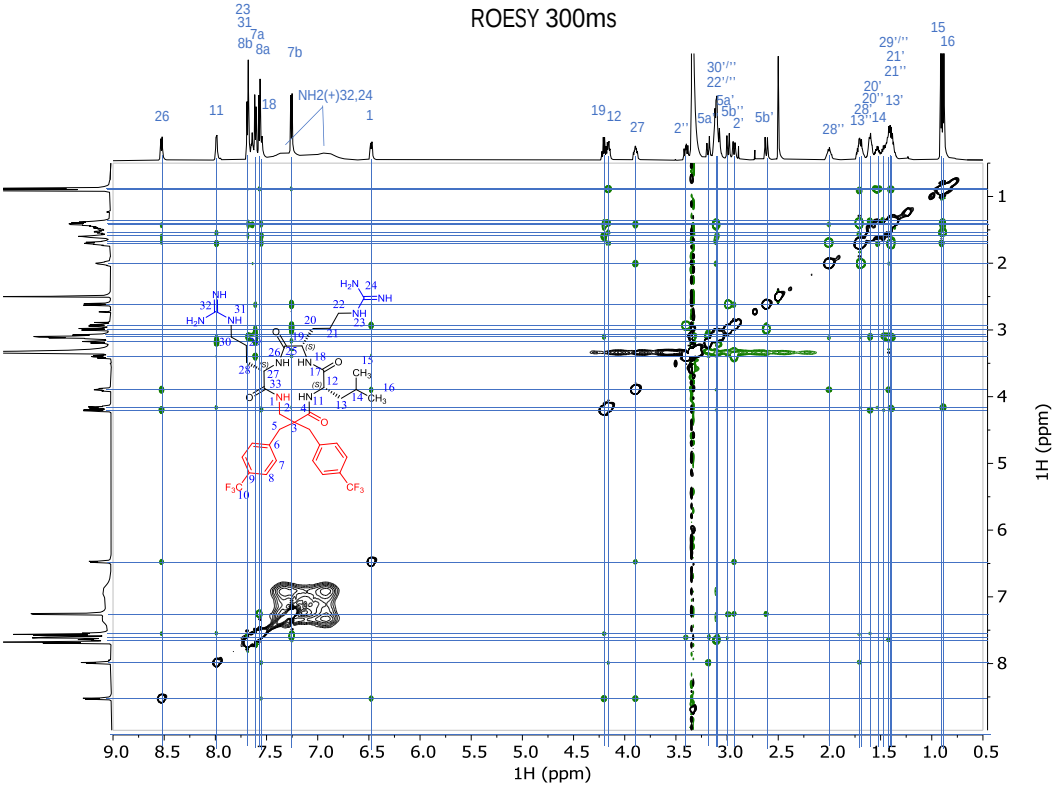

Figure S29. ROESY (300ms spinlock duration) spectrum of **002.**

Table S1. Purity (%) and retention time (min) of the synthesised peptides, and percent yield (%) of the reactions.

Entry	Sequence	Purity (%)	Retention time (min)	Percent Yield (%)
001	c(Lys-$\beta^{2,2}$-Leu-Lys)	97.80	6.23	15.8
002	c(Arg-$\beta^{2,2}$-Leu-Arg)	99.52	6.38	21.87
003	c(Leu-Lys-$\beta^{2,2}$-Lys)	97.43	5.30	21.63
004	c(Leu-Arg-$\beta^{2,2}$-Arg)	97.87	5.46	25.89
011	c(*D*-Lys-$\beta^{2,2}$-Leu-Lys)	100.00	6.07	33.04
021	c(*D*-Arg-$\beta^{2,2}$-Leu-Arg)	99.33	6.18	22.48
031	c(Phe-Lys-$\beta^{2,2}$-Lys)	100.00	5.33	14.03
041	c(Phe-Arg-$\beta^{2,2}$-Arg)	98.56	5.47	19.06
006	c(Arg-$\beta^{2,2}$-Arg-Arg)	97.16	5.08	25.07

Table S2. Theoretical monoisotopic mass (Da), and theoretical and observed m/z ions during HRMS of the synthesised peptides.

	Monoisotopic mass (Da)	$[M+H]^+$		$[M+2H]^{2+}$		$[M+3H]^{3+}$	
Peptide	Theoretical	Theoretical	Observed	Theoretical	Observed	Theoretical	Observed
001	756.3798	757.3871	757.3872	379.1972	379.1975	253.1339	-
002	812.3921	813.3994	813.3994	407.2033	407.2036	271.8046	-
003	756.3798	757.3871	757.3872	379.1972	379.1974	253.1339	-
004	812.3921	813.3994	813.3994	407.2033	407.2036	271.8046	-
011	756.3798	757.3871	757.3874	379.1972	379.1977	253.1339	-
021	812.3921	813.3994	813.3995	407.2033	407.2039	271.8046	
031	790.3641	791.3714	791.3717	396.1893	396.1897	264.4620	-
041	846.3764	847.3837	847.3836	424.1955	424.1960	283.1327	-
006	855.4091	856.4164	856.4163	428.7118	428.7122	286.1436	286.1438